DEVELOPMENT OF A HIGHLY POTENT BISPECIFIC ANTIBODY FORMAT TARGETING THE NOVEL TUMOR-SPECIFIC ANTIGEN CLDN18.2

DISSERTATION ZUR ERLANGUNG DES GRADES
„DOKTOR DER NATURWISSENSCHAFTEN"

AM FACHBEREICH BIOLOGIE
DER

JOHANNES GUTENBERG UNIVERSITÄT MAINZ

VORGELEGT VON

JULIA HOLLAND

GEBOREN IN MAINZ

BRÜGGEN, DER 11. NOVEMBER 2014

MITGLIEDER DER PROMOTIONSKOMMISSION

Dekan:

Gutachter:

Gutachter:

Tag der mündlichen Prüfung: 22.01.2014

EHRENWÖRTLICHE ERKLÄRUNG

Hiermit versichere ich, dass ich die vorliegende Dissertation selbständig und ohne unerlaubte Hilfe verfasst und keine anderen als die angegebenen Hilfsmittel und Quellen benutzt habe. Ich habe weder anderweitig versucht, eine Dissertation einzureichen oder eine Doktorprüfung durchzuführen, noch habe ich diese Dissertation oder Teile derselben einer anderen Prüfungskommission vorgelegt.

Brüggen, der 11. November 2014

Julia Holland

SUMMARY

Due to multiple immune evasion mechanisms of cancer cells, novel therapy approaches are required to overcome the limitations of existing immunotherapies. Bispecific antibodies are potent anti-cancer drugs, which redirect effector T cells for specific tumor cell lysis, thus enabling the patient's immune system to fight cancer cells.

The antibody format used in this proof of concept study–bispecific ideal monoclonal antibodies termed BiMAB–is a tailor-made recombinant protein, which consists of two fused scFv antibodies recognizing different antigens. Both are arranged in tandem on a single peptide chain and the individual variable binding domains are separated by special non-immunogenic linkers. The format is comprised of a scFv targeting CLDN18.2–a gastric cancer tumor associated antigen (TAA) –while the second specificity binds the CD3 epsilon (CD3ε) subunit of the T cell receptor (TCR) on T cells.

For the first time, we compared in our IMAB362-based BiMAB setting, four different anti-CD3-scFvs, respectively derived from the mAbs TR66, CLB-T3, as well as the humanized and the murine variant of UCHT1. In addition, we investigated the impact of an N- versus a C-terminal location of the IMAB362-derived scFv and the anti-CD3-scFvs. Thus, nine CLDN18.2 specific BiMAB proteins were generated, of which all showed a remarkably high cytotoxicity towards CLDN18.2-positive tumor cells.

Because of its promising effectiveness, 1BiMAB emerged as the BiMAB prototype. The selectivity of 1BiMAB for its TAA and CD3ε, with affinities in the nanomolar range, has been confirmed by *in vitro* assays. Its dual binding depends on the design of an N-terminally positioned IMAB362 scFv and the consecutive C-terminally positioned TR66 scFv.

1BiMAB provoked a concentration and target cell dependent T cell activation, proliferation, and upregulation of the cytolytic protein Granzyme B, as well as the consequent elimination of target cells.

Our results demonstrate that 1BiMAB is able to activate T cells independent of elements that are usually involved in the T cell recognition program, like antigen presentation, MHC restriction, and co-stimulatory effector molecules. In the first *in vivo* studies using a subcutaneous xenogeneic tumor mouse model in immune incompetent NSG[1] mice, we could prove a significant therapeutic effect of 1BiMAB with partial or complete tumor elimination.

The initial *in vitro* RIBOMAB experiments correspondingly showed encouraging results. The electroporation of 1BiMAB IVT-RNA into target or effector cells was feasible, while the functionality of translated 1BiMAB was proven by induced T cell activation and target cell lysis.

Accordingly, we could show that the *in vitro* RIBOMAB approach was applicable for all nine BiMABs, which proves the RIBOMAB concept.

Thus, the CLDN18.2-BiMAB strategy offers great potential for the treatment of cancer. In the future, administered either as protein or as IVT-RNA, the BiMAB format will contribute towards finding solutions to raise and sustain tumor-specific cellular responses elicited by engaged and activated endogenous T cells. This will potentially enable us to overcome immune evasion mechanisms of tumor cells, consequently supporting current solid gastric cancer therapies.

[1] NOD scid gamma (NSG):NOD.Cg-Prkd^{scid} IL2rg^{tm1Wjl}/SzJ (Jackson laboratory, Bar Harbour, ME, USA)

TABLE OF CONTENT

LIST OF TABLES

LIST OF FIGURES

1 INTRODUCTION – TARGETED CANCER IMMUNOTHERAPY

In recent years, cancer treatment options have developed from conventional strategies to more selective, mechanism-based therapeutic approaches [1]. Conventional methods are based on surgery as the primary curative treatment, followed by chemotherapies occasionally combined with radiotherapy [2,3]. These approaches are rather unspecific and affect healthy tissues as well as the cancer. Better insights into cancer pathogenesis, gained by the extensive research in this field, allowed the establishment of alternative therapies, which act in a more specific manner. One example are targeted therapies, which are regarded as a promising field as these drug treatments specifically bind to 'target' structures restricted to cancer tissue. This group is dominated by four drug classes. For example, there are small molecule-based kinase inhibitors like Gleevec®, as well as retinoids such as Targretin® or Panretin®, and recombinant cytokine therapies such as Ontak®. The predominantly used drug class is tumor-targeting monoclonal antibodies (mAb) [4]. All of these approaches aim to specifically eliminate tumor cells and inhibit tumor progression. However, the efficacy of these methods is limited by the highly diverse cancer phenotypes and its effective strategies 'to evade immune destruction', making the identification of a suitable target difficult. The quest to find appropriate targets and their matching anti-cancer drugs is commonly based on random high-throughput screening, focusing on their anti-proliferative effects in cytotoxicity assays [5]. Most of these targets are overexpressed on tumor cells, but their expression is not always restricted to malignant tissue, as they can play central roles in normal tissue development and maintenance [6]. Consequently, the elimination of these healthy cells along with the malignant cells can cause severe side effects in patients during drug treatment. These have been reported with all conventional therapies.

The lack of novel appropriate target molecules, which are completely absent from normal tissues, can be seen as the bottleneck in the generation of optimized cancer therapeutics. The benefits of such treatment are believed to be an improvement in efficacy and safety of anti-cancer therapy, and thus an increase in the overall survival and quality of the patients' life. Yet, there are only few targets described that fulfill this requirement of high specificity. This problem was named by Phillips *et al.* [7] the 'pipeline problem'.

The Biotech company Ganymed Pharmaceuticals AG, in collaboration with TRON gGmbH and the Gutenberg University Medical Center Mainz, are committed to validating novel cancer target structures for therapeutic use in order to address the 'pipeline problem'. A general cancer target pipeline, which will hold biomarkers of primary and metastatic solid cancers appropriate for targeted therapeutic approaches, is planned. Biomarkers suitable for targeted therapeutic approaches are crucial for cancer growth, proliferation, and survival, uniquely expressed in cancer tissues but absent on most normal tissues. The identification of these 'ideal targets' with the required high specificity is a key prerequisite to minimize the risks of toxic effects during treatment. A collection of 'ideal targets' will be used for the development of a cancer therapeutics toolkit that will allow the eradication of malignant cells by a strategy of individualized combinatorial therapy. Parallel treatment options are anticipated, with the combined application of small molecules, antibodies, bispecific antibodies, vaccines, virus-like particles, and siRNA amongst others, all targeting the same tumor associated antigen (TAA).

1.1 CLAUDIN-18 SPLICE VARIANT2–A BIOMARKER FOR GASTRIC CANCER

The cell surface antigen claudin-18 splice variant 2 (CLDN18.2) was described by Sahin *et al.* [8] as a pan-cancer target. It is expressed in a diverse variety of primary lesions and metastases of human epithelial tumor entities and is maintained in disseminated cancer cells [8].
This antigen is ectopically expressed at significant levels on esophageal, pancreatic [9], lung, and gastric adenocarcinoma cells. These are examples of cancers with so far unmet medical needs. The patients primarily benefiting from a treatment targeting CLND18.2 are those who suffer from primary or metastatic gastric or esophageal tumors [8].
CLDN18.2 is present in 70 % of all characterized gastric cancer entities [8], of which 90 % to 95 % are diagnosed to be adenocarcinomas [10]. The other 5 - 10 % comprise lymphomas, gastrointestinal stromal tumors (GIST), and carcinoid tumors.
Zagouri *et al.* [11] reported gastric cancer to be the second leading cause of cancer related death, with approximately 930,000 new incidences diagnosed annually (8.6 % of all new cancer cases). For 2008, ~640,000 new male gastric cancer patients and ~350,000 female patients were estimated worldwide (Figure 1) [12]. For 2013, about 21,000 new incidences of stomach cancer just in the United States were predicted by the American Cancer Society [12].
Newly diagnosed gastric cancer patients frequently present an already advanced disease, resulting in a relatively poor prognosis [2] with a 5-year survival rate of less than 5.5 % and median survival times of less than 6 months [8]. Thus, there is a high medical need for a gastric cancer biomarker such as CLDN18.2, which might improve the treatment options in this field.

1.1.1 CLDN18.2–TARGET STRUCTURE AND TISSUE EXPRESSION PATTERN

The target molecule CLDN18.2 is a member of the claudin family and belongs to the class of tight junction proteins. CLDN18.2 is involved in cell signaling, barrier functions of epithelia and endothelia, and the maintenance of the cytoskeleton [13–15]. The CLDN18.2 protein sequence is highly conserved across species [16, 17].
The encoded 24 kDa protein contains four transmembrane domains and two short extracellular loops, while the N- and C-termini are located in the cytoplasm (Figure 2-A).
CLND18.2 is one of two splice variants described for CLDN18. The expression of both CLDN18 isoforms is regulated by different tissue specific promoters [17].

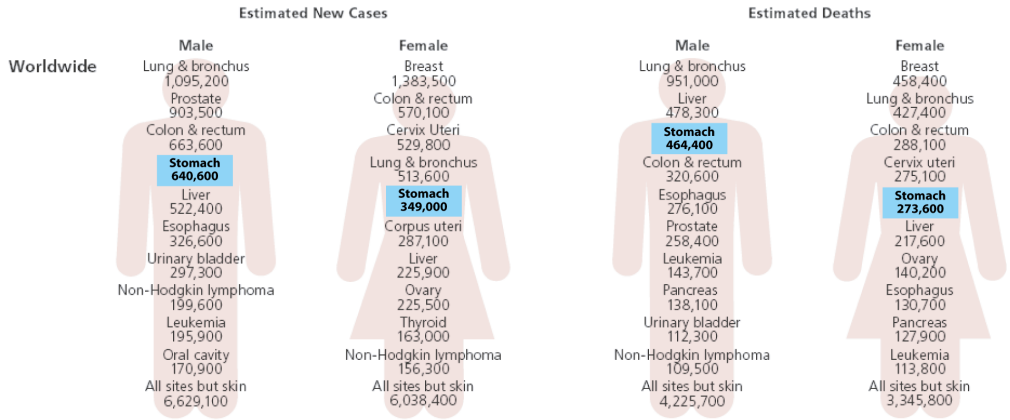

Figure 1: Estimated new cancer cases and deaths worldwide for leading cancer sites in 2008.
Stomach cancer is one of the leading causes of cancer death in men and in women. About 738,000 people worldwide died from stomach cancer in 2008. Blue rectangles highlight the gastric cancer incidences. Modified from American Cancer Society *et al.*[12]

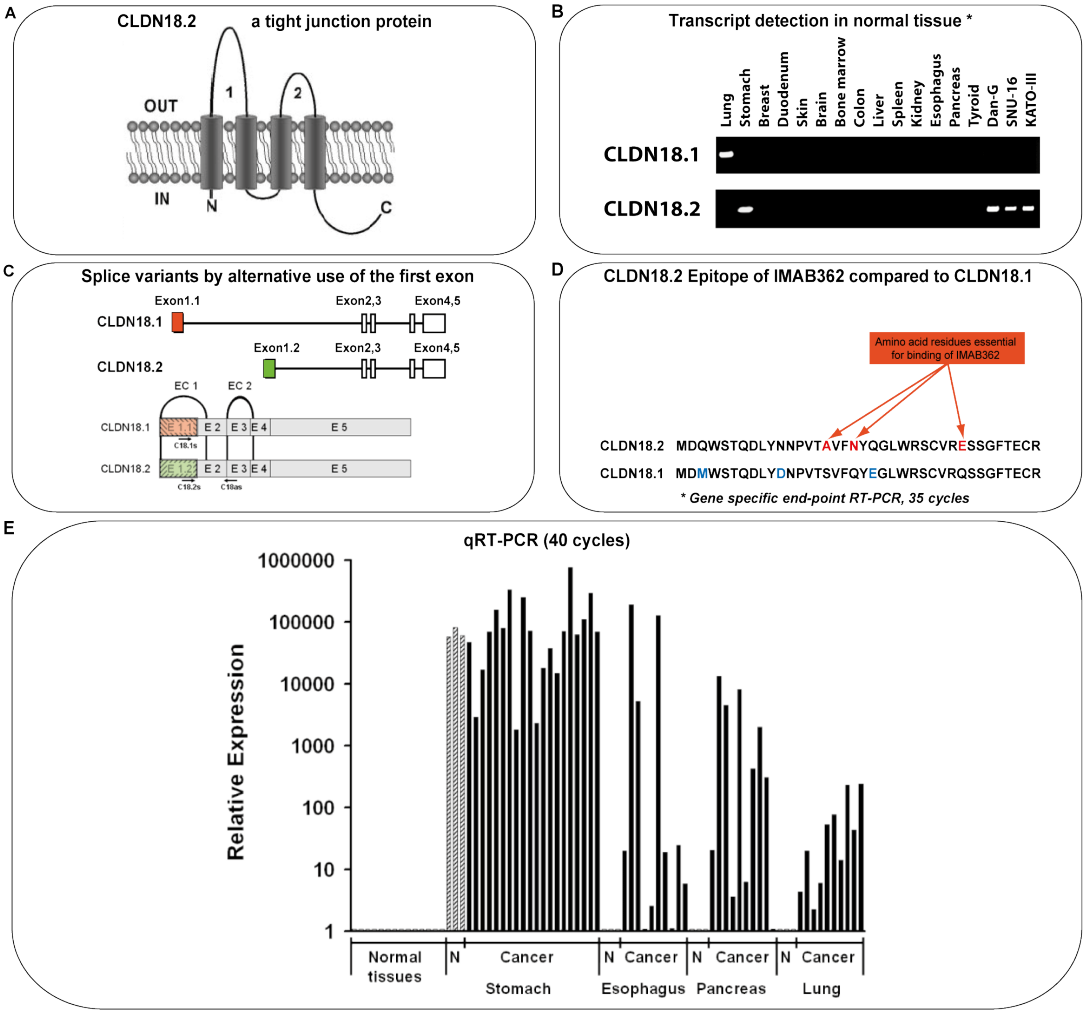

Figure 2: Compilation of CLDN18.2 characteristics

(**A**) Protein model of the tight junction protein CLDN18.2. Transmembrane regions are indicated by cylinders, extracellular loops by arches (1 and 2). (**B**) Profiles of both CLDN18 transcripts in a human panel of normal tissues, and tumor cell lines by end-point RT-PCR. (**C**) Genomic structure of the CLDN18 locus and the exon composition of both CLDN18 variants are shown. Colored boxes indicate exons that are unique for CLDN18.1 (red-E 1.1) or CLDN18.2 (green-E 1.2). Beneath, the mRNA transcripts of CLDN18 variants are depicted; arches indicate the positions encoding for the two extracellular domains. Arrows specify the primers used for RT-PCRs. (**D**) CLDN18.2 epitope sequence of IMAB362.The relevant regions of CLDN18.1 and CLDN18.2 are compared, amino acids (AA) relevant for IMAB362 binding sites are highlighted in red. AA differences not essential for IMAB362 binding are highlighted in blue. (**E**) Relative expression of CLDN18.2 in a human panel of normal tissues (N), primary tumor specimens, and tumor cell lines assessed by qRT-PCR. AA indicates amino acids; CLDN18, claudin-18; N, normal tissue qRT, quantitative real-time PCR. Pictures were modified from [8, 18].

While the first isoform (CLDN18.1) is solely present in the lung, as shown by RT PCR, splice variant 2 (CLDN18.2) is exclusively expressed in the stomach (Figure 2-B).

CLDN18.1 and CLDN18.2 differ in their first exon (Figure 2-C). There are further differences within the first extracellular loop of the two isoforms (Figure 2-D). This structural difference is targeted by the monoclonal antibody (mAb) IMAB362 (Claudiximab) developed by Ganymed Pharmaceuticals AG. It exclusively binds to CLDN18.2 [8]. Based on tissue stainings with IMAB362, it was revealed that the CLDN18.2 protein is a highly selective gastric lineage marker expressed in short-lived differentiated gastric epithelial cells in the abdominal mucosa [16]. Besides its presence in the mucosa, the expression of CLDN18.2 is strictly constrained to tumor tissue (Figure 2-E).

It was further shown that it is absent from the gastric stem cell zone [8]. Due to this selective expression, CLDN18.2 is not detectable in toxicity-relevant human tissues such as lung and liver (Figure 2-B&E), which qualifies CLDN18.2 as an 'ideal target' [16, 8].

1.2 CLINICAL VALIDATION OF IMAB362 IN GASTRIC CANCERS TARGETING CLDN18.2

The standard treatment options for patients suffering from gastric cancer are surgery, chemotherapy, and radiation therapy. Alternative treatment options for gastrointestinal stromal tumors (GIST) are two drugs from the targeted therapy class of drugs. These two drugs, Sutent® (sunitinib) and Gleevec® (imatinib mesylate), were approved in 2006 and 2008, respectively, by the US Food and drug administration (FDA).
For use in gastric cancer treatment, further targeted drugs modulating different signal transduction pathways are currently in clinical development [11]. These targeted agents include angiogenesis inhibitors and agents targeting the epidermal growth factor receptor (EGFR), cell cycle matrix metalloproteinases, cyclooxygenase-2 (COX-2), mammalian target of rapamycin (mTOR), or the proteasome [11].
Additional drugs used for the treatment of gastric cancer are the mAbs Trastuzumab, targeting HER2/neu, Bevacizumab, targeting the vascular endothelial growth factor (VEGF), and Cetuximab, targeting the epidermal growth factor receptor (EGFR). As single treatment agents, they all failed in clinical trials with gastric cancer patients [8]. However, these antibodies may be promising in combination with chemotherapy. This is presently under investigation in clinical trials, though there currently is no official approval of these drugs.
Another promising drug for a single treatment use is the mAb IMAB362, which may fill the gap in gastric cancer therapy. IMAB362 is currently in clinical phase II trials for the treatment of late-stage patients with advanced gastroesophageal cancer. Three characteristics define CLDN18.2 as an attractive and 'ideal target' for antibody based solid cancer immunotherapy: firstly, CLDN18.2 is involved in tumor-promoting cellular functions [16]. Secondly, due to its location in the outer cell membrane and its exposed extracellular loops, CLDN18.2 is easily accessible for mAb binding. Thirdly, it is expressed on numerous cancer entities but not on normal tissue, except for gastric mucosa. On normal tissue, the cellular organization prevents access of IMAB362. Therefore, IMAB362 has the potential to exclusively treat malignant tissue [16]. In summary, CLDN18.2 can indeed be regarded as an 'ideal target' and allow the development of the potent mAb IMAB362 with an excellent safety profile.
The safety of IMAB362 allows a much broader therapeutic window regarding the dosage in contrast to previously approved mAb therapies (Figure 3). Among common mAbs, the recommended dosage is often set to be functionally suboptimal to avoid conceivable side effects. Consequently, the narrow therapeutic windows only offer limited therapeutic success. The 'ideal mAbs' from Ganymed Pharmaceuticals are designed to be applicable in a wider concentration range. This results in potent anti-tumoral effects without the high risk of toxicity in patients. The safety of the IMAB362 treatment was extensively assessed in preclinical animal models. These tests raised no concerns [16]. IMAB362 is produced in CHO cells by standard recombinant expression technology [19].
In preclinical studies, IMAB362 proved to inhibit tumor growth and eradicate cancer cells by mechanisms such as complement-dependent cytotoxicity (CDC) and antibody-dependent cellular cytotoxicity (ADCC). IMAB362 binding alone leads to proliferation inhibition of CLDN18.2-expressing target cells *in vitro* and *in vivo*, as compared to control cells treated with CLDN18.2 siRNA. Thus, the mAb IMAB362 proved to operate via several separate but synergistic modes of action [20].

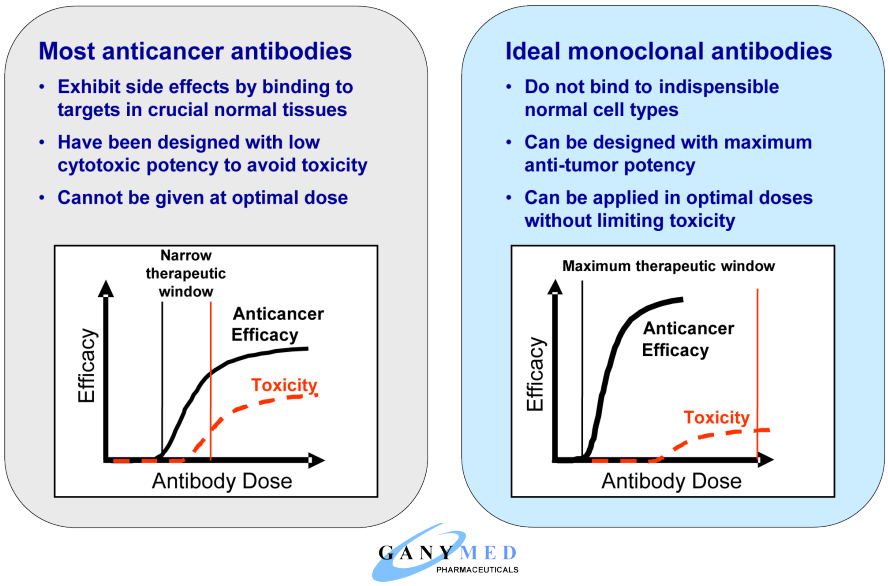

Figure 3: Pharmacological advantages of Ganymed´s ideal antibodies–IMABs
Modified from Sahin *et al.* [18].

IMAB362 is currently under investigation in clinical trials for the treatment of gastric and gastro-esophageal adenocarcinomas (clincaltrials.gov: NCT00909025 and NCT01197885, manuscripts in preparation [9]).
The determination of the maximum tolerated dose of a single infusion, as well as the evaluation of immunogenicity, pharmacokinetic, and anti-tumoral efficacy of IMAB362, were in the focus of the investigation.
Patients suffering from advanced gastric and gastro-esophageal adenocarcinoma that relapsed from previous therapy were treated in a phase I study with IMAB362. The results demonstrated an excellent safety profile and tolerability of IMAB362 [20].
In September 2010, Ganymed started a phase IIb trial (clincaltrials.gov: NCT01630083) with patients suffering from advanced adenocarcinoma of the stomach or lower esophagus. IMAB362 treatment, either as monotherapy or in combination with the chemotherapeutics Epirubicin, Oxaliplatin, and Capecitabine (EOX), is being compared to the conventional first-line treatment EOX alone [21]. Here, the safety profile and anti-tumoral effects are of major interest.
Additionally, the application of the aminobisphosphonate Zoledronic Acid (ZA) and Interleukin-2 (IL-2) in combination with IMAB362 is currently investigated in a further phase I trial [22]. ZA-treated dendritic cells (DCs) were highly effective in activating and expanding autologous human Vgamma9/Vdelta2 T cells (gammadelta-(γδ) T cells) [23–25]. These effector γδ T cells constitute less than 5 % of the peripheral blood leucocytes (PBLs) and are part of the innate immune responses against microbes, stressed cells, and tumor cells [23].
Since the antitumoral effects of γδ T cells have been demonstrated [23, 25], and several phase I-II trials that investigate the activity of ZA plus IL-2 in solid tumors [26] are ongoing, this new therapeutic approach is about to be used in combination with a IMAB362 treatment.
In order to extend the anticipated cancer therapeutic toolkit with the prospect of combinatorial therapies for CLDN18.2 (as mentioned in chapter 0), the respectable characteristics of the mAb IMAB362 were translated in this study into the promising format of a bispecific antibody.

1.3 BISPECIFIC ANTIBODIES AND T CELL-BASED CANCER IMMUNOTHERAPY

At present, two innovative strategies in cancer immunotherapy bear a high potential for success: Therapeutic antibodies (targeted therapies) and T cell-based immunotherapies. With regard to T-cell-based immunotherapies, several technologies have emerged aiming to raise T cell responses specifically against cancer. Broad interest has been aroused by the potential involvement of the patient's own immune cells, e.g. cytotoxic effector T cells, to manipulate them to trace cancer cells. These cells are capable of eliminating cancer cells by their cytolytic potential. Once T cells are activated, a mechanism of serial target cell killing is initiated. Proliferation consequently mobilizes a large number of T cells to defend the patient against cancer.
The therapeutic approach of directing effector T cells into the tumors for cancer treatment is supported by the finding of Galon *et al.* [27] and Wahlin *et al.* [28]. The authors show that higher levels of immune effector cells within the tumor tissue are beneficial for the patient´s outcome and correlate with a good prognosis. Thus, several strategies such as vaccination, adoptive T cell transfer, and administration of T cell activating or engaging pharmaceuticals were pursued to recruit them to malignant tissue and to induce onsite T cell responses.
During these intense developments, a new key player emerged that was able to bridge T cell engagement with antibody therapy, namely bispecific (bs) antibodies (Abs).
Numerous new technologies were developed to empower antibody therapeutics [29]. The aim was to maintain the target selectivity and safety profiles of the Immunoglobulin G (IgG) mAb class, but to overcome their limitations of restricted tissue penetration [30] and potential immunogenicity [31].
Several recombinant immunotherapeutic drug-formats were formed, of which the bsAb approach was one of the most promising. BsAbs were designed to redirect autologous effector T cells towards specific tumor cell lysis. The main premise is that the specific recruitment and activation of the patient's immune effector T cells to the tumor tissue enables the patient's own immune system to fight against the cancer cells [29]. This retargeting strategy finally allowed a combination of the T cell-based and antibody-based immunotherapies.
The strategy was already introduced 20 years ago, when the first bsAb was generated in 1985 as a hybrid-hybridoma antibody [32].The first bsAbs demonstrated impressive antitumoral activity [33–35], but the success of the format was hampered by issues of immunogenicity, low efficacy, and production difficulties [36].
Today's antibody engineering techniques are able to circumvent several of these obstacles. Genetic engineering facilitated numerous designs of chimeric antibody-based molecules, addressing the distinct requirements needed for each individual drug and specific therapeutic indication [37, 36, 29]. One of the most promising engineering approaches involves the design of bispecific-single-chain antibodies (bs-scAbs).They allow the revival of the concept of bispecifics, redirecting immune responses to the tumor site.

1.3.1 CONCEPT OF THE BISPECIFIC-SINGLE-CHAIN ANTIBODY FORMAT

Various different bispecific-single-chain antibody (bs-scAb) therapy approaches have been intensively studied. One of the most important innovations was the design of recombinant antibody formats composed of two antibody building blocks of the same type, the single-chain-variable-fragment (scFv).
To construct a bs-scAb, only the antigen binding part of an antibody, the variable fragment (Fv), is used. A variable fragment (Fv) consists of the variable domain of the heavy (V_H) and the variable domain of the light (V_L) chain.

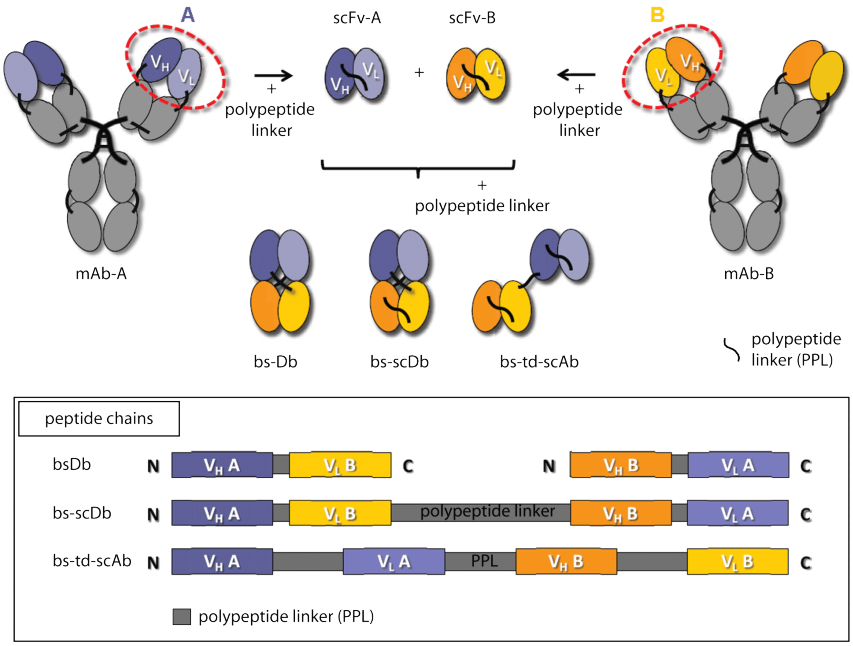

Figure 4:Scheme of two recombinant bispecific antibody formats: Diabodies and tandem-scFvs

The variable domains of two mAb A (in purple) and B (in yellow) are fused by a polypeptide linker to design the corresponding scFv-A or scFv-B. Either these scFvs assemble to bs-Db by itself or they are fused by an additional linker to bs-scDb or bs-td-scAb. In the "peptide chains" box underneath, the domain assembly for bs-Db, bs-scDb and bs-td-scAb and their polypeptide linker are shown from their N- to C-terminus. Bs indicates, bispecific; mAb, monoclonal antibody; Db, Diabody; scDb, single-chain Diabody; PPL, polypeptide linker; scFv, single chain variable fragment; V, the variable region of the heavy (H) and light (L) chain; td, tandem; scAb, single-chain antibody. Modified from Baum *et al.*[38]

The V_H and V_L domains combine with their respective constant regions to form the heavy and the light chains. The separate IgG heavy and light chains are covalently connected by several disulfide bonds, whereas the interaction between V_H and V_L is not covalent.

Instead, a recombinant Fv is engineered as a single polypeptide chain, termed scFv, in which a peptide linker fuses the C-terminus of one V_H domain to the N-terminus of the V_L domain [39, 40]. The application of these recombinant scFv techniques has revolutionized the entire bsAb field. Especially with the help of scFvs – used as building blocks – several recombinant bsAb formats were developed.

Prominent examples are bispecific Diabodies (bs-Db) or bispecific-tandem-single-chain-antibodies (bs-td-scAb). Both formats combine two scFvs derived from the variable domains of antibody A and antibody B specific for two different antigens (Figure 4-scFv-A & scFv-B). The bispecific Diabody format comprises two dissimilar scFvs (V_{HA}-V_{LB}, V_{HB}-V_{LA}), but each chain itself is incapable of binding the respective antigens.

The assembly of a heterodimer with two functional antigen-binding sites is promoted by pairing of the V_H domains of the first polypeptide chain with the V_L domains from the second scFv [41]. The compact format was termed Diabody (bs-Db) [42] (Figure 4-bs-Db). Its peptide chain design from the N-to the C-terminus of both scFvs is depicted in the box of Figure 4. The Diabody format can be further stabilized by fusing both scFvs covalently using a third polypeptide linker, which is then a bispecific-single-chain Diabody (Figure 4-bs-scDb).

To generate the second format, a bs-td-scAb, a longer linker of 13-30 AA [43] is introduced between the V_H and V_L in contrast to the short linker (≤ 12 AA) used in Diabodies. The specifically designed long linker of bs-td-scAb allows proper refolding, optimal positioning, and rotational flexibility of the binding domains. This may be needed for simultaneous binding to two antigens positioned on cell

membranes of two distinct cells [44]. An additional third linker fuses both scFvs to one polypeptide chain leading to the formation of a bs-td-scAb (Figure 4 bs-td-scAbs) [45].

1.3.2 DIFFERENCES IN PEPTIDE- AND BS-SCABS-MEDIATED INDUCTION OF T CELL ACTIVATION

As described above, immunotherapies aim to enhance the patient's immune response against cancer by utilizing the T cells' mode of action [46].
'Regular T cell activation' and cytotoxic mechanisms of T cells are initiated by the specific recognition of a major histocompatibility complex (MHC)-presented antigen-peptide via the T cell receptor (TCR; Figure 5-A) [50].
The formation of the peptide-mediated cytolytic synapses and the initiation of the cytotoxic T cell program take place only after MHC dependent T cell activation by an APC, which is considered the 'regular T cell activation'. Accordingly, the 'regular process' is hereafter termed 'peptide-mediated T cell activation'.
In order to fully activate T cells during the peptide-mediated T cell activation, additional costimulatory signals such as cytokines or B7 (CD80, CD86), that are offered by peptide-bearing antigen presenting cells (APCs), are moreover necessary (Figure 5-A).
In order to evade the natural cytotoxic T cell responses, cancer cells can develop multiple immune evasion mechanisms, such as down-modulation of MHC, resistance to induced apoptosis, inhibition of T cell activity via expression of NK cell inhibitory receptors, and a tumor environment not permissive to T cell infiltration [47–49]. This often results in an immune tolerance of the tumor by the patient's inherent immune system.
Thus, new ways have to be found to activate cytotoxic T cells regardless of their 'regular activation program'. The central goal of the bispecific anti-tumor approach is to break the immune tolerance of the tumor even in the absence of MHC presentation and TCR contribution.
While the processes of peptide-mediated and bs-scAbs-mediated T cell activation are similar, they do vary markedly in their induction.
In contrast to the peptide-mediated T cell activation, the induction of bs-scAb-mediated T cell activation occurs independent of both the specific binding of TCRs to MHC I/II [51, 52] and the presence of costimulatory signals such as CD28 or B7-ligand [53]. This independence from co-administration of costimulatory agents is an attractive feature of bs-scAb-mediated cancer immunotherapies.
Most other T cell-retargeting-antibody-therapies were hampered by their need for T cell co-activation, which has been circumvented by the bs-scAbs' mode of action, which will be explained in more detail in chapter 1.3.3.
Consequently, the ability to raise and maintain a tumor-specific T cell response is still a challenge, but the recruitment and activation of T cells in the tumor by bs-scAb is one strategy to finally reach this aim.
Hence, bs-scAbs when implemented alone or in combination with current cancer treatments might enhance therapeutic achievements. They can be described as a navigator to help the T cells to find, infiltrate, and eliminate the cancer in a MHC and costimulatory molecule independent way;
simply bypassing tumor immune evasion strategies, e.g. MHC down regulation, which tend to limit existing T cell therapies [54].

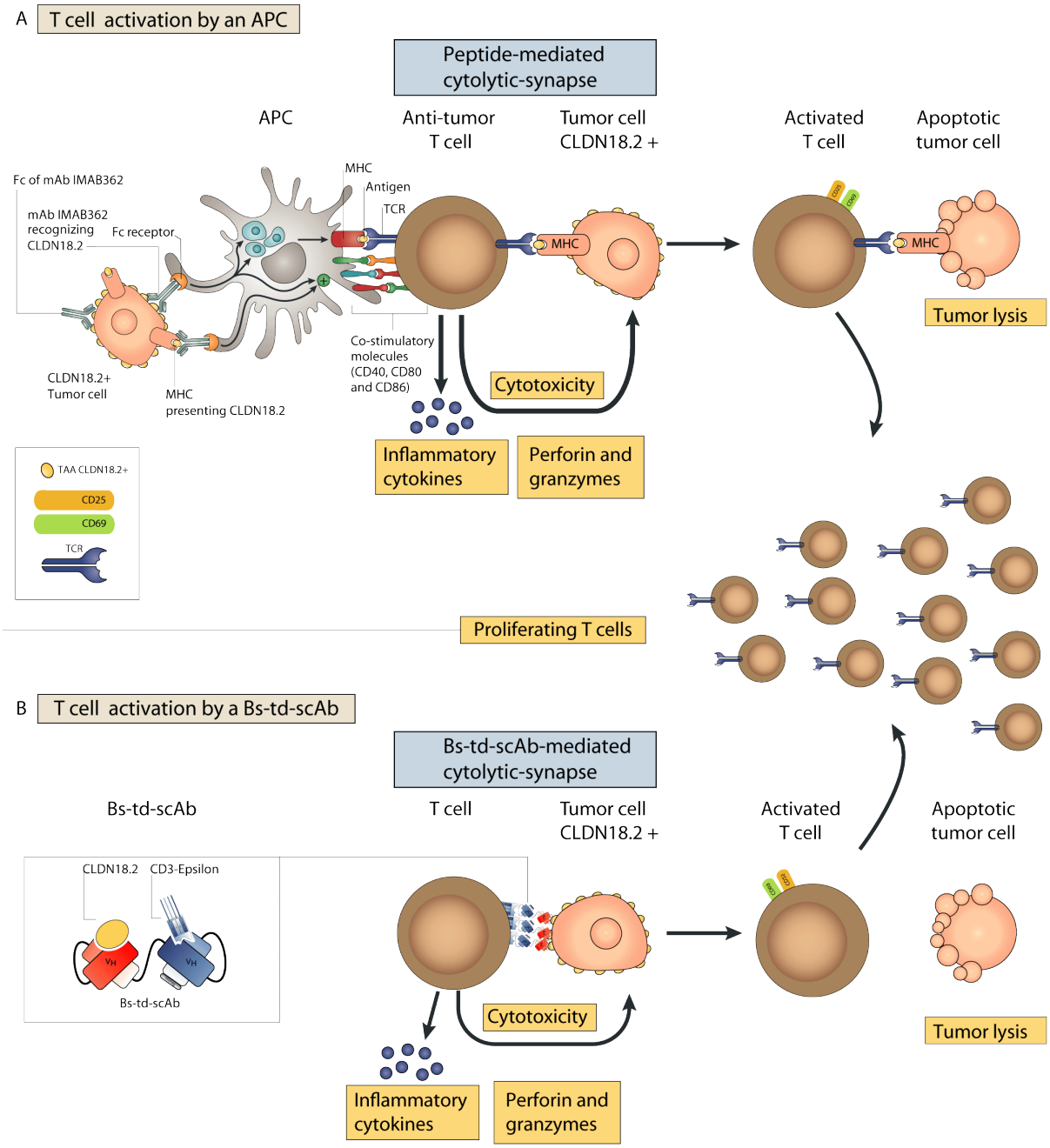

Figure 5: Peptide-mediated versus bs-scAb-mediated T cell activation

(**A**) Targeted agents can boost the priming of antigen presenting cells (APC) and the activities of tumor-specific T cells. Monoclonal antibodies such as IMAB362 (anti-CLDN18.2) bind to tumor cells and promote phagocytosis. Tumor cell phagocytosis is driven by the recognition of the crystalline fragment (Fc) of IMAB362 through the APC´s Fc receptor, which consequently increases the presentation of tumor antigens by APCs. This affects APC-mediated priming of T cells. Fc receptor-mediated opsonization also enhances the expression of co-stimulatory molecules such as CD40, CD80, and CD86 on the APC surface, promoting T cell activation. T cell activation leads to tumor cell lysis via the perforin and granzyme cytotoxic pathway. Activated T cells proliferate to generate a large pool of enduring anti-tumor T cells, even after completion of immunotherapies.
(**B**) T cell activation by bs-td-scAb results from the clustering of CD3 epsilon (CD3ε) on the surface of T cells. The bs-td-scAb binds simultaneously CD3ε and the TAA CLDN18.2 on the surface of the target cell, activating the T cells. Activated T cells lyse the tumor cell via the perforin and granzyme cytotoxic pathway and proliferate in order to generate more T cells. This process is initiated independently of both the specific binding of TCRs to MHC I/II or the presence of costimulatory signals such as CD28 or B7-ligand. APC indicates antigen presenting cell; Bs-td-scAb, bispecific –tandem-single-chain-antibody; CD3ε, CD3 epsilon; Fc, fragment crystalline; MHC, major histocompatibility complex; TCR, T cell receptor; Modified from Vanneman *et al.* [1].

1.3.3 MODE OF ACTION OF BS-SCABS

Bs-scAb formats are designed to engage T cells via binding to their CD3 epsilon (CD3ε) chain and then recruiting them to malignant tissue. CD3ε is a subunit of the TCR complex on the surface of the T cell usually involved in the regular T cell activation process. Monovalent binding to the CD3ε does not initiate T cell activation [55]. Recruited T cells are solely activated in the presence of a defined TAA. Bs-scAb-mediated T cell activation is therefore a safe and specific process.
Upon multivalent dual ligand binding, a clustering of the CD3 complex occurs. This initiates a conformational change in the CD3-epsilon (CD3ε) subunit, which is thought to be a central mechanism within the T cell activation process [56]. Thus, only the linkage to the TAA by bs-scAbs leads to clustered CD3-receptor complexes on the surface of T cells, which induces their activation [56, 44]. In this way, the bs-scAbs mimic the effects of natural MHC class I-peptide interaction and triggering of the TCR [57].
Indeed, from that point bs-scAbs-mediated T cell activation continues like the 'regular cytotoxic program' of T cells. As stated before, there is no difference in the remaining process of T cell activation and cytotoxic program, induced by either peptide- or bs-scAb. Both activation processes induce a cascade of signals that are transmitted into the nucleus of the T cell, initiating several processes on site reviewed by Smith-Garvin *et al.* [58]. Consequently, T cells redirect their cytotoxic potential towards the cancer target cells (Figure 5-B).
T cell activation comprises several detailed aspects that can be detected on the molecular level. Three of these methods are of particular interest for this study and will therefore be highlighted in the following paragraphs.

ACTIVATION MARKERS

It is possible to differentiate between three stages of activation: The early, the intermediate, and the late activation stages. Early activation is shown by T cells that only express the marker CD69 on their surface 1 h post-activation,CD69+/CD25-[2] [59]. CD69 is the human C-type lectin leukocyte receptor involved in T cell proliferation [60]. Its expression peaks around 20 h after the initiation of T cell activation [59].
The second stage of T cell activation is indicated by the upregulation of the cell surface marker CD25, which is a synonym for the alpha chain of the Interleukin-2 (IL-2) receptor. Its accessibility for mAb binding increases throughout late T cell activation [61, 62]. Advanced T cell activation starts after 24 h [59] and is characterized by the presentation of both early and late activation markers on the cell surface (CD69+/CD25+).
Finally, the late stage of T cell activation is defined by the sole presentation of CD25 (CD25+/CD69-) and is expected between 48-72 h after activation [59]. Upregulation of activation markers can easily be analyzed using flow cytometry (Figure 5) [59].

GRANZYME B AND PERFORIN CYTOTOXIC PATHWAY

During the priming of T cells, cytotoxic T cells are activated and so-called cytolytic synapses are formed between target and T cells [52], leading to the initiation of the granzyme/perforin cytotoxic pathway [63].
Thus, cytotoxic T cells induce target cell elimination by the release of the contents of lytic granules, resulting in the lysis of the target cells. Lytic granules are secretory vesicles containing the pore-forming protein perforin and the serine protease Granzyme B [63]. Both are effector molecules used

[2] CD designates cluster of differentiation

by T cells to eliminate infected, degenerated, or malignant cells. In CD8+ effector T cells, the effector molecules are pre-produced and stored in lytic granules awaiting the activation of the cytotoxic T cells [64]. CD4+ T cells do not store the molecules; therefore, they first need to produce the content of lytic granules.
Upon T cell stimulation, a further increase in the production of the lytic substance Granzyme B in cytotoxic T cells is common. These newly produced effector molecules are aimed either at refilling secretory vesicles or for a direct release into the cytolytic synapse [65]. After formation of the cytolytic synapse with the target cell, lytic granules migrate to the site of contact. Both molecules are released via exocytosis into the cytolytic synapse [66, 67].
By a not yet fully understood mechanism, these molecules are capable of penetrating the membrane of the target cells in a process often termed 'pore formations'. After entering through these newly formed pores, Granzyme B is able to activate intracellular caspases, and thereby induce the apoptosis of the cancer target cells [68]. Thus, the lysis of target cells indirectly indicates the activation of T cells and their cytotoxic response against cancer. While they pass through the full activation process, they can simultaneously trigger serial target cell killing [69].The upregulation of perforin and Granzyme B can be measured via flow cytometry.

T CELL PROLIFERATION

Another method to assess T cell activation is the measurement of T cell proliferation. T cells release the T cell growth factor IL-2 that has an autocrine effect on T cell proliferation: upon upregulation of CD25, all subunits of the high affinity IL-2 receptor assemble and are capable of binding to the secreted IL-2, initiating in turn the T cell proliferation pathway. CD4+ as well as CD8+ T cells are involved in this activation process and consequently clonally expand. Subsequently, proliferation generates an abundance of polyclonal activated effector T cells around the target cells (Figure 5-A), enabling potent cancer cell elimination even at initially low effector to target ratios [70]. T cell proliferation can also be assessed by flow cytometry.

1.3.4 ADVANTAGES OF THE BS-SCABS OVER THE BS-IGG FORMAT

The efficacy of conventional bs-IgG formats was primarily limited by suboptimal T cell recruitment and issues with large-scale production, purification, immunogenicity, suboptimal activation and the need for an abundance of T cells for efficient cancer cell lysis. The new class of bs-scAbs have addressed these issues and have several advantages when compared with bispecific-IgG (bs-IgG) formats.
One factor that limited the biological activity of most tumor-directed bs-IgG was the need for high concentrations of bsAb for efficient target-cell lysis in patients. However, high yields could not be realized because of limited drug production efficiencies.
Recombinantly designed bs-scAbs overcame the shortcomings of conventional bs-IgG productions. For example, the problem of homodimer formation was elegantly circumvented by bs-scAbs, as they are expressed on a single polypeptide chain [37]. The production of these proteins either in *E. coli* (Diabodies) or in mammalian cell culture (bs-td-scAbs) led to satisfactory yields of the desired protein as reported by Kufer *et al.* [71]. Affinity purification by a poly-histidine tag attached to the C-terminus and size exclusion chromatography enabled preparation of functional bs-scAbs.
Furthermore, drug concentrations needed for clinical efficacy with bs-scAbs are much lower than with bs-IgGs. Consequently, the required amount of protein for bs-scAbs is accordingly lower than reported for bs-IgGs. For example, in the case of non-Hodgkin´s lymphoma (NHL), the serum levels required for the bs-scAb Blinatumomab were five orders of magnitude lower for a successful clinical response compared to the mAb Rituximab [29]. Besides, the use of low drug doses may result in

fewer elicited immune responses against these bs-scAbs, which might be a further benefit of this format.
Regarding the lack of the Fc-region, bs-scAbs are less toxic, as no crosslinking with other cells carrying the Fc-receptor occurs [44]. Due to the small size of e.g. bs-td-scFvs, which have a size of approximately 60 kDa–about a third of the size of a bs-IgG–serum half-life is relatively short, which also limits side effects that can be provoked by these highly active molecules.
Certainly, the rapid clearance of bs-scAbs from the body also has disadvantages regarding the application frequency in a therapeutic setting. On the other hand, their small size should allow an efficient penetration into malignant tissues [54]. At low concentrations it may result in better clinical efficiencies than observed for bs-IgGs. In addition, its small size ensures a close proximity between T cell and target cell epitopes, which enables a highly conditional T cell activation [72]. Activated T cells redirect their cytotoxicity against TAA+ target cells without any requirement for pre- or costimulation of effector T cells.
This mode of action improved the effectiveness of bsAb formats particularly at very low effector to target ratios [71]. In summary, bs-scAbs are capable of overcoming several of the drawbacks reported for bs-IgG formats, and therefore allow a revival of the bs-Ab class in cancer therapeutics.

1.3.5 BS-SCABS IN CLINICAL TRIALS

Three different bs-scAbs are currently the most promising formats, while two of them are already undergoing extensive investigations in the pre-clinic and clinical trials reviewed by May *et al.* [29] and Müller *et al.* [73]. These three bs-scAb formats are termed BiTE, DART, and TandAbs (Figure 6).
The tetravalent tandem antibodies (TandAbs) from Affimed Therapeutics AG are the best-known representatives of the bs-Db format in clinical trials [30]. Two bs-scDbs actually assemble into a 110 kDa TandAb that contains two binding sites for each antigen. Due to their size, TandAbs have a longer serum half-life compared with heterodimeric Diabodies or bs-td-scAbs [74].
The clinical candidate AFM13 targets CD30 and CD16A (or FcγRIIIa) for the selective activation of natural killer cells (NK), dendritic cells (DC), and macrophages [75]. A well-tolerated safety profile was determined for AFM13 in a phase I trial in 2010. However, a comparison of bispecific T cell engagers (BiTEs) and TandAbs shows that the BiTE format has a 1,000-fold higher efficacy in B cell lysis [76].
The second promising format is a dual affinity-retargeting antibody (DARTs) from MacroGenics. DARTs belong also to the class of single-chain antibodies, which actually is a disulfide-linked bs-scDb. To each scFv either a C_{kappa} domain or the hinge region of a natural IgG1 antibody is fused, which allows a disulfide bridge formation.

Table 1: Tumor associated antigens targeted by bs-td-scAb

TAA	Tumor associated antigen
CD19	B-lymphocyte antigen CD19
CD20	B-lymphocyte antigen CD20
CEA	carcinoembryonic antigen
CSPG4	chondroitin sulfate proteoglycan 4
EGFR	epidermal growth factor receptor
EpCAM	epithelial cell adhesion molecule
EphA2	ephrin type-A receptor 2 tyrosine kinase
HER2neu	human epidermal growth factor receptor 2
MUC-1	mucin-1
PSMA	prostate-specific membrane antigen

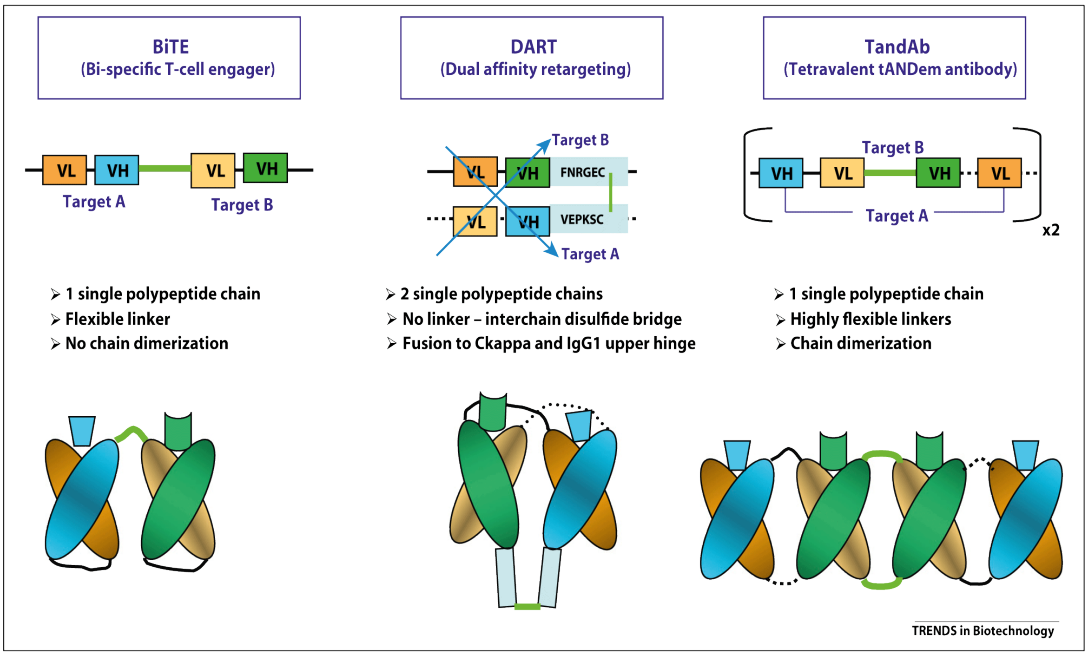

Figure 6: Schematic representations of bispecific single-chain-based scaffolds.
(**Top**) The linear drawings show heavy and light chain variable domain concatenations for three bispecific antibody formats: BiTEs, DARTs, and TandAbs. (**Bottom**) Pictures correspond to 3D rearrangement of variable heavy and variable light chains to create the different antigen binding sites. (Target A in blue); (target B in green). Modified from Wurch et al. [30].

Although *in vitro*, the CD19 and CD3 DART molecule outperformed the corresponding BiTE; there is so far no DART in clinical development. The clinical efficacy of DARTs still has to be proven.
The BiTE format from Micromet AG/Amgen representing the bs-td-scAb format has been evaluated by its particular success in clinical trials [36]. BiTEs targeting the following common cancer antigens, which are summarized in Table 1, have already been generated: CD19, EpCAM, PSMA, MUC-1, EGFR, HER2, CD20, CSPG4, EphA2, CD33, and CEA.
In the case of the BiTE targeting CD19 (Blinatumomab), the variable domains of the scFv binding the invariant CD3ε chain of the TCR complex were derived from the mouse mAbs TR66. With all other BiTEs, the variable domains derived from the mouse mAb L2K. The latter was preferred by Micromet because of its crossreactivity with cynomolgeous and human CD3ε. TR66 can only bind human CD3ε.
In addition, the scFv derived from L2Kwas deimmunized by deleting potential T cell epitopes via phage display selection. Accordingly, the new scFv was termed diL2K. Micromet protected this new procedure of deimmunized scFv generation against anti-CD3ε by patent law. Thus, diL2K and this scFv generation procedure can only be used by Micromet/Amgen, in contrast to the freely accessible scFv derived from TR66.
By targeting CD3ε, the BiTE engages T cells [77] that are, besides NK-cells, considered the most potent cells within the immune system for killing malignant cells [78].
BiTEs have to be expressed in eukaryotic cells [79]. Expression of e.g. Blinatumomab in *E. coli* resulted in only nonfunctional protein [80]. The final bsAb protein has a molecular mass of about 55 kDa. This is small enough to allow good penetration of tumor tissue as it is known that molecules smaller than mAbs distribute more homogenously in tumor tissue [81].
However, these bs-td-scAbs are just large enough not to be cleared too rapidly by the kidney. The estimated half-life of this protein in humans is 2 h [44]. Thus, it has to be administered continuously to guarantee a permanent distribution of the antibody within the body.

Several clinical trials with continuous application by portable mini-pumps of the bs-td-scAb proved the feasibility and efficacy of this approach [44].
The most clinically advanced BiTE is Blinatumomab (targeting CD19), which is able to activate T cells *in vitro* at low concentrations in the picomolar range. The first clinical responses occurred in non-Hodgkin's lymphoma (NHL) patients treated with a dose of 15 $mg \times m^{-2}$ per day. Their serum levels were about 10,000-fold below the serum levels reported for the treatment with the mAb rituximab at a dose of 375 $mg \times m^{-2}$ per week in NHL patients [82,30]. The high efficacy at such low concentrations might explain the promising results in several clinical trials of lymphoma and leukemia patients, who still remain in remission two years after treatment [44].
This remarkable efficacy can be related to the bs-td-scAb induced serial target cell lysis provoked by T cells after activation. The proliferation of T cells, leading to an abundance of effector cells at the site of activation, supports the efficient killing. Patient treatment with Blinatumomab was well tolerated and all occurring adverse events were fully reversible [57].
Apart from hematologic malignancies, a BiTE targeting EpCAM (MT110) is under investigation in a Phase I study with patients suffering from advanced EpCAM+ solid tumors. To control the adverse events, dexamethasone was added to the treatment [83], resulting in a stable disease in 38 % of the patients [30].
This bs-td-scAb treatment was slightly less effective than the treatment of lymphomas with Blinatumomab, but as treatment of solid tumors is considerably more complicated, the results still appear promising. There are many differences in the tissue of solid tumors and normal tissue regarding the vasculature, interstitial pressure, cell density, tissue structure, and in the composition of the extracellular matrix [84].
These differences result in a prolonged retention of macromolecules in the vasculatures and a reduced diffusion of macromolecules into the tumor tissue [37]. This also holds true for T cells recruited by the BiTEs. Thus, Wurch *et al.* [30] hypothesized that these mechanisms might have permitted less infiltration of effector cells into the malignant tissue, causing a less potent response as in the lymphoma scenario.
Another challenge is given by the target EpCAM. EpCAM is known not to be an 'ideal target' as its expression is not completely restricted to cancer tissue, which in turn confines the range of dosing [85]. For example, recommended doses of EpCAM targeting mAb ING-1 (IgG class) were only 0.10 $mg \times kg^{-1}$ to exclude the severe side effect of pancreatitis in patients caused by higher concentrations of this antibody in phase I trials [86]. Accordingly, to judge the potency of this bsAb class, further results from targeting solid tumors are awaited.

A bs-td-scAb-specific for an 'ideal target' such as CLDN18.2 might change the current setting entirely. Targeting only cancer cells might allow the usage of a high antibody dose, probably resulting in a high efficacy of the bsAb.
Consequently, this auspicious bs-td-scAb format was used for the approach to develop bs-td-scAbs termed BiMABs (Bispecific ideal monoclonal antibodies) for the treatment of gastroesophageal adenocarcinomas. They can bispecifically bind the 'ideal target' CLDN18.2 on the surface of TAA positive target cells and the CD3ε chain on the T cell effector cell surface.

1.4 A NEW STRATEGY FOR DRUG APPLICATION– RIBOMABS– IVT-RNAS ENCODING BIMABS

Drug production, especially of recombinant protein, is considered time and cost intensive. Thus, alternative ways were explored to rapidly produce, administer, and test our bs-scAbs.
Pharmacologically optimized synthetic messenger RNA (mRNA) has recently emerged as an attractive and promising alternative for established therapeutic agents such as proteins [87].
In vitro transcribed-RNA (IVT-RNA) is designed to mimic the function of naturally occurring mRNAs. It was shown several years ago that administered IVT-RNA is translated into the encoded protein after transfection [88, 163, 189]. The protein synthesis occurs in the cytoplasm utilizing the protein synthesis machinery of the target cell [89, 90]. By this way, the patients' cells are engaged to produce the desired drug substances themselves.
Consequently, IVT-RNA application instead of protein delivery can be a fast and affordable alternative to the complex, laborious and time-consuming procedure of GMP protein production, purification, and quality assurance [91]. Since IVT-RNA production is less elaborate and can easily be upscaled [92], it is feasible to deliver IVT-RNA for cellular uptake in therapeutic settings.

The use of IVT-RNA in a bs-td-scAb context may furthermore be ideal to overcome a major drawback of bs-td-scAb protein therapy, i.e. their short *in vivo* bioavailability. Due to renal clearance, the normal biological half-life of the 55 kDa small bs-td-scAb ranges between minutes and two hours [44]. In order to reach a steady level of protein within the organism during a protein-injection-therapy, frequent or continuous application of protein drug would be required.

Using IVT-RNA bs-td-scAbs, termed RIBOMABs, offers the possibility of improving this setting. The pharmacologically effective dosing of RIBOMABs might lead to a sustained expression of BiMAB protein over a certain timeframe. A sustained translation of IVT-RNA of up to several days *in vivo* has already been described by Sohn *et al.* [93].
As the BiMAB proteins are produced by the organism itself, the drug's immunogenicity may be reduced, which would lead to a general improvement in the tolerance and bioavailability of the protein. Within this time slot of sustained expression, the continuous translation of IVT-RNA can result in an anticipated constant level of the drug, as it continuously compensates the fast renal clearance of the small bispecific antibodies.
In this manner, the IVT-RNA approach might improve the pharmacokinetics of bs-td-scAbs without the need for frequent injections that are usually performed for small protein therapies. This in turn should drastically increase the patients' quality of life. Moreover, a conceivable enhancement in the therapeutic effect by the constant level of the drug is expected.
Besides this still prospective attempt to improve the therapeutic setting, there is another major advantage of IVT-RNA application in the process of bs-td-scAbs development.
The translation of IVT-RNA enables a direct evaluation of the bsAbs' function, omitting the time-consuming protein production. Moreover, this new technique is a valuable feature to quickly screen for suitable bsAb candidates. Transfected cells are immediately assessed in cytotoxicity assays in order to directly evaluate the potency of bsAb candidates, just as described for bs-td-scAb proteins.

To the best of our knowledge, this is the first report describing the development of IVT-RNA based bs-scAbs. Once this technology is matured, the mentioned advantages of a therapeutic IVT-RNA approach will possibly outweigh those of the common and established approach using protein drugs.

1.5 OBJECTIVES OF DOCTORAL DISSERTATION

The advances in the field of bispecific biotherapeutics for the treatment of cancer have been demonstrated with the market approval of the bsAb Catumaxomab (TRION Pharma GmbH) in 2009, and by the promising results of clinical trials with the bs-td-scAb Blinatumomab (Micromet AG/AMGEN).
This thesis was intended to add to the success of bsAbs with the development of a potent recombinant bispecific-tandem-single-chain antibody, termed "BiMAB," that selectively targets the strictly tumor-associated antigen CLDN18.2 and simultaneously recognizes CD3ε of the TCR complex.
To qualify as an efficient cancer immunotherapeutic agent, the BiMAB format had to meet certain requirements. Briefly, these involved the redirection of T cells towards the CLDN18.2 positive tumors, the subsequent activation of endogenous T cells in close proximity of the malignant cells, and in consequence, the mediation of T cell effector functions to eliminate tumor cells independent of costimulatory signals, antigen presentation and MHC restriction. Accordingly, the anti-tumor antibodies should be capable of both bypassing the complex T cell regulation and breaking the immune tolerance of the tumor.
One of the major aims of this thesis was the evaluation of four different well-known anti-CD3-mAbs, to identify an anti-CD3-scFv suitable for the BiMAB setting. Furthermore, the impact of the consecutive order of the two scFvs on the effectiveness of the BiMAB variants was addressed in this study, as the scFvs sequence can affect BiMAB expression and performance.
To generate the required material, a modular recombinant antibody-engineering platform was designed to obtain a variety of CLDN18.2-specific BiMABs. This study describes the *in vitro* characterization and selection procedure of those engineered BiMABs. Apart from the highly tumor-specific efficacy of the BiMABs, affinity and sensitivity were important criteria to be considered in the selection process. All recombinant proteins were produced in mammalian cells, purified via immobilizing metal affinity chromatography, characterized with biochemical techniques, and functionally tested *in vitro*. Particular parameters of interest were the observation of a cytolytic synapse formation, T cell activation, and cytotoxicity towards TAA positive target cells. The above-defined criteria enabled us to narrow down the selection of candidates to one preferred BiMAB prototype with therapeutic efficacy. Only this BiMAB prototype was characterized in depth, including the evaluation of the *in vivo* BiMAB protein efficacy in a subcutaneous xenograft tumor mouse model.
Besides protein-based therapeutics, the development of nucleic acid-based therapeutics has raised remarkable interest in the past few decades as a new category of biologics. IVT-RNA recently emerged from this category as an attractive and promising tool for non-viral gene delivery, due to its several advantages over DNA therapeutics. Considering this, an *in vitro* proof of concept for the application of *in vitro* transcribed (IVT) RNA-BiMABs, termed RIBOMABs, was attempted after testing the applicability of the BiMAB as protein therapeutics. The primary advantage of the innovative RIBOMAB therapy is the circumvention of expensive and time-consuming protein production and purification methods.
The CLDN18.2-specific BiMAB strategy creates a high potential of raising tumor-specific T cell responses during the treatment of solid tumors. The challenges of bispecific antibodies, such as large-scale protein production and the cost-effective purification, might be elegantly solved by this novel RIBOMAB application approach.

2 MATERIALS & METHODS

2.1 MATERIALS

All manufacturers and their location of the company are mentioned in this part of the thesis either in the tables or within the text. Therefore, they will not be mentioned in the remaining main chapters of this work. Abbreviations are defined in Table 21 in the appendix.

2.2 HARDWARE

Table 2: Hardware

Hardware designation	Hardware manufacturer
ABI Prism 7300 Real Time PCR System	Applied Biosystems/Life Technologies GmbH, Darmstadt, Germany
Äkta Purifier 10 FPLC system	GE Healthcare Life Sciences, Munich, Germany
Analytical balance	Sartorius AG, Göttingen, Germany
flow-cytometry Aria cell sorter	BD Biosciences, Heidelberg, Germany
Bath circulator Julabo F10	Julabo Labortechnik, Seelbach, Germany
BioAnalyzer 2100	Agilent Technologies, Palo Alto, USA
Cell incubator	Heraeus Instruments, Hanau, Germany
Centrifuge 5810,Multifuge-X1R,-X3R	Heraeus Instruments, Hanau, Germany
Centrifuge Mikro 22R	Hettich, Tuttlingen, Germany
Clean bench Bio wizard Golden GL-200	Kojair, Vilppula, Finland
CO2 Incubator	Binder, Tuttlingen, Germany
counting chamber Neubauer	LO - Laboroptik GmbH, Bad Homburg, Germany
Duo Cycler	VWR International, Darmstadt, Germany
Electro Square Porator ECM 830	BTX Instrument Division, Harvard Apparatus, Inc. Holliston, MA ,USA
flow-cytometry Calibur	Becton Dickinson, Heidelberg, Germany
flow-cytometry Canto II	Becton Dickinson, Heidelberg, Germany
Fluorescence microscope DM RXA	Leica Microsystems, Wetzlar, Germany
Gel documentation/UV system	Intas, Göttingen, Germany
Gene Pulser II	Bio-Rad Laboratories, Munich, Germany
Heating magnetic stirrers ARE	VELP Scientifica, Usmate, Italy
Horizontal electrophoresis s. (wide) Mini Sub-Cell GT	Bio-Rad Laboratories, Munich, Germany
Horizontal electrophoresis system Sub-Cell GT/Model90	Bio-Rad Laboratories, Munich, Germany
HTP equipment Starter Set A	Macherey-Nagel, Düren, Germany
Hydro Flex plate washer	Tecan Austria GMBH, Grödig, Austria
Image Quant LAS 4000	GE Healthcare Europe GmbH, Freiburg, Germany
Inverted microscope Wilovert	Hund, Wetzlar, Germany
Luminescence reader infinite M200	Tecan, Crailsheim, Germany
Membrane vacuum pump	KNF Neuberger, Freiburg, Germany
Membrane vacuum pump MPC 301 Zp	Ilmvac, Ilmenau, Germany
Microbiological incubator	Heraeus Instruments, Hanau, Germany
Microbiological incubator INCU-Line 115	VWR International, Darmstadt, Germany
Microscope Wilovert S	Hund, Wetzlar, Germany

Hardware designation	Hardware manufacturer
Microwave Inverter	Panasonic Deutschland, Hamburg, Germany
Mini Cell X Cell Sure Lock	Invitrogen Life Technologies GmbH, Darmstadt, Germany
Mini shaker MS2	IKA Labortechnik, Staufen, Germany
Mini Shaver	Philips, Eindhoven, Netherlands
Multifuge X1	Heraeus Instruments, Hanau, Germany
Multifuge X3R	Heraeus Instruments, Hanau, Germany
Multipette® plus	Eppendorf, Hamburg, Germany
Multitron Shaking incubator	Infors AG, Bottmingen, Swiss
NanoDrop® 1000 UV-Vis Spectrophotometer	PEQLAB Biotechnologies, Erlangen, Germany
NanoDrop® 2000c UV-Vis Spectrophotometer	PEQLAB Biotechnologies, Erlangen, Germany
Nikon EclipseTi / T100-F	Nikon GmbH Mikroskope, Düsseldorf, Germany
NucleoVac 96 Vacuum Manifold	Macherey-Nagel, Düren, Germany
Pico 21 Centrifuge	Heraeus Instruments, Hanau, Germany
Power supply Power Pac HC	Bio-Rad Laboratories, Munich, Germany
QIAvac 24 Plus Vacuum Manifold	QIAGEN, Hilden, Germany
QIAxcel System	QIAGEN, Hilden, Germany
Steritop Filter Units	Merck Millipore, Billerica, MA, USA
Table centrifuge Mikro 22R	Hettich, Tuttlingen, Germany
Thermo cycler T3	Biometra, Göttingen, Germany
Thermo mixer compact/comfort	Eppendorf, Hamburg, Germany
Titramax 1000+ Incubator	Heidolph Schwabach, Germany
Ultrospec 2100 pro Spectrophotometer	Amersham Pharmacia, Uppsala Sweden
Vortex Wizard	VELP Scientifica, Usmate, Italy
Vortexer VF2	IKA Labortechnik, Staufen, Germany
Vortex-Genie 2	Scientific Industries, New York, USA

2.2.1 CONSUMABLES

Were mainly used from Nunc (Wiesbaden, Germany), Costar, (New York, USA), Greiner Bio one, (Essen, Germany), Becton Dickinson, (Heidelberg, Germany), SARSTEDT AG & Co. KG (Nümbrecht, Germany), Thermo Scientific, Pierce (Bonn, Germany), QIAGEN, (Hilden, Germany), Invitrogen Life Technologies GmbH (Darmstadt, Germany).

2.3 CHEMICALS AND REAGENTS

Were mainly used from Sigma-Aldrich Chemie (SAC) Holding (Taufkirchen, Germany), AppliChem (Darmstadt, Germany), Merck (Darmstadt, Germany), Invitrogen Life Technologies GmbH (Darmstadt, Germany), Thermo Scientific (St. Leon-Rot, Germany), Roth (Karlsruhe, Germany).

2.3.1 RESTRICTION ENZYMES

All restriction enzymes used were produced by New England Biolabs (Frankfurt, Germany) or Thermo Scientific Fermentas (St. Leon-Rot, Germany).

2.3.2 KITS

Table 3: Kits

Kits designation	Kits manufacturer
Fixation/Permeabilization Solution Kit	BD Biosciences, Heidelberg, Germany
Magnetic activated cell sorting (MACS) CD4+ T Cell Isolation Kit human	Miltenyi Biotec, Bergisch Gladbach, Germany
Magnetic activated cell sorting (MACS) CD8+ T Cell Isolation Kit human	Miltenyi Biotec, Bergisch Gladbach, Germany
Magnetic activated cell sorting (MACS) Pan T Cell Isolation Kit II human	Miltenyi Biotec, Bergisch Gladbach, Germany
Magnetic activated cell sorting (MACS) Pan T Cell Isolation Kit II murine	Miltenyi Biotec, Bergisch Gladbach, Germany
MEGA clear Kit	Ambion, Austin, USA
MinElute PCR Purification Kit	QIAGEN, Hilden, Germany
mMESSAGE mMACHINE T7 Ultra Kit	Ambion, Austin, USA
NucleoSpin 96 Plasmid	Macherey-Nagel, Düren, Germany
NucleoSpin Plasmid Mini Kit	Macherey-Nagel, Düren, Germany
NucleoSpin8 Plasmid	Macherey-Nagel, Düren, Germany
Pierce ECL Western Blotting Substrate	Thermo Scientific, Pierce, Bonn, Germany
Qiafilter Plasmid Maxi (Midi) Kit	QIAGEN, Hilden, Germany
QIAGEN Plasmid Plus Midi/Maxi/Mega Kit	QIAGEN, Hilden, Germany
QiaQuick Gel Extraction Kit	QIAGEN, Hilden, Germany
Qiaquick MinElute PCR Purification Kit	QIAGEN, Hilden, Germany
QiaQuick PCR Purification Kit	QIAGEN, Hilden, Germany
RNeasy Mini Kit	QIAGEN, Hilden, Germany
Super Signal West Femto Chemiluminescent Substrate	Thermo Scientific, Pierce, Bonn, Germany
SYBR® Green Real-Time PCR Master Mix	Invitrogen Life Technologies

2.3.3 ANTIBODIES AND ENZYME-CONJUGATES

Applied antibodies were distributed by BD Pharmingen/ Biosciences (Heidelberg, Germany), Jackson Immunoresearch DIANOVA Vertriebs-Gesellschaft GmbH (Hamburg, Germany), Ganymed-Pharmaceuticals (Mainz, Germany), Sigma-Aldrich Chemie Holding GmbH (Taufkirchen, Germany).

Table 4: Antibodies and enzyme-conjugates

Antibodies and enzyme-conjugates designation	Manufacturer
7-AAD	BD
Alkaline Phosphatase-conjugated AffiniPure Goat Anti-Mouse IgG Fcγ Fragment	Jackson Immunoresearch
Allophycocyanin-conjugated AffiniPure F(ab')2 Fragment Goat Anti-Human IgG + IgM (H+L),	Jackson Immunoresearch
Anti-6×His-Tag mouse monoclonal antibody DIA 900	Jackson Immunoresearch
anti-Granzyme B-PE	BD
CD69-APC Mouse-Anti-human	BD
APC-AffiniPure Goat-anti-mouse IgG (H+L)	Jackson Immunoresearch
CD3-FITC (SK7)	BD
CD8-APC (SK1)	BD
IMAB362 (Claudiximab)	Ganymed-Pharmaceuticals
CD4-FITC Mouse-Anti-human	BD
mumAB anti-Claudiximab 8B1F3	Ganymed-Pharmaceuticals
CD25-PE Mouse-Anti-human	BD
Peroxidase conjugated Goat Anti Mouse IgG (Fc-specific) A0168-	Sigma-Aldrich Chemie
Propidium iodide solution 1.0 mg×mL^{-1} P4864-10 ML	Sigma-Aldrich Chemie

2.3.4 MEDIA

MEDIA FOR MOLECULAR BIOLOGY METHODS

LB-medium
1.0 % Trypton [w/v]
0.5 % Yeast-Extract [w/v]
1.0 % NaCl [w/v]
•dissolve in H2O dist
•autoclave

LB agar
1.0 L LB medium
15.0 g Agar
•autoclave

SOC medium
5.0 g Yeast extract
20.0 g Trypton
0.,5 g sodium chloride
2.0,5 mL potassium chloride (1 M)
•ad. 1 L H2O dest
•autoclave
•add 20 mL Glucose (1 M, sterile)

MEDIA FOR CELL BIOLOGICAL METHODS

NugC4 medium (M)
500.0 mL RPMI-M containing Glutamax
10.0 % FCS (heat inactivated)
0.5 % Penicillin (100 U×mL^{-1}) / Streptomycin (100 µg×mL^{-1})

HEK293 medium
500.0 mL DMEM:F12-M containing Glutamax
10.0 % FCS (heat inactivated)
0.5 % Penicillin (100 U×mL^{-1}) / Streptomycin (100 µg×mL^{-1})

Murine DC medium
500.0 mL RPMI-M containing Glutamax
10.0 % FCS (heat inactivated)
1.0 % Sodium pyruvate (100 mM)
1.0 % Non-essential-amino acids (NEAA) (100x)
0.5 % Penicillin (100 U×mL^{-1}) / Streptomycin (100 µg×mL^{-1})

Human DC medium
500.0 mL RPMI-M containing Glutamax
5.0 % Human serum-Type AB (heat inactivated)
1.0 % Sodium pyruvate (100 mM)
1.0 % Non-essential amino acids (NEAA) (100x)
0.5 % Penicillin (100 U×mL^{-1}) / Streptomycin (100 µg×mL^{-1})

Freezing medium
70.0 % RPMI-M containing Glutamax
20.0 % FCS or Human serum –Type AB
10.0 % DMSO (pure)

2.3.5 BUFFER

BUFFER AND SOLUTIONS FOR MOLECULAR BIOLOGY METHODS

Loading buffer
0.25 % Bromphenol blue
0.25 % Xylene cyanole FF
0.25 % Orange G
1.0 mM EDTA pH 8.0
40.0 % Sucrose
•in H2O dest

TAE 50 x stock solution
242.0 g TrisBase
57.1 mL Glacial acetic acid
100 mL 0.5 M EDTA pH 8.0
•ad 1 L H_2O dest
•autoclave

TAE gel (1 %)
1.5 g Agarose
150.0 mL 1 x TAE
• dissolve agarose by boiling
•cool down to 55 °C
•add 75.0 µL ethidium bromide (0.05 M)

BUFFERS FOR CELL CULTURE, FLOW CYTOMETRY AND MACS

Luciferin –solution
1 mg×mL^{-1} Luciferin
50 mM HEPES
Add 1 mL H_20
flow-cytometry buffer
5.0 % FCS
2.0 mM EDTA pH 8.0
•prepare in 1×DPBS
PI-buffer
•dilute Propidium iodide (PI) to a concentration of 1 µg×mL^{-1} with flow-cytometry buffer

Fixative solution
Dilute the 3× concentrate BD Stabilizing Fixative 1:3 in deionized water at RT

MACS buffer
5.0 % Human serum albumin 20 % (HSA)
2.0 mM EDTA pH 8.0
•prepare in 1×DPBS

BUFFERS FOR ANIMAL EXPERIMENTS

Erythrocyte lysis buffer
8.29 g NH_4Cl
1.0 g $KHCO_3$
37.2 mg EDTA pH 8.0
•complete the volume up to 1 L with H_2O dist
•adjust pH to 7.29
•filter sterile

Anesthesia mixture
2.5 mL Ketamine (50 mg×mL^{-1})
1 mL Rompun (2 %)
6.5 mL H2Odist

BUFFERS AND SOLUTIONS FOR PROTEIN BIOCHEMISTRY

Running buffer preparation
50.0 mL 20X NuPAGE® SDS Running buffer (MOPS)
fill up to 1.0 L H2O dest

Coomassie brilliant blue staining solution
0.1 % Coomassie
in 50 % ethanol
10 % acetic acid
•in H2O dest

Decolorizing solution:
20.0 % ethanol
7.5 % acetic acid
•in H2O dest

10x NuPAGE® Transfer buffer
Tris-Glycine transfer buffer:
29.0 g Tris Base
144.0 g Glycine
200.0 mL Methanol
in 800 mL H2O dest

Blocking buffer
10.0 % Milk powder (w/v)
0.05 % Tween20 (v/v)
in 1×DPBS

Phosphate buffered saline PBS wash buffer 10 x PBST
0.02 % Tween 20
in 1×DPBS

Buffer 1 (pH 7.4):
500 mM NaCL
50 mM NaH_2Po_4
10 mM imidazole
in 1×DPBS, adjust with 2 M NaOH

Buffer 2 (pH 7.4):
500 mM NaCL
50 mM NaH_2Po_4
250 mM imidazole
in 1×DPBS, adjust with 5 M HCl

Storage buffer (pH 7.4):
200 mM L-Arginin-monohydrochloride
800 mL H_2O adjust with 5 M HCl,
fill up to 1 L

Imidazole buffer (pH 7.4)
500 mM Imidazole
In 1×DPBS, adjust with 5 M HCl

ELISA washing buffer
1x DPBS
0.05 % Tween

ELISA antibody buffer:
1x DPBS
3 % BSA

AP Alkaline phosphatase buffer (pH 9.8):
105,14g Diethanolamin
700 mL ultrapure water
500 µL MgCl2
Fill up to 1 L with ultrapure water
adjust pH with 5 M HCl

Substrate solution
AP buffer (pH 9.8)
1.5 mg pNPP per mL AP buffer

2.4 EUKARYOTIC CELL LINES

Table 5: Cell lines

Cell line	Origin of cells	reference	media
CHO-K1 WT	Chinese hamster ovary cells	ATCC CCL-61	DMEM:F12+10.0 % FCS+ 0.5 % Pen/Strep
HEK293T	Human embryonic Kidney epithelial cells	ATCC CRL-11268 [94]	DMEM:F12+10.0 % FCS+ 0.5 % Pen/Strep
HEK293	Human embryonic Kidney epithelial cells	ATCC CRL-1573 [95]	DMEM:F12+10.0 % FCS+ 0.5 % Pen/Strep
HEK293-CLDN18.2	Human embryonic Kidney epithelial cells stably transfected with CLDN18.2	[8]	D-MEM:F12 Glutamax; 10.0 % FCS,0.5 % Pen/Strep,
HEK293-CLDN18.1	Human embryonic Kidney epithelial cells stably transfected with CLDN18.1	[8]	D-MEM:F12 Glutamax; 10.0 % FCS,0.5 % Pen/Strep,
NugC4	Human gastric cancer cell lines, adenocarcinoma and partial signet-ring cell carcinoma	JCRB0834 [96]	RPMI1640 medium with 10 % fetal calf serum, 0.5 % Pen/Strep
KATOIII	Humane pancreatic carcinoma cell-line	[97]	RPMI 1640 medium supplemented 20 % fetal calf serum.
Dan-G	Humane pancreatic adenocarcinoma cell-line	[98]	RPMI 1640 medium supplemented with 10 % fetal bovine serum, 0,5 % P/S 1 % Hepes, 1 % Sodium Pyrovat.

2.5 MOLECULAR BIOLOGICAL METHODS

Methods for manipulation of DNA are described by Sambrook *et al.* [99] and molecular biological reagents were used according to the manufacturer's instructions. Gene segments flanked by restriction endonuclease cleavage sites were synthesized by a commercial provider of automated gene synthesis (GeneArt AG). Synthesized DNA stretches were sub cloned into appropriate expression vectors and amplified in *E. coli* Top10 (Invitrogen)/NEBalpha (NEB) or XL Blue (Invitrogen). Used plasmids are named in Table 7. All buffers used are mentioned in chapter2.3.5 and media were listed in chapter 2.3.4.

2.5.1 OLIGONUCLEOTIDE PRIMER

Table 6: Oligonucleotide primer

Oligonucleotide primer name	Sequence	Length	Type
05_iMAB362_rev	GGACATGGTCACTTTCTCGCC	21	Seq.
06_5_T7-for_pSTI	CTCACATGTTCTTTCCTGCG	20	Seq.
07_pSTI-rev1	TTTAGCTCTCGACGCAGCAATG	22	Seq.
08_pSTI-rev2	CTTGATTTCCAGCTTGGTGCC	21	Seq.
09_5_CLDN_for	GGCACCAAGCTGGAAATCAAG	21	Seq.

Oligonucleotide primer name	Sequence	Length	Type
10_5_iMAB362_for	GGCAACTCCTTCGATTACTG	20	Seq.
11_tailreverse	ATGAACAGACTGTGAGGACTG	21	Seq.
11a_iMAB362_for2	GGCGAGAAAGTGACCATGTCC	21	Seq.
12_pcDNA3_rev	GGCAACTAGAAGGCACAGTC	20	Seq.
13_pcDNA3_for	GGCTAACTAGAGAACCCACTG	21	Seq.
23_5_CLDN18hu_rev	CCAGTAGCTGGTGAAGGTGTAG	22	Seq.
25_5_TR66hu_for	GCGTGTCCTACATGAACTG	19	Seq.
28_5_UCHT1-MM_for	GGTGAAGCTTGCCACCATGAACTCC	25	Seq.
30_3_iMAB362_for	GGCAACTCCTTCGATTACTG	20	Seq.
32_5_CLB-T3_for	GGAGAAGCTTAGCCACCATGAACTTCG	27	Seq.
CLDN18.2 for	TGGCTCTGTGTCGACACTGTG	21	RT PCR
CLDN18.2 rev	GTGTACATGTTAGCTGTGGAC	21	RT PCR
HPRT for	TGACACTGGCAAAACAATGCA	21	RT PCR
HPRT rev	GGTCCTTTTCACCAGCAAGCT	21	RT PCR

2.5.2 PROTEIN EXPRESSION PLASMIDS

pcDNA™3.1/myc-His(+) A, B, & C mammalian expression vectors Invitrogen-Life Technologies GmbH (Darmstadt, Germany) were used for protein expression in mammalian cells.
The plasmid pEGFP-C1 (Becton Dickinson, Heidelberg, Germany) was used in control settings to express the reporter gene eGFP.

2.5.3 IVT-RNA TEMPLATE PLASMIDS

Plasmid constructs used as templates for *in vitro* transcription (IVT) of coding sequences (CDS) for example luciferase or BiMABs were based on pST1-2hBgUTR-A120 described previously by Holtkamp *et al.* [100].
To guarantee a seamless insertion of only the CDS into the IVT-RNA expression plasmid, the multiple cloning sites of the expression plasmid pST1-2hBgUTR-A120 were modified. An expression plasmid was designed, containing the type IIS restriction site BsmBI. Moreover, upstream of the recognition site an additional alpha-Globin 5′-UTR (described by [101]) together with a Kozak sequence was associated assuring a direct in-frame ligation of the BiMAB-CDS with this features.
The desired sequence for this new MCS was ordered at GeneArt and cloned into the pST1 plasmid. To assemble the new plasmid -pST1-BsmBI- the common MCS from plasmid pST1-2hBgUTR-A120 was excised by both restriction enzymes SpeI and XhoI. Compatible ends of the new MCS named MCS-BsmBI were than ligated into pST1-2hBgUTR-A120.
The name of this plasmid was given according to the name of the added restriction site: pST1-BsmBI. The correctness of the MCS within this new construct pST1-BsmBI was verified by sequencing.

2.5.4 PHARMACOLOGICALLY OPTIMIZED SYNTHETIC MRNA

Generally, IVT-RNAs are synthesized by *in vitro* transcription from a digested DNA plasmid [92]. Optimizations of the IVT-RNA design using cis-acting structural elements enhanced RNA stability and thus translational efficiency [100] (Figure 7-A).

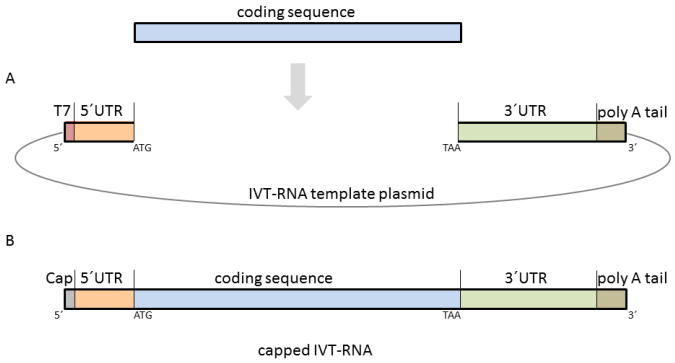

Figure 7: Typical structure of a mature eukaryotic synthetic mRNA
(**A**) A template plasmid for *in vitro* transcribed mRNA is depicted in that the coding sequence (CDS) can be inserted by cloning techniques. (**B**) A fully processed mRNA includes a 5' cap, a 5' UTR, the coding region, a 3' UTR, and a poly (A) tail.

The used template plasmid offers five cis-acting structural elements for the generation of optimized IVT-RNA (Figure 7-B) listed from the 5´to its 3´end:

- The special mARCA cap structure
- The 5´untranslated region (UTR)
- The codon optimized coding sequence (CDS) beginning with the start codon at the 5´end and ending with the stop codon at the 3´end
- The 3´UTR
- The stretch of repeated adenine nucleotides termed poly A-tail at the 3´end containing approximately 120 residues

The cap, a specially altered nucleotide on the 5' end of precursor messenger RNA, allows the ribosome to be recruited and thus facilitates the translation of the mRNA [102]. Moreover, the cap plays an important role in the mRNA stabilizing processes [103]. A chemically modified cap-analog termed mARCA used during the IVT-RNA synthesis pharmacologically enhances the synthetic stabilization of the 5´end of IVT-RNAs [104].
IVT-RNA stability cab be further improved by three plasmid-encoded elements introduced by Holtkamp *et al.* [100]. As described for naturally occurring mRNAs, the coding region of IVT-RNAs is flanked by untranslated regions (UTRs).
First, a 5´human alpha globin sequence (5´UTR) directly joined to a commonly known Kozak sequence (gccgccaccATGG) upstream of the start codon enabled advanced stability. Second, two sequential 3´UTRs of the human beta-globin genes [100] were cloned in-between the CDS and the poly(A) tail. Third, a long poly(A) tail at the 3´end of the IVT-RNAs (for example A80-A120) inhibits decapping as well as degradation of mRNA. Combined with the modified mARCA cap structure, they greatly increased the expression efficiency in dendritic cells [105].
However, improvements in translation are cell type dependent [87] and accordingly have to be tested for each cell type. An additional optimization of the ORF-codon-usage corresponding to the organism in which translation is required can enhance the process as well. Thus, IVT-RNA drugs can be effortlessly customized using traditional DNA engineering methods.

USED PLASMIDS

Table 7: Used plasmids

plasmid name	plasmid function	antibiotic resistance
MCS-BsmB I	new MCS for pST1-2hBgUTR-A120	Ampicillin
pST1-Luciferase	IVT-RNA production	Kanamycin
pST1-BsmB I	IVT-RNA production	Kanamycin
pST1-2hBgUTR-A120	IVT-RNA production	Kanamycin
pEGFP-C1	mammalian expression	Kanamycin
pcDNA3.1	mammalian expression	Ampicillin

2.5.5 DNA SEQUENCING

All cloned constructs were verified by sequencing. Single read sequence service from MWG Eurofins (Ebersberg, Germany) was chosen. Purified DNA was sent with appropriate sequencing primers (Table 6) to determine the presence/orientation/accuracy of the insert sequence and the length of 3´polyA sequence.

2.5.6 SEQUENCE ORIGIN, DESIGN OF BIMAB CONSTRUCTS, AND CLONING INTO EXPRESSION VECTORS

The bispecific tandem single chain antibodies (bs-td-scAbs) constructs were produced by the method of gene synthesis (GeneArt-Life Technologies GmbH, Regensburg, Germany) and codons were optimized by GeneArt's GeneOptimizer® software. In Table 8 the implemented codon usage is explained.

Table 8: Codon usage

codon abbreviation	explanation
HS	*Homo sapiens*
MM	*Mus musculus*
CHO	*Chinese hamster ovary*

2.5.7 DESIGN OF THE BIMAB AND THE ELEMENTS REQUIRED FOR A BIMAB PROTEIN ASSEMBLY

Each BiMAB was designed as a bispecific-tandem-single chain variable fragment (bs-td-scFv). In this context bispecific indicates that this type of antibody offers two single-chain variable fragments (scFv) but with specificities for two different targets.
The BiMAB contains a binding domain specific for the human T cell receptor component CD3 and a second for the human tumor associated antigen (TAA) CLDN18.2. These two binding sites are lined up one behind another (tandem).
The possible consecutive orders from N- to C-terminus are depicted in Figure 8. The first possibility was to engineer the antibody starting with the TAA-specific scFv positioned at the N-terminus. Consequently, the anti-CD3ε scFv would follow at the C-terminus (Figure 8-A). The second option was to design the same bispecific antibody in reverse order, starting with the CD3ε-specific scFv at the N-terminus (Figure 8-B).
This principle is summarized in more detail for each BiMAB in Figure 9 and Table 18. Both consecutive orders were engineered for each BiMAB.

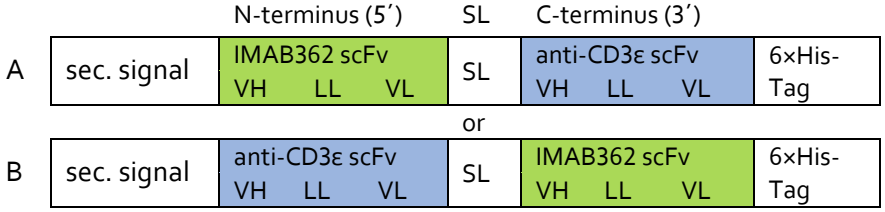

Figure 8: Consecutive order of both scFvs within the BiMAB format.

The bispecific tandem single chain antibody constructs (bs-td-scAb) comprises two scFvs: One specific for the human T cell receptor component CD3ε (anti-CD3ε scFv-blue) and the other for the human tumor-associated antigen CLDN18.2 (IMAB362-scFv-green). The corresponding scFvs for each construct were arranged from N- to C-terminus in two consecutive orders specified by A and B. Sec. indicates secretion signal; LL, long linker; SL, short linker; scFv, single-chain-variable-fragment; VH, variable heavy; VL, variable light.

This technique enabled the production of a recombinant fusion protein that is capable of binding two distinct targets at the same time. The binding sites were derived from the variable regions of the corresponding parental monoclonal antibody (mAb). The highly CLDN18.2-specific and bio-effective mAb IMAB362 (kindly provided by Ganymed Pharmaceuticals AG, Mainz, Germany) was used for building the tumor antigen-specific binding site.

The binding sites were composed of the variable heavy- (V_H) and the variable light-chain (V_L) regions. Due to relative weak non-covalent interactions of those variable domains, an additional stabilizing element is necessary to create binding scaffolds. This stabilizing element was implemented via a covalent linker. It was positioned between the C-terminus of the relevant V_H and the N-terminus of the V_L [106]. In this approach, a flexible hydrophilic peptide linker (long-linker; LL) was used to stabilize this kind of binding molecule kinetically.

This long-linker is composed of a 3 times repeated 5 amino acid long glycine- and serine-rich element $(GGGGS)_3$ [107]. In order to allow the exchange of individual domains an *Eco*RV restriction site was enclosed within this linker sequence. In this way, the current minimal binding domain was engineered to be capable of binding CLDN18.2. Because this fragment is composed of a single peptide chain, it is commonly termed single-chain variable fragment (scFv), which is the smallest known active antibody format [54].

As this part of the bispecific antibody holds the specificity of the cancer tumor associated antigen CLDN18.2, the second part should target the immune effector cells. Our intention was to engage effector T cells for cancer cell lysis. For that reason, the T cell surface glycoprotein CD3ε was considered suitable as molecular target. Accordingly, taking advantage of this Major Histocompatibility Complex (MHC) independent T cell activation mechanism by targeting the epsilon chain of the CD3 receptor was intended.

The designed anti-human-CD3ε-scFvs were derived from the variable domains of four chosen mAbs: the murine mAb UCHT1, the humanized mAb UCHT1, the murine mAb CLB-T3 and the murine mAb TR66. Their nomenclature (NC) and citations are listed in Table 9. Again, the flexible hydrophilic peptide linker (long linker) composed of a 3 times repeated 5 amino acid glycine and serine rich element $(GGGGS)_3$ was used to build scFvs specific for the CD3ε-chain.

Table 9: CD3 variable domain sequence origin and internal nomenclature

	nomenclature (NC)		citation
1.	humanized UCHT1	UCHT1-HS	[108]
2.	murine UCHT1	UCHT1-MM	[109]
3.	murine CLB-T3	CLB-T3	[110]
4.	murine TR66	TR66	[34]

Subsequently each anti-CD3-scFv was fused to the CLDN18.2-specific scFv via a third linker creating a bispecific molecule on a single peptide chain. This third linker is composed of only one glycine-serine element (SGGGGS) termed short-linker (SL). In this way, the tandem-single-chain antibody format was generated, providing specificities for two distinct epitopes thus being bispecific.
In order to allow the exchange of individual scFv domains a *Bam*HI restriction site was integrated within this short-linker sequence. Furthermore, an in-frame secretion signal sequence was introduced at the N-terminus of all BiMAB constructs, during the protein production process. This should guarantee the accurate protein secretion from the cellular cytoplasm into the culture medium.
If the endogenous secretion signal of the mAb was identified, this sequence was selected for scFv generation. For the sake of simplicity the secretion signal of IMAB362 was chosen (MGWSCIILFLVATATGVHS) for all the remaining scFvs. For Ni-NTA-affinity-purification of the protein, a 6×His-Tag was fused to the C-terminus of the construct.
The BiMAB constructs were generated via gene synthesis by GeneArt®. Therefore, the BiMAB sequences were uploaded and a codon optimization was implemented by GeneArt's GeneOptimizer® software. The program's implicit option to reduce undesired restriction sites within the sequence was used. Restriction sites used for cloning steps or *in vitro* transcription were protected and all other redundant restriction sites were eliminated by codon optimization.
The BiMAB formats were successively ordered from GeneArt as Chinese Hamster Ovary (CHO) or human (HS) codon optimized recombinant antibody DNA-constructs. Information on specificity, sequence origin from monoclonal antibodies (mAb), codon usage, additional sequence features, and references of all applied domains are summarized in Figure 9, Table 18 and Table 19.

CLONING

In detail, the DNA sequences were provided with a 5′ *Hin*dIII, *Btg*ZI, and a *Nco*I restriction site, which enables cloning into either protein or IVT-RNA expression plasmids. The following Kozak consensus sequence GGCGCCACC was inserted between the *Btg*ZI site and the start codon, to allow a proper translation of the BiMABs. Two stop codons and several DNA restriction enzyme sites (*Pme*I, *Xba*I, *Not*I, *Xho*I) were integrated at the 3′end.
The design of 1BiMAB was slightly different from the CHO codon optimized CLDN18.2-specific BiMABs. Briefly, the DNA sequence was provided with only a 5′ *Hin*dIII, 5′*Nco*I and a 3' *Xba*I restriction site for cloning and a codon optimization appropriate for the production in human cells (Homo sapiens [HS]).
An altered 3′long-linker sequence, coding for a 18 amino acid long peptide [VE$(GGSGGS)_2$GGVD], was inserted to join the V_H and V_L domains of the CD3 binding scFv.
All used bs-td-scAbs were cloned using the restriction sites *Hin*dIII and *Xho*I (XbaI in the case of 1BiMAB) inserted into the standard mammalian expression vector pcDNA3.1. Successively they were cloned into IVT-RNA expression plasmids pST1-BsmB. Coding sequences were cloned 5′ with one of the following restriction enzymes *Hin*dIII/*Bsm*BI/*Nco*I and 3′by *Xho*I or *Xba*I. A schematic overview of the cloning procedures is shown in Figure 10.

2.5.8 RT PCR

According to the manufacturer's protocol of the RNEasy Mini Kit total RNA extraction from cells was prepared. Next, using superscript II reverse transcriptase 5 µg of the total RNA was transcribed into cDNA. Using oligonucleotides (Table 6) specifically amplifying the transcripts of interest, expression of the corresponding genes was measured via SYBR Green incorporation into the amplified sequences. As an internal control, the resulting CT-values of the gene of interest were related to the

CT-values of a housekeeping gene, HPRT. For the calculation of the Delta CT values following formula was used: $\Delta CT = CT[Target] - CT[HPRT]$

2.5.9 *IN VITRO* TRANSCRIBED RNA SYNTHESIS

The production of *in vitro* transcribed (IVT-) RNAs has become a routine laboratory procedure. In this chapter, the preparation of sufficient amounts of active single-stranded RNAs by a T7-RNA-polymerase with additional steps of RNA purification is described. To generate templates for IVT-RNA, plasmids were linearized downstream of the poly(A)-chain and purified by phenol/chloroform extraction and sodium acetate precipitation.
Linearized vector DNAs were quantified spectrophotometrically and subjected to *in vitro* transcription using commercial kits according to the manufacturer's instructions.[100].Finally the linearized vector DNA was *in vitro* transcribed into mRNA with the Ambion mMessage mMachine T7 ultra kit. In this kit, a modified cap analogue is used, called ARCA cap (anti reversed cap analogue) that prolongs the duration of RNA translation. The reaction batch was incubated for approx. 2–3 h at 37 °C. Afterwards, the solution was incubated with 1 µL Turbo DNaseI for 30 min at 37 °C in order to eliminate any remaining template DNA.
To gain pure RNA, the sample was purified via the Ambion MegaClear Kit. Quantification of IVT-RNA was done by spectrophotometric measurements using the NanoDrop device and quality was controlled by the BioAnalyzer device. Agilent´s 2001 BioAnalyzer was used according to the manual instructions employing the Kit Eukaryote Total RNA Nano from the company Agilent Technologies, Inc.

2.6 CELL BIOLOGICAL METHODS

Common established cell culture techniques, equipment, and principles provided by [111] and [112] were used. All buffers used are mentioned in media were listed in 2.3.4. If no additional terms and conditions are mentioned, cells were handled with aseptic cell culture techniques and cultivated in sterile incubators at 37°C and 5 % CO_2. Supplemental for the media composition for each cell line respectively is described in Table 5. To allow for the detection of mycoplasma contaminations all cells were regularly examined using the Kit MycoAlert® Mycoplasma Detection according to the manufacturer's instructions.

2.6.1 MICROSCOPIC ANALYSIS

Phase contrast microscopy was performed with a Wilovert S inverted microscope (Hund, Wetzlar, Germany) over a period from 6 h to 48 h. Pictures of cells were taken using a Nikon camera Nikon Eclipse TS100-F and processed by the Nikon Imaging software NIS-Elements Documentation D3.10.

2.6.2 DETERMINATION OF CELL DENSITY BY NEUBAUER CHAMBER

Calculation of cell density and total cell number were determined by use of a Neubauer chamber in combination with Trypan Blue. The cell density/number and percent vitality can be calculated by using the equations below:

$$\textbf{Cell density}\ [\textbf{mL}] = \frac{\text{cells count of 2 quadrants}}{\text{number of counted quadrants}} \times \text{dilution factor} \times 10^4$$

$$\textbf{Total cell number} = \text{cell density} \times \text{volume of cell suspension [mL]}$$

2.6.3 FICOLL ISOLATION OF PERIPHERAL BLOOD MONONUCLEAR CELLS (PBMCS) FROM BUFFY COATS

Human PBMCs were freshly isolated from human blood of healthy donors. Peripheral blood mononuclear cells (PBMC) were isolated by density gradient centrifugation according to standard protocols. 25 mL of blood was diluted with 25 mL DPBS + 2 mM EDTA. Subsequently, 35 mL of this mixture was layered on 15 mL Ficoll. Samples were centrifuged for 25 min at RT at 1,900 rpm decelerating the centrifuge at level 3 to preserve phase separation. After centrifugation, an interface below the top of the plasma layer could be observed, which contained the mononuclear cells. Then, the peripheral blood mononuclear cells (PBMCs) were collected using a pipette, washed three times with cold DPBS supplemented with 2 mM EDTA and counted (Determination of cell density by Neubauer chamber).

2.6.4 EFFECTOR CELL PREPARATION

By magnetic-activated cell separation (MACS) the human T cells were separated from PBMCs using the Pan T Cell Isolation Kit II (negatively selected T cells) or using the CD4-positive T Cell Isolation Kit human and CD8-positive T Cell Isolation Kit human according to the manufacturer's instructions (chapter 2.3.2). Enrichment of T cells was verified for purity by flow cytometric analysis.

ISOLATION OF T CELL SUBTYPES

PBMCs of one donor were divided into four fractions and T cells were differently isolated from these fractions using different methods. One fraction remained untouched using these PBMCs for the assay. The second fraction was used in a negative[3] selection of all T cells via the Pan T cell kit. For the third fraction, the MACS separation kit for CD4-positive T cells was used and for the last fraction, the kit for CD8-positive T cells was used. Some of the CD4-positive and CD8-positive T cells were mixed to get another T cell-test-solution. These T cells were mixed in a ratio of CD4-positive to CD8-positive, which resembles that of the donor. This ratio was determined via flow cytometry analysis of the PBMC population and T cell activation was assessed at five different time points– after 8 h, 16 h, 24 h, 48 h, and 72h.

T CELL PROLIFERATION ANALYSIS BY CFSE STAINING

T cell proliferation assays were prepared according to standard protocols [1a].
A cytotoxicity assay was prepared according to chapter 2.6.5. Data was acquired by flow-cytometry Canto II. The decrease in CFSE signal indicating T cell proliferation was determined by FlowJo´s software tool "proliferation."

DETECTION OF THE SERINE PROTEASE GRANZYME B

To detect the upregulation of proteolytic molecules during T cell activation provoked by the bs-td-scAbs, the determination of serine protease Granzyme B via flow cytometric analysis was done. A cytotoxicity assay according to chapter 2.6.5 was prepared. Samples included T cells alone, T cells with 1 and 5 ng×mL^{-1} 1BiMAB, T cells together with NugC4 cells, and T cells with 1 and 5 ng×mL^{-1} 1BiMAB in the presence of NugC4 cells.
After 96 h of coincubation, the T cells were harvested, collected in 5 mL round bottom tubes, washed and stained with a 1:1000 7-AAD DPBS solution to counterstain dead cells for 30 min at 4°C. Then cells were treated according to the manual instructions of the Fixation/Permeabilization Solution Kit and subsequently stained with PE-conjugated Mouse Anti-Human Granzyme B antibody for 20 min at RT. After washing with DPBS, cells were resuspended in flow-cytometry-buffer and data

[3] All other PBMC cells were labeled by beads. All T cells remained unlabeled and were collected as flow through during MACS isolation.

was acquired using a flow-cytometry Canto II.
The upregulation of Granzyme B was defined by comparing the fluorescence signal strength to those of control samples. Control samples contained T cells in the absence (T cells) or presence (T cells + NugC4) of TAA-positive target cells.

2.6.5 COINCUBATION OF EFFECTOR AND TARGET CELLS

Each cell line described in Table 5 was used for this type of assay. Unless otherwise stated, 1×10^5 target cells were coincubated in a final volume of 2 mL DC-medium together with effector cells in an effector to target ratio of 5:1 using a six well tissue culture plate. If cells were cultured in another well format, all parameter settings were adapted reflecting the above-described conditions.

2.6.6 LUCIFERASE-BASED CYTOTOXICITY ASSAY USING BIMAB PROTEINS

In order to be able to determine the target cell killing induced by BiMABs at low levels a luciferase-based cytotoxicity assay was established. Target cell lysis was induced by coincubation with effector cells in the presence of different concentrations of tumor associated antigen-specific BiMAB proteins. Using this assay a quantitative measurement of target cell lysis over more than 48 h in a high throughput manner is possible.
A principle of this assay is that the measured luciferase expression correlates with the amount of viable cells. From this, the target cell lysis within each sample can be calculated. Target cells were either stably expressing the firefly luciferase or cells were electroporated with luciferase IVT-RNA prior to usage in this assay. If cells were electroporated with luciferase-IVT-RNA, six hours later the luciferase expression was confirmed by the Luciferase expression bioassay (chapter 2.6.7).
Each sample was performed at least in duplicate but most of the time in triplicate. Unless stated otherwise, a dilution row ranging from 1-100 $ng\times mL^{-1}$ were prepared along with a blank sample that contained no BiMAB protein used as a negative control. A concentration of 5 $ng\times mL^{-1}$ caused sufficient cell lysis in a reproducible manner and was further used as the standard concentration in these assays. In a flat bottom 96-well plate 1×10^4 target cells per well were analyzed. The assay was conducted in DC-medium and the final volume per well was adjusted to 100 µl.
Human effector cells were prepared as described in chapter 2.6.4. The effector cells used were PBMCs, and CD3-positive T cells. The effector cells were added in an E:T ratio of 5:1. The assay plates were incubated for a period of 4-144 h at 37°C, 5 % CO2. 30 min prior to the measurement, 50 µL of luciferin solution was added per well, followed by an incubation-time in the dark until the measurement started.
Luciferase catalyzes the oxidation of luciferin, which results in emission of light that is measureable as luminescence using a micro plate reader (Luminescence reader infinite M200 from Tecan). The intensity of the luminescence is proportional to the number of viable cells. By correlating this luminescence to that of a reference sample (Lmin), the percentage of specific target cell lysis can be calculated with the following formula:

$$\textbf{specific lysis}[\%] = 1 - \frac{(\text{luminescence test sample} - \text{Lmax})}{(\text{Lmin} - \text{Lmax})} \times 100$$

The minimum lysis (Lmin) was assessed in samples containing target and effector cells in the absence of BiMAB protein, corresponding to luminescence values, representing 100 % living cells. The maximal lysis (Lmax) was assessed in samples containing target and effector cells in the presence of BiMAB protein. Here 10 µL 2 %Triton X-100 was added to achieve the total lysis of all cells prior to measurement, whereby the intensity of unspecific background luminescence emerging from the media or the 96 well plates could be determined.
To determine BiMAB independent or undesired impacts on the target cells further control samples were implemented. Target cells were incubated in the absence of effector cells with BiMAB proteins

in order to exclude direct impact of BiMAB proteins on the target cells. For these samples, corresponding Lmin and Lmax were prepared as well. In general, alloreaction of the T cells was observed by coincubation of target cells and T cells in the absence of any BiMAB. In order to examine a TAA independent effect on the target cell viability further control BiMABs were implemented, using the Plac1 (BiMAB3) and TargetX (BiMAB4) or GT512 (BiMAB2) specific BiMABs.
BiMAB2/BiMAB4/BiMAB3 share the identical CD3 binding moiety with the TR66 BiMABs, but target cancer cells expressing the TAA GT512/TargetX/Plac1, respectivley. This TAA was not presented on the surface of the used target cells, thus serving as a negative control for TAA independent effects, which would be triggered by the CD3ε binding scaffold (3'TR66). The parental monoclonal antibody IMAB362 was applied as an additional control for the V_H and V_L binding domains of CLDN18.2. 5 ng×mL^{-1} IMAB362 were added to target cells alone or to target cells coincubated with T cells. Several further modifications of this assay were performed, whilst criteria such as E:T ratio, BiMAB concentrations and the effector cell subset were also varied.

DOSE-RESPONSE CURVE CALCULATION BY CYTOTOXICITY ASSAYS

Target cell lysis was determined by a Luciferase-based cytotoxicity assay using BiMAB proteins and incubation times of 48 h. The specific lysis was plotted against the logarithm of used BiMAB concentrations using Prism software (Graph Pad Software Inc., version 5.04). The dose-response curves were calculated by the nonlinear fit principle using the "log (agonist) vs. response - Variable slope" model. Calculated concentrations of the half-maximal lysis (EC50) were used as indicator for specific BiMAB efficacy.

2.6.7 IVT-RNA ELECTROPORATION

To prevent the degradation of IVT-RNAs the temperature was kept at 4°C to minimize RNase activity throughout the whole RNA electroporation procedure. Additionally RNase-free consumables and RNase inhibitor RNaseZap® were employed and all working steps were carried out as quickly as possible.
After the final resuspending of cells in X-vivo medium with a cell density of 2x10^7 cells×mL^{-1}, 250 µl of this cell suspension was transferred to a pre-cooled electroporation cuvette (4 mm gap). 5-20 µg IVT-RNA were then added to the cuvette, carefully mixed, and successively electroporated by the application of an electrical pulse to the cuvette using the Electro Square Porator ECM 830.
The electroporation parameters used for different cell types are listed above. Immediately after electroporation, cells were gently decanted into a 15 mL falcon containing 5 mL of pre-warmed DC-medium. Residual cells were counted and were used in assays or for cultivation.

Table 10: Parameters used for the electroporation of different cell types

Cuvette type	Cell line	Voltage	Pulse length	Pulse number	Interval length	Opt. Temp.
4 mm	HEK293T	250 V	2 ms	5	400 ms	4°C
4 mm	human CD4+/CD8+	500 V	3 ms	1	400 ms	4°C
4 mm	NugC4	250 V	12 ms	2	400 ms	4°C
4 mm	MCF-7	200 V	12 ms	2	400 ms	4°C
4 mm	Kato III	250 V	12 ms	2	400 ms	4°C
4 mm	DU145	250 V	12 ms	2	400 ms	4°C
4 mm	PA-1	200 V	12 ms	2	400 ms	4°C

LUCIFERASE EXPRESSION BIOASSAY

In various experiments, different cells were electroporated with IVT-RNA. In order to prove expression of electroporated IVT-RNA, a luciferase-based expression bioassay was applied as a control step in all experiments, whenever electroporation of cells was performed. Luciferase catalyzes the oxidative decarboxylation of Luciferin to oxyluciferin, which results in emission of light that is measurable as luminescence [113].

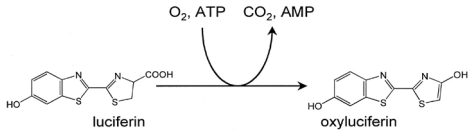

Figure 9: Luciferin luminescence reaction

Firefly luciferase catalyzes the oxidative decarboxylation of luciferin in the presence of ATP, O_2, and Mg_2, producing yellow-green light (λmax= 560 nm) and the product oxyluciferin [113].

Cells electroporated either with luciferase-IVT-RNA alone or with a mixture of BiMAB IVT-RNA and luciferase IVT-RNA, were incubated for six hours at 37°C, 5 % CO_2. 30 min prior to the measurement 50 µL of luciferin solution was added into each well, followed by incubation of the plate in the dark at 37°C for 30 min until measurement. The luciferase expression was analyzed by a micro plate-reader Infinite M200 from Tecan. The luminescence signal was compared to the signal of cells that were not electroporated. Increased luminescence signals thus prove the expression of electroporated IVT-RNAs.

LUCIFERASE-BASED CYTOTOXICITY ASSAY USING IVT-RNA

If cells were electroporated with IVT-RNA BiMABs, the luciferase-based cytotoxicity assay was correspondingly altered. Steps that differ from the protein assay are listed here. Cells were electroporated as described in chapter 2.6.7. Next, cells were coincubated with effector cells in the desired E:T ratio for lysis determination. Different from the assay above, the reference samples for normalization (Lmin) in this case were composed of the electroporated cells in the absence of effector cells. For each distinct electroporated cell-sample, an individual Lmin sample was required. The electroporation efficiency was determined by the luciferase expression bioassay.

2.6.8 TRANSIENT TRANSFECTION FOR SMALL SCALE PROTEIN PRODUCTION

The human embryonic kidney cell line HEK293T was used for transient transfections. Two days prior to transfection $1x10^7$ HEK293T cells were plated on 14.5 cm tissue culture dishes in 20 mL cell specific media. To remove residual FCS, cells were washed with DPBS containing 2 mM EDTA. Then, cells were incubated in 20 mL of plain DMEM/F-12 medium without FCS or antibiotics.
For transfection 20 µg of the circular expression plasmids were diluted in 0.5 mL plain DMEM/F-12 medium. Linear PEI (75 µL of a 1 mg×mL^{-1} solution) were added to the DNA mixture and rigorously vortexed. After 15 min incubation at RT, the DNA-PEI complexes were added drop wise to the cells. To distribute the mixture evenly on the cells the dishes were gently panned and then incubated at 37°C, 5 % CO_2. After 24 h, the media was exchanged for plain DMEM/F-12 and the cells were incubated for additional 48 h at 33°C, 5 % CO_2. The supernatant was harvested and the cells were incubated in fresh media for additional 48 h at 33°C, 5 % CO_2. The cell supernatant was harvested a second time and sterile filtered with 0.2 µm syringe filters.

2.6.9 STABLE TRANSFECTION

In order to get producer cell clones that stably produce CLDN18.2 bs-td-scAb the cell lines HEK293 or CHO-K1 WT, described in chapter 2.4, were taken.

PEI TRANSFECTION

For stable transfections of HEK293, $1x10^7$ HEK293 cells were plated on 14.5 cm tissue culture dishes in 20 mL cell specific media two days prior to transfection. To remove residual FCS cells were washed with DPBS containing 2 mM EDTA. Then cells were incubated in 20 mL of plain DMEM/F-12 medium without FCS or antibiotics. For transfection 20 µg of the linear expression plasmids were diluted in 0.5 mL plain DMEM/F-12 medium.
Linear PEI (75 µL of a 1 $mg \times mL^{-1}$ solution) were added to the DNA mixture and rigorously mixed. The DNA-PEI complexes were added drop wise to the cells after 15 min incubation at RT. To distribute the mixture evenly on the cells the dishes were gently panned and then incubated at 37°C, 5 % CO_2. After 24 h, the media was exchanged by plain DMEM/F-12 and transfected cells from this time on were selected by addition of 0.8 $mg \times mL^{-1}$ of the selective antibiotic G418 sulfate.

SELECTION OF PRODUCER CLONES

In order to get a BiMAB protein-producing cell that stably yields high amounts of BiMAB a producer cell clone derived from a single cell was generated. Single cell sorting using the flow cytometry cell sorter flow-cytometry Aria was a pragmatic way to acquire single cell cloning of stable transfected bulk cell populations.
Immunofluorescence staining (chapter 2.8.1) and an IMAB362 specific ELISA (Spectrophotometric detection of BiMABs by an IMAB362-specific ELISA assay) were used to identify cell clones that steadily and sufficiently produced BiMABs. Because a general higher expression of BiMABs was observed for HEK293 cells, they were chosen as producer cell line. If a cell clone was appropriate, cells were expanded and frozen for further use.

LARGE SCALE BIMAB PRODUCTION

According to the manufacturer's instructions one producer cell clone was incubated in a 10-layer Cell Factory and cultured in its defined media until confluent. Subsequently the media was exchanged for FCS free media. The supernatant was collected every 3-5 days for up to 4 weeks, directly filtered with 500 mL Steritop Filter Units and stored at 4°C until FPLC-purification. The amount of BiMAB in this cell culture supernatant was roughly determined prior to FPLC purification by polyacrylamide gel electrophoresis followed by Coomassie staining and Western blot analysis. For this, an aliquot of the supernatant was concentrated as described in chapter: 2.7.3.

2.7 PROTEIN BIOCHEMICAL METHODS

Commonly established techniques, equipment, and principles provided by current protocols in protein science [114] were used. All buffers used are mentioned in chapter 2.3.5

2.7.1 PURIFICATION OF BIMABS BY AFFINITY CHROMATOGRAPHY VIA HIS-TAG

BiMAB proteins were enriched from the collected cell culture supernatant by immobilized metal affinity chromatography (IMAC). According to the manufacturers protocol the His Trap FF 5 mL column attached to an ÄKTA Purifier 10 FPLC system was used to purify BiMAB from the filtered supernatant.

First, the column was equilibrated with buffer1, then the cell culture supernatant was loaded onto the column with a flow rate of 5 mL×min^{-1}. The column was subsequently washed with buffer1 to remove unbound protein contaminants. Afterwards, bound protein was eluted using a stepwise gradient of buffer 2. The whole FPLC purification process was monitored by determination of UV 260 nm and 280 nm.
An immediate dialysis against 1x DPBS using a Slide-A-Lyzer G2 Dialysis Cassette was performed, followed by an additional dialysis against the 200 mM arginine storage buffer. SDS-PAGE and Coomassie-staining and Western blot analysis were carried out to test the quality and purity of the BiMAB proteins. Additionally the concentration of BiMAB was determined. The purified protein was aliquoted and stored at -80°C for long time storage or kept at 4°C for immediate use.

2.7.2 SMALL SCALE PURIFICATION OF BIMABS

Ni-NTA spin columns were used to isolate BiMAB proteins from the supernatant as described in the manual. Proteins were eluted in 300 µL of a 500 mM imidazole buffer, kept at 4°C for direct usage or for long time storage at -20°C.

2.7.3 CONCENTRATION BY PROTEIN FILTER

The supernatant was concentrated 5×–10× by Centricon Centrifugal Filter Devices, according to the manufacturer's protocol.

2.7.4 SDS-PAGE AND COOMASSIE-STAINING

For the separation of proteins according to their electrophoretic mobility, sodium dodecyl sulfate polyacrylamide gel electrophoresis (SDS-PAGE) was used. Concentrated and non-concentrated supernatants were separated on NuPAGE Novex 4–12 % Bis-Tris gels with the help of the given Invitrogen device XCell SureLock™ Mini-Cell according to the manufacturer´s instructions using the NuPAGE® LDS Sample buffer, NuPAGE® Reducing Agent, Novex Sharp Pre-stained protein standard and the NuPAGE® MOPS SDS Running buffer. Subsequently, the gels were stained with 100 mL of Coomassie brilliant blue staining solution.
Then, the gel was gently shaken on an orbital shaker or rocker for 1 h or until the signals from the protein were visible. After the staining solution was discarded, the gel was placed in a loosely covered flask containing 100 mL of decolorizing solution and gently moved again until the gel appeared transparent. The gel was washed in 100 mL of ultrapure water for 10 min on a shaker. Afterwards, a photograph from the gel was taken using a scanner.

2.7.5 WESTERN BLOT ANALYSIS

Western blot analysis was carried out to detect BiMAB protein via its 6×His-Tag. After the electrophoretic separation of proteins via SDS-PAGE, proteins were blotted on a PVDF membrane using the XCell II™ Blot Module and the membrane was transferred into a 50 mL reaction tube.
Between each step, the blot was washed three times for 5 min each in PBS-wash buffer. In order to eliminate nonspecific binding sites the membrane was blocked using the blocking-buffer for 60 min at RT prior to the incubation with the corresponding first and secondary antibodies. The blot was incubated with each antibody at RT on a shaker platform for 1 h or at 4°C over night. The primary antibodies was diluted in a 1×PBST-buffer containing 3 % BSA and the secondary antibodies was diluted in the blocking-buffer.
First, the blot was incubated with the primary anti-6×His-Tag antibody, which was diluted 1:500. After washing, membranes were incubated with an Fc-specific secondary peroxidase-conjugated goat-

anti-mouse IgG antibody diluted 1:10,000. An additional washing step was performed and finally the signals were visualized by a substrate and recorded by an ImageQuant LAS 4000 Imager. Incubation of the blot using the substrate Pierce ECL was 1 min or 5 min when using SuperSignal West Femto Chemiluminescent substrate.

2.7.6 DETERMINATION OF PROTEIN CONCENTRATION

SPECTROPHOTOMETRIC DETECTION OF BIMABS BY A NANODROP DEVICE

Bs-td-scAbs concentration was determined by measurement at 280 nm with a NanoDrop 2000c under consideration of the extinction coefficient and the molecular weight of BiMABs determined via the ProtParam tool (http://web.expasy.org/protparam/).

SPECTROPHOTOMETRIC DETECTION OF BIMABS BY AN IMAB362-SPECIFIC ELISA ASSAY

In order to be able to quantify the concentration of the CLDN18.2-specific BiMAB protein in the cell culture supernatant, a specific ELISA was established using an idiotypic antibody that specifically binds to the variable domains of IMAB362. 200 µL of ELISA washing buffer per well was used per washing step by the Hydro Flex plate washer. Each washing step was repeated twice and all incubation steps were executed at RT while shaking on the shaking platform Titramax 1,000+ Incubator. FPLC purified 1BiMAB protein was diluted in 1×DPBS within the range of 0.3125–20 ng×mL^{-1} and consequently applied for the calculation of a calibration curve.
BiMABs were immobilized by their 6×His-Tags onto the Ni-NTA plates. All supernatants were diluted 1:10,00 in ELISA antibody buffer and successively 100 µL were implemented per well. 1 h after incubation washing was performed followed by the incubation with the anti-idiotypic antibody against the V_H-V_L domains of IMAB362 with a final concentration of 0.5 µg×mL^{-1} in ELISA antibody buffer. Incubation was performed for 1 h followed by the washing procedure. The next staining occurred through the incubation with the secondary AP-conjugated goat anti-mouse-Fc antibody that was diluted to a final concentration of 300 ng×mL^{-1} in ELISA antibody buffer.
Finally, after another washing step 100 µL of substrate solution was added. Wells containing, supernatant not containing BiMABs and anti-IMAB362 plus secondary antibody served as negative controls. After 30 min the absorption at 405 nm with an excitation wavelength of 492 nm with an Infinite M200 Tecan micro plate-reader was measured.
Curve fitting was performed using the software tool: Dose-response-log (inhibitor) vs. response-variable slope (four parameter) test from GraphPad Prism. Concentrations of the BiMAB proteins were determined by interpolation from the implemented 1BiMAB calibration curve.

COLORIMETRIC DETERMINATION OF PROTEIN AMOUNTS

Protein concentrations were determined using Coomassie staining compared to staining intensities of BSA, which was used as a protein standard. Gel electrophoresis followed by Coomassie staining, including the purified 1BiMAB and a BSA standard ranging from 0.05, 0.1, 0.5, 1.0 to 5.0 µg, were performed to confirm the concentration already measured by the NanoDrop device. Signal strength of the 1BiMAB sample was compared with BSA signal strength to calculate the respective protein concentration.

2.8 BIOCHEMICAL AND IMMUNOLOGICAL METHODS

2.8.1 BIMAB DETECTION BY IMMUNOFLUORESCENCE LABELING OF CELLS

The expression of BiMABs by transient or stably transfected cells was analyzed by immunocytochemical methods such as immunofluorescence labeling. For this, microscope slides confluently covered with 2×10^5 of the adherent cells HEK293, HEK293T, or CHO-K1 were prepared. Permeabilization of cells was achieved by incubation of slides for 20 min in 2 % formaldehyde dissolved in 1×DPBS and afterwards slides were washed three times with a blocking buffer (1×DPBS supplemented with 5.0 % BSA and 0.2 % Saponin).
Then, cells were stained at RT for 30 min with the primary anti-6×His-Tag antibody diluted 1:500 in blocking buffer. This was followed by a 3 h staining at RT with secondary Cy3-conjugated goat-anti-mouse IgG diluted 1:500 in blocking buffer. Cells were finally embedded in Glycergel-mounting medium containing the Hoechst 33342 dye and stored at 4°C protected from light. The BiMAB expression was verified under the microscope and photographs were taken.

2.8.2 BIMAB DETECTION BY IMMUNOCYTOCHEMISTRY (ICC)

All ICC procedures were performed by the service provider IHC- unit (Tron, Mainz, Germany) according to their standard processes. After treatment, tumors were extracted, fixed in 4 % formalin, dehydrated, embedded into paraffin and three µm sections were produced. Tumor cells were detected with the help of the mouse anti-human anti-claudin18.2 monoclonal antibody 43-14AGC182 (Ganymed Pharmaceuticals) used at a concentration of 0.2 $\mu g\times mL^{-1}$. Sections from a human stomach were used as positive staining control. The negative control slides with consecutive sections were treated only with the secondary antibody and did not show any signal.

2.8.3 FLOW CYTOMETRY DIRECT/INDIRECT STAINING OF CELL SURFACE MARKERS

Cells were harvested, adjusted to the desired cell concentration, and washed in flow-cytometry buffer. Washing steps were composed of pelleting the cells by centrifugation (5 min; 1500 rpm; 4°C) and resuspending the cells in 100 µL flow-cytometry buffer. Unless otherwise stated, all stainings were performed with an incubation time of 30 min in the dark at 4°C using the anticipated antibodies solved in flow-cytometry buffer. If not indicated otherwise all fluorescently labeled antibodies were purchased from BD Biosciences as listed in Table 4.
A titration was performed for each antibody beforehand to find the optimal working concentration. The appropriate amount of desired antibody or staining component was added to reach the optimal concentration and successively the flow cytometry samples were incubated. Afterwards the cells were washed twice with 2 mL of flow-cytometry buffer.
When the staining was completed, cells were finally resuspended in 100 µL fixative solution and incubated at RT for 20 min. If cells had to be stained furthermore with secondary antibodies, cells were resuspended in 50 µL of flow-cytometry buffer containing the diluted antibody or mixture of antibodies and were incubated .
Subsequently, the cells were washed twice with flow-cytometry buffer and resuspended in 100 µL fixative solution. Incubation time was 20 min at RT and the following storage of the samples in the dark at 4 °C. Flow cytometry measurements were performed on a BD flow-cytometry Calibur running Cell Quest Pro software or flow-cytometry Canto II device running flow-cytometry Diva-software (BD Bioscience) and the resulting data was analyzed using Flow-Jo software (Tree star).

FLOW-CYTOMETRY LIVE/DEAD STAINING

The number of dead cells was determined via flow-cytometry-based analysis of propidium iodide (PI) or 7-AAD incorporation into the cell nuclei. 1×10^6 cells were labeled during staining procedure with 2 µL 7-AAD in 100 µL flow-cytometry buffer, washed twice and subsequently fixed by fixative solution. Cells that were stained by a buffer containing PI as an alternative to 7-AAD, were resuspended in only 50 µL flow-cytometry buffer instead of using fixative solution. Immediately before the flow-cytometry measurement 50 µL of PI-buffer was added to the sample.

FLOW-CYTOMETRY-BASED TARGET BINDING ASSAY

Binding of the BiMAB protein to their target molecules CLDN18.2 and CD3 was assessed via flow-cytometry measurement. Target cells expressing the TAA CLDN18.2 (for example NugC4) were used to investigate the BiMAB binding. The specific binding of BiMABs to CD3 was tested by using T cells. In addition, a cell line that does not express any of the two epitopes (HEK293) was used to rule out an unspecific binding of the BiMABs. All steps of this staining procedure were prepared as described in chapter 2.8.3. 1×10^5 target cells were transferred to 5 mL round bottom tubes and incubated for 30 min with various concentrations of the respective BiMAB solved in flow-cytometry buffer.
Binding of the BiMABs was followed by a washing step and the subsequent staining with 3.3 $\mu g\times mL^{-1}$ anti-6×His tag mAb. After washing, the cells were incubated with a 1:200 dilution in flow-cytometry buffer of the APC-conjugated goat-anti-mouse secondary antibody in combination with 7-AAD (Flow-cytometry live/dead staining). Then, cells were washed twice and resuspended in 100 µL fixative solution. The mean fluorescence intensity (MFI) of the histograms reflecting the BiMAB-binding was calculated.
Several controls were implemented to detect background staining of the cells. Each antibody (the highest used concentration of the respective BiMABs, too) was tested alone to detect a probable appearance of a background signal. Additional control samples were stained with either primary anti-6×His tag mAb and successively the secondary goat-anti-mouse APC antibody, or each concentration of BiMAB protein and after that the APC-conjugated goat-anti-mouse secondary antibody. If a low direct background binding of the secondary goat-anti-mouse APC antibody to BiMABs or directly to the cells was observed, normalization of the mean fluorescence intensity (MFI) values of each sample had to be considered. In this case, the MFI of this particular control was subtracted from the respective MFI of corresponding samples.
Relative BiMAB binding depicted in percentage was calculated by normalizing to the highest APC signal, which was set as 100 % BiMAB binding. Percentages of 1BiMAB binding were plotted against the indicated 1BiMAB concentrations.

<u>Flow-cytometry-based detection of tumor associated antigen (TAA) expression levels</u>
The respective epitope expression on the cell surface of the implemented target cells was determined within the experiment. CLDN18.2 expression was verified by using 10 $\mu g\times mL^{-1}$ mAb IMAB362 and consecutively stained with APC-labeled secondary goat-anti-human antibody for 10 min at 4°C in the dark. CD3 expression was detected by incubating with a direct-labeled FITC-anti-CD3 mAb.

FLOW-CYTOMETRY-BASED SATURATION BINDING ASSAYS

Saturation binding experiments were carried out to determine equilibrium binding curves for the used target cells. Cells from a confluent flask were trypsinized, washed with flow-cytometry buffer and finally 1×10^5 cells per well were added to a 96 well plate in triplicates. In general, centrifugation

of cells was performed at 1,500 rpm for 5 min at 4°C and supernatant was discarded after centrifugation of the plate by rapidly inverting/dumping the plate one time.
After pelleting of cells, they were incubated for 30 min at 4°C with various concentrations of the respective BiMAB diluted in 100 µL flow-cytometry buffer. The cells were resuspended in the antibody solution by careful pipetting to allow an equivalent binding of BiMAB to the TAA exposed on the target cell surface. After the incubation time, samples were washed twice with flow-cytometry buffer.
In order to detect bound BiMAB, cells were resuspended in 50 µL of flow-cytometry buffer containing the primary antibody (6×His-Tag) and incubated at 4°C for 30 min.
Cells were washed once with flow-cytometry buffer to remove unbound primary antibody and were resuspended in 100 µL of the appropriate secondary antibody (goat anti mouse-APC) solved in flow-cytometry buffer. The next incubation period required 30 min at 4°C and cells were washed twice with flow-cytometry buffer afterwards.
Binding was analyzed by flow cytometry on a flow-cytometry Canto II device running flow-cytometry Diva software using the high-throughput-sampler (HTS). The mean fluorescence intensity values of APC were normalized to the respective strongest signals and plotted against various concentrations of BiMABs.
The KD values were obtained by computational analysis using GraphPad Prism (version 5.04 for Windows, GraphPad Software, San Diego California USA) Calculations were obtained by performing Prism model: Nonlinear regression with binding saturation-one site - total and nonspecific binding.

FLOW-CYTOMETRY-BASED T CELL ACTIVATION AND CELL CYTOTOXICITY ASSAY

For this kind of assay 1×10^5 target cells were coincubated in 2 mL DC-medium with 5×10^5 T cells using a six well plate. Varying effector-to-target ratios (E:T) or testing different BiMAB dilutions were the variables in this assay.
However when further E:T ratios were varied, the sample volume and number of target cells remained identical, while the concentration and, accordingly, the number of effector cells were adapted. BiMAB was tested in a concentration ranging from 0.001–1000 ng×mL^{-1}.
Control samples contained target or T cells alone with and without BiMAB protein: Six controls were implemented to assure the correct interpretation of the T cell activation results. Three out of these six samples were composed of coincubated T cells and cancer cells, comprising first the blank sample, second the parental mAb IMAB362 (exclusively binding to the TAA CLDN18.2), and third the control BiMABs (BiMAB4/BiMAB3/BiMAB2).
In order to exclude a BiMAB independent activation of T cells due to allo-reactivity of the T cells, the first control, a mixture of only T cells and cancer cells, was investigated. Comparing the level of activation of all samples with reference to this blank value, the BiMAB induced effects were revealed. By targeting only the TAA (IMAB362-2.control sample) or CD3 (BiMAB4/BiMAB3/BiMAB2– 3. control sample) the mediated effects of single target binding on T cells were verified.
In the next three controls, target cell independent effects were measured using T cells in the absence of cancer target cells. The samples containing either mAb IMAB362 (fourth control) or 1BiMAB (fifth control) were compared to the T cell activation of untreated T cells (sixth control).
For the determination of target cell lysis, several controls were necessary. The same first three controls, described for the T cell activation assay, were utilized in the cytotoxicity assay as well. T cell independent effects were measured using only the target cells (blank sample) or target cells in combination with BiMABs or IMAB362.
At indicated time points, cells were harvested by gentle scraping with Cell Scrapers and transferred to 5 mL round bottom tubes. Remaining cells were resuspended in flow-cytometry buffer, harvested again by gently scraping, and transferred into the matching round bottom tubes. Cells were centrifuged and washed with flow-cytometry buffer.

Staining occurred according to the procedure described in chapter 2.8.3. After incubation at 4°C in the dark for 30 min with a mixture of mouse anti-human CD3-FITC, mouse anti-human CD69-APC, and mouse anti-human CD25-PE antibodies (optional CD45-V500), cells were washed and pellets were resuspended in 50 µL cold flow-cytometry buffer. During the measurement, cells were kept in the dark and on ice. Directly before flow-cytometry measurement, 50 µL freshly prepared propidium iodide buffer was added to distinguish live from dead target cells.
Target cell lysis was monitored by propidium iodide uptake into the cell nuclei, while lysed cells appeared PI-positive. Accordingly, dead target cells were quantified by gating the CD3/CD45 negative target cell population and the amount of PI-positive cells was defined. In order to measure T cell activation, cells were gated for PI negativity, CD3 positivity and the percentages of T cell populations expressing for the following combinations of activation markers (CD69+/CD25-), (CD69+/CD25+) and (CD25+/CD69-) were determined.
The flow cytometric data were analyzed by the software FlowJo and were depicted using the software Graph Pad Prism. The status of activation was subdivided into three stages marked by the expression of two differentiation markers, expression of CD69 alone:(CD69+/CD25-), as early activation state, expression of CD69 and CD25 in combination (CD69+/CD25+) as advanced stage and expression of CD25 alone (CD25+/CD69-) as late stage. The sum of the percentages determined for the different activation stages, represents the total percentage of all activated T cells, and it is depicted as a stacked bar graph.
Either for T cell activation or for determining the BiMAB-mediated target cell lysis, ten thousand events were analyzed per sample using flow cytometry. Samples were acquired on the flow-cytometry Canto II device. All activation and cytotoxicity samples were performed in duplicates and repeated twice. The total percentage of activated T cells was calculated for each sample and the standard deviation of duplicates is indicated by error bars on top of the stacked bar graphs.

2.9 *IN VIVO* MODELS

All animals were between 6 to 12 weeks of age and were obtained either from Jackson laboratory (Bar Harbour, ME, USA) or from the University of Mainz animal facility. All experiments were performed according to the German Animal Protection Law and to the GV-SOLAS guidelines with permission from the responsible local authorities.

2.9.1 MOUSE STRAINS

NOD scid gamma (NSG)

NOD.Cg-Prkd^{scid} IL2rg^{tm1Wjl}/SzJ (Jackson laboratory, Bar Harbour, ME, USA).
The mouse strain commonly known as NOD scid gamma (NSG), belongs to the immunodeficient models. These mice have the severe combined immune deficiency mutation (scid) and additionally an IL-2 receptor gamma chain deficiency resulting in the lack of mature T cells, B cells, or functional NK cells.

2.9.2 ADEQUATE ANIMAL HOUSING

All animal experiments in human xenograft models were performed in NOD.Cg-Prkd^{scid} IL2rg^{tm1Wjl}/SzJ mice (Jackson laboratory, Bar Harbour, ME, USA) characterized by T-, B-, NK-cell deficiency, and lack of macrophage function (Jackson Lab., Bar Harbor, ME USA). The mice were maintained under sterile and standardized environmental conditions (20 ± 1 °C RT, 50 ± 10 % relative humidity, 12 h light:12 h dark-rhythm). Animals were kept in individually ventilated cages to achieve

specified pathogen free conditions (SPF). They received autoclaved food and bedding and acidified (pH 4.0) drinking water.

2.9.3 ANESTHESIA AND SACRIFICE OF MICE

Mice were anesthetized by intraperitoneal (ip) injection of 150-200 µl anesthesia mixture with an insulin syringe (29G). Mice were regarded as "under anesthesia" when a footpad reflex was not detected anymore. Sacrifice of mice was performed by cervical dislocation.

2.9.4 BLOOD RETRIEVAL

For preparation of white blood cells, blood was obtained via retro-orbital bleeding under anesthesia. 100-150 µl blood was retrieved from the retro-orbital vein via a micro hematocrit capillary tube and transferred to a clean flow-cytometry tube. In order to remove erythrocytes, cells were incubated with 300 µl erythrocyte lysis buffer for 3-5 min at RT. The lysis reaction was then stopped with addition of 2 mL 1×DPBS that was followed by centrifugation (300xg, 8 min, RT). Cells were resuspended in 200 µl 1×DPBS medium and further analysis of cells was performed by flowcytometry described in chapter 2.9.6.

2.9.5 ORGAN DISSECTION

The pathology of animals, retrieval of organs and preparation of cell suspensions were performed. Tumor tissue and spleen were isolated and stored PBS at RT until further *ex vivo* analysis. In some cases the gastrointestinal tract (caecum, colon, duodenum, ileum, jejunum, esophagus, and rectum), the kidney, the liver, and the lungs, were additionally removed and fixed for further histopathological analysis. Tumor tissue was dissected and organs infiltrated by tumor metastasis were immediately fixed in 10 mL Roti-Histofix 4 % for immunohistochemical analysis.

PREPARATION OF SINGLE CELL SUSPENSIONS FROM MURINE SPLEENS

NSG mice were sacrificed by cervical dislocation. After that, the spleen was removed and placed in a 1.5 mL tube with 500 µL PBS. The tip of a 5 mL syringe served as a grinder to homogenize the spleen while the homogenate was being filtered through a cell strainer (70 µm) into a 50 mL tube. After centrifugation of the splenocyte suspension (1200 rpm, 8 min, RT), the pellet was resuspended in 5 mL erythrocyte lysis buffer for 3-5 min at RT.
The lysis reaction was stopped through the addition of 25 mL 1×DPBS and cells were pelleted by centrifugation (1200 rpm, 8 min, RT). After resuspending the cells in PBS or DC-medium, the cell density was calculated and further analysis of the cells was performed by flow cytometry as described in chapter 2.9.6. Some cells were frozen for experiments at a later time point. In case of freezing, the splenocytes were resuspended in 1 mL heat inactivated fetal bovine serum supplemented with 10 % DMSO instead of erythrocyte lysis buffer. Samples were immediately frozen at -80°C and stored until samples from all mice from one experiment were complete for further investigations.

2.9.6 ANALYSIS OF ENGRAFTMENT OF HUMAN T LYMPHOCYTES

Splenocyte samples were thawed. All cells were washed twice with warm DPBS. One million splenocytes per sample were incubated with fluorophore-conjugated mAbs for 20 min at 4°C in the dark. The percentage of engrafted human T cells was determined by antibody staining (anti-CD45-APC, anti-CD3-FITC and anti-CD4-FITC, anti-CD8-APC).
Flow cytometric analysis was conducted with a flow-cytometry Calibur. Staining occurred according

to the procedure described in chapter 2.8.3. Directly before flow-cytometry measurement, 50 µL freshly prepared propidium iodide (PI) buffer was added to distinguish live from dead target cells. Target cell lysis was monitored by PI uptake into the cell nuclei, while lysed cells appeared PI-positive. Accordingly, dead target cells were excluded by gating the PI negative target cell population. In order to quantify CD4-positive and CD8-positive T cells, cells were gated for the respective markers. The percentages of T cell populations expressing for the following combinations of activation markers (CD4+/CD8-), (CD4+/CD8+) and (CD8+/CD4-) were determined.

2.9.7 ADOPTIVE TRANSFER OF EFFECTOR CELLS

The intraperitoneal (ip) injection route was employed to adoptively transfer human PBMCs as effector cells. PBMCs were isolated according to the procedure described in chapter 2.6.3 and cells were stained for flow-cytometry analysis to document the percentage of T cells in the PBMC cell suspension for injection (chapter 2.9.6). Cells were stored on ice until ip inoculation into mice was performed. An indicated number of cells, resuspended in 200 µl PBS, was injected ip into the mice using a 0.5 mL syringes with a sterican cannula (Ø 0,45 x 25 mm, 26G).

2.9.8 ENGRAFTMENT OF TUMOR CELLS

Prior to tumor inoculation, respective exponentially growing tumor cells HEK293-CLDN18.2 (chapter 2.4) were cultivated and harvested. The cells were counted (chapter 2.6.2) and vitality of cells was ensured (chapter 2.6). Cells were stained for flow-cytometry analysis to document the current TAA expression level (chapter 2.8.3). Cells were stored on ice until subcutaneous (sc) inoculation into mice was performed. CLDN18.2-expressing target cells were applied sc to 8 weeks old NSG mice using a sterican cannula (Ø 0,45 x 25 mm, 26G) and 1 mL syringes.

2.9.9 HUMAN XENOGRAFT MODEL

A mouse model with engrafted human T cells after PBMC injection was established in order to investigate the therapeutic potential of BiMAB proteins *in vivo*. Prior to tumor inoculation, respective exponentially growing tumor cells HEK293-CLDN18.2 (chapter 2.4) were cultivated and harvested. The cells were counted (chapter 2.6.2) and vitality of cells was ensured (chapter 2.6).
Cells were stained for flow-cytometry analysis to document the current TAA expression level (chapter 2.8.3) and stored on ice until subcutaneous (sc) inoculation into mice was performed. CLDN18.2-expressing target cells were applied sc to eight weeks old NSG mice using a sterican cannula (Ø 0,45 x 25 mm, 26G) and 1 mL syringes.
Five days after tumor cell inoculation mice were stratified according to their tumor volume into groups receiving PBMCs or not. Mice without tumor growth were excluded from the experiment. On the same day, PBMCs were isolated from human blood of healthy donors and used for effector cell engraftment in these mice. $2x10^7$ PBMCs diluted in 200 µL 1×DPBS were injected ip on the day of isolation to the experimental treatment groups designated with "PBMC".
With "PBS" designated treatment groups received 200 µL plain 1×DPBS intraperitoneally instead and served as control without human effector cells. Group "PBS/vehicle" comprised four mice (n=4), "PBS/1BiMAB" 5 mice (n=5). The human effector cells themselves can cause a graft-versus-host reaction against murine tissue. That can lead to a deterioration of the state of health of the mice. In order to differentiate between a graft-versus-host reaction and therapeutic effects of the BiMAB, a corresponding negative control –"PBMC/vehicle"– was implemented covering 13 mice (n=13).
The therapy group –"PBMC/1BiMAB"– enclosed 15 mice (n=15).
One day after DPBS or PBMC application the 1BiMAB therapy was started. Injection of 5 µg purified 1BiMAB protein diluted in 200 µL of DPBS per animal were applied ip. The mice of the vehicle

groups received ip 200 µL of storage buffer diluted in 1×DPBS to resemble the composition of the 1BiMAB injection. The injections occurred on a daily basis over a period of 22 days.
The tumor volumes were monitored twice per week using a digital calibrated caliper. Volumes of the tumors were calculated according to the following formula: $\mathrm{mm}^3 = \frac{\mathrm{length} \times \mathrm{with}^2}{2}$. Mice exhibiting tumors that exceeded the volume of 500 mm^3 were sacrificed by cervical dislocation. If severe symptoms of graft-versus-host disease or a drastic decline in the state of health was observed, these distinct mice were sacrificed as well.

2.9.10 DETERMINATION OF THERAPY INFLUENCE ON BODY WEIGHT

In order to judge the state of health of mice the body weight measurement was the apparent criterion that was monitored. The body weight of each mouse was examined twice per week using a laboratory scale. A loss of body weight above 10 % indicated impaired health. A weight-loss of ≥ 20 % indicated massive impaired health and therefore was an abort-criterion. These mice were directly sacrificed.

2.9.11 APPLICATION TECHNIQUES

Used application techniques were intravenous (iv) injection via the tail vein, subcutaneous (sc) application under the skin of the right abdominal flank and intraperitoneal (ip) injection into the body cavity according to GV-SOLAS guidelines. For all injections syringes (0.3×12mm, 0.01-1 mL, Braun) were used.

2.10 STATISTICAL METHODS

Data are given as mean and its standard deviation (SD). The number of replicate-samples is stated in the figure description of each experiment. Statistical analysis was performed by GraphPad Prism version 5.04 for Windows, GraphPad Software, San Diego California USA, www.graphpad.com employing Two-way ANOVA with the Bonferroni multiple comparison test where indicated and respective P-values were provided. P-value between $P < 0.05$ and $P < 0.0001$ was considered statistically significant.

3 RESULTS–BiMAB THE PROOF OF CONCEPT

3.1 SUCCESSIVE CLONING OF BiMAB PLASMIDS

Considering the issues of the objective of this study the design of numerous bispecific-single-poly-peptide-chain-antibodies was required. The overall aim was not only to design several of these BiMAB constructs, but also to develop a platform with a modular design for each BiMAB. This allows for the simple removal and a bare fit in of a newly-inserted scFv-element. By this means, it permits the easy expansion of the platform at any time point. The second goal was the easy and fast transfer of the BiMAB constructs from protein expression plasmids into IVT-RNA expression plasmids. For both goals, it was necessary to find matching restriction sites for a manageable consecutive cloning.

3.1.1 DESIGN

Considering the above-mentioned requirements, all BiMAB were designed in-silico. Detailed information on the BiMAB design and a comparison of all BiMAB elements for each BiMAB respectively can be found in chapter 2.5.6, Figure 9, Table 18, and Table 19.
The BiMAB constructs were generated via gene synthesis using GeneArt®. Therefore, the BiMAB sequences were uploaded and a codon optimization was implemented by GeneArt's GeneOptimizer® software. The BiMAB formats were successively ordered at GeneArt as Chinese Hamster Ovary (CHO) or human (HS) codon optimized recombinant antibody DNA-constructs.

3.1.2 CLONING

To briefly recap only the key-points of the BiMAB cloning, all used bispecific antibody DNA constructs were cloned via their 5´ *Hin*dIII and 3´ *Xho*I restriction enzyme sites (*Xba*I in the case of 1BiMAB) into the standard mammalian expression vector pcDNA™3.1/myc-His (+).
Whenever it was necessary, 5´scFv-domains were exchanged by HindIII and BamHI restriction and 3´scFv-domains by *Bam*HI and *Xho*I restriction. The final assembly of the BiMAB fragments, their restriction sites, and the consecutive cloning steps are listed in Figure 10.
Subsequently the cloning of BiMAB sequences from mammalian expression plasmids into IVT-RNA expression plasmids named pST1 was performed. To guarantee a seamless insertion of only the CDS, a new expression plasmid was created, suitable for the desired cloning platform, termed pST1-*Bsm*BI (chapter 2.5.3).
For the transfer two restriction sites were used. This was either the integrated restriction enzyme site 5´*Btg*ZI in combination with 3´*Xho*I, or the recognition sites 5´ *Nco*I in combination with 3´*Xho*I. The coding sequence of BiMABs digested with 5´*Btg*ZI/ *Nco*I and 3´*Xho*I were ligated into plasmid pST1-*Bsm*BI, previously treated with 5´*Bsm*BI and 3´*Xho*I.
After each cloning step, all constructs were verified by sequencing via MWG´s single read sequence service and only those matching the alignment entirely (100 %) were taken for further downstream applications.
A further selection criterion for correct pST1-BiMAB clone selection was the length of the polyA tail. The aim was to obtain IVT-RNA expression plasmids, which at least offered a polyA tail length of 80 AA that should guarantee an appropriate RNA stability.

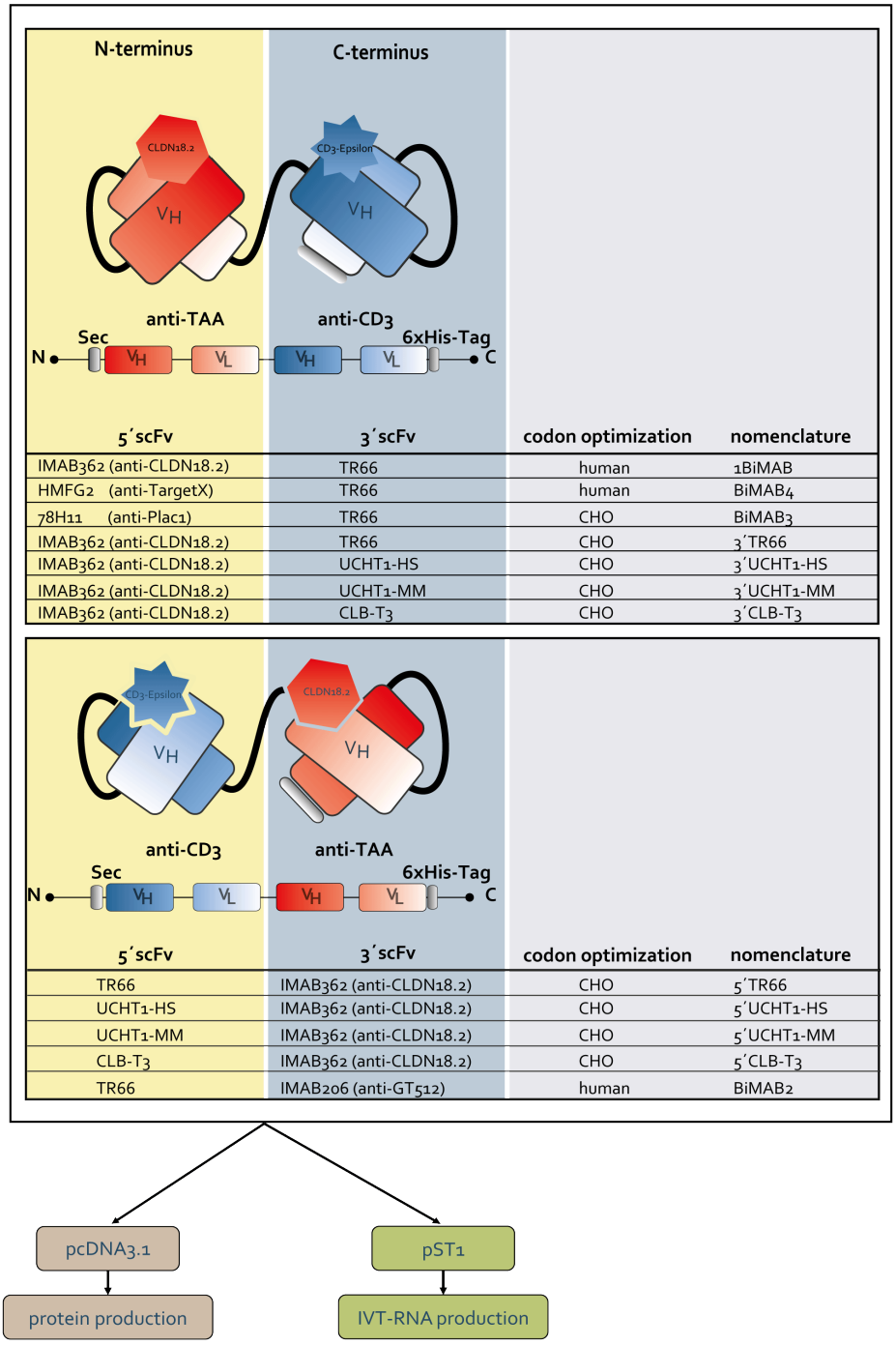

5´scFv	3´scFv	codon optimization	nomenclature
IMAB362 (anti-CLDN18.2)	TR66	human	1BiMAB
HMFG2 (anti-TargetX)	TR66	human	BiMAB4
78H11 (anti-Plac1)	TR66	CHO	BiMAB3
IMAB362 (anti-CLDN18.2)	TR66	CHO	3´TR66
IMAB362 (anti-CLDN18.2)	UCHT1-HS	CHO	3´UCHT1-HS
IMAB362 (anti-CLDN18.2)	UCHT1-MM	CHO	3´UCHT1-MM
IMAB362 (anti-CLDN18.2)	CLB-T3	CHO	3´CLB-T3

5´scFv	3´scFv	codon optimization	nomenclature
TR66	IMAB362 (anti-CLDN18.2)	CHO	5´TR66
UCHT1-HS	IMAB362 (anti-CLDN18.2)	CHO	5´UCHT1-HS
UCHT1-MM	IMAB362 (anti-CLDN18.2)	CHO	5´UCHT1-MM
CLB-T3	IMAB362 (anti-CLDN18.2)	CHO	5´CLB-T3
TR66	IMAB206 (anti-GT512)	human	BiMAB2

Figure 9: Design of the bispecific-tandem-single-chain-antibodies–BiMABs

The sequences of four different anti-human CD3-scFvs were selected for BiMAB cloning. Each anti-CD3-scFv was either positioned at the N-terminus (5´scFv-lower panel) or at the C-terminus (3´scFv upper panel) of the protein. Anti-CD3 specifies the anti-CD3-scFv; anti-TAA classifies the specificity of this tumor targeting scFv. Those scFvs are derived from the indicated mAb, which are specific for one of four TAA: CLDN18.2, GT512, Plac1, and TargetX. BiMAB3, BiMAB4, and BiMAB2 serve as control BiMABs in subsequent experiments. The nucleotide codon usage of each BiMAB is indicated in an additional column. Each construct got its own nomenclature to distinguish between the domain orientation, its different CD3-scFv, and its TAA binding specificity. All BiMAB constructs were cloned into the mammalian protein expression plasmid pcDNA3.1 (Invitrogen) and subsequently into an IVT-RNA template plasmid named pST1 derived from the pGEM3Z-vector (Promega, Madison, WI). IMAB indicates ideal monoclonal antibody; -HS, humanized; IVT, *in vitro* transcribed; -MM, murine; mAb, monoclonal antibody; Sec, secretion signal; scFv, single-chain-variable-fragment; V, the variable region of the heavy (H) and light (L) chain; 6×His-Tag, Hexahistidine-tag.

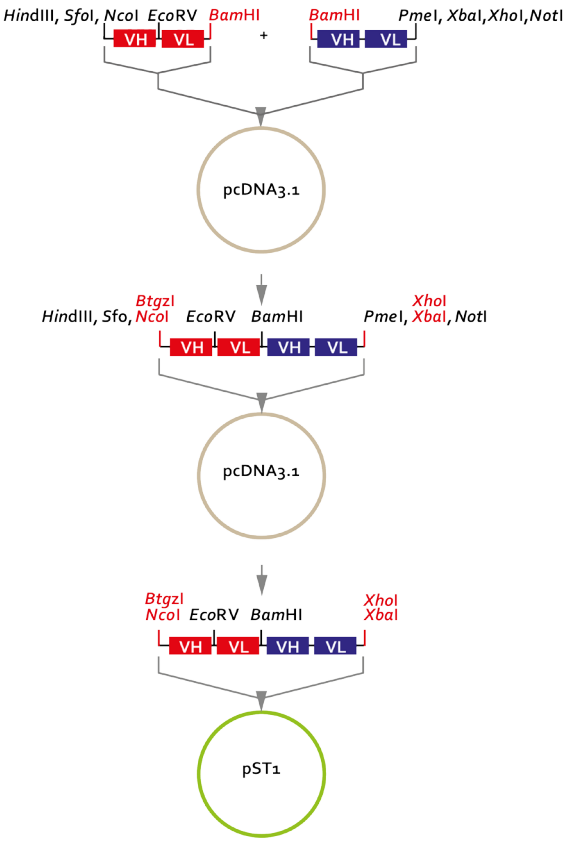

Figure 10: Scheme illustrating the chronology of cloning BiMABs into expression and template plasmids

BiMABs were cloned into the protein expression plasmid pcDNA3.1. Exchange of the 5′or 3′scFv sequences can be done at the 5′end via HindIII and BamHI, and at the 3′end via BamHI and XhoI/XbaI. For IVT-RNA production, inserts were subcloned into IVT-RNA template plasmids pST1-BsmBI. The cloning procedure, plasmids, and restriction sites are depicted in this figure. V specifies the variable region of the heavy (H) and light (L) chain of the corresponding scFvs.

3.2 BiMAB PROTEINS ARE EXPRESSED BY MAMMALIAN CELLS

The first downstream application after cloning was the *in vitro* production of all CLDN18.2 specific BiMAB proteins and BiMAB3 by cell culture technologies. Briefly, several BiMABs– directed against CLDN18.2 and the human CD3ε chain–were transiently expressed in HEK293T cells, to generate high amounts of products as is our preference. Production was prepared for small-scale purification via Ni-NTA spin columns. BiMABs were eluted from spin columns using a 500 mM Imidazole solution. Aliquots of these purified proteins either were kept at 4°C for immediate use or stored longer term at -20°C. Initial assays were performed in order to analytically characterize and compare the performance of the eight CLDN18.2-specific BiMABs.
Distinct determination of BiMAB protein quality and quantity was done by protein analysis methods such as immuno-cyto-chemical staining, sulfate polyacrylamide gel electrophoresis (SDS-PAGE), immuno-Western blot, and enzyme-linked immunosorbent assay (ELISA).

3.2.1 IMMUNO-CYTO-CHEMICAL AND WESTERN BLOT DETECTION OF PURIFIED BiMABs PRODUCED BY HEK293 (T) CELLS

The production and secretion of all BiMAB proteins was confirmed via immuno-chemical stainings using a 6×His-Tag specific antibody. Results are illustrated in Figure 11-A and -B. In A the nuclei were immuno-cyto-chemically (ICC) stained in blue with the Hoechst cell stain. The 6xHis-Tags were stained in red, and an overlay of both is shown.
The BiMAB protein production by cells transfected with 1BiMAB or the control BiMAB3 was proven and visible as the red stained cells. The eGFP transfected cells and the non-transfected cells were used as negative controls and showed no staining, as expected. Correspondingly, the BiMAB production could be proven for the transient BiMAB expressions (data not shown). BiMAB protein contained in the supernatant (SN) were further verified by SDS-PAGE and Coomassie staining (data not

shown) and a subsequent Western blot shown in Figure 11-B. Under reducing conditions, the polypeptide chains of all BiMABs were detected by the 6×His-Tag-specific antibody and an Fc-specific secondary peroxidase-conjugated antibody. The mass estimation of approximately 55 kDa for each BiMAB is derived from the mobility of those fragments in the SDS page. The sizes matched accurately with the expected molecular weight calculated from the DNA sequences. The molecular weights as well as the number of AA residues for each BiMAB are summarized in the appendix in Table 20. While all BiMABs are similar in size, there is a considerable variance in their expression level; even though, the same amount of SN was loaded for each BiMAB. The amount of protein detected suggested an elevated production of UCHT1-BiMABs–regardless of whether the humanized or the murine version was used (except for 3´UCHT1-MM).
The conclusions were drawn that all BiMAB-proteins were transiently produced but a prominent disparity in the level of protein synthesis for all BiMABs was identified. These assumptions could be verified for all CLDN18.2 specific BiMABs by ELISA quantification as reflected in Table 11.

3.2.2 QUANTIFICATION OF BIMAB USING AN IMAB362 SPECIFIC ELISA

For the quantification of the nine BiMAB variants present in the harvested supernatants, an IMAB362 specific ELISA was used. BiMAB protein concentrations in supernatant were determined by interpolation from a 1BiMAB calibration curve. Curve fitting was performed using the software GraphPad Prism[4]. Calculated values are summarized in Table 11, wherein C_{BiMAB} specifies the BiMAB concentrations. The proportions and the variance within the BiMAB expression levels, which were already identified in the Western blots, were confirmed by the ELISA experiment.

Table 11: BiMAB concentrations determined via ELISA

BiMAB	C_{BiMAB} [µg×mL^{-1}]
3´UCHT1-MM	9,18
5´UCHT1-MM	21,34
3´UCHT1-HS	3,52
5´UCHT1-HS	21,46
3´TR66	3,18
5´TR66	2,55
1BiMAB	16,87
3´CLB-T3	2,07
5´CLB-T3	2,92

The murine UCHT1 (5´UCHT1-MM) and the humanized UCHT1-BiMAB (5´UCHT1-HS) appear to be the best expressed BiMABs by HEK293T cells, resulting in 20 µg×mL^{-1} recombinant protein. The expression of 5´UCHT1-MM with ~10 µg×mL^{-1} was less than 50 % compared to murine 3´UCHT1-MM BiMABs. The third best-expressed transgene was 1BiMAB with a concentration of 17 µg×mL^{-1}.
Low expression levels in the range of single digit protein concentrations (2–6 µg×mL^{-1}) were gained with BiMABs 3´and 5´CLB-T3, 3´UCHT1-HS, as well as 5´TR66 and 3´TR66.
The protein yield obtained with BiMAB 3´CLBT3 was the lowest with 2 µg×mL^{-1}. The concentration of BiMAB3 could not be determined by the IMAB362-specific ELISA. Therefore, the protein concentration was estimated in respect to Western blot signals. Comparison of the Western blot signals (Figure 11-B) showed that BiMAB3 had a similarly low expression level as the BiMAB 3´CLB-T3. According to this, BiMAB3 is believed to have approximately a concentration of 1 µg×mL^{-1}.

[4] Dose-response-log (inhibitor) vs. response-variable slope (four parameter) test, GraphPad Prism Software version 5.01 for Windows, San Diego California USA, www.graphpad.com").

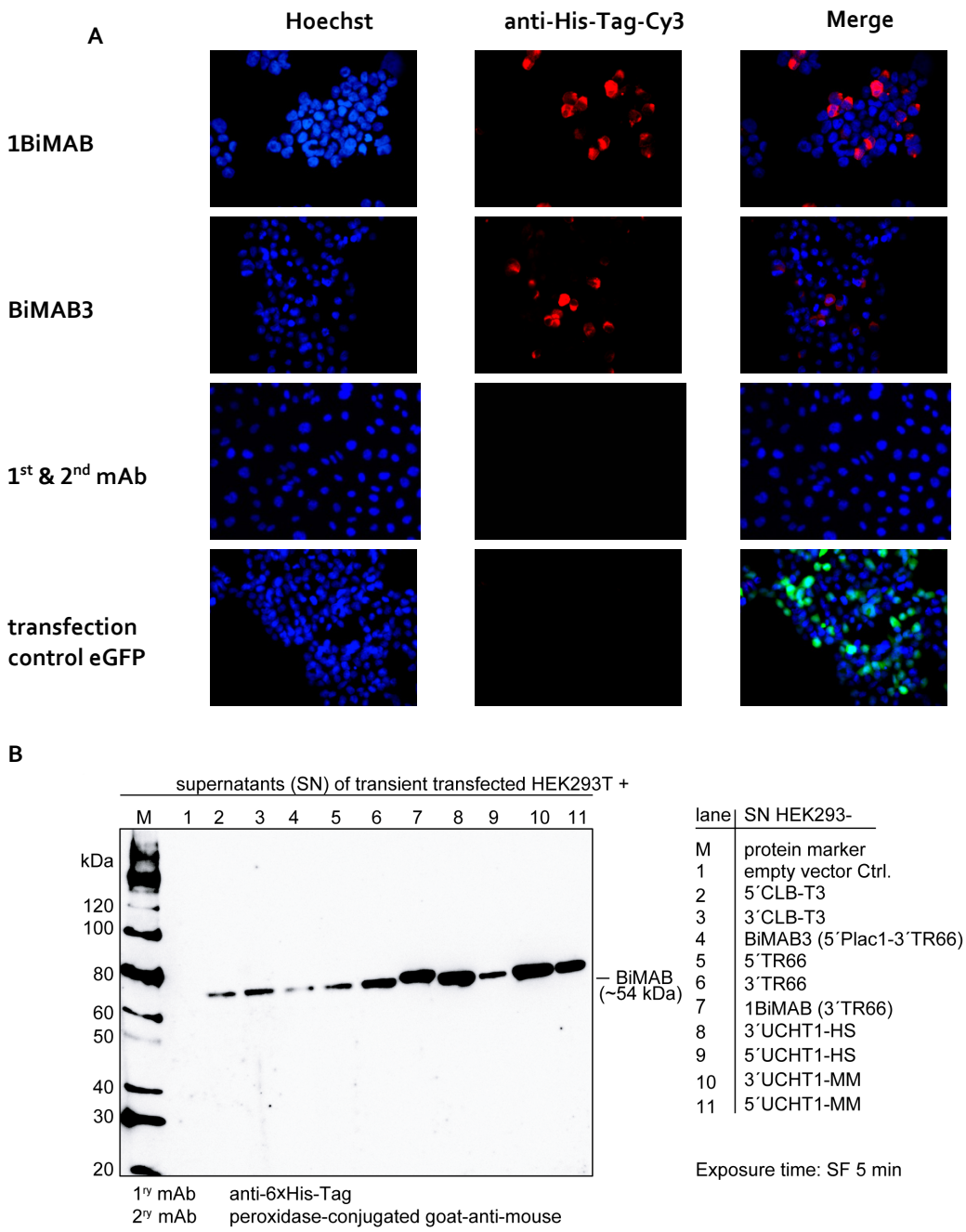

Figure 11: BiMAB proteins produced by transfected HEK293(T) cells

(A) 1BiMAB was detected in stably transfected HEK293 cells via ICC staining. The produced 1BiMAB protein (red) is detected by a primary (1^{ry}) 6×His-Tag-specific mAb and a secondary (2^{ry}) goat-anti-mouse IgG (H+L)-Cy3. CHO cells are indicated by Hoechst (blue) stained nuclei. Overlay of both pictures can be seen in the right panel titled "Merge". Cells transfected with transgenes of BiMAB3 (5´Plac1-3´TR66) or eGFP were used as controls. (**B**) Analysis of BiMAB protein quality and quantity via Western blot is shown. Equal volumes of SN were loaded onto 10 % Bis-Tris gels. The molecular weights of the different BiMAB proteins range from 53.37 to 54.19 kDa. Detection was performed with a 6×His-Tag-specific mAb as 1^{ry} mAb and an Fc-specific 2^{ry} peroxidase-conjugated goat-anti-mouse IgG antibody. Time of exposure was 5 min. SuperSignal West Femto Luminol/Enhancer solution® (SF) was used as development substrate. Molar masses are indicated in kDa at gel-margin. eGFP, specifies enhanced green fluorescent protein; kDa, kilo Dalton; Hoechst, blue fluorescent dye-Hoechst; ICC , immuno-cyto-chemical; M, protein marker; mAb, monoclonal antibody; SN, supernatant; 5´, N-terminal arrangement of the scFv within the BiMAB; 3´, C-terminal arrangement of the scFv within the BiMAB.

3.3 *IN VITRO* STUDIES-SELECTION OF PROMISING BIMABS

With the aim of identifying the best candidate, all BiMAB proteins were examined with regard to the following three main requirements:

1. Specificity for the tumor selective associated antigen CLDN18.2
2. An active anti-CD3-scFv capable of recruiting T cells
3. A beneficial consecutive order for both scFvs within the respective BiMAB format

With the aim of testing these properties for all of the BiMAB proteins, the first attempt was to test the potency in mediation of effector cell redirected lysis of CLDN18.2-positive target cells.

3.3.1 ALL CLDN18.2-SPECIFIC BIMABS INDUCED A POTENT TARGET CELL LYSIS

An easy and convenient screening procedure was f, which compares the efficiency of all CLDN18.2-specific BiMABs. For this, the BiMAB triggered target cell lysis as a screening criterion first was examined *in vitro*, as determined via a Luciferase-based cytotoxicity assay. CLDN18.2 endogenously expressing NugC4 cells, that stably express luciferase, were taken as target cells. The cell surface expression of both BiMAB epitopes–CD3 and CLDN18.2–were evaluated via flow cytometric analysis on cancer target cells, T cells, and epitope-negative control cells used for the assay.
Only T cells were positively stained by the anti-CD3 mAb (Figure 12-B), while NugC4-luc cells, and the negative control cell line HEK293 showed no CD3 expression. In the same manner, an expression of CLDN18.2 was detected only on the surface of NugC4-luc cells (Figure 12-C) but not on T cells or HEK293 cells. This selective expression of both epitopes allowed the BiMABs to specifically link cancer target cells via their TAA to the CD3ε of T cells.
The target cells were incubated for 48 h with CD3+ human T cells at an effector to target ratio (E:T) of 5:1 in the presence of 5 ng×mL^{-1} BiMAB. By comparing the data of all nine BiMABs, differences in the performance were observed regarding the tumor cell killing potential (Figure 12). Repetitions of the experiment confirmed that 1BiMAB is the fastest mediator of target cell lysis. 60 % of target cells were already eradicated after 16 h, rising to approximately 100 % after 48 h.
After 1BiMAB, the recombinant proteins 5′and 3′TR66 (shown in Figure 12–black lines) as well as 5′and 3′UCHT1-MM (shown in Figure 12–blue lines) were the best in eliciting the desired effector functions of T cells. However, all four showed a less constant progression in tumor cell lysis and proved to be less efficient compared to 1BiMAB.
Other than the 5′CLB-T3 and 3′UCHT1-HS, the remaining BiMABs also managed to trigger T cell responses with a target cell lysis of between 96 %-99 % after 48 h.
All BiMABs were compared with each other for each time point by means of statistical analysis[5] (data not shown). Nevertheless, through this analysis it became clear that five BiMABs (1BiMAB, 3′& 5′UCHT1-MM and 3′& 5′TR66) were all highly effective. Therefore, the differences in lysis between those five BiMABs were not significant.
The next objective was to identify the beneficial consecutive order of the scFvs. For each of the five best BiMABs, a comparison of both scFv orientations for each BiMAB protein showed no statistically significant differences in potency.

[5] Two-way ANOVA with the Bonferroni multiple comparisons test was performed using GraphPad Prism version 5.04 for Windows, GraphPad Software, San Diego California USA, www.graphpad.com

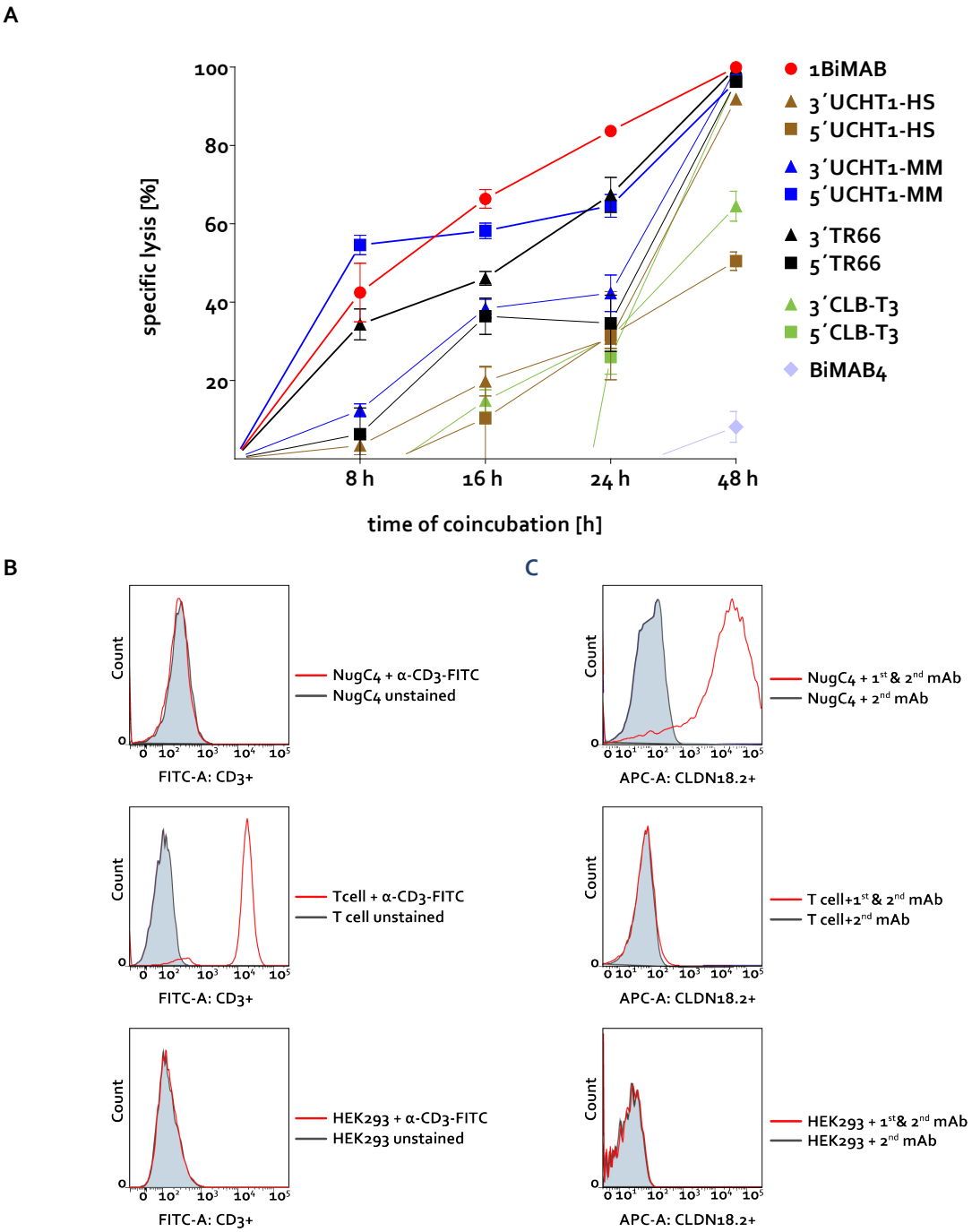

Figure 12: Outcome of induced cancer cell lysis depended on the used BiMAB protein

A kinetic of target cell lysis mediated by all generated BiMAB proteins monitored over 48 h is shown in (**A**). The respective cancer target cell line (NugC4-luc) was coincubated with freshly isolated T cells. An effector to target ratio (E:T) of 5:1 was chosen. Coincubation was performed in the presence of 5 ng×mL^{-1} Ni-NTA column purified BiMABs or the control BiMAB4. Potency to induce specific cancer cells lysis was quantified with the luciferase-based cytotoxicity assay in a 96 well format. Error bars indicate standard deviations (SD) of triplicates. Results are a representative of two experiments. (**B**-**C**) The cancer target cells (NugC4-luc), T cells and a negative control cell line were validated for target antigen expression. The respective histograms reflecting antibody binding are presented. 5×10^5 CLDN18.2 endogenously expressing NugC4-luc cells, 5×10^5 CD3 endogenously expressing human T cells or 5×10^5 CLDN18.2 and CD3 negative HEK293 cells were stained with a FITC labeled anti-CD3 mAb shown in (**B**) or first stained with the mAb IMAB362 and second with the corresponding APC-conjugated antibody depicted in (**C**). Control stainings included secondary APC-conjugated antibody alone. 5´ specifies N-terminal arrangement of the anti-CD3-scFvwithin the BiMAB; 3´, C-terminal arrangement of the anti-CD3-scFv within the BiMAB.

Table 12: The statistical significances with respect to the lysis efficiency comparing 1BiMAB with every other BiMAB6

1BiMAB vs BiMAB	8 h	16 h	24 h	48 h
5′TR66	ns	ns	**	ns
3′TR66	ns	ns	ns	ns
5′UCHT1-MM	ns	ns	ns	ns
3′UCHT1-MM	ns	ns	*	ns
5′CLB-T3	****	****	***	ns
3′CLB-T3	**	**	**	ns
5′UCHT1-HS	*	***	**	**
3′UCHT1-HS	ns	*	**	ns
Ctrls.				
MP002	****	****	****	****

significance signature	
****	P < 0.0001
***	P < 0.001
**	P < 0.01
*	P < 0.05
ns	P > 0.05

To define the best performing BiMABs besides 1BiMAB, it was tested if 1BiMAB-mediated lysis is significantly higher compared to all other BiMABs (Table 12). Those BiMABs, that showed no significantly lower tumor cell lysis compared to 1BiMAB, were considered to have the best potential for targeted therapies. Consequently, the BiMABs 3′TR66, 5′TR66, 3′UCHT1-MM, and 5′UCHT1-MM were considered the most potent BiMABs.

In order to examine a TAA independent impact of BiMABs on the target cell viability in general Plac1-/TargetX-specific control-BiMABs and IMAB362 were implemented as negative controls. The TAAs Plac1 and TargetX were not presented on the surface of the used target cells (determined by flow cytometric analysis, data not shown), thus the control BiMABs offered binding opportunities only via their CD3ε binding scaffold (3′TR66).

In this scenario, no effect by the anti-CD3-scFv on the viability of treated target cells was measured in the absence or presence of T cells. A further control applied was the parental monoclonal antibody IMAB362 exclusively binding to CLDN18.2. 5 ng×mL^{-1} IMAB362 was added to target cells alone or to target cells coincubated with T cells, but no impact on the target cells was measured at this concentration.

Taken together, all CLDN18.2-specific BiMABs were able to redirect the T cells towards the cancer target cells thereby specifically inducing effective target cell elimination. This effect was only obtained in the presence of both CD3 and CLDN18.2 epitopes allowing simultaneous binding. Hence, it was concluded that 1BiMAB, the CHO codon optimized TR66 BiMABs, and UCHT1-MM BiMABs were the most effective formats in mediation of target cell lysis. These five BiMABs were taken forward for further investigations.

3.3.2 FUNCTIONAL PROTEIN CHARACTERIZATION OF 5 SELECTED BIMABS

The five BiMAB proteins described in 3.3.1 were selected for a deeper characterization. NugC4 cells expressing CLDN18.2 endogenously were used to investigate the binding capacity of the five anti-CLDN18.2 scaffolds. In addition, freshly isolated human T cells were used to investigate the binding to each anti-CD3-scFv.

[6] Two-way ANOVA with the Bonferroni multiple comparisons test was performed using GraphPad Prism version 5.04 for Windows, GraphPad Software, San Diego California USA, www.graphpad.com

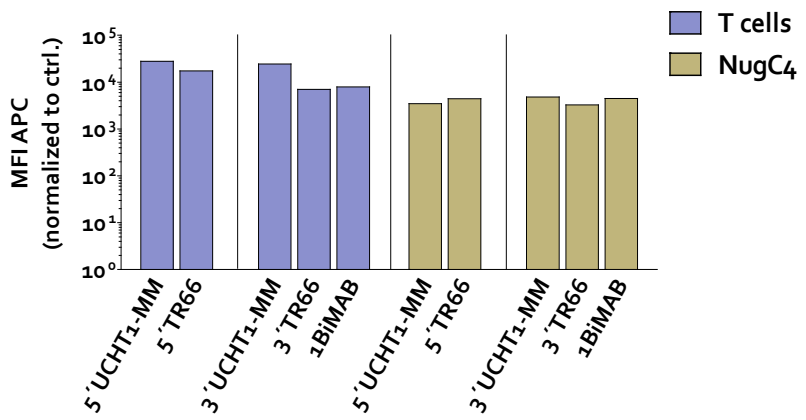

Figure 13: All five selected BiMABs were capable of binding CLDN18.2 and CD3

The binding capability of the Ni-NTA-column purified BiMABs was determined by flow cytometry. A verification of BiMAB specific binding to 1×10^5 T cells or cancer target cells is illustrated. Panels show normalized APC mean fluorescence intensity (MFI) of histograms reflecting BiMAB binding. Binding of 250 ng BiMAB was detected by a primary 6×His-Tag-specific mAb and a secondary APC-labeled-goat-anti-mouse mAb. Values were normalized to the control sample stained by primary and secondary mAb only. Further negative control samples included staining with the secondary goat-anti-mouse APC antibody alone, the primary 6×His-Tag specific mAb alone, and the secondary goat-anti-mouse APC antibody in the presence of BiMAB. 5´ specifies N-terminal arrangement of the anti-CD3-scFv within the BiMAB; 3´, C-terminal arrangement of the anti-CD3-scFvwithin the BiMAB.

To rule out an unspecific binding of the BiMAB proteins, target cells that express neither CLDN18.2, as verified by flow cytometry and RT-PCR, nor the CD3 receptor complex–as verified by flow cytometry–were tested in a flow-cytometry-based binding assay. The cell surface expression levels of each epitope were separately determined for each cell type utilized in this experiment. The cell surface expression of the TAA was confined to target cells and this of the CD3 receptor-complex to T cells (data not shown).No unspecific binding of any BiMAB to HEK293T control cells was detectable. The binding experiment was performed with cumulative concentrations of BiMAB. For simplicity, only one concentration of BiMAB–250 ng–per sample is shown in Figure 13. In this experiment, the specific binding of BiMABs to the CD3 receptor-complex on T cells and the target epitope CLDN18.2 could be verified for all antibodies. The results conclusively show that all five BiMABs bound bi-specifically to both desired epitopes.

3.3.3 POTENT INDUCTION OF T CELL ACTIVATION BY SELECTED BIMABS

In order to choose the best BiMAB candidate, each BiMABs´ ability to activate T cells was examined. To determine the efficacy of the five previously selected BiMABs in more detail, the correlation of T cell activation and lysis had to be investigated. Using the cancer target cell line NugC4, with an E:T ratio of 5:1 and a BiMAB concentration of 5 ng×mL^{-1}, target cell lysis and T cell activation were assessed via the flow cytometry-based T cell activation and cell cytotoxicity assay. As expected, the efficacy of BiMAB protein induced target cell lysis strongly depends upon its ability to activate T cells. This activation can be determined by the upregulation of the cell surface markers CD69 and CD25 on T cells. In the flow-cytometry-based assay of T cell activation six controls were implemented to assure the correct interpretation of the results (Figure 14-A). Importantly, the controls showed no overall increase in T cell activation compared to the level of untreated T cells. Furthermore, none of the control samples implemented for the cytotoxicity assay showed a noteworthy impact on the target cells.

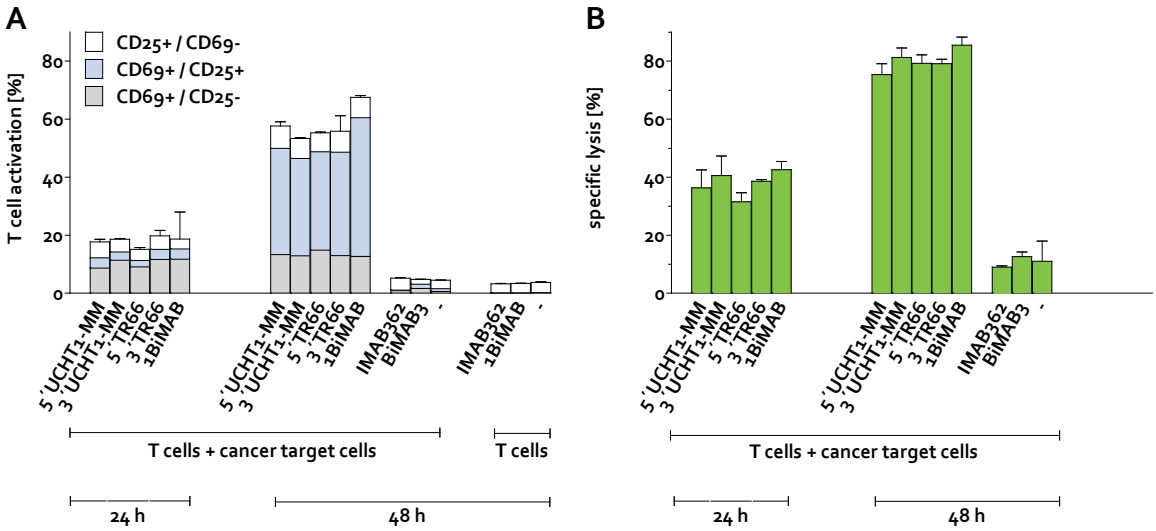

Figure 14: BiMAB induced cancer cell lysis correlates with T cell activation

Target cells [1×10^5 NugC4] were coincubated for 24 h or 48 h with 5×10^5 human T cells in the presence of 5 ng×mL^{-1} BiMAB protein. BiMAB3–specific for the TAA Plac1–as well as the mAb IMAB362 were used as control antibodies. (**A**) Expression of T cell activation markers CD25 and CD69 in response to BiMAB proteins was assessed via flow cytometric analysis. Samples contained one of five different BiMABs as specified on the X-axis. Cells were stained with a mixture of PI, and fluorophore-labeled mAbs anti-CD3, anti-CD25 and anti-CD69. By adding up the percentages (stacked bar graphs) measured for each stage of activation, the total percentage of activated T cells within a sample was shown. (**B**) BiMAB-mediated cytotoxicity of cancer cells was measured via flow-cytometry-based analysis of propidium iodide (PI) incorporation into cancer cell nuclei. The flow-cytometry data were analyzed by the software FlowJo to determine the percentage of T cell activation or target cell lysis. Error bars indicate standard deviation of duplicates within this one experiment. Results are representative of two experiments. E:T specifies effector to target ratio; 5´, N-terminal arrangement of the anti-CD3-scFv within the BiMAB; 3´, C-terminal arrangement of the anti-CD3-scFv within the BiMAB; mAb, monoclonal antibody.

However, in the presence of T cells, four CHO codon optimized BiMABs were able to activate approximately 60 % of CD3-positive (CD3+) T cells and mediated a final target cell lysis of circa 80 % after 48 h (Figure 14-B). An increase of 10 % in total T cell activation could be observed by 1BiMAB compared to the four other BiMAB proteins. After 48 h, all activated cells still showed the intermediate level of T cell activation being mainly CD69 and CD25 double positive. The maximum of the early CD69 upregulation is typically evident after 24 h and decreases thereafter, whereas CD25–being a late activation marker–reaches the highest level (being CD25+/CD69-) commonly after 72 hours [115]. Considering the still prominent high percentage of CD69+/CD25+ T cells in the assay, it was assumed that T cell activation and tumor cell lysis were still ongoing and had not reached their maximum, yet.

As seen in prior experiments, the differences in target cell lysis using this BiMAB concentration were rather small with regard to the four CHO codon optimized BiMABs. So far, 1BiMAB showed slightly enhanced lysis, probably permitted by the stronger T cell activation.

In summary, it could be demonstrated that a significant T cell activation is elicited by all five selected BiMABs in the presence of CLDN18.2-positive tumor cells. Nevertheless, with at least 10 % superiority in T cell activation, 1BiMAB had a small advantage over its competitors. Since no significant differences between these BiMABs at the present concentration have been assessed, no measurements after longer than 48 h incubation times were anticipated. Instead, a titration of the BiMAB proteins was decided, in order to find a BiMAB concentration-level that allows measurements with significant differences in BiMAB induced target cell lysis.

3.3.4 POTENT INDUCTION OF TARGET CELL LYSIS BY ALL FIVE BIMABS

In order to reveal the superiority of one BiMAB over the others, luciferase-based cytotoxicity assays with BiMAB dilution rows were performed. Increasing concentrations of 0.05, 0.1, 1.0, to 10.0 ng×mL^{-1} were applied, while the E:T ratio was adjusted to 5:1.. After 24 h and 48 h of incubation, samples were measured for luciferase signal. The IMAB362 and BiMAB4 used as negative control antibodies in this experiment did not show any cytotoxic effects towards the target cells.
As seen in prior tests, the cytotoxic efficiency of all five selected BiMABs resulted in a competent tumor cell lysis of around 95 % after 48 h at BiMAB concentrations of 1.0 and 10.0 ng×mL^{-1} (Figure 15). Slight differences were detected when comparing the lysis efficiency of all BiMABs at both time points at the lower concentration ranges (24 h: 0.05, 0.1 and 1.0 ng×mL^{-1}; 48 h: 0.05 and 0.1 ng×mL^{-1}). Based on statistical calculations [7] it was inferred that all other BiMABs induced a significant better cancer target cell lysis than BiMAB 5′TR66 (Table 13-A: 1-4) at low BiMAB concentrations.
By statistically comparing each remaining BiMAB with the other BiMABs (Table 13-A: 5-8,-B:9-10), we found the induced lysis at low concentrations (0.05 and 0.1 ng×mL^{-1}) was significantly higher for 3′TR66 and 1BiMAB. Consequently, it was concluded that at low concentrations both the 3′orientated TR66-scFvs triggered cancer target cell lysis best.
Moreover, it was found in the analysis that the lysis values of four BiMABs were closely correlating. Two BiMAB groups (Table 13-B: 9+10) could be formed consisting of two BiMABs each: Group1 = 5′UCHT1-MM and 3′UCHT1-MM; Group2 = 3′TR66 and 1BiMAB. Comparing the results of 5′UCHT1-MM to 3′UCHT1-MM, a similar efficiency at each step was detected (Table 13-B: 9). Even at the earlier time point of 24 h and at low concentrations the differences in lysis were negligible.

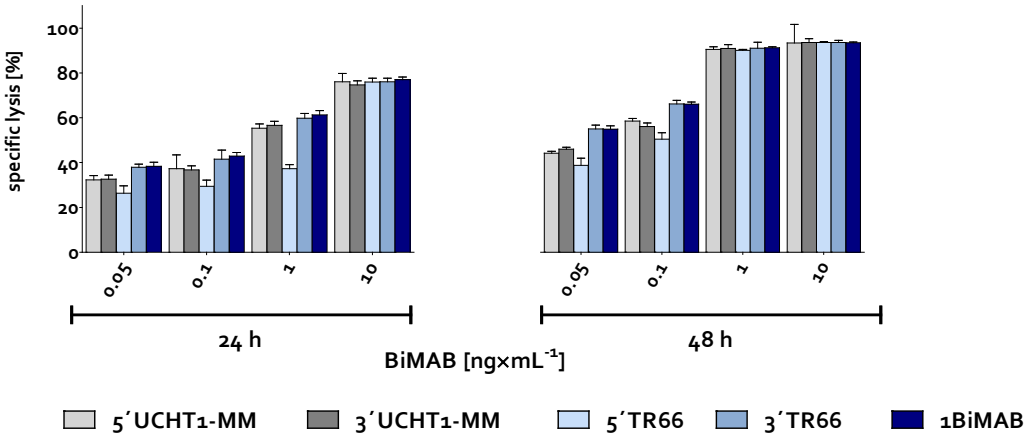

Figure 15: The titration of the five selected BiMAB proteins evidenced differences in the efficiency of target cell lysis.

A kinetic of target cell lysis mediated by BiMABs is shown. The respective cancer target cell line (NugC4-luc) was coincubated for24 h and 48 h with freshly isolated T cells. An effector to target ratio (E:T) of 5:1 was chosen. Coincubation was performed in the presence of four different concentrations of 0.05, 0.1, 1, and 10 ng×mL-1 Ni-NTA column purified BiMABs. Potency to induce specific cancer cell lysis was quantified with the luciferase-based cytotoxicity assay. Error bars indicate standard deviations of triplicates. Results are representative of two experiments. 5′ specifies N-terminal arrangement of the anti-CD3-scFvwithin the BiMAB; 3′, C-terminal arrangement of the anti-CD3-scFvwithin the BiMAB; MM, murine.

[7] Two-way ANOVA with the Bonferroni multiple comparisons test was performed using GraphPad Prism version 5.04 for Windows, GraphPad Software, San Diego California USA, www.graphpad.com

Table 13: 1BiMAB-mediated lysis is significantly higher compared to all four remaining BiMABs6

A

	BiMAB vs BiMAB	24 h				48 h			
	C_{BiMAB} [ng×mL^{-1}]	0.05	0.10	1.00	10.0	0.05	0.10	1.00	10.0
1	5′TR66 < 1BiMAB	****	****	****	ns	****	****	ns	ns
2	5′TR66 < 3′TR66	****	****	****	ns	****	****	ns	ns
3	5′TR66 < 3′UCHT1-MM	***	****	****	ns	***	*	ns	ns
4	5′TR66 < 5′UCHT1-MM	**	****	****	ns	*	****	ns	ns
5	5′UCHT1-MM < 3′TR66	**	ns	ns	ns	****	****	ns	ns
6	5′UCHT1-MM < 1BiMAB	**	**	**	ns	****	****	ns	ns
7	3′UCHT1-MM < 1BiMAB	**	**	ns	ns	****	****	ns	ns
8	3′UCHT1-MM < 3′TR66	*	ns	ns	ns	****	****	ns	ns

B

	BiMAB vs BiMAB	24 h				48 h			
	C_{BiMAB} [ng×mL^{-1}]	0.05	0.10	1.00	10.0	0.05	0.10	1.00	10.0
9	5′UCHT1-MM vs 3′UCHT1-MM	ns	ns	ns	ns	ns	ns	ns	ns
10	3′TR66 vs 1BiMAB (3′TR66)	ns	ns	ns	ns	ns	ns	ns	ns

C

	1BiMAB vs. BiMAB	24 h				48 h			
	C_{BiMAB} [ng×mL^{-1}]	0.05	0.10	1.00	10.0	0.05	0.10	1.00	10.0
11	5′UCHT1-MM	***	**	***	ns	****	****	ns	ns
12	3′UCHT1-MM	**	***	*	ns	****	****	ns	ns
13	5′TR66	****	****	****	ns	****	****	ns	ns
14	3′TR66	ns	ns	ns	ns	ns	ns	ns	ns

significance signature	
P < 0.0001	****
P < 0.001	***
P < 0.01	**
P < 0.05	*
P > 0,05	ns

Consequently, it was not possible to decide which consecutive order is favorable for the scFv of UCHT1-MM BiMAB variants. Both UCHT1-MM BiMABs appeared to be adequate candidates for pre-clinical experiments. Similarly, only minor differences between the levels of lysis were apparent between 1BiMAB and 3′TR66 (Table 13-B: 10).
The statistical significance for the differences in lysis is listed in Table 13-C: 11-14 for all four CHO codon optimized BiMABs with respect to the human codon optimized 1BiMAB.
Finally, after evaluating these results and considering the differences at low BiMAB concentrations the antibodies were rated according to their potency as follows:

1. 1BiMAB
2. 3′TR66
3. 5′& 3′UCHT1-MM
4. 5′TR66

At BiMAB concentrations higher than 1.0 ng×mL^{-1}, a respectable target cell lysis is elicited by all five selected BiMABs in the presence of CLDN18.2-positive tumor cells. When low concentrations were used, 1BiMAB was the best candidate regarding the induction of tumor cell lysis with marginal competitive advantages over 3′TR66. The latter was directly followed by 5′& 3′UCHT1-MM. All these BiMABs showed a significant better induction of target cell lysis than 5′TR66.

3.4 *IN VITRO* STUDIES– PRODUCTION AND CHARACTERIZATION OF MOST POTENT CANDIDATE–1BIMAB

After selection of 1BiMAB as the favorite bispecific antibody prototype, we aimed to validate in more detail the functioning of 1BiMAB within the implied therapeutic setting. The anticipated parameters of interest of *in vitro* assays were the observation of specific binding, a cytolytic synapse formation, T cell activation, and cytotoxicity towards TAA-positive target cells.

3.4.1 1BIMAB PRODUCER CLONES IDENTIFIED VIA ELISA

In order to gain sufficient protein amounts for these assays, a producer cell line that stably produces 1BiMAB was generated. To generate stable producer cell clones of the CLDN18.2 specific 1BiMAB, the Chinese Hamster Ovary cell line CHO-K1 and human embryonic kidney cell line HEK293 were chosen. The production of 1BiMAB by the cell line was first verified by immunofluorescence (IF) staining (Figure 12).
Because the protein production in CHO-K1 cells was less efficient regarding the positive stained cells (data not shown), the stable cell line generation was done with HEK293 cells only. Single cell cloning of this cell line via flow-cytometry sorting followed only when the previous IF staining revealed a sufficient amount of cells producing the bs-td-scAb.
For the subsequent detection of 1BiMAB in cell culture supernatant of HEK293 cells, a BiMAB specific ELISA (chapter 2.7.6) was used. Supernatants of HEK293 clones, which were positive tested for secretion of 1BiMAB, were collected over two weeks for a second test.
In this analysis, the 1BiMAB production was again checked for consistency, which could be detected in five (#1, #16, #28, #35 and #40) out of 26 HEK293-1BiMAB cell clones. Clones #1, 28, 35 and 40 had been chosen for expansion. Their 1BiMAB production efficiency was again quantified via an ELISA. All clones except for #35 expressed high levels of 1BiMAB and consecutive supernatant collections were possible. Finally, clone #28 was chosen as 1BiMAB producer clone and expanded in a 10-layer cell factory resulting in the collection of several liters of supernatant.

3.4.2 FEASIBILITY OF 1BIMAB PROTEIN PURIFICATION AND ANALYSIS

1BiMAB was purified by immuno-metal-affinity-chromatography (IMAC) as described in chapter 2.7.1. A representative SDS-PAGE analysis of the purified 1BiMAB from several fractions is shown in Figure 16-A. The FPLC chromatogram commonly displayed two peaks within the 1BiMAB elution process (data not shown).
Analysis of the elution fractions by SDS-PAGE revealed a band of the expected size (~54 kDa) as well as other bands in the fractions representing peak 1 (lane 3 and 4). The most prominent ones were approximately ~50 kDa and ~70 kDa in size. Those undefined fractions were discarded, the eluted protein from peak 2 was pooled (lane 5-10) and used for further experiments. Quality and purity of 1BiMAB were confirmed by Western blot analysis using reducing conditions. The Western blot analysis (Figure 16-B) revealed only a single band at the expected size of approximately ~54 kDa for the bs-td-scAb. None of the other proteins that co-eluted in peak 1 has been detected by the anti-6×His-Tag antibody in these pooled fractions.
Therefore, it was concluded that the contaminants of peak 1 were not degraded forms of the BiMAB, but rather unrelated host cell proteins that were separated. We gained 1BiMAB protein with a defined size of 54 kDa, which was dialyzed twice against PBS and finally against 200 mM arginine buffer.

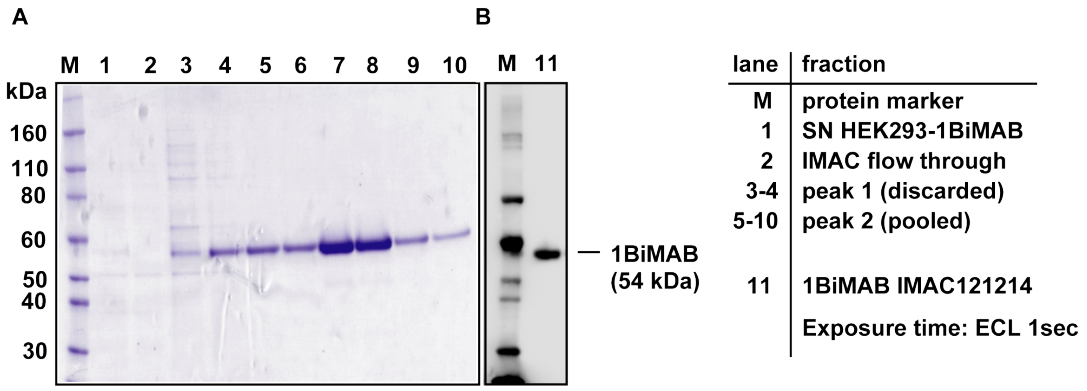

Figure 16: 1BiMAB protein could be purified from HEK293 supernatant via IMAC.

(**A**) Supernatant (SN) of monoclonal HEK293-1BiMAB#28 cells cultured without FCS was used to purify 1BiMAB by IMAC. Different fractions collected during the purification procedure were loaded on a 4-12 % Bis-Tris gel. A Coomassie staining of 1BiMAB in the following fractions was prepared: supernatant, flow through, and eight fractions of eluates. Only fractions of the IMAC peak 2 were pooled for further investigations and dialyzed against 200 mM arginine buffer. In (**B**) the pooled and dialyzed 1BiMAB protein is shown in a Western blot detected by a 6×His-Tag-specific mAb as 1^{γ} mAb and an Fc-specific 2^{γ} peroxidase-conjugated goat-anti-mouse IgG antibody. The protein was prepared using reducing conditions. ECL indicates enhanced chemiluminescence; IMAC, immobilized metal Ion affinity chromatography; kDa, kilo Dalton; M, protein marker; SN, supernatant.

3.4.3 PURIFICATION OF 1.3 mg 1BiMAB PROTEIN PER LITER SUPERNATANT

BiMAB concentration was determined by measurement at 280 nm with a NanoDrop 2000c under consideration of the extinction coefficient and the molecular weight of 1BiMAB. Protein parameters were determined (Table 14) via the ProtParam tool provided by the Expert Protein Analysis System (ExPASy)[8].

Several liters of 1BiMAB containing supernatant of HEK293-1BiMAB clone #28 were then collected. The mean value for all purified 1BiMAB protein yields was 1.3 mg per liter of cell culture supernatant. Purified protein was aliquoted and stored at -80°C for long time storage or kept at 4°C for immediate use.

Table 14: Protein parameter calculated by ProtParam tool

ExPASy-ProtParam calculated sample information	
Absorbtion260/280	0.63
Ext. Coeff. $\times 10^{-3}$ [M^{-1} cm^{-1}]	124.15
MW [kDa]*	54.19

1BiMAB QUANTIFICATION VIA A BSA CALIBRATION CURVE

1BiMAB quantification was achieved by protein determination according to a BSA standard. Gel electrophoresis including 1BiMAB and a BSA standard (0.05, 0.1, 0.5, 1 and 5.0 µg) followed by Coomassie staining, was performed to confirm the concentration already measured by the NanoDrop device.

Signal strength of 1BiMAB sample was compared with BSA signal strength to determine the protein concentration. The resulting concentration for 1BiMAB was 0.056 mg×mL^{-1} coincided well with the spectrophotometric data.

[8] http://web.expasy.org/protparam/

3.4.4 PURIFIED 1BIMAB PROTEIN–FUNCTIONAL CHARACTERIZATION

After the successful protein production, testing of several anticipated characteristics and functions of the 1BiMAB protein was required. Therefore, the tumor selectivity, the recruitment, and the activation of T cells; as well as the potency of redirected killing of tumor cells were more closely investigated using the following *in vitro* cell culture assays.

1BIMAB NANOMOLAR AFFINITY DETERMINATION BY SATURATION BINDING

The binding properties for 1BiMAB were verified by checking the specific binding to its two epitopes: CLDN18.2 and CD3ε. The binding specificities of 1BiMAB were studied by flow cytometric analysis, testing HEK293-CLDN18.2 cells expressing CLDN18.2 but not CD3. Human T cells that are positive for the TCR subunit CD3ε (CD3+) but negative for CLDN18.2 were analyzed the same way.
The expected cell surface expression of both epitopes was confirmed by flow cytometry for each cell line (data not shown). The concentration dependent binding of 1BiMAB to either freshly isolated human T cells or HEK293-CLDN18.2 cells was confirmed.
The affinity of 1BiMAB for CLDN18.2 and CD3ε was determined in this saturation-binding assay. The relative 1BiMAB binding was plotted against the increasing concentrations of 1BiMAB (Figure 17). The binding equilibrium was determined to be in the nanomolar range for both binding sites[9].
To rule out an unspecific binding of 1BiMAB, target cells that express neither CLDN18.2 nor CD3 (tested by flow cytometry–Figure 12) were subjected to the flow-cytometry-based binding assay. Unspecific binding of 1BiMAB to HEK293-Mock cells was not detectable (data not shown). The complete displacement of 1BiMAB by its parental mAb IMAB362 confirmed the specific binding of 1BiMAB to its target CLDN18.2 (data not shown).

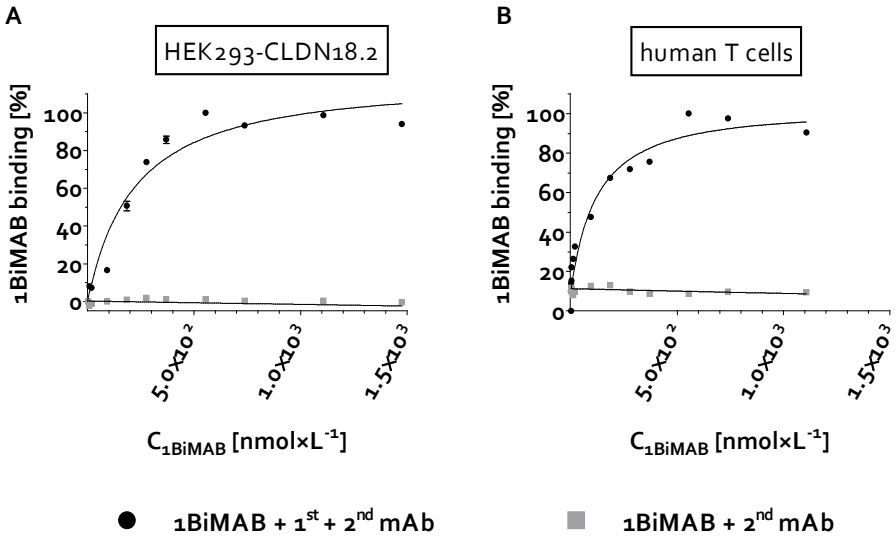

Figure 17:Binding affinities for 1BiMAB defined by saturation binding lay within the nanomolar range
Saturation binding of 1BiMAB to HEK293 cells stable transfected with CLDN18.2 (**A**) and human T cells were investigated (**B**). Cells were incubated with concentrations of serially diluted 1BiMAB. Bound BiMAB was quantified with flow cytometry after staining with 1ry 6×His-Tag-specific mAb followed by a 2ry APC labeled goat-anti-mouse mAb. MFI was normalized to the respective strongest signals and plotted against various concentrations of 1BiMAB.

[9] The half-maximal binding values were obtained by computational analysis using GraphPad Prism (version 5.04 for Windows, GraphPad Software, San Diego California USA). Calculations were obtained by performing Prism model: Nonlinear regression with binding saturation-one site - total and nonspecific binding.

STRICT TAA-DEPENDENT TARGET CELL BINDING AND LYSIS BY 1BIMAB

Specific binding was evaluated for 1BiMAB considering the TAA CLDN18.2 and its structurally similar splice variant CLDN18.1. HEK293 cells, overexpressing either the antigen CLDN18.2, CLDN18.1, or empty vector stably transfected HEK293 (Mock control), were chosen for binding assays and luciferase-based cytotoxicity experiments. Cell lines are listed in Table 15.
A specific concentration-dependent binding of 1BiMAB to cells expressing CLDN18.2 was measured (Figure 18-A), but no binding was detected when using the highest concentration of 1,000 ng×mL^{-1} of the splice variant CLDN18.1 or the Mock cells.
No signal was detected using 1,000 ng×mL^{-1} of the control BiMAB2 with any of the three cell lines, excluding unspecific binding of BiMABs. For the use in a luciferase-based cytotoxicity assay, HEK293-CLDN18.2, HEK293-CLDN18.1, and HEK293-Mock cells were electroporated with luciferase IVT-RNA to gain cell lines expressing luciferase. In this assay, 1BiMAB elicited a highly significant lysis of CLDN18.2-positive cells after 48 h compared to all control samples (Figure 18-B).

STRICT TAA-DEPENDENT T CELL ACTIVATION TRIGGERED BY 1BIMAB

To further prove the target dependency of 1BiMAB, the induced T cell activation using cell lines that have various expression-levels of the TAA (Figure 18-D) ranging from high (green) to low (brown) to very low or no expression (blue) were examined; the cell line MCF7 served as negative control (dark blue). The expression levels were determined in two independent experiments by quantitative RT-PCR. (qRT-PCR data was kindly provided by a colleague). The chosen cell lines are listed in Table 15.

Table 15: Tumor cell lines used and their origin

Cell line	Cancer type	CLDN18.2 expression
HEK293-CLDN18.2	stably transfected	high
HEK293-CLDN18.1	stably transfected	none
HEK293-Mock	stably transfected	none
NugC4	Gastric lymph node cancer	medium
DAN-G	Pancreatic cancer	low
MKN7	Gastric cancer	none
KP-4	Pancreatic cancer	none
SNU1	Gastric cancer	none
MCF7	Breast cancer	none

All cell lines were tested in the flow cytometry-based T cell activation assay. The status of activations mediated by 5 ng×mL^{-1} 1BiMAB was assessed via flow cytometry after 144 h of coincubation (Figure 18-C). Almost 100 % of T cells coincubated with NugC4 cells and 1BiMAB were in the late state of activation being CD25+/CD69- whereas approximately 75 % of T cells were activated in the presence.
However, in contrast to the previously activated CD25+/CD69- T cells, which were co-incubated with NugC4 cells, T cells coincubated with DAN-G were mainly CD69+/CD25+, indicating an ongoing T cell activation. During the 144 h of coincubation, cells were microscopically observed to assess the induction of T cell activation detectable by T cell clustering.
In comparison to the cell line NugC4, offering a high expression of the TAA CLDN18.2, only a late induction of T cell activation was observable by microscope and measurable via flow cytometry. Thus, the progression speed of T cell activation seemed to be greatly influenced by the expression level of the TAA on the target cell surface.

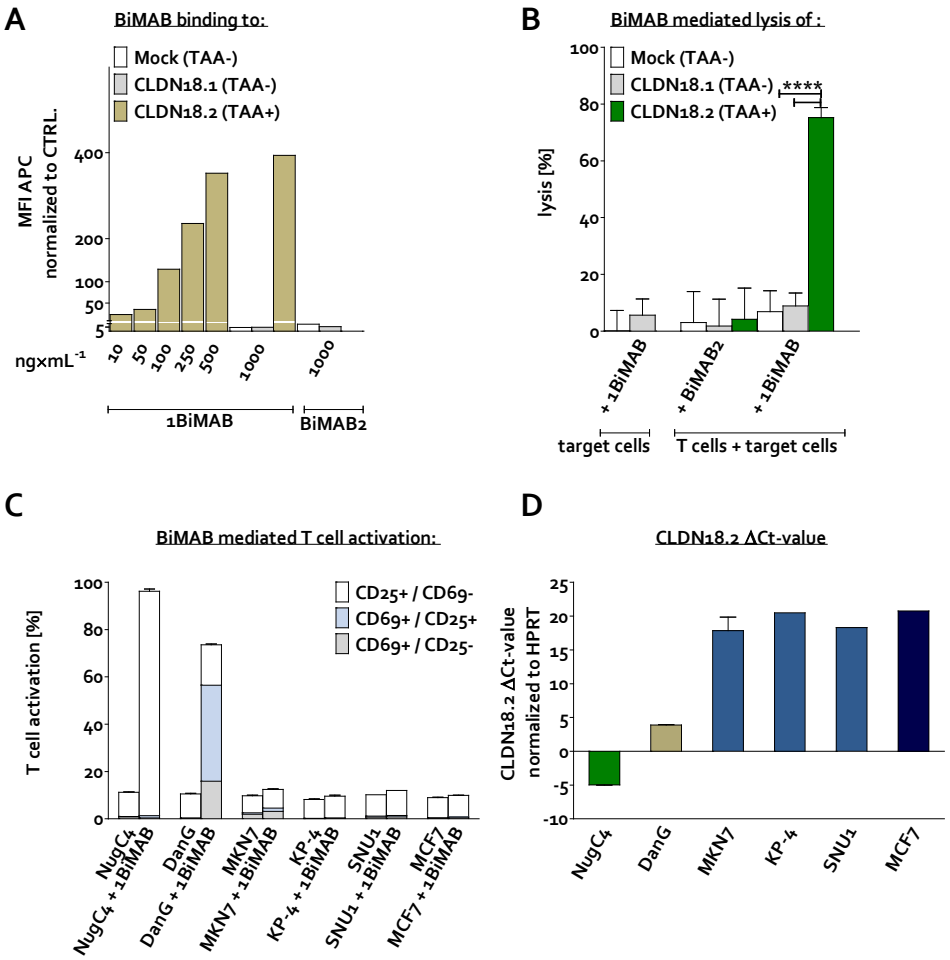

Figure 18: 1BiMAB binding, T cell activation and target cell lysis is strictly TAA dependent.

In (**A**) the focus of investigation laid on the binding to the transgene CLDN18.2 (TAA+), its isoform CLDN18.1 (TAA-), and the corresponding Mock HEK293 cell line (TAA-). Binding of 1BiMAB with increasing doses from 10-1000 ng×mL^{-1} were used. The comparison of binding properties of 1BiMAB to all three-cell lines is shown using the highest concentration of 1000 ng×mL^{-1} of 1BiMAB and control BiMAB2. The stain occurred using a primary 6×His-Tag-specific mAb and a secondary APC-labeled-goat-anti-mouse mAb. APC mean fluorescence intensity (MFI) of histograms reflecting BiMAB binding was assessed by flow cytometry and was analyzed using FlowJo software. Background MFI signal (measured for the sample using primary and secondary mAb only) were subtracted from the MFI of all samples. In (**B**) the specificity of cytotoxic activity of 1BiMAB in the presence or absence of the TAA CLDN18.2 was under investigation. The ability to induce TAA-specific cancer cell lysis was quantified by a luciferase-based cytotoxicity assay. Target cells were electroporated with 5 µg luciferase IVT-RNA. 1×10^4 target cells were then coincubated with 5×10^4 T cells including 5 ng×mL^{-1} 1BiMAB or control BiMAB2 in a 96 well format. In further controls, target cells together with 1BiMAB were incubated in the absence of T cells. Error bars indicate the standard deviation of six replicates. (**C**) 1BiMAB induced T cell activation only in the presence of the TAA. Cancer cells were incubated for 144 h in the presence or absence of 5 ng×mL^{-1} 1BiMAB protein together with human T cells. An E:T ratio of 5:1 was used. Expression of T cell activation markers was detected by four-color flow cytometry using a mixture of PI, and fluorophore-conjugated mAbs anti-CD3, anti-CD25, and anti-CD69. Error bars show standard deviations of duplicates. (**D**) Cancer cell lines were tested for levels of expression of tumor-associated antigen via qRT-PCR. qRT-PCR data was generated from the total RNA of the six indicated tumor cell lines. The breast cancer cell line MCF7 (dark blue bar) was chosen as CLDN18.2-negative control. NugC4 and DAN-G cancer cell lines were chosen as positive control cell lines (green and brown bars). ΔCt-values of CLDN18.2 expression were normalized by subtracting the Ct-value of the housekeeping gene HPRT and were calculated from two independent experiments. mAb indicates monoclonal antibody; CLDN18.2 (TAA+), CLDN18.2 expressing HEK293 cell line; CLDN18.1 (TAA-), CLDN18.1 expressing HEK293 cell line but TAA negative; Mock (TAA-), Mock HEK293 cell line but TAA negative; APC, allophycocyanin; ****, highly significant ($p<0.0001$).

However, in the absence of TAA expression or in the presence of the highly related surface molecule CLDN18.1, 1BiMAB showed no T cell activation *in vitro* even after an extensive coincubation time of 144 h (Figure 19). No signs of unspecific activation in the absence of CLDN18.2 were observed, but a specific activation was measured via flow cytometry using a pancreatic cancer cell line (DAN-G) that expresses only low levels of CLDN18.2. In conclusion, 1BiMAB strictly targeted CLDN18.2-positive cells and T cells, resulting in the highly selective and specific activation of effector cells.

3.4.5 EVIDENCE OF 1BIMAB-MEDIATED T CELL ACTIVATION AND CYTOLYTIC FUNCTION

In this chapter, 1BiMAB´s mode of action was further investigated. The interaction between 1BiMAB and T cells, the recruitment of different T cell subsets, characteristics of their activation as well as the association with target cell lysis was verified.

1BIMAB INDUCED FORMATION OF CYTOLYTIC SYNAPSES

The picture in Figure 19-E is a model illustrating the process of a cytolytic synapse formation initiated by bs-td-scAbs. In this setting, 1×10^5 NugC4 cells cultured in human DC-medium were coincubated at an E:T ratio of 5:1 with freshly isolated T cells in the presence of 5 ng×mL^{-1} 1BiMAB. Pictures were taken with a Nikon Eclipse TS100 inverted microscope 24 h after coincubation.
1BiMAB visibly redirects several T cells to its target, forming a cytolytic synapse (labeled by an arrow in Figure 19-A). The formation of a cluster of T cells surrounding and covering the cancer cell (labeled by an arrow in Figure 19-B) characterizes the successful activation and proliferation of a T cell initiated by its physical linkage to a tumor cell.
The next step is an efficient target cell lysis. In comparison with the control samples (Figure 19-C and D) an increase in the total number of effector cells was obvious. As control, NugC4 target cells were coincubated with T cells in the absence of BiMAB (Figure 19-C). In Figure 19-D, the control BiMAB3 (5´Plac1-3´TR66) was added to the cells. Control BiMAB3 shares the same CD3 binding arm as 1BiMAB but is restricted to the TAA Plac1 that is not expressed by NugC4 cells.
Both controls show no signs of cytolytic synapse formation, T cell clustering, or target cell killing. This confirms that only the crosslink between CLDN18.2 and the CD3ε chain mediated by 1BiMAB leads to a specific activation of T cells.
Microscopic analysis was further included in *in vitro* assays as a visibility control. Any assumptions concerning T cell activation and cytotoxicity that were derived from observations of these visibility controls were verified by *in vitro* T cell activation and cytotoxicity assays. Results of these analyses are described in the next chapters.

1BIMAB INDUCED T CELL PROLIFERATION DEPENDENT ON THE PRESENCE OF TAA

To assess the microscopically observed 1BiMAB triggered T cell proliferation, CFSE labeled T cells were incubated with CLDN18.2-positive target cells at an E: T ratio of 5:1 in the presence of 5 ng×mL^{-1} 1BiMAB protein. CFSE fluorescence was analyzed using flow cytometry to trace the proliferation of lymphocytes induced by 1BiMAB (Figure 20-B). CFSE is retained within the cells and evenly distributed in dividing cells, resulting in a bisecting reduction of the CFSE intensity with each division. Here the fluorescence is presented as distinct peaks in a histogram view (Figure 20-A). Each peak indicates a generation of proliferating T cells, while the number of peaks directly correlates with the number of cell division cycles.

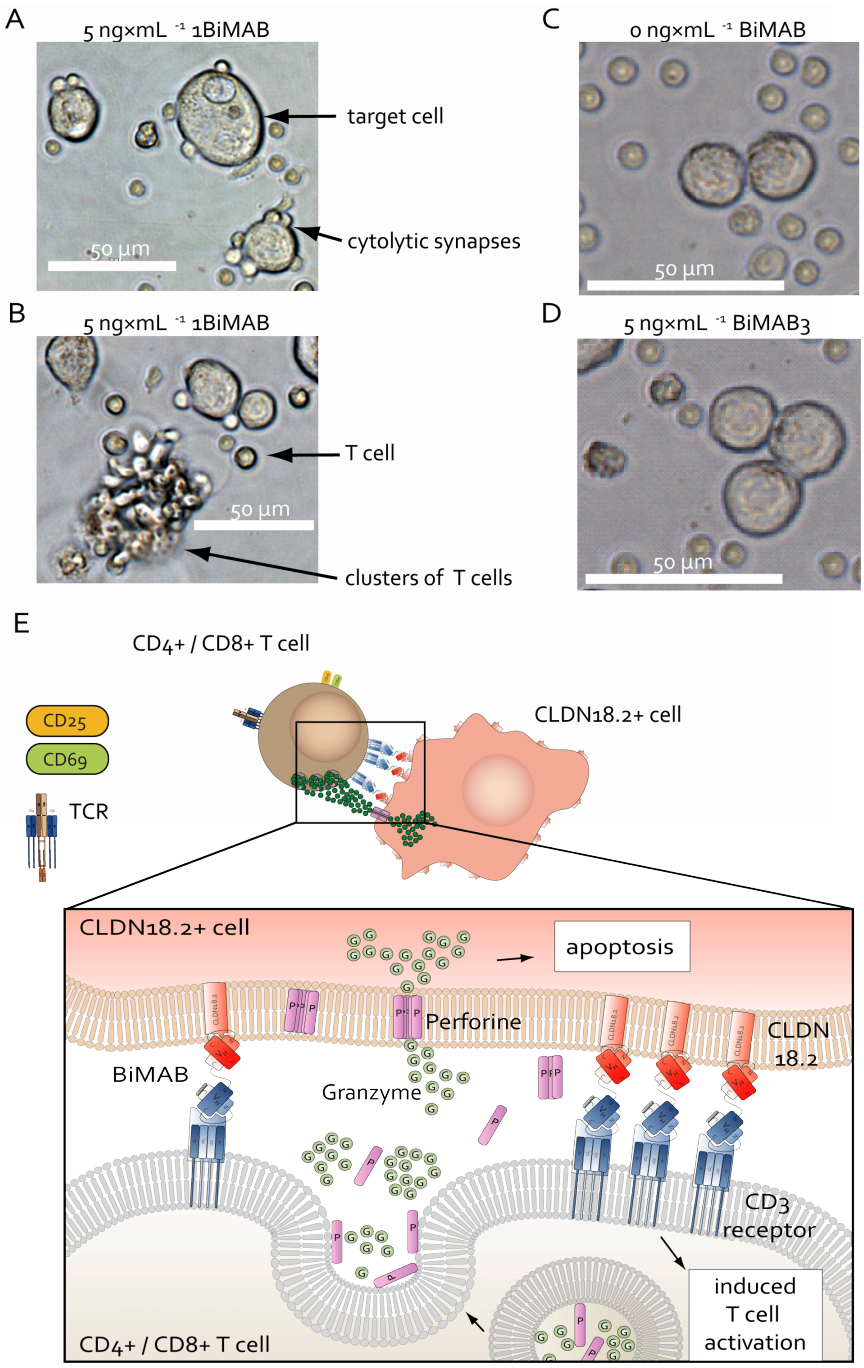

Figure 19: 1BiMAB induced cytolytic synapse formation as visualized by microscopic imaging

(**A&B**) Microscopic image of 1BiMAB triggered cytolytic synapses and T cell clustering. Black arrows indicate the noteworthy details: T cell alone, clustering T cells, vital cancer cells, or the formed cytolytic synapse between T cells and cancer cells. (**C&D**) Microscopic images of control samples are depicted. In this assay cancer cells [1×10^5 NugC4] were coincubated with 5×10^5 human T cells at an E:T of 5:1. Coincubation lasted 24 h, using a six well format in the presence of 5 ng×mL^{-1} FPLC purified 1BiMAB (**A&B**). Either 0 ng×mL^{-1} BiMAB (**C**) or 5 ng×mL^{-1} Ni-NTA purified control BiMAB3 (**D**) were added to control samples. The scale bar represents 50 µm. (**E**) is a cartoon illustrating the cytolytic synapse between T cells and cancer cells induced by 1BiMAB and the resulting induced cellular mechanisms are shown. E:T specifies effector to target ratio; FPLC, fast protein liquid chromatography; G, Granzyme; Ni-NTA, nickel-nitrilotriacetic acid; P; Perforin; CD4+, CD4-positive T cells; CD8+, CD8-positive T cell; CLDN18.2+ cell, CLDN18.2-positive cells.

A

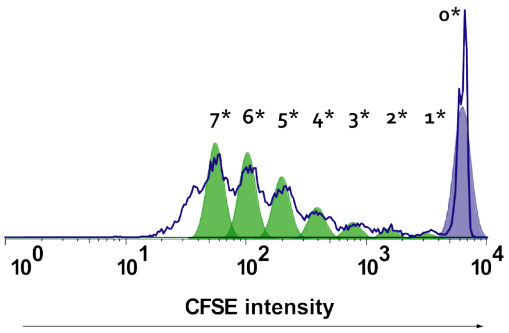

B

*		T cells + CC + 1BiMAB	T cells + CC	T cells + 1BiMAB	T cells
Generation	0	29.87	99.82	97.81	96.31
	1	1.32	0.02	2.06	3.49
	2	2.43	0.01	0.09	0.15
	3	3.75	0.00	0.00	0.01
	4	7.23	0.00	0.01	0.03
	5	14.17	0.00	0.03	0.01
	6	19.51	0.00	0.00	0.00
	7	21.71	0.15	0.00	0.00
total proliferation		70.13	0.18	2.19	3.69

Figure 20: 1BiMAB mediates T cell proliferation dependent on the presence of the TAA CLDN18.2

A mixture of CD4 and CD8 positive T cells were enriched from freshly isolated PBMCs and labeled with 8 µM CFSE. Afterwards, T cells were cocultured with or without TAA-positive cancer cells (NugC4) at a ratio of 5:1 in the presence or absence of 5 ng×mL-1 1BiMAB. The decrease in CFSE signal indicating T cell proliferation was determined after 5 days by flow cytometry. In the left panel (A), the different generations of proliferating T cells are shown in detail. T cell proliferation of one representative sample (T cells + CC + 1BiMAB) is depicted. T cell proliferation for distinct generations was detected by FlowJo´s software tool "proliferation." Each generation is indicated by a green label and a numbered asterisk. Depicted in blue is the initial T cell population, termed generation zero ("0*"). The right panel (B) gives a brief overview of the percentages of T cell proliferation for the indicated samples. CFSE stands for carboxyfluorescein succinimidyl ester; CC, cancer target cells; E:T, effector to target ratio; *, generation of proliferating T cells.

The asterisk zero indicates the position of the undivided T cells (blue peak = generation 0), whereas asterisk one to seven indicate the successive generations of proliferating T cells (green peaks). The amount of proliferating T cells in percent for each sample is given in the table of Figure 20-B.
A clear proliferative effect, mediated by 1BiMAB (a total of 70.13 % proliferating T cells) in the presence of the TAA on NugC4 cells, was observed, while in the absence of 1BiMAB only 0.18 % of T cells proliferated (99.82 % T cells in generation 0).
T cells alone, in the presence or the absence of 1BiMAB, did not show any increase in proliferative properties either.

INDUCTION OF CONSIDERABLE GRANZYME B ACCUMULATION IN HUMAN T CELL BY 1BIMAB

We next investigated the lytic potential of T cells activated by 1BiMAB protein. Special consideration was put to the pro-apoptotic enzymes contained in the lytic granules. Upon stimulation, cytotoxic T cells increase the production of the lytic effector molecule Granzyme B.
These newly produced effector molecules are aimed either for refilling of secretory vesicles or for a direct release into the cytolytic synapse [65]. In this assay, the upregulation of the effector molecule Granzyme B was measured (Figure 21) in response to 1BiMAB engagement of cytotoxic T cells for target cell lysis.
A strong upregulation of Granzyme B, mediated by 1BiMAB was observed in flow cytometric measurements. Two defined concentrations 1.0 and 5.0 ng×mL^{-1} of 1BiMAB protein were tested. Both concentrations induced an increase in Granzyme B accumulation within the T cells causing a 20-fold higher MFI of the Granzyme B-PE antibody compared to control samples.

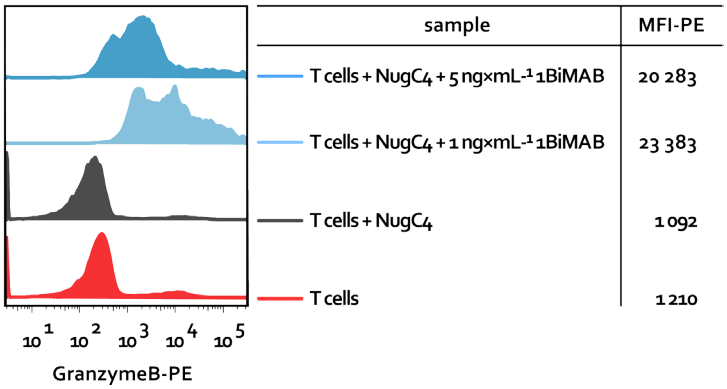

Figure 21: 1BiMAB induces the upregulation of Granzyme B production in human T cells

The influence of T cell activation on Granzyme B production in human T cells mediated by 1BiMAB was investigated. T cells were incubated in the presence of cancer cells (NugC4; E:T = 5:1) with 0 ng×mL^{-1}, 1 ng×mL^{-1} or 5 ng×mL^{-1} 1BiMAB. T cells alone served as a further control. After 96 h of coincubation, T cells were harvested followed by an intracellular staining with an anti-GrB-PE mAb for flow cytometric analysis. The MFI of anti-Granzyme B-PE was calculated from histograms using FlowJo software. For normalization, the MFI signal of unstained sample T cells + cancer cells + 5 ng×mL^{-1} 1BiMAB was subtracted from all samples. MFI stands for mean fluorescence intensity. PE indicates phycoerythrin; mAb, monoclonal antibody.

DOSE DEPENDENT 1BIMAB-MEDIATED T CELL EFFECTOR FUNCTIONS

The cytolytic potential of T cells (isolated from four different donors) triggered by 1BiMAB was determined in a cytotoxicity assay and the results are shown in Figure 22-A. Increasing concentrations of 1BiMAB ranging from 0.001-5,000 ng×mL^{-1} resulted in a dose-dependent increase of lytic activity of the T cells.

Comparing the strength of lysis among T cell donors, a high variability was noted. At low concentrations of between 0.001 and 0.1 ng×mL^{-1} 1BiMAB, an initial lysis of around 10-20 % could be determined for T cells of donors 1 and 2 after 48 h coincubation, whereas donor 4 showed no 1BiMAB-mediated lysis until that time point.

A much higher lysis was observed for the T cells from donor 3 starting with 54 % lysis at the lowest concentration. Nevertheless, EC_{50} values from the dose-response curves that certified a potent 1BiMAB activity in the picomolar range between 11-459.1 pg×mL^{-1} could be defined.

The different trends of the four curves clearly indicate that each population of T cells had their own sensitivity, reactivity, and responsiveness in this cytotoxicity assay. Regardless of these differences, all T cells were recruited by 1BiMAB for a total lysis of target cells reaching 80 –100 %.

For a closer look at the T cells, the *de novo* expression of T cell activation markers CD25 and CD69 mediated by 1BiMAB protein was assessed during a cytotoxicity experiment presented in figure 12-B. Correlations between the dose dependent lysis of target cells and T cell activation were revealed. In the absence of 1BiMAB a total of ~6 % of T cells were in an activated state, whereas 3.25 % of T cells were in the early stage of activation (CD69+/CD25- T cells), 0.09 % in the median stage (CD25+/CD69- T cells) and 3.15 % in the late stage of activation (CD25+/CD69- T cells).

A concentration dependent T cell activation was observed with increasing concentrations of 1BiMAB. In the presence of target cells and after 48 h incubation time with 0.001 ng×mL^{-1} 1BiMAB, there was already an upregulation of CD69 in ~9 % of the T cells.

In all other samples, the amount of early-activated T cells expressing CD69 but not CD25 reached values between 22-30 %.

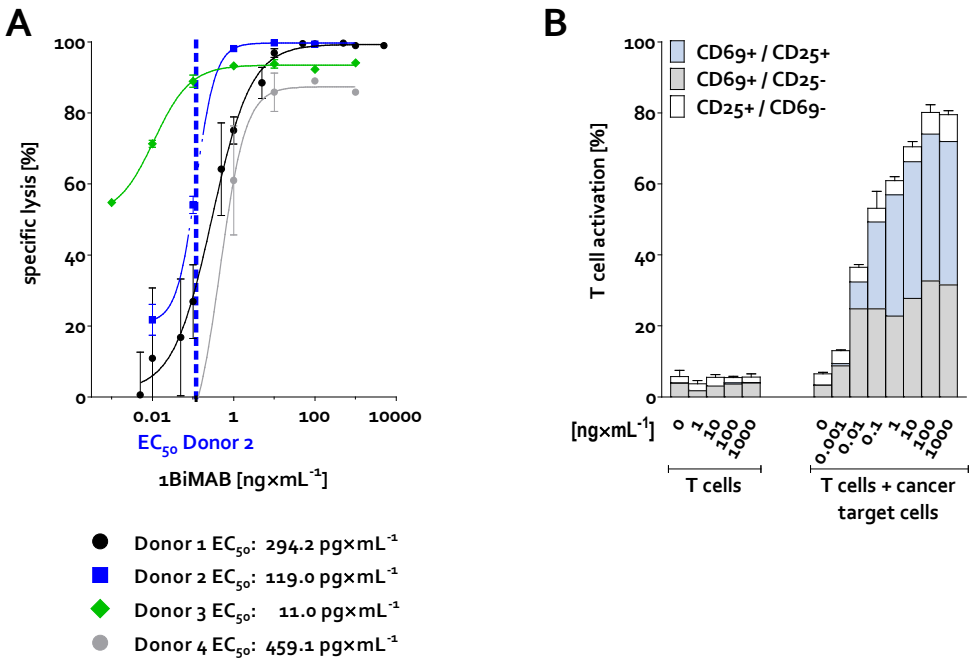

Figure 22: 1BiMAB induced T cell effector functions in a donor- and dose-dependent manner

(**A**) Cytotoxic activity induction by 1BiMAB is T cell donor dependent. Dose-dependencies were analyzed for T cells from four selected healthy donors. Cancer cell lysis was determined by the luciferase-based cytolytic assay after 48 h. EC50 for donor 2 is depicted representatively by a vertical blue dotted line. (**B**) T cell activation in response to different doses of 1BiMAB is shown. T cells isolated from the blood of a healthy donor were cocultured with NugC4-luc cancer cells at an E:T of 5:1 in the presence of indicated 1BiMAB concentrations for 48 h. Samples were subjected to a four-color staining using a mixture of PI, and fluorophore-conjugated anti-CD3, anti-CD25, and anti-CD69 mAbs and analyzed via flow cytometry. The PI negative and CD3-positive subpopulation was investigated for the expression of the activation marker CD25 and CD69. Error bars give standard deviations of the replicates. EC50 indicates half-maximal effective concentration.

The upregulation of the late activation marker CD25 was clearly initiated at a 1BiMAB concentration of 0.01 ng×mL^{-1}, resulting in an increase of up to 7.53 % CD69+/CD25+ T cells. At this concentration, no changes were determined for T cells in the late stage of activation (CD25+/CD69-).
At higher concentrations ranging from 0.1-1000 ng×mL^{-1} 1BiMAB mediated an even higher upregulation of CD25 with between~24-41 % of T cells expressing CD69+/CD25+, in a dose dependent manner. When the higher concentrations of 1BimAB were added, the number of CD25+/CD69- expressing T cells ranged from 3 % slightly increasing with 1BiMAB concentrations up to 7.52 %.
A clear shift from the median to the late stage of activation indicated by a significant increase in CD25+/CD69- T cells was not observed after 48 h. In any case, the maximum percentage of CD25+/CD69- T cells was not expected earlier than 72 h after activation [115].
However, by adding together the percentages of the different activated T cell populations from each sample, the dose dependent increase in T cell activation became even more evident. This led to a conclusion that is consistent with the lytic kinetics: an increasing dose of 1BiMAB protein leads to an increase of total activated T cells.

1BiMAB-MEDIATED ACTIVATION OF CD4- AND CD8-POSITIVE T CELLS

The contribution of different T cell subtypes in redirecting target cell lysis mediated by 1BiMAB is investigated in this chapter. PBMCs from one donor were divided into four fractions. From each fraction either CD4-positive, CD8-positive or total T cells were isolated while the fourth PBMC fraction remained untouched (chapter 2.5.6). A further T cell population was created by mixing CD4-positive and CD8-positive cells in a ratio, which resembles that of the whole T cell fraction.
The effector function of all T cell populations in the presence of 5 ng×mL^{-1} 1BiMAB and tumor cells was measured at five different time points– after 8 h, 16 h, 24 h, 48 h, and 72 h as depicted in Figure 23-A.
The total percentage of activated T cells after 48 h was between 70 % and 80 %. Thus, all five T cell groups– CD4-positive, CD8-positive, the mixture of CD4-positive & CD8-positive t cells, Pan-T cells, and PBMCs–were activated by 5 ng×mL^{-1} 1BiMAB. Regarding the late activation (48 h-72 h), all subsets were more or less equally activated (Figure 23-C).
Comparing all subsets of T cells in Figure 23-B, the fastest T cell activation was observed in CD8 after 8 h while CD4 T cells were not activated yet. However, the CD4 T cells subset showed the highest percentage of CD69 expression in comparison to all other subsets after 16 h.
A synergistic effect in T cell activation by the combination of CD4-positive and CD8-positive T cells compared to the usage of CD8-positive T cells alone was not observed. It even seems as if CD4-positive T cells regulated the reactivity of CD8-positive T cells.
At the earliest time-point of 8 h little or no activation could be observed in the three samples that contained a mixture of CD4-positive and CD8-positive T cells. (CD4+ & CD8+ T cells, Pan-T cells, as well as in the samples of PBMCs.) In contrast, 40 % of the T cells in the group of CD8-positive where already activated after 8 h.
The influence of CD4-positive T cells might be due to the action of regulatory T cells (Tregs), constitutively expressing CD4+/CD25+. It has been shown by others that Tregs are a common constituent of the T cell population and modulate the effector function of immune cells thus keeping a balanced immune response [116, 117].
The control BiMAB3 that shares the same scFv for CD3 as 1BiMAB but has a different TAA binding specificity elicited no T cell activation in this assay. Neither did the TAA CLDN18.2-specific parental mAb IMAB362. Several additional control samples were tested to exclude 1BiMAB independent effects influencing the T cell activation.
All five T cell groups were studied for activation either in the absence of 1BiMAB protein (T cells + NugC4-luc) or in the absence of target cells (T cells + 1BiMAB). None of these controls showed an unspecific activation of the respective T cell subtype (data not shown).
To summarize the principle point, CD4-positive T cells responded to 1BiMAB similarly as CD8-positive T cells with the main difference being the delayed onset of CD4-positive T cell activation. A clearly enhanced or reduced T cell activation was not observed when comparing the results of CD8-positive T cells with regards to the other outcomes. Consequently, it seems that a mixture of CD4-positive and CD8-positive T cells sustained an intermediate activation level between both T cell subtypes.

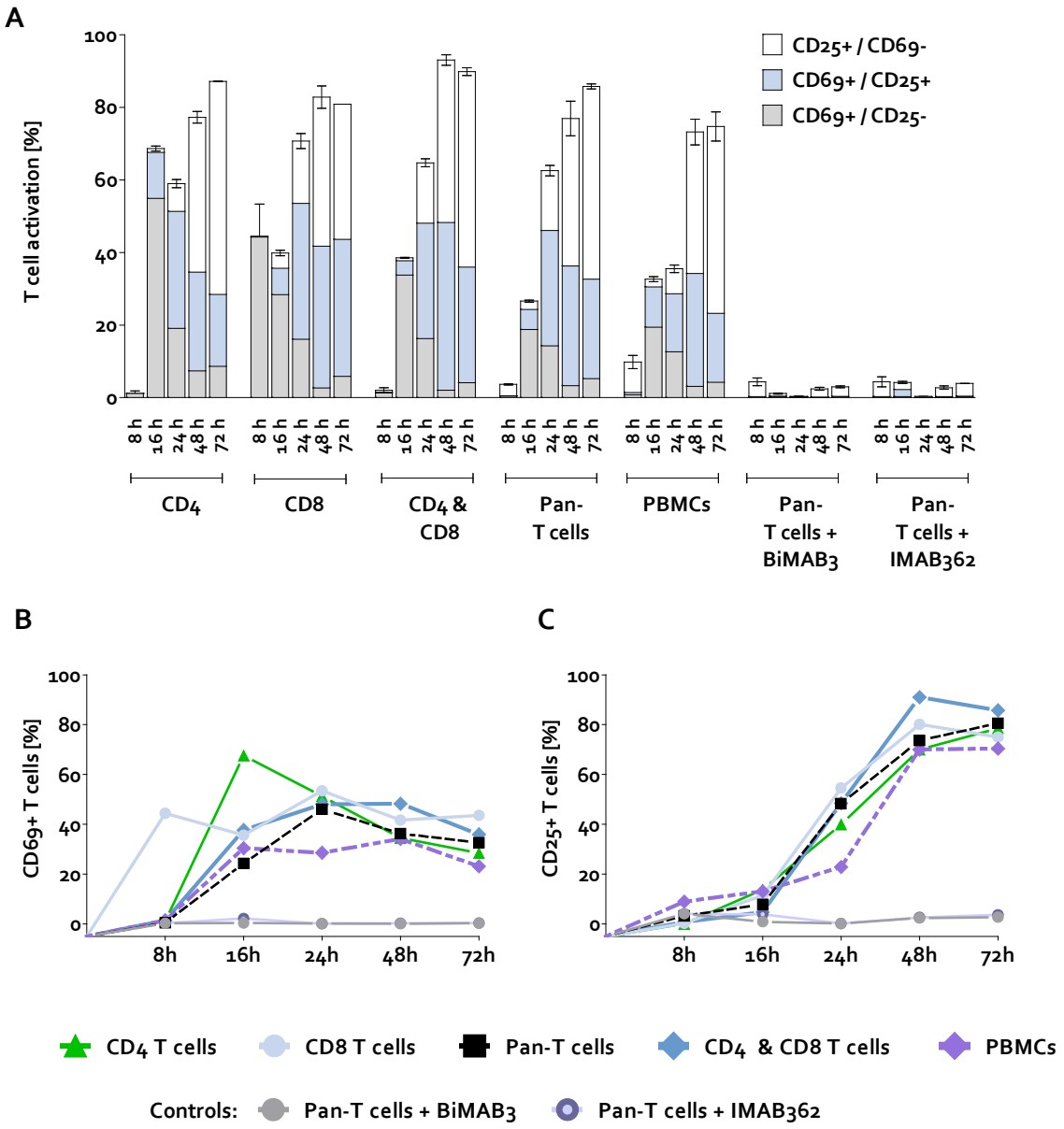

Figure 23: CD8 and CD4-positive effector cells contribute to 1BiMAB-mediated T cell activation

Five different effector cell subsets were isolated: PBMCs, CD4-positive T cells (CD4), CD8-positive T cells (CD8), CD4- and CD8-positive T cells together (CD4 & CD8), and "untouched" T cells (Pan-T cells). All subsets were enriched via MACS separation from one donor of human PBMCs. T cells and NugC4-luc cancer target cells were incubated at an E:T ratio of 5:1 in the presence of 5 ng×mL^{-1} 1BiMAB. After the indicated time points (8 h,16 h,24 h,48 h and 72 h), a five-color flow cytometry analysis of CD3, CD25, CD69 and CD45 expression on the cell surface of effector cells was done using a mixture of PI, and fluorophore-conjugated mAbs. An overview is given in (**A**) for 1BiMAB-induced T cell activation of different PBL subsets.

In (**B-C**) T cell activation kinetics (%) are shown for all indicated PBL subsets. Panels show progressive early CD69+ and late CD25+ expression due to T cell activation.

More explicit in (**B**) are the percentages of T cell populations determined by flow cytometry, positive for the early activation marker CD69. CD69+/CD25- & CD69+/CD25+ T cells are depicted for each subset, respectively.

In (**C**) effector cell subsets are positive for the late activation marker CD25 (CD25+/CD69- & CD25+/CD69+). Error bars indicate standard deviation of duplicates. PBMCs indicates peripheral blood mononuclear cells; BiMAB3, (5´Plac1-3´TRR66) Ctrl.-BiMAB; PBL, peripheral blood lymphocytes, "untouched T cells, no MACS beads are attached to T cells during T cells separation.

CD8- AND CD4-POSITIVE T CELLS BOTH CONTRIBUTE TO REDIRECTED TARGET CELL LYSIS BY 1BIMAB

Corresponding to the T cell activation assay, the ability of 1BiMAB to mediate target cell killing was measured by each T cell group, via a luciferase-based cytotoxicity assay. All samples were normalized to L_{min} consisting of Pan-T cells and target cells but no BiMAB.
The comparison of the data in Figure 23 illustrates differences between all T cell subsets with regard to L_{min}.
As already indicated by the T cell activation data, CD4-positive T cells were also involved in the process of 1BiMAB-mediated target cell killing, but compared to the Pan-T cell subset they had somewhat delayed kinetics.
Most effective lysis was found using the CD8-positive T cells population, providing the highest cytotoxicity values. T cells from the Pan-isolated group or the mixture of CD4-positive & CD8-positive T cells had almost identical lytic efficiencies. The control BiMAB3 triggered no target cell lysis.
Finally, it can be summarized that 80 % of all kinds of T cells isolated by MACS separation were activated by 1BiMAB and contributed to the target cell lysis. Therefore, a clear correlation for each T cell subtype is apparent between the curves of total activation and their target cell lysis.

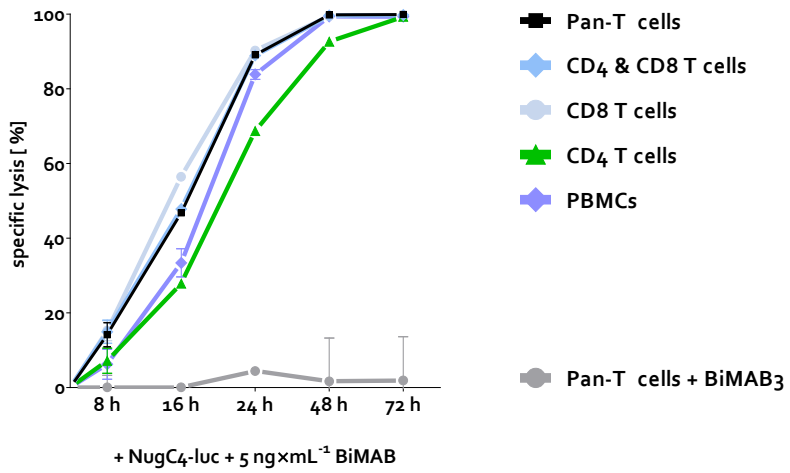

Figure 24: 1BiMAB induced cancer cell lysis engaging different subsets of effector cells
Effects of five different PBL cell subsets on cancer cell lysis induced by 1BiMAB were observed in a 72 h kinetic analysis. Five different effector cell subsets were isolated: PBMCs, CD4-positive T cells (CD4), CD8-positive T cells (CD8), CD4- and CD8-positive T cells together (CD4 & CD8), and "untouched" T cells (Pan-T cells). T cells were incubated at an E:T ratio of 5:1 with NugC4-luc cancer target cells in the presence of 5 ng×mL^{-1} 1BiMAB. The relative contribution of CD4-positive or CD8-positive T cells to redirected cancer cell lysis was determined after the indicated time points by luciferase-based cytotoxicity assay. Values determined for the samples of Pan-T cells in the presence of target cells were used as 0 % lysed cells (L_{min}). Samples containing Pan-T cells together with target cells in the presence of 5 ng×mL^{-1} 1BiMAB treated with 20 % Triton X-100 served for determination of 100 % lysed cells (L_{max}). Lmin and Lmax were than used to calculate specific cell lysis. PBMCs indicates peripheral blood mononuclear cells; PBL, peripheral blood lymphocytes, BiMAB3, (5´Plac1-3´TRR66) Ctrl.-BiMAB; E:T, effector to target ratio.

1BiMAB INDUCED POTENT LYSIS OF CANCER TARGET CELLS AT LOW E:T RATIOS

Different effector to target ratios (E:T) were verified in the next experiment to determine the efficiency of T cell-mediated target cell lysis. A constant concentration of 5 ng×mL^{-1} 1BiMAB with NugC4-luc target cells and Pan-T cell-isolated effector cells were used in this luciferase-based cytotoxicity assay to test the range of E:T from 0.3:1 to 10:1.
After 24 h of incubation even at a low E:T ratios of 0.3:1 a substantial target cell lysis of over 30 % was measured. For both time points, an increase in target cell lysis using accelerating E:T ratios was observed, whereas at an E:T ratio of 5:1 a sort of saturation was reached. The maximal target cell lysis reached approximately 95 % after 24 h and 99 % after 48 h.
The observed correlation between increasing E:T ratios and increasing target cell lysis once more confirmed that 1BiMAB-mediated cytotoxicity is dependent on effector cell recruitment. The effective lysis of 85 % target cells even at the lowest E:T ratio of 0.3:1 indicated clearly that each T cell must have lysed more than one target cell.
Hence, each T cells was able to execute several target cell killings after 1BiMAB recruitment. No lysis was observed using 1BiMAB in the absence of T cells.

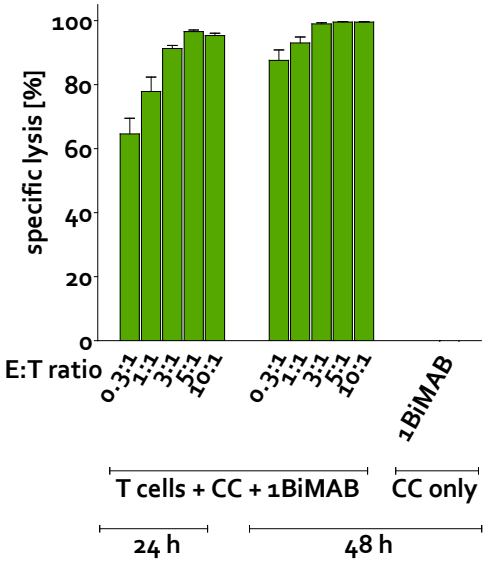

Figure 25: Effective target cell lysis at low E:T ratios using 1BiMAB
The effect of E:T ratios on redirected cancer cell lysis mediated by 1BiMAB was tested in a luciferase-based cytotoxicity assay. Therefore different E:T ratios of 10:1, 5:1, 3:1, 1:1 and 0.3:1 were tested using Pan T cells and 1×10^4 cancer target cells (NugC4-luc). A 1BiMAB concentration of 5 ng×mL^{-1} was used. In further controls, target cells together with 1BiMAB were incubated in the absence of T cells. Error bars indicate the standard deviation of three replicates. CC indicates cancer target cells; E:T, effector to target ratio.

3.5 *IN VIVO*– 1BIMAB TREATMENT REDUCES TUMOR SIZE IN A XENOGENEIC TUMOR MOUSE MODEL.

Next, the question of the therapeutic efficacy of the 1BiMAB protein *in vivo* was addressed. Therefore, a xenogeneic tumor mouse model with engrafted human T cells was established and verified. The mouse strain NOD.Cg-Prkd^{scid} IL2rg^{tm1Wjl}/SzJ commonly known as NOD scid gamma (NSG), belongs to the immunodeficient mouse models. These mice have the severe combined immune deficiency mutation (scid) and additionally an IL-2 receptor gamma chain deficiency resulting in the lack of mature T cells, B cells, or functional NK cells.

3.5.1 *EX VIVO* FUNCTIONALITY TEST OF T CELLS PREVIOUSLY ENGRAFTED IN NSG MICE

The aim of this experiment was to evaluate *ex vivo* the cytotoxic functions of previously engrafted human T cells. To adoptively transfer human PBMCs as effector cells, 2×10^7 PBMCs resuspended in 200 µl PBS, have been injected intraperitoneal (ip) into the mice.
NSG mice were subcutaneously (sc) injected with HEK293 stably expressing CLDN18.2. Splenocytes from five mice bearing a tumor with a volume of over 25 mm^3 (day 31 after PBMC engraftment) and assessable engrafted T cells were taken for the *ex vivo* assay. Splenocytes from each mouse were prepared and thereof human T cells were isolated via a MACS separation kit. These T cells were used in a flow cytometry-based cytotoxicity and T cell activation assay. After 72 h using 5 ng×mL^{-1} 1BiMAB in the presence of target cells, a T cell activation of 75 % was reached and a target cell lysis of 70 %, using the positive control with freshly isolated human T cells. T cell activation for each mouse donor was given but intensities of the response varied from around 30 % to nearly 80 % activated T cells. Nevertheless, similar to the positive control the *ex vivo* T cells were all able to lyse 50 %-60 % of the target cells.
These results clearly prove that 1BiMAB-mediated an obvious T cell activation of *ex vivo* used T cells and managed a 1BiMAB dependent lysis of TAA-positive target cells. This indicates that use of human T cells in a xenogeneic tumor mouse model leads to functional engrafted effector T cells, which are in turn capable of an effective tumor cell lysis (Figure 26).

3.5.2 PROLONGED SURVIVAL DUE TO 1BIMAB TREATMENT IN A XENOGENEIC MOUSE MODEL

We used immune deficient NSG mice carrying xenografted CLDN18.2-positive tumors to determine the efficacy of 1BiMAB in tumor growth reduction. CLDN18.2 overexpressing HEK293 cells were inoculated sc to eight weeks old mice (Figure 27-A). Five days after tumor cell inoculation mice were stratified according to their tumor volume into groups receiving 2×10^7 PBMCs or 1×DPBS.
"PBS" designated treatment groups received plain 1×DPBS ip and consequently served as controls. Groups designated by "vehicle" belonged also to the group of control mice because they received the BiMAB storage buffer instead of the bispecific antibody. The therapy group–"PBMC/1BiMAB"–enclosed 15 mice (n=15) that received ip 5 µg purified 1BiMAB protein per animal. One day after PBMC application the 1BiMAB therapy started. The applications occurred constantly on a daily basis over a period of 22 days. The tumor volumes were monitored twice per week. Mice exhibiting tumors that exceeded the volume of 500 mm^3 were sacrificed. If severe symptoms of graft versus host disease or a decline in the state of health was observed, mice were sacrificed as well.
Kaplan-Meier survival curves (Figure 27-B) demonstrated that mice treated with 1BiMAB (group 4) had a significantly higher survival rate ($p< 0.0001$) than those receiving vehicle (group 3). The survival of 11 mice was significantly prolonged by 1BiMAB treatment (Figure 28-A, Table 17). 1BiMAB treatment in the absence of effector cells considerably slowed the tumor growth rate but did not prevent tumor outgrowth.

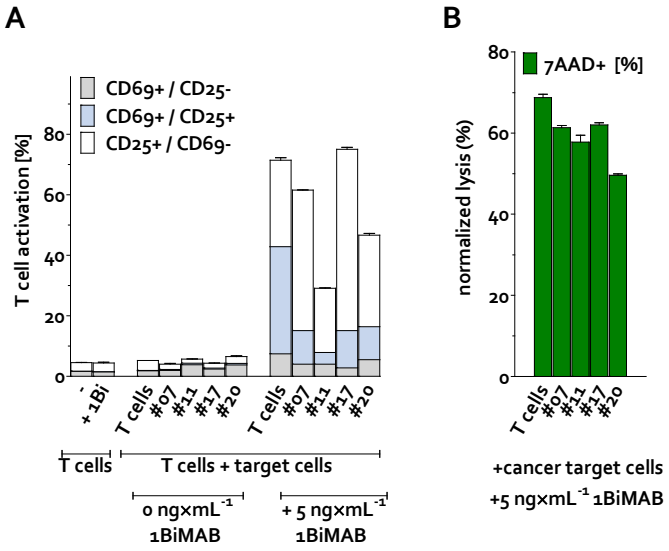

Figure 26: 1BiMAB induces effector functions of *ex vivo* human T cells

To reconstitute NSG mice with human effector cells, 2×10^7 PBMCs have been injected intraperitoneal (ip) into the mice. 31 days after PBMC engraftment, splenocytes from five NSG mice were taken for the *ex vivo* assay. In (**A**) 1BiMAB-mediated T cell activation [%], is shown; while the percentages of 1BiMAB-mediated cytotoxicity of cancer cells was assessed in figure (**B**). Samples contained T cells from mouse donors (#07, #11, #17, #20) as specified on the X-axis. T cells freshly isolated from a human buffy coat (entitled T cells) were used as positive control samples. Target cells [1×10^5 NugC4] were coincubated for 72 h with 5×10^5 T cells in the absence (control samples, 0 ngxml^{-1} 1BiMAB) or presence (test samples, 5 gxml^{-1} 1BiMAB) of 1BiMAB. Cells were stained with a combination of 7-Aminoactinomycin-D (7-AAD) and fluorophore-conjugated mAb against CD3, CD25, CD45, and CD69. Cells were studied by flow cytometry. Data analysis was done using the software FlowJo. Cytolysis was assessed by 7-AAD incorporation into target cell nuclei. In order to normalize the lysis values, the amount of 7-AAD+ cells measured in the control sample was subtracted from the percentages of target cell lysis determined in the respective test samples. Error bars indicate standard deviation (SD) of duplicates within this one experiment.

Consequently, mice treated with 1BiMAB and engrafted T cells (group 4) showed a significantly higher survival ($p< 0.0022$) than group 2 receiving 1BiMAB without engrafted effector cells. Thirteen days after the end of the treatment, the experiment was ended and the engraftment of human T cells in the spleens of mice was evaluated.
Additionally, immunocytochemistry (ICC) was performed examining the tumor tissue in order to provide evidence of tumor infiltrating T cells and CLDN18.2 expression of target cells. An anticipated long lasting follow up after the treatment was not feasible because mice relatively quickly developed severe symptoms of graft versus host disease (GVHD).

3.5.3 TUMOR SIZE REDUCTION IS RELIANT ON THE QUALITY OF HUMAN T CELL AND TUMOR CELL ENGRAFTMENT IN XENOGENEIC TUMOR MOUSE MODEL

The engraftment of human T cells can be verified by flow cytometric analysis of the peripheral blood or the splenocytes of mice that received human PBMCs. The median engraftment of CD3+/CD45+ cells within the total population of spleen cells in Group 4 was 50 %±24.42. In Group 3 a median of 66 %±14.95 engrafted cells was reached versus 0.1 %±0.1 in control group 1 & 2. To check the functionality and efficiency of the bispecific antibody, it was obligatory to stain the expression of the TAA CLDN18.2 within the xenograft tumors. Tumor cells were detected with the help of the anti-CLDN18.2 monoclonal antibody 43-14AGC182 (Ganymed Pharmaceuticals; ICC samples were kindly generated by colleagues).

Table 16: Significant differences in median tumor size

treatment groups	G2 (n=5)	G3 (n=13)	G4 (n=15)
G1 (n=4)	ns	ns	*
G2 (n=5)	-	ns	**
G3 (n=13)	ns	-	**
G4 (n=15)	**	**	-

significance signature [10]	
**	P < 0.01
*	P < 0.05
ns	P > 0.05

In eight of 15 tumors, 1BiMAB mediated a decrease in tumor growth (Group 4) even up to the complete elimination of malignant tissue (Figure 28-A). Thus, the mean tumor size of group 4 (Table 17) was significantly smaller in comparison to group 1 (P value = 0.039[10]), group 2 (P value = 0.0055) and group 3 (P value = 0.0019).
Whereas no significant differences were determined, comparing tumor sizes of control groups (Table 16). Due to the 1BiMAB-mediated removal of the tumors, no ICC analysis could be performed. Strong expression of the target antigen CLDN18.2 could be detected in nearly all remaining tumors, with the exception of two small tumors that were treated with 1BiMAB (Figure 28-A). Here, no residual CLDN18.2 expression was detectable.
It is noticeable that within some tumors distinct areas could be identified that do not express any CLDN18.2, indicative for the presence of genetically divergent tumor cell clones. The size of three remaining 1BiMAB treated tumors did not exceed 50 mm^3, but their TAA expression was restricted only to certain areas. CLDN18.2-positive (red staining) and negative cells (blue staining) within the tumor of mice #7.5 treated with 1BiMAB in the presence of PBMCs are shown representatively in Figure 28-B.
Accumulations of CD3-positive T cells were more frequently found in CLDN18.2-expressing areas of tumors showing positive and negative areas of CLDN18.2 expression. However, most CD3-positive cells were equally spread throughout the whole tumor tissue, but in some cases an increased presence of CD3-positives occurred along the outer edge of the TAA-positive tumors (data not shown).Yet, a clear statement based on the results of CD3 staining is not possible.
To summarize the main findings, the final assumption is that 1BiMAB treatment mediated a significant reduction of tumor sizes up to the eradications of eight complete tumors. Although, the loss of TAA within the malignant tissue led to missing responses to 1BiMAB therapy, there was still a significant higher survival rate in the treatment group, proving the therapeutic efficacy of 1BiMAB *in vivo*.

[10] The Unpaired t test was performed using GraphPad Prism version 5.04 for Windows, GraphPad Software, San Diego California USA, www.graphpad.com.

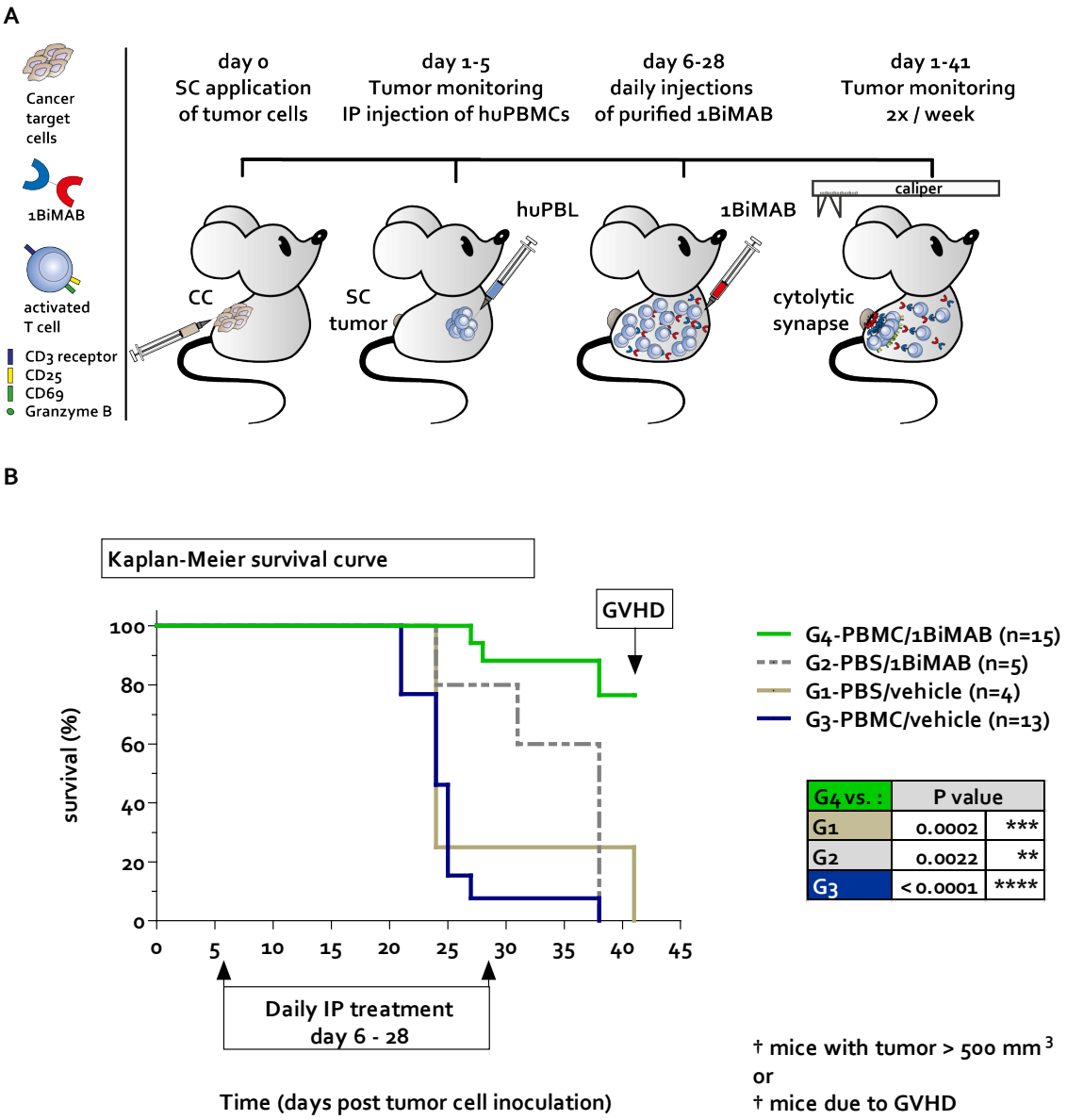

Figure 27: 1BiMAB mediates prolonged survival in a xenogeneic tumor mouse model

(**A**) The time schedule for tumor treatment is depicted. In (**B**) the Kaplan-Meier survival curves are shown for all four mice groups. NOD.Cg-Prkd^{scid} IL2rg^{tm1Wjl}/SzJ (NSG) (immuno-incompetent) mice were injected sc with 1x10^7 HEK293 stably expressing CLDN18.2. Five days later 2x10^7 human PBMC effector cells were injected ip to groups G3 and G4. Control groups (G1 and G2) received PBS only. Daily ip application of 5 µg 1BiMAB per animal or vehicle as control started at the following day. Therapy was administered for 22 days and tumor sizes were measured in the consecutive 14 days. Mice with tumors exceeding the volume of 500 mm^3 were sacrificed (†). Severe symptoms of graft-versus-host disease were observed by a drastic decline in the state of health at day 42, which was the abort-criterion for this experiment. P values were calculated by Graph Pad Prism[11]. CC indicates cancer target cells; G, group; ip, intraperitoneal; PBMC, peripheral blood mononuclear cells; PBS, phosphate buffered saline; sc, subcutaneous; †, sacrificed.

[11] The Log-rank (Mantel-Cox) Test was performed using GraphPad Prism version 5.04 for Windows, GraphPad Software, San Diego California USA, www.graphpad.com.

A **Table 17: Tumor free survival after 1BiMAB therapy**

Group	G1	G2	G3	G4
Effector cells	PBS	PBS	PBMCs	PBMCs
Treatment	vehicle	1BiMAB	vehicle	1BiMAB
Mean size of all tumors [mm^3]	707.4	1057	739.6	220.8
Tumor n ≥500 mm^3	3/4	5/5	13/13	4/15
Tumor n <500 mm^3	1/4	0/5	0/13	3/15
Mean size of tumors <500 mm^3 [mm^3]	438.51	-	-	5.57
Tumor free	0/4	0/5	0/13	8/15

B

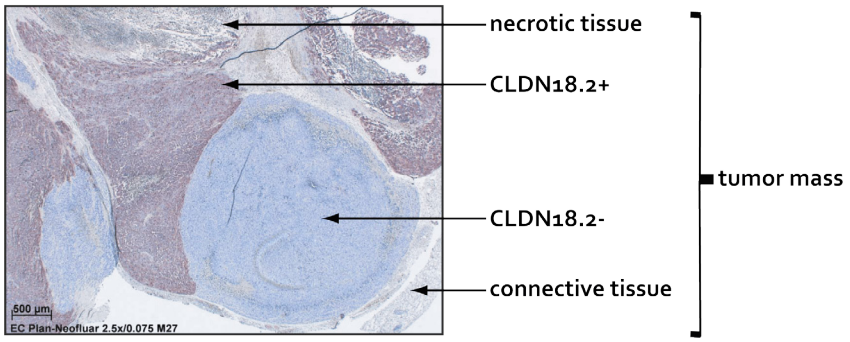

Figure 28: Heterogeneous distribution of TAA in xenogeneic engrafted HEK293-CLDN18.2 tumors have an impact on 1BiMAB-mediated tumor size reduction

Treatment and outcome of the four different mice groups is summarized in Table 17 (A). Immune deficient NSG mice were sc injected with $1x10^7$ HEK293 cells stably expressing CLDN18.2. Five days later $2x10^7$ human PBMC effector cells were injected ip to groups 3 and 4. Control groups (G1 and G2) received PBS only. 1BiMAB therapy was administered for 22 days. Animals were sacrificed as soon as the tumor volume exceeded 500 mm^3. (B) The development of tumor heterogeneity in CLDN18.2 expression on extracted tumor tissues is depicted. After treatment, tumors were extracted, fixed in 4 % formalin, dehydrated, embedded into paraffin and 3 µm sections were produced. Tumor tissue staining occurred with TAA CLDN18.2-specific antibody 43_14A GC182. G stands for group; ip, intraperitoneal; n, number; PBMC, peripheral blood mononuclear cells; PBS, phosphate buffered saline; sc, subcutaneous; vehicle, drug product buffer.

3.6 SUMMARY OF THE *IN VITRO* AND *IN VIVO* CHARACTERIZATION OF 1BIMAB PROTEINS

The identification of the most potent BiMAB candidate directed against CDLN18.2 and CD3 in this drug discovery process was achieved by *in vitro* comparison of nine different bs-td-scAbs. All BiMAB variants showed specific binding to target and T cells, a respectable T cell activation and effective target cell killing but 1BiMAB showed consistently an enhanced efficiency in both categories.
For this reason, 1BiMAB was chosen for the drug discovery studies, examining some of the BiMAB characteristics in more detail. We reached a median production efficiency of 1.3 mg 1BiMAB protein per one liter of supernatant acquired from stable transfected HEK293 cells.
The highly specific selectivity of 1BiMAB, with affinities in the nanomolar range, and potent efficacy EC_{50} in the range of: 11-459.1 pg×mL^{-1} has been affirmed for 1BiMAB by several *in vitro* assays. Redirection of T cells to the tumor and activation was shown to be selectively mediated by 1BiMAB.
Moreover, the *in vivo* efficacy of 1BiMAB was demonstrated by a xenogeneic tumor model in NSG mice. The growth of subcutaneous tumors was inhibited or even eradicated by 1BiMAB treatment and survival of mice was significantly prolonged.
The results show the *in vitro* and *in vivo* potency of 1BiMAB selectively targeting the TAA CLDN18.2. The BiMAB approach appeared to be a promising strategy for the therapeutic treatment of solid tumors. That way, the first main goal was reached, the proof of concept of the BiMAB prototype. This was followed by the attempt to confirm the IVT-RNA approach for this BiMAB principle.

3.7 RIBOMABS –IVT-RNA-BASED BISPECIFIC ANTIBODIES

The drug development experiments certified 1BiMAB to be a highly selective, specific, and potent bispecific antibody.
Protein production, purification, and analysis of bispecific-single-chain antibodies are laborious and time-consuming procedures. Our intention was to find an alternative way to rapidly produce, administer, and test the bispecific antibodies.
Thus, we chose to implement *in vitro* transcribed messenger RNA (IVT-RNA) encoding for bispecific antibodies. This RNA can be brought into organisms via several ways of application: electroporation, lipofection, or injection of naked IVT-RNA.
Cells that incorporate the IVT-RNA translate it *in vivo* into the BiMAB protein. The proteins will be secreted by the cells into their surroundings, ready to pursue its job. Thus, we implemented a very cost efficient approach in contrast to the complex, and expensive protein production procedures. Cost efficiency is given due to a rapid production, handy purification, and quality assurance of IVT-RNA as shown in the next chapter. Moreover, by the direct test of BiMAB formats as IVT-RNA in *in vitro* functional assays the screening speed is drastically increased.

3.7.1 BIOANALYZER QUALITY ASSURANCE OF BIMAB IVT-RNA AND CONCENTRATION ESTIMATION OF CELLULAR EXPRESSED 1BIMAB PROTEIN

For all BiMABs described in chapter 3.1, the respective IVT-RNAs were produced, comprising the structural modifications described by Holtkamp *et al.* [100]. This was considered important for IVT-RNA stability and translational efficiency. The quality of IVT-RNA was determined by the BioAnalyzer device.
The protein *in vitro* translated from 1BiMAB IVT-RNA was detected by the IMAB362-specific ELISA. The supernatant of producing cancer target cells (NugC4) was analyzed 48 h after electroporation with 20 µg×mL^{-1} IVT-RNA. 1.91 ng×mL^{-1} of 1BiMAB protein were measurable as soluble protein in the collected supernatant (Data not shown).

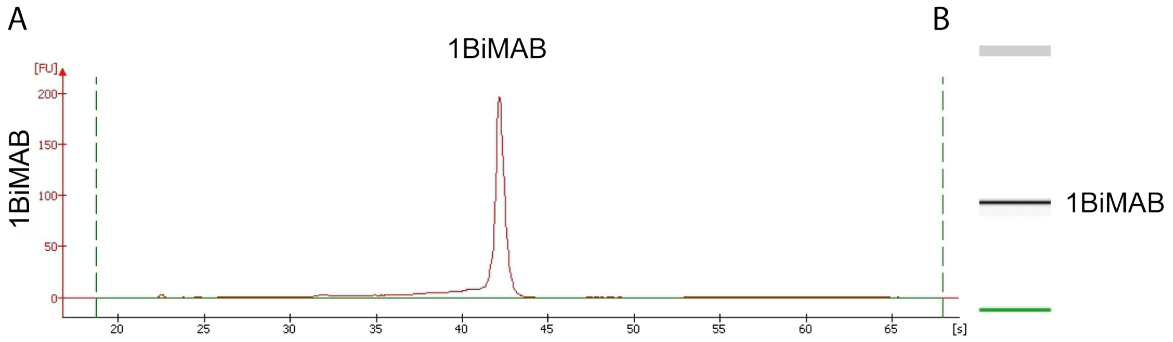

Figure 29: Pure IVT-RNA is produced by *in vitro* transcription

The quality of 1BiMAB IVT-RNA is depicted. The purity and quality control of IVT-RNA was ascertained by analysis with the 2100 BioAnalyzer device. A representative electropherogram of purified 1BiMAB IVT-RNA is shown in Figure 29–A (left side). It displays one distinct peak and its correlating clear band (Figure 29–B (right side)) of the expected size (~2000 nt) proving a pure 1BiMAB-IVT-RNA production without degraded RNAs.

3.7.2 CHARACTERIZATION AND PROOF OF CONCEPT USING IVT-RNA CANDIDATE 1BIMAB

1BiMAB IVT-RNA was tested in several *in vitro* experiments to prove the main ideas of the concept. We addressed 1BiMAB dependent T cell activation and target cell killing.

MICROSCOPIC OBSERVATION OF 1BIMAB IVT-RNA-MEDIATED CYTOTOXICITY AND T CELL CLUSTERING

A cytotoxicity assay was prepared to test the functionality of IVT-RNA encoding 1BiMAB protein. 1BiMAB was translated from IVT-RNA (80 µg×mL^{-1}) transiently transfected into NugC4 cells using electroporation.
As indication of T cell activation, a clear clustering of T cells around the electroporated target cells was observed (Figure 30, lower right, indicated by white arrows).
In addition, a drastic reduction of target cells was noticeable, illustrating 1BiMAB-mediated cytotoxicity. Whereas in control samples (lower left) that were electroporated with IVT-RNA encoding luciferase none of these effects were visible.
In conclusion the observed T cell clustering together with the target cell killing strongly indicate the translation of the IVT-RNA to a functional 1BiMAB protein.

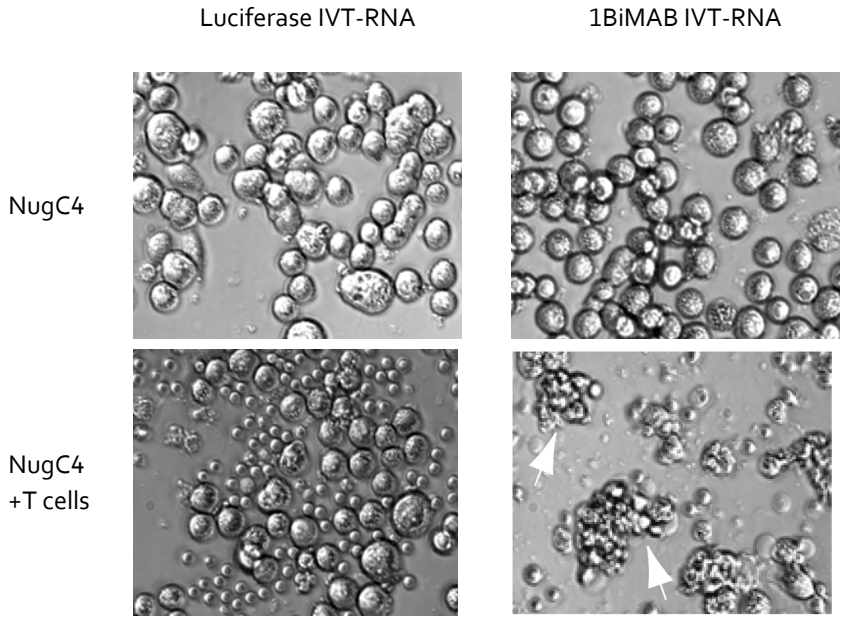

Figure 30: 1BiMAB IVT-RNA induced cancer target cell lysis could be visualized by microscopic imaging
A microscopic image of 1BiMAB triggered cancer target cell lysis and T cell clustering indicated by white arrows was taken. Microscopic images of control samples are accompanying. 5x10^6 cancer target cells were electroporated with 80 µg×mL^{-1} of 1BiMAB or control IVT-RNA encoding luciferase. Cancer cells [1×10^5 NugC4] were incubated for 24 h either alone or together with 5×10^5 CD8-positive human T cells using a 96 well plate format. IVT indicates *in vitro* transcribed.

1BIMAB IVT-RNA IS TRANSLATED AND FUNCTIONALLY SECRETED INTO THE SUPERNATANT

The aforementioned assumptions –based on the microscopic observations –needed to be verified and quantified. One question was if only 1BiMAB-electroporated target cells are lysed by T cells or if also non-electroporated target cells are attacked when added to the cell mixture.
One concern was that the electroporation or the translation of 1BiMAB might harm the target cells resulting in false-positive lysed target cells and therewith hamper a correct interpretation of the results.

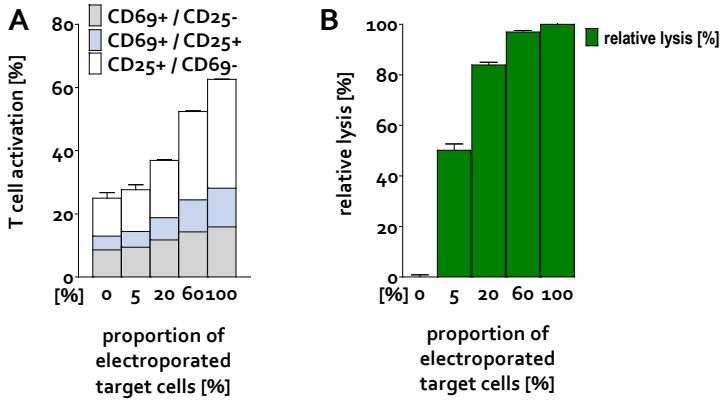

Figure 31: 1BiMAB-mediated T cell activation and cancer target cell lysis was not restricted to 1BiMAB releasing target cells.

T cell activation mediated by 1BiMAB is depicted in (**A**). While in (**B**) the 1BiMAB-mediated lysis of cancer cells was assessed. A series of diverse mixtures that are comprised of different proportions of electroporated and non-electroporated cancer cells was used. These mixtures contained 5 % electroporated versus 95 % non-electroporated cancer cells (5 %:95 %, 0 %:100 %, 20 %:80 %, 60 %:40 %, and 100 %:0 %). Cancer cells were electroporated with 20 µg×mL^{-1} 1BiMAB IVT-RNA prior to coincubation. Target cells [1×10^5 NugC4] were coincubated for 48 h with 1×10^6 human CD8-positive T cells in a six well format. An E:T ratio of 10:1 was chosen. Cells were stained with a mixture of propidium iodide (PI) , and three fluorophore-conjugated mAbs anti-CD3, anti-CD25, and anti-CD69. The data was evaluated via flow cytometry analysis and percentages were calculated using the software FlowJo. Cancer cell lysis was measured via PI incorporation into cancer cell nuclei. The mean PI value of the control samples using non-electroporated NugC4 cells in the presence of CD8-positive T cells was subtracted from all samples. The mean value of lysis determined for the samples composed of 100 % electroporated cancer target cells coincubated with CD8-positive T cells was set to 100 % 1BiMAB-mediated cancer cell lysis. The remaining values were consequently normalized to this value. Error bars indicate standard deviation (SD) of replicates. E:T indicates effector to target ratio.

Another consideration was that during or after secretion, 1BiMAB binds to its respective 'producer target cell' and is not disposable for neighboring cells. This is likely to happen due to its high affinity for its TAA CLDN18.2. Consequently, T cells would recognize and lyse only the BiMAB-tagged 'producer cells'.

To investigate this hypothesis, target cells were electroporated with 20 µg×mL^{-1} 1BiMAB or 20 µg×mL^{-1} luciferase IVT-RNA. Successful transfection was routinely confirmed via the luciferase expression bioassay (chapter 2.6.7) 6 h after electroporation. A mixture of transfected NugC4 cells with different proportions of non-electroporated target cells was used in a flow cytometry-based T cell activation and cytotoxicity assay.

With this assay, we were able to demonstrate that a significantly higher proportion of cells was lysed than just the electroporated target cells. Already 5 % electroporated target cells elicited 50 % of relative cancer target cell lysis. This indicated that secreted 1BiMAB protein was disposable in the culture dish and mediated target lysis irrespective of the cell origin of 1BiMAB.

The higher the proportion of electroporated target cells the higher was the respective target cell lysis, referring to a higher 1BiMAB protein concentration of translated 1BiMAB protein. According to the escalating proportions of electroporated cells within the samples, also increasing amounts of activated T cells were observed.

Within the control samples, no increased T cell activation or target cell lysis was measurable (data not shown). These control cells were electroporated with luciferase IVT-RNA and mixed in the same manner as described for 1BiMAB samples.

The results demonstrate that 1BiMAB IVT-RNA transfection is not only a feasible approach for *in*

vivo BiMAB production and its secretion but also leads to functional 1BiMAB protein that induces target cell lysis.

1BiMAB IVT-RNA INDUCED A STRONG CONCENTRATION DEPENDENT T CELL ACTIVATION AND A POTENT CANCER TARGET CELL LYSIS

Increasing concentrations of 1BiMAB IVT-RNA were electroporated, in order to display the dependency of T cell activation and target cell killing on mRNA bioavailability (Figure 32).
An ascending T cell activation and subsequent target cell lysis was obtained that started at concentrations of 1.2 µg×mL^{-1} and using 4 µg×mL^{-1} then significantly increased by ~40 % 1BiMAB IVT-RNA to >60 %. With the highest amount of 40 µg×mL^{-1} 1BiMAB IVT-RNA 90 % of T cells were activated and 80 % target cells were lysed after 48 h.
The high percentages of CD69+/CD25- and CD69+/ CD25+ T cells indicated that T cell activation was still in progress and target cell lysis was not at its maximum yet. A 1BiMAB independent decrease in the number of viable cells of around 20 % was assessed in all control samples via their PI+ stain (spontaneous lysis).
Controls comprised electroporated target cells alone or coincubated target and effector cells in the absence of 1BiMAB. The detected dose dependent T cell activation and lysis proves that effects were reliant on the presence of 1BiMAB. 1BiMAB induced effects were highly significant using 4 µg×mL^{-1} IVT-RNA or more[12].

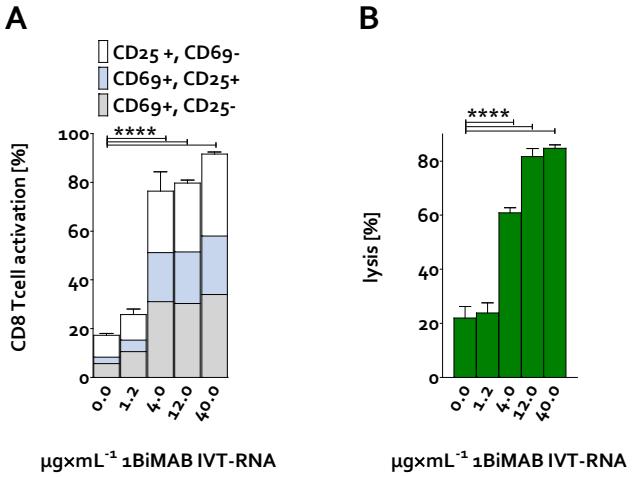

Figure 32: Expression of 1BiMAB IVT-RNA induced T cell effector functions in a dose-dependent manner

1BiMAB In (**A**) the T cell activation, in response to increasing amounts of 1BiMAB IVT-RNA, was assessed. The correlation between electroporated 1BiMAB IVT-RNA amount and the induced lysis of cancer cells is presented in (**B**). Target cells [1×10^5 NugC4] were coincubated for 48 h with 1×10^6 human CD8-positive T cells in a six well format. An E:T ratio of 10:1 was chosen. Prior to coincubation cancer target cells were electroporated with the indicated amounts of BiMAB IVT-RNA plus luciferase IVT-RNA to electroporate 40 µg×mL^{-1} IVT-RNA per sample in total. Cells were stained with a mixture of PI, and fluorophore-labeled mAbs CD3, CD25, and CD69. Cancer cell lysis was assessed via PI incorporation into cancer cell nuclei. Data were evaluated via flow cytometry analysis and percentages were calculated using the software FlowJo. Error bars indicate standard deviation (SD) of duplicates within one experiment. Results are representative of two experiments. EP specifies electroporation; IVT, *in vitro* transcribed; mAb monoclonal antibody; E:T, effector to target ratio; ****, highly significant (p< 0,0001).

[12] The 1way ANOVA- One-way analysis of variance– together with the Post test: Bonferroni's Multiple Comparison were performed using GraphPad Prism version 5.04 for Windows, GraphPad Software, San Diego California USA, www.graphpad.com.

Higher doses of IVT-RNA for electroporation up to 240 µg×mL^{-1} were likewise tested but resulted in cell death (data not shown). Consequently, the favorable dose of 1BiMAB IVT-RNA for *in vitro* assays was determined to be between 12 and 40 µg×mL^{-1}. 20 µg×mL^{-1} IVT-RNA was further used in most of the assays.

LYSIS OF CANCER TARGET CELLS MEDIATED BY 1BIMAB IVT-RNA STARTED AT AN E:T RATIO OF 0.3:1

Next, we examined the influence of the effector to target ratios on T cell activation and target cell lysis. The target cell killing is a T cell dependent procedure and therefore the application of increasing amounts of T cells is expected to result in increasing lysis.
In this flow cytometry-based cytotoxicity and T cell activation assay, CD8-positiveT cells were used as effector cells. NugC4 target cells were electroporated with 20 µg×mL^{-1} 1BiMAB IVT-RNA. 5x10^{6} NugC4 target cells were coincubated with T cells. The E:T ratios ranged from 0.3:1 to 10:1.
After 48 h of coincubation with 1BiMAB-expressing target cells, 1BiMAB mediated a T cell activation of 55 %.
As expected, higher E:T ratios did not result in higher T cell activation because higher T cell numbers have had to be activated in comparison to samples with low E:T ratios. The process of T cell activation was still at the beginning as indicated by the low percentages of CD25+/CD69- T cells.
In the control samples comprising only electroporated target cells, roughly 20 % PI-positive cells were measured.
It was demonstrated that electroporation of target cells alone led to maximally 20 % spontaneous lysis. Even in the luciferase transfected control samples with an E:T ratio of 10:1 the spontaneous lysis was under 20 %.

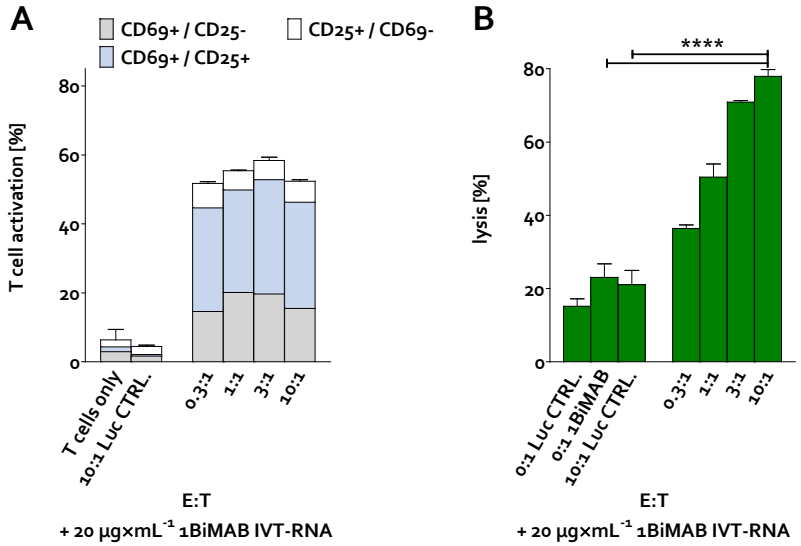

Figure 33: Efficiency of cancer target cell lysis was dependent on the effector to target ratio

In (**A**) the induction of T cell activation, in (**B**) the 1BiMAB-mediated lysis of cancer cells dependent on the E:T ratio is shown. Cancer target cells were electroporated with 40 µg×mL^{-1} 1BiMAB IVT-RNA. As a control 40 µg×mL^{-1} of luciferase IVT-RNA (Luc Ctrl.) were electroporated into cancer cells. [1×10^{5} NugC4] were coincubated for 48 h with different amounts ranging from 0.3 to 10×10^{5} human CD8-positive T cells in a six well format. Indicated E:T ratios were used. Cells were stained with a mixture of PI, and fluorophore-labeled mAbs CD3, CD25, and CD69. Cancer cell lysis was measured via PI incorporation into cancer cell nuclei. The data was evaluated via flow cytometry analysis and percentages were calculated using the software FlowJo. Error bars indicate standard deviations (SD) of duplicates (samples: T cells only, 0.3:1; 1:1.) or triplicates (remaining samples) within one experiment. Results are representative of two experiments. E:T, specifies effector to target ratio; mAb monoclonal antibody; ****, highly significant (p< 0,0001).

This indicates that T cells in the absence of 1BiMAB were not able to induce lysis. Hence, the difference in induced cell lysis at an E:T ratio of 10:1 between controls and 1BiMAB transfected samples were determined to be highly significant[13] (as indicated by asterisks).
In contrast to the T cell activation, we observed corresponding increases in target cell lysis according to the accelerating E:T ratios. Even at a low E:T ratio of 0.3:1 a beginning target cell lysis of over 30 % (10 % over background) was measured. The maximal lysis after 48 h reached approximately 80 %. Thus, we confirmed that the efficacy of 1BiMAB IVT-RNA-mediated target cell lysis correlated to the amount of present T cells.

1BiMAB IVT-RNA CAN BE ADMINISTERED TO TARGET OR TO EFFECTOR CELLS

In accordance with existing practices in cancer immunotherapy as for example, adoptive T cell transfer, the purpose of the next experiment was to test effector cells as 1BiMAB IVT-RNA recipients. Therefore, we compared the induced T cell activation and target cell lysis after electroporation of T cells and target cells. The results of separate experiments are summarized in Figure 34.
48 h after electroporation of 1BiMAB IVT-RNA into T cells (Figure 34-A**)** approximately 60 % T cells were activated in the presence of target cells, while luciferase electroporation did not influence the T cell activation status.

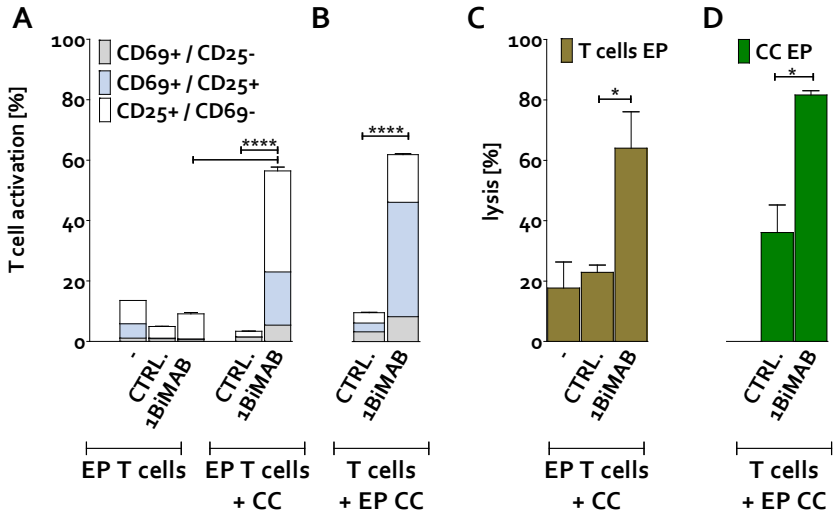

Figure 34: 1BiMAB IVT-RNA expressed by T cells showed a similar potent induction of cancer target cells lysis and T cell activation as detected with 1BiMAB expressed by cancer target cells.

In (**A**) and (**B**) the 1BiMAB-mediated T cell activation 48 h after electroporation of T cells or cancer cells is shown. While in (**C**) and (**D**) 1BiMAB induced lysis of cancer cells after 24 h was assessed. At an E:T ratio of 10:1, target cells [1×10^5 NugC4] were coincubated with 1×10^6 human CD8-positive T cells. Prior to coincubation T cells in (**A** & **C**) or cancer target cells in (**B** & **D**) were electroporated either with 20 $\mu g\times mL^{-1}$ 1BiMAB or with control IVT-RNA. Control IVT-RNA used for transfection of T cells was eGFP (A) and luciferase IVT-RNA for cancer cells (**B**). In the experiments (**C**) and (**D**) luciferase was used as control IVT-RNA. Cells were stained with a mixture of PI, and three fluorophore-conjugated mAbs (anti-CD3, anti-CD25, and anti-CD69). Cancer cell lysis was measured via PI incorporation into cancer cell nuclei. The data was evaluated via flow cytometry analysis and percentages were calculated using the software FlowJo. Error bars indicate standard deviation of replicates. CC specifies cancer target cells; E:T, effector to target ratio; EP, electroporated; mAb, monoclonal antibody; ****, highly significant ($p< 0,0001$); *, significant ($p< 0,05$).

[13] The 1way ANOVA- One-way analysis of variance– together with the Post test: Bonferroni's Multiple Comparison were performed using GraphPad Prism version 5.04 for Windows, GraphPad Software, San Diego California USA, www.graphpad.com.

In the absence of target cells, comparing the untreated T cells to the 1BiMAB or luciferase IVT-RNA transfected cells, no activation could be measured. In another independent experiment, using electroporated target cells–depicted in Figure 34-B, a good agreement with the experimental results of T cell electroporation was found.
Congruently one further experiment is shown in Figure 34-C, in which target cell lysis mediated by electroporated T cells is depicted. In contrast, in Figure 34-D the target cell lysis 24 h after electroporation of target cells was investigated.
By subtracting the spontaneous lysis of control samples (Ctrl.) from the results of 1BiMAB transfected samples the remaining lysis values can be specified as specific target cell lysis. At this early time point of 24 h, already 40 % specific target cell lysis was determined for samples containing either electroporated T cells or electroporated target cells.
The differences in comparison to the spontaneous lysis of control samples were considered significant [14](indicated by asterisks). Thus, these four experiments allowed a comparison of T cell activation and target cell lysis between electroporated T cells and target cells.
From the results, it was concluded that electroporation of T cells, as a treatment option using 1BiMAB IVT-RNA, is possible. Furthermore, it is important to notice that not only electroporation but also the translation of 1BiMAB IVT-RNA was feasible for target cells as well as for T cells. This finding expands the possibilities of 1BiMAB IVT-RNA application.

3.7.3 PROOF OF BIMAB IVT-RNA CONCEPT TESTING ALL CLDN18.2-SPECIFIC BIMABS

In the experiments before, we preliminary tested the feasibility of 1BiMAB IVT-RNA to induce T cell activation and target cell lysis of CLDN18.2-positive target cells. In these tests, 1BiMAB IVT-RNA provoked the desired effects. Despite the proven applicability and *in vitro* functionality after electroporation, it was important to demonstrate that the IVT-RNA application is assignable for each conceivable BiMAB.

INDUCTION OF A POTENT TARGET CELL LYSIS AND T CELL ACTIVATION MEDIATED BY ALL NINE CLDN18.2-SPECIFIC IVT-RNA BIMABS

The following experiments intended to finally prove the main concept of the BiMAB IVT-RNA approach. Nine CLDN18.2-specific BiMAB IVT-RNAs, differing in the CD3 binding domain sequence and orientation, were compared in a flow cytometry-based T cell activation and cytotoxicity assay. In detail we electroporated 20 $\mu g \times mL^{-1}$ of each BiMAB into NugC4 target cells. 48 h later, T cell activation and target cell lysis for each BiMAB were determined via flow cytometry, respectively.
All CLDN18.2-specific BiMABs considerably activated the T cells.
The difference in activation and lysis between control and CLDN18.2-specific BiMAB samples was highly significant[15]. For some BiMABs differences in the efficacy to induce T cell activation were clearly observable, while controls remained completely inactivated.
Correspondingly, all CLDN18.2-specific BiMABs induced an effective target cell lysis between 80 % and 90 %, whereas the highest spontaneous lysis among all controls reached maximally 23 %.
Besides luciferase IVT-RNA, further controls for example the Plac1-specific RIBOMAB–targeting a non-expressed TAA–was implemented in this assay as a new negative control.

[14] The unpaired t test was performed using GraphPad Prism version 5.04 for Windows, GraphPad Software, San Diego California USA, www.graphpad.com.

[15] The 1way ANOVA- One-way analysis of variance– together with the Post test: Bonferroni's Multiple Comparison were performed using GraphPad Prism version 5.04 for Windows, GraphPad Software, San Diego California USA, www.graphpad.com.

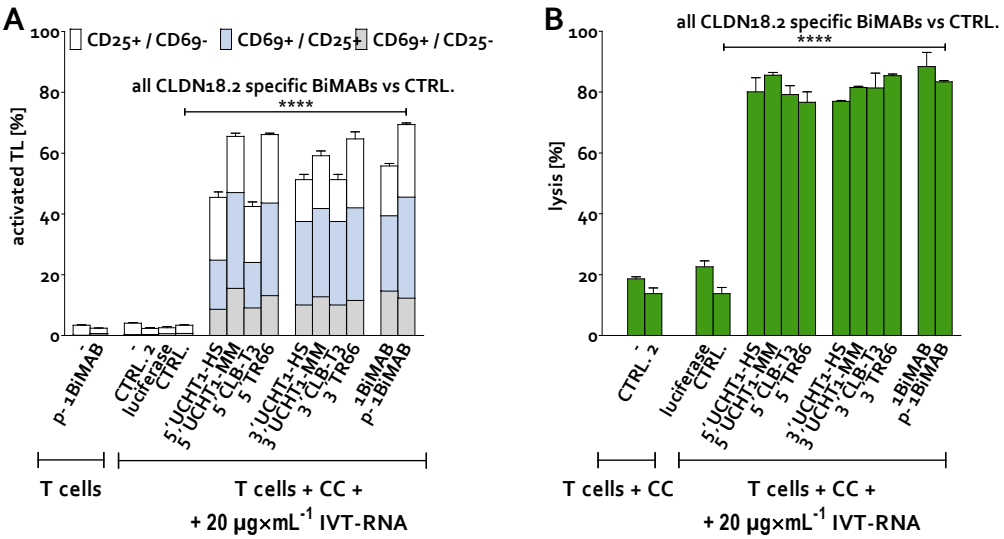

Figure 35: All CLDN18.2-specific RIBOMABs were capable of cancer target cell lysis induction and T cell activation

In (**A**) expression of T cell activation markers CD25 and CD69 in response to expression of nine different CLDN18.2-specific BiMAB IVT-RNAs was assessed. In (B) BiMAB-mediated cytotoxicity was assessed via PI incorporation into cancer cell nuclei. The data was evaluated via flow cytometric analysis and percentages were calculated using the software FlowJo. Samples contained one of nine different IVT-RNA BiMABs specified by labeling of the X-axis. Cancer cells [1×10^5 NugC4] were coincubated for 48 h with 5×10^5 human T cells. An E:T ratio of 5:1 was chosen and cancer cells were electroporated with 20 µg×mL^{-1} BiMAB IVT-RNA prior to coincubation. The IVT-RNA of a BiMAB-specific for an irrelevant TAA (Ctrl..) served as control. Besides the CLDN18.2-specific mAb IMAB362 (Ctrl. 2–Ganymed Pharmaceuticals) and the 1BiMAB protein (p-1BiMAB) were further used as protein controls. Cells were stained with a mixture of PI, CD3-FITC, CD25-PE and a CD69-APC mAb. Error bars indicate standard deviation (SD) of duplicates within one experiment. Results are representative of two experiments. CC specifies cancer target cell; E:T, effector to target ratio; IVT-RNA *in vitro* transcribed RNA; mAb, monoclonal antibody;, ****, highly significant (p< 0,0001).

1BiMAB protein in the absence or presence of target cells served as additional evaluation control. In the presence of target cells, the efficacy to mediate T cell activation was significantly better using 1BiMAB protein rather than IVT-RNA, but lysis mediated by the IVT-RNA was slightly better than protein-induced effects.
Briefly speaking, all CLDN18.2-specific BiMAB IVT-RNAs were able to redirect T cells, provoked their effector functions, and finally resulted in an effective target cell lysis that had–compared to 1BiMAB protein–equivalent efficacies.

3.7.4 SUMMARY–PROOF OF CONCEPT FOR RIBOMABS

The BiMAB IVT-RNA plasmids were successfully cloned and nine different IVT-RNAs were produced encoding for CD3- and CLDN18.2-specific proteins. The electroporation of IVT-RNA into target or effector cells was successful. Thereby translation of control–luciferase IVT-RNA indicated the production of functional proteins in both T cells as well as tumor cells. Additionally, after 1BiMAB IVT-RNA electroporation, it was possible to determine the 1BiMAB protein concentration via ELISA. This confirmed the translation of transfected 1BiMAB IVT-RNA transgenes. Translated 1BiMAB protein induced cytotoxicity and T cell activation in a concentration dependent manner.
In summary, this preliminary data showing the functionality of RIBOMABs suggests the suitability for an application in therapeutic settings. Future aims of our research will be to further generate profound knowledge regarding the *in vitro* and *in vivo* behavior of RIBOMABs.

4 DISCUSSION

4.1 THE BISPECIFIC ANTIBODY APPROACH "BIMAB" IN CANCER IMMUNOTHERAPY

In the last couple of years, various bispecific antibody (bsAb) approaches have been analyzed; however, one of the most promising approaches examined was of particular interest for us: the bispecific-tandem-single-chain- antibodies (bs-td-scAbs).
This concept has already been used by others to redirect and activate circulating T cells against tumor cells [118–120]. This setup was the most promising approach for our purpose as an effective T cell activation can be induced without any costimulation by CD28 or B7-ligand, thus circumventing the main disadvantage of most existing T cell receptor engaging antibody therapies.
We adopted the currently most effective and promising approach, designing a bs-td-scAb termed BiMAB, which recruits T cells to solid tumors expressing the proprietary surface differentiation tumor antigen CLDN18.2. In the BiMAB format, two scFvs were recombinantly joined by a short glycine-serine (SGGGGS) peptide linker. For this purpose, the variable domains of the mAb IMAB362 (Ganymed Pharmaceuticals) were converted into a single-chain-variable-fragment (scFv). The second scFv binds the invariant CD3ε chain of the TCR complex. By targeting CD3ε, which is known to be a T cell activating receptor, the BiMAB engages T cells, which are some of the most potent effector cells within the immune system for eradicating tumor cells.
Information on several other monoclonal antibodies (mAb) with a well-defined specificity for the human CD3ε chain has been published [121]. There is evidence that at least four mAbs have a good ability to induce MHC independent T cell activation [122,123]. In order to choose the best T cell engaging anti-CD3-scFv, we validated all four in a comparative study.

4.2 MODULAR DESIGN FOR AN EXPANDABLE BIMAB CLONING PLATFORM

The challenge in this comparative study of new bsAbs was not only the creation of truly equivalent constructs, which is mandatory for drawing comparisons, but also to generate an efficient and modular setup of the creation process itself.
Our intention was to design a platform consisting of modules that can be rapidly generated and substituted, providing the potential for future expansion by substituting modules for the formation of new specificities. In this study, we established a DNA-based modular design to create a flexible and expandable BiMAB cloning platform. Dividing the BiMAB nucleotide-constructs into several single modules allowed the careful consideration of all intended requirements.
The newly designed IVT-RNA expression plasmid pSTI-BsmBI is the first module of this building set; the second module is the mammalian expression plasmid pcDNA3.1.
Further modules are the eight 3′- or 5′- scFvs specific for the CD3ε chain, the 3′- and 5′- CLDN18.2-specific scFvs, as well as all scFvs for the assembly of the control BiMABs. In total, eight different scFvs binding the CD3ε subunit were designed as modules for the platform. Those scFvs were derived from the mAbs TR66, CLB-T3, the murine (UCHT1-MM) and humanized mAb UCHT1 (UCHT1-HS).
Besides the comparison of different anti-CD3-scFvs, the organization of the scFvs within the BiMAB construct was of interest. As reported by Lu *et al.* [124], it is possible that the sequential arrangement of the binding domains within a bispecific construct can have a significant impact on expression levels, stability, antigen binding properties and efficacy of the protein. The modular concept of all constructs permitted the testing of both possible orders for the scFv within each BiMAB setting.

Additionally, it was anticipated to test the functionality of all BiMABs as an IVT-RNA version, the RI-BOMABs. As previously mentioned, the platform comprises two different expression plasmids: one plasmid for protein expression, and the other one for the IVT-RNA expression.
In summary, the platform was used for the production of more than twenty BiMAB-plasmids within this study. Moreover, the development and design of this modular concept is a powerful instrument to continuously generate BiMABs specific for well-known TAAs as well as newly discovered targets beyond CLDN18.2. The principle of this modular design enables a process characterized by rapid standard cloning procedures and recyclable modules, which significantly reduces cost.

4.3 PROPERTIES OF CLDN18.2-SPECIFIC BIMABS

One major aim of the present study was the comparison of nine different CLDN18.2 bs- scAbs in order to find the best BiMAB prototype for cancer immunotherapy treatment. Hence, all protein BiMABs were transiently expressed by HEK293T cells previously transfected with the mammalian expression plasmids pcDNA3.1.

4.3.1 EVALUATION OF BIMAB PRODUCTION EFFICIENCIES

BiMAB expression levels were verified using SDS-PAGE and Western blot. All constructs yielded a single protein band in Western blot under reducing conditions, with the expected molecular size of approximately 55 kDa indicating the absence of degradation products (Figure 11). An IMAB362-specific ELISA verified the hexahistidine-tagged-proteins as CLDN18.2-specific BiMABs and confirmed variable expression levels of the BiMABs (Table 11). The yields varied from a maximum of nearly 50 mg×L^{-1} to a minimum of 1 mg×L^{-1}.
A comparison of the protein yields revealed that BiMABs N-terminally carrying the anti-CD3-scFv of UCHT1 were highly expressed, whereas all other BiMABs were expressed at considerably lower levels. However, we found that protein expression levels of one protein varied between four different transient expression experiments. The variation was primarily caused by different transfection efficiencies. Therefore, a comparison of BiMAB yields following transient expression only provides an indication of the production efficiency of a particular BiMAB protein.
Considering the results of four independent transient expression experiments, it appears that the sequence of the scFvs within the BiMAB had no clear impact on BiMAB expression levels. While all BiMABs, compared to the UCHT1 BiMABs, were expressed at a similarly low level, the differences between each 5′and 3′BiMAB were not significant.
We found no publications containing information about any impact of the consecutive order of scFvs within a tandem-single-chain-antibody. However, none of the publications reported on the absence of influence of a consecutive sequence of scFvs. It might be that either no analysis on this has yet been conducted, or that, corresponding to the results of this study, no significant or conclusive results have been obtained by the scientific community.
Thus, we conclude from the expression experiment results that the anti-CD3-scFv derived from UCHT1 has a higher expression level, compared to all other anti-CD3-scFvs. UCHT1-MM exhibited a clearly higher protein production, while the sequence of scFvs within the BiMAB seemed to have no significant influence on expression levels.
Differences like codon optimization also have an impact on BiMAB expression [125]. 1BiMAB is optimized for expression in human cells, whereas the other BiMABs were designed for expression in CHO cells.
In contrast to initial expectations, the yields of CHO codon optimized BiMAB proteins produced in stably transduced CHO cells were not sufficient for protein purification (data not shown). Therefore,

all BiMABs were produced in HEK293 cells. However, in accordance with 1BiMAB´s codon optimization, 1BiMAB protein was efficiently produced by stably transfected human HEK293 cells.
As 1BiMAB was selected as the prototype for the CLDN18.2 bs-td-scAbs and consequently needed to be more closely characterized, we continued with HEK293 as a suitable producer cell line for stable expression.
The up-scaled routine production of 1BiMAB and its FPLC-purification were feasible.
Control BiMAB2 and BiMAB4 were purified, like 1BiMAB, from the supernatant of stably transfected HEK293 cell lines using affinity purification, and subsequently tested for functionality. The proteins were formulated in a 200 mM arginine buffer to ensure their stability.
The yields were sufficient to perform the intended *in vitro* and *in vivo* assays. Nevertheless, we assume that a suitable commercial protein expression system, which is typically used for antibody production, can increase these production efficiencies.
The fact that BiMABs are functionally secreted from the mammalian producer cells (SN has been tested in cytotoxicity assays – data not shown), and the straightforwardness of its purification via Ni-NTA affinity chromatography, significantly simplifies the procurement of antibody material compared to other bsAb formats.
Thus, efficient 1BiMAB production will allow bypassing of production difficulties, such as extremely low yields that are commonly described for most other bsAb classes [126]. The efficiency of 1BiMAB in target cell lysis at low protein concentrations and low E:T ratios is a profitable characteristic of the protein. In view of its compelling therapeutic efficiency, we assumed that the demand for 1BiMAB protein, which will be required for pre-clinical use, could probably be met by its expression in mammalian cells.

4.3.2 BINDING SPECIFICITIES AND MONOVALENT BINDING AFFINITIES

In addition to protein production aspects, we validated a concentration dependent specific binding of 1BiMAB and its four CHO codon optimized competitors, 3´& 5´UCHT1-MM as well as 3´& 5´TR66 (Figure 13), to either target or T cells.
Binding to CLDN18.2+ cells seemed to be equivalent regardless of scFv location within the BiMABs. For T cell binding, these results differed. 5´anti-CD3-scFvs offered a slightly higher MFI than 3´. This holds true for all variants except for BiMAB 3´UCHT1-MM. This BiMAB showed nearly the same MFI as 5´UCHT1-MM. It is possible that the different binding properties (for example differences in the 'on-off rate') of these scFvs for CD3ε are reflected. BiMAB binding was highly selective for cells expressing either its TAA or CD3ε, while cells like HEK293T, which do not express any of the epitopes the BiMAB recognizes, were not bound.
Though direct evidence for simultaneous dual binding has not yet been realized, it was indicated through the BiMAB-induced efficient cell lysis.
Binding affinities in the nanomolar range for both scFvs to the cell line HEK293-CLDN18.2 and to human T cells were determined for the FPLC purified 1BiMAB protein (Figure 17). We detected a stronger binding affinity for the TAA CLDN18.2 than for CD3ε.
This was reported by Bortoletto *et al.* [127] as a favorable attribute of bsAb designed for cancer therapy. Jacob *et al.* [128] described an affinity constant of $K_{aff} = 3.6\times10^{-8}$ M for the mAb TR66, whereas the equilibrium dissociation constant for the L2K scFv of Micromet was 1×10^{-7} M [129]. The binding affinity of 1BiMAB´s TR66-derived scFv was in between these values, which suggested 1BiMAB as a notable prototype.
In order to compare the CLDN18.2 binding affinities of 1BiMAB with its parental antibody, we determined the binding strength of the parental mAb IMAB362 for HEK293-CLDN18.2 and human T cells by flow cytometry.
We measured an equilibrium binding in the nanomolar range (data not shown) comparable to results

obtained for 1BiMAB. Binding to the TAA was found to be three times stronger using IMAB362 than 1BiMAB. A slightly stronger binding of mAb in comparison to scFv binding was also described by Bird *et al.* [130] and might result from the higher avidity (bivalent binding) [131] of mAbs in contrast to a monovalent binding of the TAAs by BiMABs.
Ganymed Pharmaceuticals described a slightly better binding affinity of the mAb IMAB362 for CLDN18.2. This could be due to the use of different and multiple parameters for the determination of the binding affinity. As such, the results are a function not only of 1BiMAB's binding affinity, but also of the affinity of 1^{ry} and 2^{ry} detection antibodies.
Furthermore, saturation in this binding assay depends on the quantity of the CD3-receptor or of the TAA on the cell surface, which can vary donor- and condition-dependent. Hence, a direct labeling of the antibodies and subsequent affinity measurement would be a more accurate way to determine binding affinities in a flow cytometry-based assay.
The binding parameters can also be determined by methods based on surface plasmon resonance (SPR), such as the Biacore instrument or comparable devices. However, no peptide representatives for the epitopes of both scFvs were available at the time for such assays.
Results of these tests would be more accurate as they are independent of target cell conditions and binding affinities of added antibodies. These strategies should be pursued in future drug development procedures.
Nevertheless, even if the suggested methods confirm that 1BiMAB has this somewhat more-moderate affinity for CLDN18.2 , it seems that it did not hamper 1BiMAB´s efficacy at all. The tumor target binding of BiTEs can vary between affinities of 10^{-8} M and 10^{-9} M without significantly influencing the EC_{50} values [72].
This suggests that, in contrast to mAb of the IgG class, higher affinity binding only has a small impact on the potency of this bs-td-scAb format. Low expression of the TAA CLDN18.2 on normal tissues and a greatly increased expression on tumors [16] creates a good therapeutic window for BiMABs, without the requirement for extremely high affinities.
Nevertheless, both antibodies - 1BiMAB and IMAB362 - bound specifically, which was confirmed by several binding controls (data not shown). For example, BiMAB2 was taken as a control BiMAB to exclude unspecific binding. An IgG antibody with the same backbone (heavy and light chains) as IMAB362, but with different complement determining regions (CDRs), was used as an equivalent control for IMAB362.
Both control antibodies did not show any binding to the HEK293-CLDN18.2 cell line. In further experiments, it was revealed that specific binding occurred only via their antigen-binding site. In these assays, 1BiMAB (fluorescently labeled by 1^{ry} and 2^{ry} antibodies) that had already bound to the TAA+ cells was competitively displaced by abundantly provided IMAB362, and vice versa: IMAB362 could also be competitively displaced by 1BiMAB.
Hence, the binding of both antibodies to this cell line occurred only with their antigen binding sites. IMAB362, control IgG, BiMAB2, and 1BiMAB were additionally tested for binding to the irrelevant HEK293-Mock cell line, but no antibody binding was detected (data not shown).
Furthermore, no binding took place using cell lines that expressed molecules that were highly related to the TAA such as the CLDN18 splice variant one expressed by HEK293 cells, as has been demonstrated for IMAB362 by Sahin *et al.* [8]. In additional investigations, mediation of T cell effector functions that indirectly indicate antibody binding were investigated with further gastric cancer cell lines not expressing CLDN18.2, such as the gastric or pancreatic carcinoma cell lines MKN7, SNU1, KP-4, and the breast cancer cell line MCF7. Again, no unspecific activation was detected.
In summary, a concentration dependent binding of 1BiMAB to CLDN18.2+ cells and cells expressing the CD3ε on their cell surface has been confirmed in this study.

4.3.3 SAFETY PROFILES AND SPECIFICITIES OF ALL BIMABS

Along with efficacy, the most important aspect in the development of a drug is the safety. Several controls in each assay have to prove the accuracy of the required mode of action, without the generation of any concomitant effects.
BiMAB2, BiMAB3, and BiMAB4 were used as negative-control-antibodies in the experiments, because their target antigens were not expressed by the cancer cell lines used.
IMAB362 also served as a negative control because this mAb is not supposed to elicit any effects in the absence of NK cells or monocytes.
As expected, none of the negative controls showed an unspecific induction of lysis. Therefore, we proved that monovalent binding of only one scFv on its own did not result in tumor cell lysis. Neither the anti-CD3-scFv alone (BiMAB2, 3, or 4) nor the TAA-specific binding domains of the mAb IMAB362 induced T cell activation.
These controls were additionally tested in the presence of T cells or target cells alone and provided the evidence that the BiMAB format only activated T cells when it was simultaneously linked to its TAA CLDN18.2.
Correspondingly, using the above test conditions, none of the CLDN18.2-specific BiMABs[16] elicited T cell activation or were tumoricidal. These findings were consistent with those described by Brischwein *et al.* [55] and Dreier *et al.* [129] as 'target cell dependent T cell activation' by BiTE antibodies. Target cell dependent T cell activation has been explained as the effect of "clustering and activation of T cell receptors by only the small fraction of BiTE antibodies presented to T cells on the surface of target cells" [44].
Although the direct T cell activation mechanisms by bs-td-scAbs are not yet completely understood, this mode of action was reviewed as follows: "Monovalent binding to the CD3 complex by BiTEs is apparently not sufficient to lead to a full-blown T-cell activation. Only when BiTEs are arrayed on the surface of a target cell (i.e. are presented to T cells in a polyvalent form) do they cause robust T-cell signaling, redirected lysis and a cascade of subsequent events" [72]. Wolf *et al.* declared this target cell dependent T cell activation by bsAbs to be the major premise for a secure drug [72].
Unspecific T cell activation in patients can provoke symptoms of cytokine release syndrome that can result in multiple organ dysfunctions, which is what happened to volunteers during the testing of the drug TGN1412 [132].
In the absence of TAA expression, 1BiMAB showed no T cell activation *in vitro* even when EC_{50} values for redirected lysis were exceeded 10-fold (Figure 22) nor by measuring after an extensive coincubation time of 144 h (Figure 18). Thus, no signs of unspecific T cell activation using CLDN18.2 negative target cell lines were observed, but a specific activation was measured by flow cytometry when using a pancreatic cancer cell line (DAN-G) that expresses only low levels of CLDN18.2.
In comparison to target cells with a higher TAA expression, T cell activation by 1BiMAB was clearly decelerated. The cells were under continuous microscopic observation, so that T cell activation and target cell lysis would not be missed. Despite the slowdown in T cell activation, we microscopically observed a clear clustering of T cells around the DAN-G target cells, a formation of cytolytic synapses, lysis of target cells, and an increased number of T cells, indicating proliferation during these 144 h.
Therefore, these *in vitro* results allowed us to draw the conclusion that the efficacy of our BiMAB format is definitely dependent on TAA surface expression, making it suitable to specifically retarget and activate T cells only towards CLDN18.2+ cancer cells. A particularly outstanding and promising property of 1BiMAB is therefore its potency to effectively target cells that only have low expression

[16] With the exception of the 5'TR66-BiMAB, this was excluded from the selection pool in the next chapter for that very reason.

of the target antigen. Furthermore, the requirement for dual binding was confirmed by the absence of antitumor activity or T cell activation when using the control BiMABs. In conclusion, the prototype 1BiMAB functioned *in vitro* as a highly specific and thus a safe drug.

4.3.4 SELECTION OF THE MOST EFFECTIVE BIMAB IN CANCER CELL ELIMINATION

In this study, nine recombinant bispecific antibodies targeting the TAA CLDN18.2 were under investigation for their potential use in gastric cancers. We confirmed the functionality of all BiMABs in cytotoxicity assays.
Seven out of nine BiMABs were able to induce a target cell lysis of over 90 % (Figure 12). One out of these seven BiMABs showed a late onset of target cell killing with a low lysis value until 24 h (5′CLB-T3), but then reached a high lysis value after 48 h. This indicates a high potency of this BiMAB once it started its action.
On the other hand, the results could also mean that, compared to the other BiMABs, a much higher activation threshold is present until T cell triggering is initiated. This results in an undesirable delay of T cell recruitment. CLB-T3 is described as a mAb with a high avidity for the CD3 complex [123], which might be the reason for the delayed activation.
High avidity seems to be suboptimal for T cell recruitment, as Viola *et al.* [133] reported that "high affinity of binding prevents antibodies from serially triggering TCRs [T cell receptors]".
Moreover, Bortoletto *et al.* [127] concluded that the reduction in binding affinity to CD3 results in improved T cell activation. Thus, he concluded that binding to CD3ε of an anti-CD3 antibody, which is characterized by a high 'on-off rate', is more efficient in triggering T cell activation. Therefore, the long-lasting binding of CLB-T3 scFvs to the CD3 complex might have delayed the progress in T cell triggering. This characteristic may be of advantage for certain therapeutic applications.
Nevertheless, we prefer BiMABs with an anti-CD3-scFv that offers the above mentioned high 'on-off rate'. Using our approach, the BiMABs we selected were able to effectively induce T cell activation without delay, in correlation with a steady progress in target cell lysis. Five BiMABs fulfilled these criteria, and choosing them restricted the selection of anti-CD3 scaffolds to those scFvs solely derived from mAbs TR66 and UCHT1-MM.
Besides OKT-3, UCHT1-MM is the most intensively studied antibody in the field of anti-CD3 antibodies and is described as an effective T cell activating antibody [134]. The high incidence of UCHT1-MM usage, and the initial selection of mAb TR66 by Micromet for their BiTE format, reflect their superior properties compared with other anti-CD3 mAbs, which supports our selection. From the results, we concluded that the choice of specific anti-CD3-binding domains could differently affect the *in vitro* cytotoxic efficacy. In addition to their good producibility, their potency in tumor cell lysis strongly supported our selection of UCHT1-MM and TR66.
Differences between these five BiMABs were identified using further characterizing *in vitro* assays (Figure 12, Figure 14, Figure 15). Epitope binding, T cell activation, and target cell lysis were all considered. However, the assays did not show a clearly superior candidate. On the other hand, the experiments revealed major differences in target cell lysis between both CHO codon optimized TR66-BiMABs, especially in titration assays.
5′TR66 was significantly less efficient than 3′TR66 in inducing target cell lysis at low BiMAB concentrations. In this particular case, the position of the anti-CD3-scFvs within these two BiMABs indicated a benefit of its C-terminal orientation. Moreover, a slight T cell activation in the absence of target cells and sporadic minor toxic effects on target cells were observed in further samples lacking T cells, which disqualified 5′TR66 as drug candidate. Hence, considering the uncertain results obtained from usage of 5′TR66, the number of candidates could be reduced to four BiMABs.

The remaining four BiMABs showed a specific binding to both of their target-epitopes: CLDN18.2

and CD3ε, which led to a comparable T cell activation, and consequently to efficient target cell lysis. Thus, all four BiMABs had almost the same potential for their selection as a promising drug prototype candidate. The differences in T cell activation and target cell lysis were not significant.
The high expression levels of UCHT1-MM BiMABs and the extremely fast induction of target cell lysis accounted for the selection of 5′UCHT1-MM. However, the observed differences in target cell lysis efficiency and T cell activation by 3′or 5′UCHT1-MM, respectively, were not consistent. Sometimes 5′ UCHT1-MM showed the best results, whilst in other cases the 3′BiMAB was better. Both BiMABs were highly effective, but the results could not be referred to one of the BiMABs because the results alternated. This made it difficult to select one as the preferred BiMAB.
In contrast, both BiMABs containing the TR66 scFv (3′TR66 or 1BiMAB) delivered more consistent results . Both BiMABs take advantage of the same C-terminal positioned TR66-scFv. Their different codon optimization (1BiMAB–Homo sapiens (HS); 3′TR66–Chinese hamster ovary (CHO)) resulted in a nucleotide sequence difference of 16 %[17], while the remaining 84 % are identical.
They have a high AA sequence similarity of 97 % within their complete BiMAB open reading frame with only five amino acids (AA) not matching[18]. These different AA (highlighted) are located in the long linker forming the 3′anti-CD3-scFv of 1BiMAB. The AA sequence for 1BiMAB – **VE**(GG**S**GGS)$_2$GG**VD** – was juxtaposed to the AA sequence of the 3′long linker – (GGGGS)$_3$ –belonging to 3′TR66.
It has been published by Jiang *et al.* [135] and Digiammarino *et al.* [136] that differences in the linker may lead to completely different antibody properties, because the physiological attributes of the linker may affect the flexibility between the binding domains. In this study, no major differences between both BiMABs (1BiMAB & 3′TR66) have been observed.
1BiMAB was assigned the highest priority in the ranking list because this BiMAB repeatedly showed a better efficiency in the triggering of T cells and the induction of target cell lysis compared to 3′TR66 and both UCHT1-MM BiMABs, which can be seen e.g. by a comparison of the lysis curves in Figure 12. While 1BiMAB offered a consistent progression in lysis, the lysis mediated by the remaining BiMABs increased gradually. In addition to the finding that 1BiMAB had a slightly better protein expression yield than 3′TR66, our choice was further supported by the fact that 1BiMAB protein expression, in contrast to 3′TR66, 3′-and 5′UCHT1-MM, is possible in both human (HEK293) and in CHO cells.
The remaining three BiMABs 3′TR66, 3′UCHT1-MM, and 5′UCHT1-MM may be of future use as potent alternatives for the removing of CLDN18.2 positive cells, and will be kept in mind as 'reserve players'/substitutes.
In summary: to select a lead molecule, we considered defined properties of the BiMAB format such as protein expression, selective and specific BiMAB-binding, T cell activation, and target cell lysis throughout our screening process. In these screening rounds, 1BiMAB best met the pre-established criteria to proceed to the next drug discovery stage: the characterization of the prototype. Further molecular analysis of 1BiMAB including quantification of expression levels from stable mammalian expression systems, degradation analysis by SDS-PAGE and Western blot analysis, as well as the determination of binding affinities by flow cytometric analysis, showed encouraging properties confirming 1BiMAB as a promising bs-td-scAb prototype.

[17] Clone Manager Professional Edition 9.02 using the function compare two sequences as assembled DNA alignment of both strands referring to the method of FastScan-MaxQual

[18] Clone Manager Professional Edition 9.02 using the function compare two sequences as amino acids referring to the algorithms of BLOSUM62

4.4 EVALUATION OF 1BIMAB

In our setting, we wanted to target the novel TAA CLDN18.2 using a T cell recruiting bs-td-scAb. Until now, this newly described target has only been verified using the mAb IMAB362 in the IgG mAb format produced by Ganymed Pharmaceuticals AG. Thus, a direct extrapolation of the BiMAB data onto already existing bs-scAb formats was not feasible.

4.4.1 SETUP DIFFERENCES IN BS-SCAB FORMATS

In order to validate the prototype 1BiMAB, a structural comparison to other bs-scAbs is mandatory to determine the major differences. To date, the bs-td-scAb targeting CD19 and CD3 (CD19×CD3; termed Blinatumomab, MT103), is the best described bs-td-scAb. This molecule has been compared extensively to numerous other bs-scAb formats binding CD19 as a model antigen. The most promising formats were the TandAb and DART setup. The described comparison of the formats of BiTEs, TandAbs, DARTs, and BiMABs should reveal their differences and put them into a common context. While the BiMABs offer a complete new specificity in binding the TAA CLDN18.2 instead of the model antigen CD19, their setup is structurally most similar to the bs-td-scAb format of the CD19×CD3 BiTE Blinatumomab.

Small structural differences between them were revealed, such as the assembly of the variable domains, which is as follows: $V_{L(TAA)}$-$V_{H(TAA)}$-$V_{H(CD3)}$-$V_{L(CD3)}$, in contrast to the BiMAB assembly of $V_{H(TAA)}$-$V_{L(TAA)}$-$V_{H(CD3)}$-$V_{L(CD3)}$. It was stated by Dörken *et al.* [137] that variable domain arrangements have no impact on the efficacy of their BiTE single chain antibodies. The impact of the V_H/V_L domain assembly within 1BiMAB remains to be investigated.

In contrast to BiMABs and BiTEs, both formats, TandAbs and DARTs, belong to a second class of bs-scAbs, the Diabodies. The DART antibody is based on the bispecific Diabody format, but additionally it is covalently linked by a C-terminal disulfide bridge and forms a molecule of around 50 kDa [138]. The tetravalent tandem Diabody structure called TandAb is comprised of two single-chain molecules that contain four variable antibody domains in an orientation that prevented intramolecular pairing [74]. The homodimeric self-assembly generates a 114 kDa antibody [139]. Due to their high molecular weight, TandAbs offer longer blood retention when injected into mice, offering a pharmacokinetic advantage compared to the ~55 kDa bispecific molecules [140].

Dreier *et al.* [129] admitted the possibility that differences in the efficacy of other bispecific antibody formats may result,amongst other factors,from a different potential to trigger T cells via their respective CD3ε binding scaffold. Therefore, it is important to mention that OKT3 was used as the parental anti-CD3 mAb for the construction of TandAbs [139]. However, in the first two publications on the bispecific single-chain-antibody CD19×CD3, the anti-CD3-scFv was derived from cDNA coding for the mAb TR66 [141, 142].

Thus, in the comparison-study of BiTE and DART molecules, both antibodies made use of the variable domains of the anti-CD3 mAb TR66 [138], as did 1BiMAB. Unfortunately, no publications on the direct comparison of anti-CD3-scFvs derived from the mAb TR66 with remaining well-known anti-CD3-scFvs (OKT3, UCHT1, CLB-T3), similar to our BiMAB comparison study, could be found.

As postulated by Dreier *et al.* [129], the efficacy of the TandAb using another anti-CD3-scFv was not comparable to that of bs-td-scAb. A direct comparison of a CD19xCD3 TandAb and BiTE showed the latter to be significantly more potent, whereas the CD19xCD3 DART outperformed the CD19xCD3 BiTE Blinatumomab *in vitro* by means of its more potent B cell lysis [138]. Due to the fact that the same antigen binding sites (CD19 and TR66) were used in both molecules, the authors concluded that the structural distinctions inherent in the DART antibody setup caused the difference in activity [138].

In contrast to the TandAb and BiTE format, no DART has yet been clinically validated, but results are

awaited eagerly by the bsAb community. Thus, the BiTE format is currently the best clinically validated bs-scAb format. A direct comparison of the BiMAB, TandAb, BiTE, or DART format is not feasible and not anticipated due to their scFvs targeting different TAAs. However, our aim was not to produce a competing bsAb format, but rather to generate an effective bispecific antibody that can be used in cancer therapies targeting the tumor specific antigen CLDN18.2, particularly in gastric and pancreatic adenocarcinomas. TandAbs, DARTs, and BiTEs are described as platform-technologies, which means that their cancer associated binding domain can easily be exchanged. Thus, bispecific antibodies targeting the antigens EpCAM, EGFR, PSA, CD30, CEA,CSPG4, HER2,CD33, CD20, EphA2, 17-1A, IL-1, ADAM17 as well as IGF1R have already been generated, and more are currently under investigation. 1BiMAB came along as a new bs-td-scAb adding to this list the novel promising 'ideal target' CLDN18.2.

4.4.2 *IN VITRO* PERFORMANCE AND ASPECTS OF THE MODE OF ACTION

The main goal of this study was to discover a potent recombinant bs-td-scAb for cancer immunotherapy with a strict targeting of the highly selective tumor associated antigen CLDN18.2. One critical step in the mode of action of T cell recruiting bsAbs is the formation of the so-called bs-scAb-mediated cytolytic synapse between effector and target cells.
Its formation initiates the specific tumor cell lysis. Immunofluorescence staining of molecular structures involved in the antibody-induced synapse formation can directly verify this phenomenon as shown by Offner *et al.* [52].
The formation of cytolytic synapses mediated by 1BiMAB was confirmed and recorded on microscopic pictures, which were labeled following the principle presented on the pictures of Haas *et al.* [67], as shown in Figure 19.
The process of bsAb-mediated cytolytic synapse formation and T cell activation can be indirectly confirmed by the secretion of the serin protease Granzyme B. 5 ng×mL^{-1} 1BiMAB led to an excessive induction of Granzyme B expression (Figure 21), similar to that induced by 1 ng×mL^{-1} BiTE MT110 [51]. At this concentration, a robust 1BiMAB-mediated T cell proliferation (Figure 20) was observed, comparable to that described by Brandl *et al.* [143].
To collect more information on the T cell activation mechanisms induced by 1BiMAB, we studied the dependency of T cell responses on the E:T ratio. We achieved a remarkable lysis of 60 % after 24 h with an extremely low E:T ratio of 0.3:1 (Figure 25). This indicates that 1BiMAB might support serial lysis as reported for bs-scAbs [144], which still has to be confirmed for 1BiMAB, possibly using video microscopic assays.
In conclusion, the anticipated mode of action for BiMABs, such as the induction of MHC, or costimulatory molecule independent T cell activation, the proliferation of T cells, the Granzyme B upregulation and finally the target cell lysis could be confirmed in this study. Importantly, our findings demonstrate that 1BiMAB generated potent T cell immune responses against CLDN18.2-positive targets analogous to that of antibodies of the same bs-td-scAb class against their respective targets.

T cells isolated from one donor can be categorized into several subsets. The most abundant subsets of T cells are categorized into either CD4-positive or CD8-positive T cells. We could verify the contribution of CD4-positive and CD8-positive T cells in 1BiMAB-mediated T cell activation (Figure 23) and target cell lysis (Figure 24), similar to reports on common bsAb used in the pre-clinic or clinical trials [145, 118, 142, 51]. We measured a polyclonal T cell activation demonstrated by the *de novo* expression of early and late T cell activation markers.
CD4-positive and CD8-positive T cell subsets showed comparable potencies in response to 1BiMAB, with regard to their ability to be activated and to provoke target cell lysis, compared to the Pan-T cell population. The only differences were observed in their kinetics. CD4-positive T cells needed

16 h to be activated, compared to CD8-positive T cells that needed only 8 h. This 8 h delay could also be observed in the efficacy to induce target cell lysis, and as reported for CD4-positive T cell activation by CD19xCD3 bs-td-scAbs [142, 129]. It was assumed that CD4-positive T cells initially have to produce lytic molecules such as Granzyme B and Perforin *de novo*. This would explain the delayed response.

However, a release of the contents of cytotoxic storage granules was observed in the context of CD19xCD3 bs-td-scAbs usage, directly after the activation of CD8-positive T_{EM} cells [78,51]. The examination whether 1BiMAB induced this pathways remains to be done, but the upregulation of Granzyme B in T cells as a response to 1BiMAB-mediated T cell activation has already been shown (Figure 21). This indicates the implementation of the granzyme induced apoptosis pathway by 1BiMAB.

Supplementary characterization of T cell subsets will be necessary to precisely define those T cell subsets that are recruited by 1BiMAB and subsequently determine their mode of action. Thus, it can be evaluated how 1BiMAB integrates into the immune response.

This approach can also help to find answers for the problem of 'inter-donor variations' that we observed in our *in vitro* T cell activation and cytotoxicity assays. 1BiMAB elicited a concentration dependent T cell activation in coculture experiments when added at a concentration higher than 0.01 ng×mL^{-1} (Figure 22-B). However, the efficacy of 1BiMAB-mediated T cell activation was highly variable. The level of activation of T cells could differ greatly between individual donors.

T cells of each individual donor seemed to have their own sensitivity, reactivity, and responsiveness. Correspondingly, using several T cell preparations, the inter-donor variability was also clearly reflected in the four different dose-response-curves illustrating target cell lysis (Figure 22-A).

The EC_{50} values obtained for cell lysis by 1BiMAB using different T cell donors were in a low range of 11-500 pg×mL^{-1} (> 4 donors tested). This value is not far from that of Blinatumomab with a half maximal concentration for redirected lysis between 10 and 100 pg×mL^{-1} (> 80 donors tested).

Results indicated that EC_{50} values could not be compared between experiments that used different donors. This high variability was also reported by Dreier *et al.* [129] and Hauff *et al.* [146], who only gained reproducible EC_{50} values in assays that were repetitively prepared with T cells from the same donor.

We concluded that target cell lysis might not only depend on the ability of 1BiMAB to recruit and activate T cells, but that further factors such as the health and immune status of the donor, the current activation conditions (pre/unstimulated), or responsiveness of the respective T cells might have strongly influenced the outcome of the experiments.

Dreier *et al.* [129] even indicated possible "unknown polymorphisms in the genes of T or B-cell target molecules" as a source of the high EC_{50} value variability. Thereupon, Kufer *et al.* [141] and Dreier *et al.* [129] analyzed the effector cell subsets that were activated by their bs-td-scAb molecules. It was revealed that it was the effector memory T cells (T_{EM}) double-positive for (CD45RO+/CD4+) or (CD45RO+/CD8+) that were mostly engaged by the BiTE molecules, while it seemed that naïve (CD45RA+/CD4+) or (CD45RA+/CD8+) T cells were not activated [141, 129].

This suggested that one reason for the observed variability between donors depended on the numbers of effector memory T cells. Thus, a profound knowledge of the interaction partners of 1BiMAB is necessary in order to explain these limitations and reduce or circumvent them in the cytotoxicity assays.

Moreover, differences in tumor associated antigen expression levels in target cells also play a role in inter-assay variations. T cell donor dependencies manifested in an unpredictable and variable activation time. For example, a low expression level of the TAA prolonged the time required for BiMAB-mediated activation, whilst a high expression level reduced it.

Hence, variability in the duration of T cell activation and target cell lysis is not only T cell donor dependent, but also differed with the surface expression of TAA and target cell's resistance to BiMAB induced lysis, which has previously been reported for bs-td-scAbs e.g. by Wolf *et al.* [72]. As the expression of TAA by target cell lines should resemble the situation in endogenous tumors, these fluctuations in TAA expression and the corresponding variations in the assay results were taken into account.
A way to minimize the influences of TAA expression or donor dependency on the results is the measurement of large quantities of assays combined with statistical analysis of the results as done by Dreier *et al.*[129]. However, this is only feasible if a high-throughput system for *in vitro* tests has been implemented.
To reduce the impact of quality fluctuations between different protein-batches on the dose-response curves, each 1BiMAB batch was tested after purification for its biological functionality. Thus, new and old batches were compared to each other in a parallel cytotoxicity assay.
To reproduce the EC_{50} values for 1BiMAB, it is important that theses assays should be repetitively performed using effector cells of the same donor just as shown by Dreier *et al.* [129] , but have not yet been tested
To date, the best method to pre-stimulate T cells without disturbing our assays has not been determined. Pre-stimulation of T cells would induce a potent and consistent donor-independent activation level and thus help to obtain more reproducible results.
In summary, we confirmed that 1BiMAB mediated a concentration dependent T cell activation measured by the *de novo* expression of CD69 and CD25, an increased Granzyme B accumulation in activated T cells, and a proliferation of T cells. 1BiMAB-mediated T cell activation is polyclonal and resulted in the lysis of the target cancer cells by high percentages of peripheral CD4-positive and CD8-positive T cells even at low E:T ratios. 1BiMAB's efficacy at low doses and low E:T ratios suggests a potent therapeutic effect using only small amounts of protein, though this remains to be proven in preclinical studies. All processes were shown to be target cell dependent and did not need additional expansion, pretreatment, or coactivation of effector cells. Thus, we conclude that 1BiMAB is a potent bispecific antibody *in vitro*.

4.4.3 EFFICACY OF 1BIMAB *IN VIVO*

In this study we show that 1BiMAB can effectively be utilized in the *in vivo* therapy of CLDN18.2-positive tumors in a NSG mouse xenograft model. The immuno-incompetent background of these animals has the clear benefit of evaluating drug candidates in an animal system using human tumor tissue and an artificial human immune system [118].
Eradication of CLDN18.2-positive tumor tissue relied on the recruitment of the engrafted human T cells via 1BiMAB and the generation of potent T cell immune responses against the malignant tissue. This anti-tumor activity occurred without previous stimulation of PBMCs or treatment with an anti-CD28 antibody, as described for other bsAbs [147].
We identified a high efficacy of 1BiMAB to impede tumor growth and eliminate established subcutaneous tumors (average tumor volume at treatment start: ~15 mm^3).The model allowed us to confirm a potent *in vivo* efficacy of 1BiMAB, proven by the complete elimination of the CLDN18.2-positive parts of established solid tumors. The experiment resulted in eight tumor free mice and partial responses in the remaining seven mice. The significantly prolonged overall survival following repeated treatment of mice with the low dose of 0.25 $mg \times kg^{-1}$ 1BiMAB in the presence of PBMCs (Figure 27, Figure 28) confirmed the potency of this antibody.
An explanation for the partial responses (Table 17) might be targeting-difficulties of 1BiMAB caused by TAA negative cells within the tumor. Five tumors had regions that had lost CLDN18.2 expression, and two tumors out of the seven had no remaining CLDN18.2 expression at all.

Consequently, using the xenogeneic target cell line HEK293, thought to stably express the transgene CLDN18.2, was a limitation of the current model. These cells suffered a spontaneous partial loss of TAA expression when inoculated subcutaneously (Figure 28). This indicates a genetic or epigenetic instability in the expression of the TAA. This could be due to heterogeneous distribution of TAA expression amongst the cell population (not detectable with flow cytometric measurements – data not shown) or an epigenetic influence that resulted in the down regulation of the TAA. It remains to be proven if down regulation of the TAA resulted from a selective tumor escape mechanism that would also be present in cell lines endogenously expressing CLDN18.2.
Another possible cause of the down regulation is a high susceptibility of the CMV promoter to methylation [148], causing the silencing of the transgene [149,150] CLDN18.2. In order to find alternative cell lines, we tried to engraft target cell lines endogenously expressing CLDN18.2 in NSG mice, but so far, we have failed to establish a model. Nevertheless, these results show that 1BiMAB´s mode of action is highly dependent on the presence of its TAA.
An unexpected outcome was observed in the mice of group 2 that received 1BiMAB, but was devoid of PBMCs. Compared to control mice receiving only vehicle buffer a delay in tumor growth was observed in this group. Since this effect cannot be caused by effector cells, it might be the result of 1BiMAB binding to the TAA itself. Binding of the parental mAb IMAB362 is thought to elicit anti-proliferative and proapoptotic effects [19] in CLDN18.2-positive cancer target cells. Thus, binding of the CLDN18.2-specific arm of 1BiMAB alone might also impair tumor growth to some extent.
The mice that received 1BiMAB protein injections experienced no adverse events or significant weight loss. This indicated a good overall tolerability during the treatment of the CLDN18.2 binding arm of 1BiMAB, which is capable of binding its murine orthologue.
In contrast to the anti-CLDN18.2 scFv, the anti-CD3-scFv of 1BiMAB is not cross-species reactive with rodent tissues. This implies that 1BiMAB does not recruit murine T cells (also tested by flow-cytometry binding analysis – data not shown) or interact with murine tissue. Thus, mouse models cannot be used to study side effects induced by the anti-CD3-scFv of 1BiMAB, so that a direct extrapolation from rodent models into clinical practice is not possible. Therefore, a reliable pharmacological and toxicological analysis of 1BiMAB will only be feasible in clinical studies. A surrogate BiMAB that is able to recruit murine T cells might be another alternative to study side effects in a syngeneic model.
Due to the binding specificity to human T cells only, we needed a preclinical model that mimics the human immune system. We therefore engrafted human PBMCs in these immunodeficient mice. The susceptibility of engrafted T cells to 1BiMAB redirection, effective T cell activation and induction of target cell lysis was confirmed in an *ex vivo* assay (Figure 26) with splenocytes isolated thirty days after injection of PBMCs.
The T cell mediated eradication of tumors in eight mice (Figure 27, Figure 28) further confirms the activity of the engrafted T cells. However, we are aware of the fact that the reconstituency model system only resembles a human immune system and is incomplete and artificial [151]. This is because engrafted human T cells are probably not able to behave, communicate, or interact with rodent tissue like rodent cells do. Thus, the reconstituted human immune system lacks homing signals from the microenvironment necessary for functional human hematopoiesis [152,153].
In the NOD/SCID-background, the T cells remain functional mainly in the peritoneum for only three weeks after engraftment, as described by Tary-Lehmann [153]. It was reported that after three weeks, most T cells in the peritoneum will die and only specific mouse-reactive clones remain and repopulate the mice [153,151].
This artificial and functionally limited immune system in NOD/SCID mice, consisting of mainly mouse-reactive anergic clones, is associated with the appearance of an 'anti-host response', termed graft versus host disease (GVHD) [153,152]. Accordingly, 1BiMAB's therapeutic effect occurred

within these three weeks, and utilized the still functional reconstituted immune system. Finally, following 1BiMAB treatment in our tumor model, the remaining mice were kept under observation in case of a possible relapse. However, the animals generally had to be sacrificed after a short period due to GVHD symptoms. Consequently, it was not possible to examine animals after treatment in a long-term follow up study. Nevertheless, the first *in vivo* studies of MT103 and MT110 testing efficacy were also performed in immunodeficient mice.

A frequently used therapeutic model alternative to effector cell engraftment is the simultaneous subcutaneous inoculation of target and T cells [154]. This model was termed "admixed experiments" in the review of May *et al.* [29], and entails a direct commencement of treatment whilst simultaneously measuring antibody efficacy through the delay or lack of tumor growth. These admixed experiments might resemble an early cancer treatment option or the situation in lymphomas, but these cell mixtures do not reflect the clinical situation of established solid tumors. For that reason, this tumor model would not be a suitable substitute for our experimental setup and could therefore only be used as an adjunct to collect supplementary 1BiMAB potency data.

In summary, our xenogeneic NSG tumor mouse model can reflect the setting of solid tumors in the presence of a human immune system, but it does not permit 1BiMAB safety analysis. Taking into account that we tried to study the effect of the human immune system in this type of cancer therapy, this model was potentially restricted by GVHD in the NSG background. Due to the conceivably diminished human immune system of the mouse, it is even imaginable that in a realistic clinical situation – i.e., in the presence of an intact human immune system – our therapeutic results would improve. On the other hand, patients can likewise present a disordered and impaired immune system after several rounds of chemotherapy treatment, similar to our NSG mouse model.

Despite its limitations, the model allowed us to confirm a potent *in vivo* efficacy of 1BiMAB, while the repetitive low dose of only 0.25 mg×kg^{-1} of a mouse would translate to a human dose of approximately 0.02 mg×kg^{-1} for an average (60 kg) adult. (This dose calculation bases on the formula considering the body surface area (BSA) normalization method defined by Reagan-Shaw *et al.* [155].) Bs-td-scAbs might improve antibody-based cancer immunotherapy by requiring considerably lower doses than currently approved mAbs in solid cancer therapy, such as 2 mg×kg^{-1} for Herceptin or up to 10 mg×kg^{-1} for Avastin [118]. A titration of 1BiMAB in *in vivo* dose finding experiments will provide evidence of the precise limiting dose for an effective 1BiMAB therapy and might reveal that it possibly can be smaller than the already used 0.25 mg×kg^{-1} in mice.

4.5 SUMMARY OF 1BIMAB EVALUATION

Fundamental properties of IMAB362 such as efficacy and highly selective binding of the novel and 'ideal target' CLDN18.2 were transferred to the bs-td-scAb format 'BiMAB' for therapeutic use *in vitro* and *in vivo*. Production efficiency, selective and suitable epitope affinities, specificity, a potent target cell dependent activation of T cells and resultant target cell lysis are proven characteristics of 1BiMAB. Due to its format and its effectiveness, 1BiMAB seems to be capable of overcoming several challenges in the treatment of cancer [37] such as:

1. Low ratios of T cells within the tumor tissue will not be a problem because 1BiMAB is effective even at low E:T ratios;
2. Low drug amounts in the tumor as a consequence of limited penetration into malignant tissues may be overcome by the small size of BiMABs (< 60kDa) and the need for only small 1BiMAB concentrations;
3. The suppression of anti-tumor immunity as a tumor evasion mechanism can be bypassed by the MHC independent engagement of T cells.

It is remarkable that neither pretreatment of effector cells nor costimulatory reagents are required for 1BiMAB. These *in vitro* and *in vivo* analyses show that 1BiMAB has a great potential for the treatment of solid cancers, but a more comprehensive characterization of its properties and mode of action are still outstanding. The next steps in the development of our prototype 1BiMAB as a therapeutic antibody will be discussed in the following chapter.

4.6 PERSPECTIVES– 1BIMAB IN THE DRUG DEVELOPMENT PROCESS

The primary goal of this study was the translation of the ideal mAb Claudiximab (IMAB362) into a T cell recruiting bispecific antibody recognizing the 'ideal target' CLDN18.2. The prototype–1BiMAB is at the first step of drug discovery and its development into a promising BiMAB antibody. A key next step would be a further characterization of 1BiMAB's mode of action.

Additional experiments would clarify its so far indirectly shown mode of action. For example, one could test the inhibition of the perforin- and granzymes-based apoptosis pathway by an application of abundant EGTA, or perform competition experiments using cumulative amounts of the parental monoclonal antibodies IMAB362 and TR66.

It is expected that both experimental setups will block 1BiMAB-mediated processes and consequently result in a lack of target cell lysis. The first experiment, the inhibition of the perforin- and granzymes-based apoptosis pathway, would prove the initiation of the perforin dependent apoptosis pathway by 1BiMAB. The second experiment, the application of abundant EGTA, would confirm the participation of both the perforin- and the granzymes-based apoptosis pathways within the process of tumor elimination. EGTA binds Ca^{2+} and in that way, it would inhibit the Ca^{2+} dependent perforin- and the granzymes-based apoptosis pathway. This would probably result in the absence of target cell lysis induction.

Further characterization can be obtained using common stability analyses that confirm protein functionality after altering storage conditions. It has to be evaluated whether the efficacy of 1BiMAB is impaired by exposure of 1BiMAB to realistic treatment conditions such as coincubation with fresh human serum, the use of various T-cell subsets and tumor cell lines, or by using tumor tissue and/or PBMCs from patients previously treated with chemotherapy.

The involvement of different effector cell populations has to be described in more detail. Experiments should include data analysis of the spectrum of induced cytokine- and chemokine-release, effects on T cells costimulated with CD28 and IL-2, proliferation, and the successive behavior of these cells after removal of 1BiMAB.

The activity of redirected human T cells against murine TAA-positive but human MHC negative cells

would further demonstrate the MHC class independent activation of T cells by 1BiMAB.
As strategies of combined anti-cancer therapies can elicit synergistic effects, offering an improvement to the monotherapeutic approach, a possible combination of 1BiMAB with common solid cancer therapies should be addressed throughout drug development, especially its use in combination with IMAB362 [16] or HBcAg-CLDN18.2-VLPs [156].
Additionally, it has been shown that blocking CTLA-4 drastically increased the number of infiltrating CD8-positive T cells in tumors [157]. Thus, anti-CTLA-4 could help improve the T cell recruiting antibody treatment of solid cancers by accumulating T cells in tumors. This might enhance the therapeutic efficacy of bs-td-scAbs, and could therefore be a suitable treatment partner for 1BiMAB *in vivo*.
During the drug development process, further challenges with comprehensive product characterizations will be encountered. A plethora of data has to be collected before embarking on a clinical trial, starting with bioanalytical testing including formulation research, pharmacokinetic- and drug-disposition-studies to support the drug dose finding and preclinical safety experiments.
The bio analytical work is a key element of protein characterization and supports all other processes in finding and providing optimal biochemical and biophysical analysis techniques [158].
Experiments to determine manufacturability, assurance, and quality control including determination of aggregation or degradation by size exclusion chromatography are planned for 1BiMAB or its matured derivatives. The determination of binding affinities for BiMAB antibodies via Biacore and KinExA analysis are intended.
Finally, there is a vital need to evaluate whether the reported therapeutic effects can be replicated in appropriate animal models. Therefore, the establishment of animal models that reflect the clinical setting as closely as possible is required.
In 2002, Dreier *et al.* [129] described the exchange of the TR66 scFv by a deimmunized scFv derived from the mAb L2K for the first time. The main reasons for this exchange were diL2K-scFv's cross reactivity with cynomolgeous cells, and the aim of reducing the humoral immune response against murine antibody sequences. The complementarity determining regions (CDR) of the scFv of di-L2K were mutated to create a less immunogenic scFv, whilst retaining its effectiveness [159]. These optimizations improved the format for its therapeutic application in humans, and corresponding modifications in the BiMAB format should be considered for its future drug development and preclinical testing. It remains to be seen whether a deimmunization of 1BiMAB for preclinical testing is necessary.
Despite the fact that the IMAB362 derived scFv of 1BiMAB binds CLDN18.2 in rodents with the same affinity as in humans, a surrogate anti-CD3-scFv comprising the binding domains of the Armenian hamster derived mAb 145-2C11 has been designed to gain a BiMAB for use in cross species-specific assays in rodents (not part of this study).
In conclusion, a clear demonstration of efficacy, tolerability, and stability of the BiMAB antibody candidate in cellular and animal models, which indicates its putative efficacy in human disease, will be required to define the leading drug candidate.
Meanwhile, a lot can be learned from the current IMAB362 drug development and clinical trials. It would be helpful if information gained during IMAB362's development could be extrapolated to the CLDN18.2 specific BiMAB format. A closer comparison of the characteristics of the BiMAB format with the parental mAb IMAB362 will be performed as part of the combinational treatment approaches.
The successful continuous generation of new BiMABs with our cloning platform showcases its suitability for fast and easy expansion. For example, BiMABs targeting different TAAs such as GT512 (BiMAB2), Plac1 (BiMAB3), TargetX (BiMAB4), and other known TAAs were created. Furthermore, BiMABs that are specific for the TAA CLDN18.2, but are carrying costimulatory molecules instead of

the anti-CD3-scFv, have been prepared for future investigation in cancer treatment.
An extension to a more elaborate platform is planned once the concept of the BiMAB approach has been confirmed. A drug development platform suitable for screening hundreds of bs-td-scAbs and the subsequent selection of lead candidates was not anticipated in this study. This kind of platform would require significantly faster recombinant engineering techniques, based on e.g. the bacteriophage-encoded homologous recombination function, such as the coliphage λ Red system or the RecET system from the Rac prophage [160].
In addition, even more modules would be required such as different linkers, secretion signals, or tags for purification. At this point, our platform is designed purely for the purpose of creating BiMAB prototypes suitable for our proof of concept studies, testing the TAAs discovered in biomarker discovery experiments of Ganymed Pharmaceuticals and TRON.

4.7 *IN VITRO* TRANSCRIBED MESSENGER RNA AS THERAPEUTIC APPROACH

The successful application of synthetic messenger RNAs (mRNA) in anti-tumor vaccination in mice [161],[162] as well as for gene therapy[163] has been demonstrated. Thus, mRNA emerged as an attractive and promising tool in the field of gene delivery [87].
In vitro transcribed-RNA (IVT-RNA) is designed to mimic the function of naturally occurring mRNAs. It was shown several years ago that IVT-RNA is translated into the encoded protein after transfection [88]. Protein synthesis occurs in the cytoplasm utilizing the protein synthesis machinery of the target cell [89,90]. This new treatment option to administer for instance therapeutic mRNA instead of therapeutic proteins should be feasible in a large number of patients [164].
Normally, unmodified IVT-RNA is degraded by extracellular or intracellular ribonucleases shortly after its application, indicating a major limitation of RNA as a therapeutic agent. Methods to overcome the limits of short IVT-RNA half-life, which in turn prolong RNA translation, were established [104,102,165,105] and further refined by Holtkamp *et al.* [100].
It was reviewed by Yamamoto, Kreiter, and Kuhn *et al.* [87,166,92] that with certain modifications in its structure (chapter 2.5.4), the life span of IVT-RNA is remarkably prolonged and the molecule is thus stable enough to lead to increased protein translation during transient expression of this IVT-RNA [167,168]. Thus, IVT-RNA drugs can be effortlessly customized using traditional DNA engineering methods.
These mRNA improvement-trends opened up numerous perspectives for the therapeutic application of coding RNAs. Drug production, especially of recombinant protein, is considered time and cost effective. Recombinant RNA is easy to produce in large amounts and high purity using the method of *in vitro* transcription [91]. Consequently, IVT-RNA application could be a fast and affordable alternative. Since IVT-RNA production is less elaborate, more economic than the protein procedures [91], and can easily be upscaled [92], it is feasible to deliver IVT-RNA for cellular uptake in therapeutic settings and in this way engage cells to produce the desired drug substances.
The concept of using RNA antibodies instead of mAb proteins was already described by Hoerr *et al.* [169]. With this innovative idea in mind, we used our IVT-RNA technique to rapidly produce, administer, and test our IVT-RNA-based bs-td-scAbs (RIBOMABs).
The direct *in vivo* administration of coding RNAs is an attempt to circumvent the challenges of the complex, laborious and time-consuming procedure of GMP protein production, purification, and quality assurance.
This strategy aims to induce a transient translation of administered BiMAB IVT-RNA by every susceptible cell in the organism. The translated proteins are thought to be secreted into the extracellular environment and thus can enter the lymph- and successively the vascular-system, which distributes the protein throughout the whole body.

The translation of pharmacologically stabilized RIBOMABs and post-translational modification of the BiMAB protein by the treated individual itself is thought to result in fewer immunogenic proteins, leading to an improved bioavailability, fewer injections, and thus to a far better outcome for the patients.
The first step to proof this concept by the usage of RIBOMABs, we investigated the efficacy of our IVT-RNA encoded bs-td-scAbs *in vitro*.

4.8 PROOF OF CONCEPT FOR RIBOMABS–IVT-RNA-BASED BISPECIFIC ANTIBODIES

The results obtained after the initial experiments of transient transfection of 1BiMAB IVT-RNA testing electroporation have been very promising. 1BiMAB protein produced at a concentration of approximately 2 ng×mL^{-1} could be detected in the supernatant of transfected cells.
It might even be possible that a lot more protein was secreted but had bound to the exposed TAA on the surface of target cells. Thus, there may have been a bias in the BiMAB quantification, but the main goal to confirm the IVT-RNA translation and protein secretion was reached.
This knowledge allowed us to conclude that cytotoxic effects visible under the microscope and measured by cytotoxicity assays are mediated by this IVT-RNA derived 1BiMAB protein.
Several additional tests were prepared in order to verify that 1BiMAB translated from IVT-RNA elicited the desired cytotoxic effects. Concentration dependent T cell activation and target cell lysis were proven (Figure 32).
The huge difference in effect between 1.2 and 4 µg×mL^{-1} IVT-RNA indicated a further need for titration of the IVT-RNA amounts. The smaller difference between 12 and 40 µg×mL^{-1} IVT-RNA suggested a saturated setting of the cells. The comparison of CLDN18.2 specific BiMABs (Figure 35) using 20 µg×mL^{-1} for electroporation also uncovered the necessity for further titrations to decrease the amounts of IVT-RNA.
All CLDN18.2 specific RIBOMABs showed their ability to effectively activate T cells and mediate target cell lysis but at the amount of 20 µg×mL^{-1} IVT-RNA it was not possible to find significant differences in the efficacies between the BiMAB variants. Evident variances in T cell activation by these RIBOMABs indicated significant differences in their potencies. It remains to be tested, if decreased amounts of electroporated RIBOMABs result in significant differences in efficacy, as observed using the CLDN18.2 specific BiMAB proteins.
A direct comparison of the BiMAB protein and the RIBOMAB efficiencies is required. However, once we gain more profound knowledge and information on the translation efficiency of the IVT-RNA and the resulting concentration of functional BiMAB protein in the supernatant, a more correct comparison of the efficiencies of RIBOMABs and BiMAB protein effects should be feasible.
A fact that has to be considered is that electroporation can harm and/or alter the activities of the producer cells and therefore distort results of target cell lysis or T cell activation. Thus, the finding that the process of electroporation on its own did not provoke the observed therapeutic effects was important. T cell activation after electroporation of T cells with control BiMABs or Luciferase IVT-RNA compared to not electroporated T cells was not apparent in controls (Figure 35).
The absence of unspecific activation measured by flow cytometry detecting no upregulation of activation markers CD69 and CD25 proved this. The variance of activated T cells between control samples in the different assays depended on the activation status of the individual donor. In each experiment, we measured variable percentages of RIBOMAB independent target cell death. In order to distinguish between unspecific cell death in the experiment and the RIBOMAB induced cytotoxic effects, the value of unspecific cell death of control samples was ascertained for each experiment. Control samples were either cells electroporated with control IVT-RNA or RIBOMAB electroporated cells in the absence of T cells. All results obtained from one experiment have to be related to the

value of unspecific cell death. The differences between these samples revealed the cytotoxic effects of the RIBOMABs. In that way, cytotoxic effects in all experiments were shown to be highly significant compared to the value of unspecific cell death in control samples.
By mixing electroporated and unelectroporated target cells, we could confirm that 1BiMAB mediated the lysis of both types of target cells (Figure 31). It is remarkable that even when only 5 % of the electroporated target cells expressed 1BiMAB, it was still enough to reach approximately 50 % of lysis, which again indicates a high potency of 1BiMAB.
Moreover, we showed that translation of the IVT-RNA is not restricted to a special target cell line but can be transferred to hematopoietic cells like T cells (Figure 34). This indicates a possible application of 1BiMAB IVT-RNA in a broad range of cells, which would be advantageous for a therapeutic setting.
Successful T cell transfection by electroporation of chimeric immune receptors has been already shown by Rabinovich *et al.* [170]. In our approach, we could show, not only the translation of RIBOMAB, but also the anticipated production of a functional 1BiMAB by two different cell types (NugC4 and T cells).
Furthermore, IVT-RNA of nine different CLDN18.2 specific BiMABs was translated by NugC4 target cells and they all elicited a remarkable T cell activation and target cell lysis. These initial results were all measured by flow cytometry. In order to confirm the results by an additional method, these experiments should be repeated using the luciferase-based cytotoxicity assay in the future.
Furthermore, using RIBOMAB electroporation of even more different cell lines should verify its wide-ranging applicability. Subsequently, the characterization of RIBOMABs now has to be extensively compared to the effects elicited by the 1BiMAB protein.

To our knowledge, this is the first report on the direct translation and secretion of functional anti-cancer bs-td-scAbs after electroporation of cells. The electroporated RIBOMABs were secreted as proteins, which in turn were capable of mediating significant T cell activation and target cell lysis. Accordingly, these initial results proved the concept of RIBOMABs and confirmed our *in vitro* approach to be realistic.
Moreover, bypassing the laborious work of protein production, a much faster screening for functional BiMAB candidates was possible. Their functionality was conventionally tested via *in vitro* T cell activation and cytotoxicity assays.
However, there is one aspect that was not yet addressed in this study but has to be taken into detailed consideration for future aspects, which is the alternatives of IVT-RNA delivery *in vitro* and *in vivo*. This will be discussed in more depth in the perspectives for RIBOMABs.

4.9 PERSPECTIVES–CHALLENGES AND OPPORTUNITIES IN THE DELIVERY OF RIBOMABS

An established procedure in immunotherapy with the usage of IVT-RNA delivery is the reprogramming of antigen presenting cells for HLA haplotype-independent antigen-specific vaccination, both for anti-infection and anti-cancer immunotherapy [171]. Two investigated applications of mRNA technology have emerged into the clinical setting. Either autologous dendritic cells are transfected *ex vivo* with synthetic mRNA for adoptive transfer into the patient, or naked synthetic mRNA is directly injected [172, 167].
It was shown successfully in human skin by Probst *et al.* [173] that the delivery of mRNA leads to the translation of the respective transgene in mammalian tissue. Different injection sites have been examined (intravenous, intradermal, intramuscular, intranodal, intrapinna), demonstrating that the administration route of the mRNA vaccine is critically important [174, 175].
Further application settings for synthetic RNAs are feasible as recently reviewed by Kuhn *et al.* [92].

Thus, T cells can be manipulated by synthetic mRNAs to transiently present TAA-specific T cell receptors on their cell surface. Also, a reprogramming to pluripotency and directed differentiation of human cells with synthetic modified mRNA was achieved [176]. Additional application methods for IVT-RNA-based gene delivery, not in the context of vaccination strategies, are under investigation. Xu *et al.* [177] stated that the strategies to deliver the nucleic acids into the interior of the cells always involve difficulties that affect the efficiency of the approach. In any case, a transient translation of the IVT-RNA encoded proteins has been attained. The duration of IVT-RNA bioavailability can be regulated by either the dosing of the IVT-RNA, by stabilizing modifications of the IVT-RNA itself, or by packaging of the IVT-RNA [87, 178, 164].
As the amount and time of RNA expression in the cell is regulated by its stability, a further advantage of RNA is indicated: RNA, in contrast to gene transfer via viral or plasmid DNA, exclusively gives rise to transient translation of the encoded proteins as desired for many pharmaceuticals [179]. The transient expression of RNA occurs in the cytoplasm and therefore does not require either nuclear transport or integration into the host´s genome. Thus, RNA lacks the risk of malignant transformation resulting in a far better safety profile compared to pDNA or viral transfection techniques [166,180].
Delivery technologies are so far limited to a handful of approaches reviewed by Üzgün *et al.* [181] and Pascolo *et al.* [90], the most common being electroporation described by van Tendeloo *et al.* [89] and should be feasible by these techniques in several diverse human cell types [175].
Due to a high abundance of synthetic mRNA analysis in the context of vaccination, most transfection efficiency studies are investigated in dendritic cells (DCs). Thus, the transfection efficiency numbers stated here refer to DC transfection. Lipofection seems to lead to equal or less efficient levels of translated transgene than observed for electroporation [182], which might again depend on the cell type used. In contrast to plasmid DNA (pDNA) that has to be transferred into the nucleus, the objective for mRNA transport is the cytosol of the cell, which results in high electroporation efficiencies in around 90 % of transfected cells [105].
Therefore, IVT-RNA translation results in significant higher protein expression already at early time points compared to pDNA transfection [87]. Despite that, the conditions used for pDNA electroporation have to be more stringent in order to cross both the cell and nuclear membranes, resulting in higher percentages of damaged and correspondingly fewer transfected cells [175]. In addition, electroporation efficiencies seem to be cell type dependent (unpublished observation).
In this study, the transgene was transferred by electroporation, but transfection of cells can be reached by several other mRNA delivery techniques. These techniques include the most prominent formulations, the use of cationic liposomes, carbonate apatite-cationic liposome conjugates, cationic polymers, self-replicating RNAs or gene gun bombardment [181], [166]. DOTMA and DOTAP, synthetic cationic lipids, mixed with lipofectin to form liposomes were the most extensively used cationic liposomes to efficiently transfect mRNA into different mammalian cells and most publications suggest lipoplexes for mRNA transfection [87].
Each of the different possible routes has to be carefully evaluated for RiBOMAB *in vitro* and *in vivo* administration.

4.9.1 LIMITATIONS OF DURABLE IVT-RNA TRANSLATION VIA CELLULAR RESPONSE MECHANISMS

Not only is the half-life of mRNA limiting its translation, but the innate immune system also restricts the mRNA translation. Synthetic RNA can be sensed as 'non-self RNAs' resulting in cellular immune responses indistinguishable from those of invading viral RNA. Immunostimulatory effects of RNAs hamper the translation and thereby reduce the levels and duration of expression. Therefore, investigations to circumvent these effects have special priority.
IVT-RNA can be recognized by intracellular toll-like receptors (TLR) TLR3, TLR7, TLR8 & TLR9, the

protein kinase R (PKR) and the (RIG)-I-like receptors (RLRs) [183], [184]. The TLR3 detects dsRNA, siRNA and mRNA, whereas TLR7 and TLR8 recognize ssRNAs [87]. Furthermore, cytosolic RNA receptor retinoic-acid-inducible protein I (RIG-I) was suggested to be an mRNA sensing receptor. Nonetheless, it became clear that RIG-I recognizes contaminants of *in vitro* transcribed RNA preparations. These contaminants consist of short degradation products of paired RNAs still offering a 5′triphosphate [166].
Moreover, complex secondary structures formed by single-stranded RNAs were shown to act as ligands for the RNA-dependent protein kinase, another cytosolic RNA sensor [166]. Upon detection of non-self RNA, the cell is alerted and it initiates cellular anti-viral defense mechanisms [185]. Consequently, tumor necrosis factor-alpha and/or inflammatory interferon immune responses are triggered by IVT-RNAs. The response includes induction of the interferon (IFN) response pathways, and a PKR-mediated shutdown of protein biosynthesis even up to the induction of apoptosis.
While in current RNA vaccination approaches the supportive immunostimulatory and inflammatory therapeutic effects of the synthetic RNAs are appreciated [186], they remain a major challenge in IVT-RNA-based gene transfer. Faced by this major challenge, the cellular immune response is a point that has to be addressed for a successful RIBOMABs *in vivo* application.
At the current stage, there are two major attempts to circumvent or reduce this cellular response. First, introducing modified nucleotides such as N6-methyladenosine and pseudouridine into the *in vitro* transcription reaction avoided immune responses [187]. A further purification step using high-performance liquid chromatography (HPLC) has been reported to amplify the reduction of these immune stimulatory effects [188]. These steps are able to reduce the TLR-mediated immune responses.
The second attempt is the implementation of virus-derived immune modulating proteins, which impede the upregulation of cellular defense mechanisms by interfering with dsRNA detection, and subsequent signaling cascades [176]. This in turn bypasses the activation of antiviral pathways, the shutdown of protein biosynthesis, and the interferon signaling [176].
In brief, there are several techniques to deal with the upregulation of cellular defense mechanisms induced by the presence of IVT-RNA. These approaches are probably capable of permitting sufficient transient translation of IVT-RNA for immunotherapeutic settings. Thus, until now already two *in vivo* studies using IVT-RNA have been conducted with promising results. In a first study that was introduced by Kormann *et al.* [163] the expression of therapeutic proteins after delivery of chemically modified mRNA could be demonstrated and in the second the delivery of self-amplifying RNA was shown by Geall *et al.* [189].
Both mRNA *in vivo* delivery approaches immensely encouraged our efforts to successfully administer BiMAB IVT-RNA, resulting in a transient, but sustained, expression in future. Our group is aware of the above-mentioned countermeasures against the cellular immune responses against non self RNAs and most of them are currently being tested or already realized when using RIBOMABs. Furthermore, the implementation of novel knowledge –gained about mechanisms of IVT-RNA recognition or IVT-RNA application– into the design of our IVT-RNA structures is planned. It will constantly improve the *in vivo* application possibilities of BiMAB IVT-RNAs in the future.
In conclusion, using these countermeasures and a pharmacologically effective dosing of RIBOMABs might lead to a sustained expression of BiMABs *in vivo*. We hypothesize that in this manner, the IVT-RNA approach will improve the pharmacokinetics of bs-td-scAbs without the need for frequent injections that are usually performed for small protein therapies. This in turn should drastically increase the patients′ quality of life. Additionally, a conceivable enhancement in the therapeutic effect by the constant level of the drug is expected. Thus, besides 1BiMAB protein the CLDN18.2 specific RIBOMABs particularly might change the gastric cancer treatment options.

5 REFERENCES

1. Vanneman M, Dranoff G: **Combining immunotherapy and targeted therapies in cancer treatment.** Nat Rev Cancer 2012, **12:**237–251
1a. Quah BJC, Warren HS, Parish CR: **Monitoring lymphocyte proliferation in vitro and in vivo with the intracellular fluorescent dye carboxyfluorescein diacetate succinimidyl ester.** Nat Protoc 2007, **2:**2049–2056
2. Lawson JD, Sicklick JK, Fanta PT: **Gastric Cancer.** Gastric Cancer 2011, **35:**97–127
3. Moehler M, Galle PR, Gockel I, Junginger T, Schmidberger H: **The multidisciplinary management of gastrointestinal cancer. Multimodal treatment of gastric cancer.** Best Pract Res Clin Gastroenterol 2007, **21:**965–981
4. **Targeted Cancer Therapies - National Cancer Institute** [http://www.cancer.gov/cancertopics/factsheet/Therapy/targeted]
5. Balis FM: **Evolution of anticancer drug discovery and the role of cell-based screening.** J. Natl. Cancer Inst. 2002, **94:**78–79
6. Hata R: **A New Strategy to Find Targets for Anticancer Therapy: Chemokine CXCL14/BRAK Is a Multifunctional Tumor Suppressor for Head and Neck Squamous Cell Carcinoma.** ISRN Otolaryngology 2012, **2012:**1–12
7. Phillips KA, van Bebber S, Issa AM: **Diagnostics and biomarker development: priming the pipeline.** Nat Rev Drug Discov 2006, **5:**463–469
8. Sahin U, Koslowski M, Dhaene K, Usener D, Brandenburg G, Seitz G, Huber C, Tureci O: **Claudin-18 splice variant 2 is a pan-cancer target suitable for therapeutic antibody development.** Clin Cancer Res 2008, **14:**7624–7634
9. Wöll S, Schlitter AM, Dhaene K, Roller M, Esposito I, Sahin U, Türeci O: **Claudin 18.2 is a target for IMAB362 antibody in pancreatic neoplasms.** Int. J. Cancer 2013.
10. **Stomach Cancer.**
11. Zagouri F, Papadimitriou CA, Dimopoulos M, Pectasides D: **Molecularly targeted therapies in unresectable-metastatic gastric cancer. A systematic review.** Cancer Treatment Reviews 2011, **37:**599–610
12. **Global Cancer Facts & Figures - 2nd Edition.**
13. Sanada Y, Oue N, Mitani Y, Yoshida K, Nakayama H, Yasui W: **Down-regulation of the claudin-18 gene, identified through serial analysis of gene expression data analysis, in gastric cancer with an intestinal phenotype.** J. Pathol 2006, **208:**633–642
14. Koval M: **Claudin Heterogeneity and Control of Lung Tight Junctions.** Annu. Rev. Physiol. 2012, **75:**121016121642003
15. Hayashi D, Tamura A, Tanaka H, Yamazaki Y, Watanabe S, Suzuki K, Suzuki K, Sentani K, Yasui W, Rakugi H, Isaka Y, Tsukita S: **Deficiency of Claudin-18 Causes Paracellular H(+) Leakage, Up-regulation of Interleukin-1β, and Atrophic Gastritis in Mice.** Gastroenterology 2012, **142:**292–304
16. Türeci Ö, Koslowski M, Helftenbein G, Castle J, Rohde C, Dhaene K, Seitz G, Sahin U: **Claudin-18 gene structure, regulation, and expression is evolutionary conserved in mammals.** Gene 2011, **481:**83–92
17. Niimi T, Nagashima K, Ward JM, Minoo P, Zimonjic DB, Popescu NC, Kimura S: **claudin-18_ a Novel Downstream Target Gene for the T_EBP_NKX2.1 Homeodomain Transcription Factor_Encodes Lung- and Stomach-Specific Isoforms through Alternative Splicing _TNiimi_2001.pdf // claudin-18, a novel downstream target gene for the T/EBP/NKX2.1 homeodomain transcription factor, encodes lung- and stomach-specific isoforms through alternative splicing.** Mol. Cell. Biol 2001, **21:**7380–7390
18. Sahin U: *Ideal Targets for Potent Cancer Antibody Development: CLDN18.2.* 2007

19. Ganymed Pharmaceuticals: *INVESTIGATIONAL MEDICINAL PRODUCT DOSSIER: iMAB 362 (Claudiximab)*; FEBUARY 2009.
20. Ganymed Pharmaceuticals: *Clinical Phase I Results of GANYMED's iMAB362 Antibody Demonstrate Excellent Safety*; 04.08.2010.
21. **Efficacy and Safety of IMAB362 in Combination With the EOX Regimen (Plus ZA/IL-2) CLDN18.2-positive Gastric Cancer** [http://www.cancer.gov/clinicaltrials/search/view?cdrid=736310&version=HealthProfessional&protocolsearchid=8234117]
22. **Safety and Activity of IMAB362 in Combination With Zoledronic Acid and Interleukin-2 in CLDN18.2-positive Gastric Cancer** [http://www.cancer.gov/clinicaltrials/search/view?cdrid=739282&version=HealthProfessional&protocolsearchid=8234117#ContactInfo_CDR0000739282]
23. Castella B, Riganti C, Fiore F, Pantaleoni F, Canepari ME, Peola S, Foglietta M, Palumbo A, Bosia A, Coscia M, Boccadoro M, Massaia M: **Immune modulation by zoledronic acid in human myeloma: an advantageous cross-talk between Vγ9Vδ2 T cells, αβ CD8+ T cells, regulatory T cells, and dendritic cells.** J. Immunol. 2011, **187:**1578–1590
24. Santini D, Martini F, Fratto ME, Galluzzo S, Vincenzi B, Agrati C, Turchi F, Piacentini P, Rocci L, Manavalan JS, Tonini G, Poccia F: **In vivo effects of zoledronic acid on peripheral gammadelta T lymphocytes in early breast cancer patients.** Cancer Immunol. Immunother. 2009, **58:**31–38
25. Roelofs AJ, Jauhiainen M, Mönkkönen H, Rogers MJ, Mönkkönen J, Thompson K: **Peripheral blood monocytes are responsible for γδ T cell activation induced by zoledronic acid through accumulation of IPP/DMAPP.** British Journal of Haematology 2009, **144:**245–250
26. Caccamo N, Meraviglia S, Scarpa F, La Mendola C, Santini D, Bonanno CT, Misiano G, Dieli F, Salerno A: **Aminobisphosphonate-activated gammadelta T cells in immunotherapy of cancer: doubts no more.** Expert Opin Biol Ther 2008, **8:**875–883
27. Galon J, Costes A, Sanchez-Cabo F, Kirilovsky A, Mlecnik B, Lagorce-Pagès C, Tosolini M, Camus M, Berger A, Wind P, Zinzindohoué F, Bruneval P, Cugnenc P, Trajanoski Z, Fridman W, Pagès F: **Type, density, and location of immune cells within human colorectal tumors predict clinical outcome.** Science 2006, **313:**1960–1964
28. Wahlin BE, Sander B, Christensson B, Kimby E: **CD8+ T-Cell Content in Diagnostic Lymph Nodes Measured by Flow Cytometry Is a Predictor of Survival in Follicular Lymphoma.** Clinical Cancer Research 2007, **13:**388–397
29. May C, Sapra P, Gerber H: **Advances in bispecific biotherapeutics for the treatment of cancer.** Biochemical Pharmacology 2012, **84:**1105–1112
30. Wurch T, Pierré A, Depil S: **Novel protein scaffolds as emerging therapeutic proteins: from discovery to clinical proof-of-concept.** Trends in Biotechnology 2012, **30:**575–582
31. Scott AM, Wolchok JD, Old LJ: **Antibody therapy of cancer.** Nat Rev Cancer 2012, **12:**278–287
32. Staerz UD, Kanagawa O, Bevan MJ, Staerz UD, Kanagawa O, Bevan MJ: **Hybrid antibodies can target sites for attack by T cells.** Nature 1985, **314:**628–631
33. Perez P, Hoffman RW, Shaw S, Bluestone JA, SEGAL DM: **Specific targeting of cytotoxic T cells by anti-T3 linked to anti-target cell antibody.** Nature 1985, **316:**354–356
34. Lanzavecchia A, Scheidegger D, Lanzavecchia A, Scheidegger D: **The use of hybrid hybridomas to target human cytotoxic T lymphocytes.** Eur. J. Immunol. 1987, **17:**105–111
35. Renner C, Jung W, Sahin U, Denfeld R, POHL C, Trumper L, Hartmann F, DIEHL V, van Lier R, Pfreundschuh M: **Cure of xenografted human tumors by bispecific monoclonal antibodies and human T cells.** Science 1994, **264:**833–835
36. Chames P, Baty D: **Bispecific antibodies for cancer therapy.** Curr Opin Drug Discov Devel 2009, **12:**276–283
37. Chames P, van Regenmortel M, Weiss E, Baty D: **Therapeutic antibodies: successes, limitations and hopes for the future.** British Journal of Pharmacology 2009, **157:**220–233
38. Volker Baum: **Herstellung und Vergleich zweier PSMAxCD3 Diabodies zur Therapie des Prostatakarzinoms: Inaugural-Dissertation**; 2012.
39. Huston JS, Levinson D, Mudgett-Hunter M, Tai MS, Novotný J, Margolies MN, Ridge RJ, Bruccoleri RE, Haber E, Crea R: **Protein engineering of antibody binding sites: recovery of specific**

activity in an anti-digoxin single-chain Fv analogue produced in Escherichia coli. Proc. Natl. Acad. Sci. U.S.A. 1988, **85:**5879–5883
40. Bird R, Hardman K, Jacobson J, Johnson S, Kaufman B, Lee S, Lee T, Pope S, Riordan G, Whitlow M: **Single-chain antigen-binding proteins.** Science 1988, **242:**423–426
41. Holliger P, Prospero T, Winter G: **"Diabodies": small bivalent and bispecific antibody fragments.** Proc Natl Acad Sci U S A 1993, **90:**6444–6448
42. Holliger P, Winter G: **Diabodies: small bispecific antibody fragments.** Cancer Immunology, Immunotherapy 1997, **45:**128–130
43. Desplancq D, King DJ, Lawson AD, Mountain A: **Multimerization behaviour of single chain Fv variants for the tumour-binding antibody B72.3.** PROTEIN ENG 1994, **7:**1027–1033
44. Nagorsen D, Kufer P, Bäuerle PA, Bargou RC: **Blinatumomab: a historical perspective.** Pharmacol. Ther. 2012, **136:**334–342
45. Adams GP, Schier R: **Generating improved single-chain Fv molecules for tumor targeting.** J. Immunol. Methods 1999, **231:**249–260
46. Pillay V, Gan HK, Scott AM: **Antibodies in oncology: Antibodies: From Basics to Therapeutics.** New Biotechnology 2011, **28:**518–529
47. Seliger B: **Strategies of tumor immune evasion.** BioDrugs 2005, **19:**347–354
48. Quezada SA, Peggs KS, Simpson TR, Allison JP: **Shifting the equilibrium in cancer immunoediting: from tumor tolerance to eradication.** Immunological Reviews 2011, **241:**104–118
49. Hanahan D, Weinberg RA: **Hallmarks of Cancer: The Next Generation.** Cell 2011, **144:**646–674
50. Ma Z, Finkel TH: **T cell receptor triggering by force.** Trends in Immunology 2010, **31:**1–6
51. Brischwein K, Schlereth B, Guller B, Steiger C, Wolf A, Lutterbuese R, Offner S, Locher M, Urbig T, Raum T, Kleindienst P, Wimberger P, Kimmig R, Fichtner I, Kufer P, Hofmeister R, da Silva AJ, Bäuerle PA: **MT110: A novel bispecific single-chain antibody construct with high efficacy in eradicating established tumors.** Molecular Immunology 2006, **43:**1129–1143
52. Offner S, Hofmeister R, Romaniuk A, Kufer P, Bäuerle PA: **Induction of regular cytolytic T cell synapses by bispecific single-chain antibody constructs on MHC class I-negative tumor cells.** Mol. Immunol 2006, **43:**763–771
53. Sharkey RM, van Rij CM, Karacay H, Rossi EA, Frielink C, Regino C, Cardillo TM, McBride WJ, Chang C, Boerman OC, Goldenberg DM: **A New Tri-Fab Bispecific Antibody for Pretargeting Trop-2-Expressing Epithelial Cancers.** Journal of Nuclear Medicine 2012, **53:**1625–1632
54. Elsässer-Beile U, Bühler P: **Bispecific antibodies and diabodies for cancer immunotherapy.** Immunotherapy 2012, **4:**459–460
55. Brischwein K, Parr L, Pflanz S, Volkland J, Lumsden J, Klinger M, Locher M, Hammond SA, Kiener P, Kufer P, Schlereth B, Bäuerle PA: **Strictly Target Cell-dependent Activation of T Cells by Bispecific Single-chain Antibody Constructs of the BiTE Class.** Journal of Immunotherapy 2007, **30:**798–807
56. Minguet S, Swamy M, Alarcón B, Luescher IF, Schamel WWA: **Full Activation of the T Cell Receptor Requires Both Clustering and Conformational Changes at CD3.** Immunity 2007, **26:**43–54
57. Nagorsen D, Baeuerle PA: **Immunomodulatory therapy of cancer with T cell-engaging BiTE antibody blinatumomab.** Exp. Cell Res. 2011, **317:**1255–1260
58. Smith-Garvin JE, Koretzky GA, Jordan MS: **T cell activation.** Annu. Rev. Immunol. 2009, **27:**591–619
59. Yokoyama WM, Maxfield SR, Shevach EM: **Very Early (VEA) and Very Late (VLA) Activation Antigens have Distinct Functions in T Lymphocyte Activation.** Immunol Rev 1989, **109:**153–176
60. Ziegler SF, Ramsdell F, Alderson MR: **The activation antigen CD69.** Stem Cells 1994, **12:**456–465
61. Saito Y, Sabe H, Suzuki N, Kondo S, Ogura T, Shimizu A, Honjo T: **A larger number of L chains (Tac) enhance the association rate of interleukin 2 to the high affinity site of the interleukin 2 receptor.** J Exp Med 1988, **168:**1563–1572

62. Ortega G, Robb RJ, Shevach EM, Malek TR: **The murine IL 2 receptor. I. Monoclonal antibodies that define distinct functional epitopes on activated T cells and react with activated B cells.** J. Immunol. 1984, **133:**1970–1975
63. Jenkins MR, Griffiths GM: **The synapse and cytolytic machinery of cytotoxic T cells.** Curr Opin Immunol 2010, **22:**308–313
64. Page LJ, Darmon AJ, Uellner R, Griffiths GM: **L is for lytic granules: lysosomes that kill.** Biochimica et Biophysica Acta (BBA) - Molecular Cell Research 1998, **1401:**146–156
65. Isaaz S, Baetz K, Olsen K, Podack E, Griffiths GM: **Serial killing by cytotoxic T lymphocytes: T cell receptor triggers degranulation, re-filling of the lytic granules and secretion of lytic proteins via a non-granule pathway.** Eur. J. Immunol. 1995, **25:**1071–1079
66. Stinchcombe JC, Bossi G, Booth S, Griffiths GM: **The Immunological Synapse of CTL Contains a Secretory Domain and Membrane Bridges.** Immunity 2001, **15:**751–761
67. Haas C, Krinner E, Brischwein K, Hoffmann P, Lutterbüse R, Schlereth B, Kufer P, Bäuerle PA: **Mode of cytotoxic action of T cell-engaging BiTE antibody MT110.** IMMUNOBIOLOGY 2009, **214:**441–453
68. Fischer K, Andreesen R, Mackensen A: **An improved flow cytometric assay for the determination of cytotoxic T lymphocyte activity.** Journal of Immunological Methods 2002, **259:**159–169
69. Kufer P, Mack M, Gruber R, Lutterb&#x000FC, se R, Zettl F, Riethm&#x000FC, ller G: **Construction and biological activity of a recombinant bispecific single-chain antibody designed for therapy of minimal residual colorectal cancer.** Cancer Immunology, Immunotherapy 1997, **45:**193–197
70. Wimberger P, Xiang W, Mayr D, Diebold J, Dreier T, Bäuerle PA, Kimmig R: **Efficient tumor cell lysis by autologous, tumor-resident T lymphocytes in primary ovarian cancer samples by an EP-CAM-/CD3-bispecific antibody.** Int. J. Cancer 2003, **105:**241–248
71. Kufer P, Lutterbüse R, Bäuerle PA: **A revival of bispecific antibodies.** Trends Biotechnol. 2004, **22:**238–244
72. Wolf E, Bäuerle PA: **Micromet: engaging immune cells for life.** Drug Discovery Today 2002, **7:**S25
73. Müller D, Kontermann RE: **Bispecific antibodies for cancer immunotherapy:: Current perspectives.** BioDrugs 2010, **24:**89–98
74. Cochlovius B, Kipriyanov SM, Stassar MJ, Schuhmacher J, Benner A, Moldenhauer G, Little M: **Cure of Burkitt's lymphoma in severe combined immunodeficiency mice by T cells, tetravalent CD3 x CD19 tandem diabody, and CD28 costimulation.** CANCER RES 2000, **60:**4336–4341
75. Reiners KS, Kessler J, Sauer M, Rothe A, Hansen HP, Reusch U, Hucke C, Kohl U, Durkop H, Engert A, Strandmann EP von: **Rescue of Impaired NK Cell Activity in Hodgkin Lymphoma With Bispecific Antibodies In Vitro and in Patients.** Mol Ther 2013, **21:**895–903
76. Mølhøj M, Crommer S, Brischwein K, Rau D, Sriskandarajah M, Hoffmann P, Kufer P, Hofmeister R, Bäuerle PA: **CD19-/CD3-bispecific antibody of the BiTE class is far superior to tandem diabody with respect to redirected tumor cell lysis.** Mol. Immunol 2007, **44:**1935–1943
77. Kufer P, Lutterbuse R, Bäuerle PA: **The promise of bispecific antibodies.** Discov Med 2004, **4:**325–332
78. Mack M, Gruber R, Schmidt S, Riethmuller G, Kufer P: **Biologic properties of a bispecific single-chain antibody directed against 17-1A (EpCAM) and CD3: tumor cell-dependent T cell stimulation and cytotoxic activity.** J Immunol 1997, **158:**3965–3970
79. Kipriyanov SM, Moldenhauer G, Braunagel M, Reusch U, Cochlovius B, Le Gall F, Kouprianova OA, Lieth CW von der, Little M: **Effect of domain order on the activity of bacterially produced bispecific single-chain Fv antibodies.** J. Mol. Biol 2003, **330:**99–111
80. Mack M, Riethmüller G, Kufer P: **A small bispecific antibody construct expressed as a functional single-chain molecule with high tumor cell cytotoxicity.** Proc. Natl. Acad. Sci. U.S.A. 1995, **92:**7021–7025

81. Yokota T, Milenic DE, Whitlow M, Schlom J: **Rapid tumor penetration of a single-chain Fv and comparison with other immunoglobulin forms.** CANCER RES 1992, **52:**3402–3408
82. Maloney DG, Grillo-López AJ, Bodkin DJ, White CA, Liles TM, Royston I, Varns C, Rosenberg J, Levy R: **IDEC-C2B8: results of a phase I multiple-dose trial in patients with relapsed non-Hodgkin's lymphoma.** J. Clin. Oncol. 1997, **15:**3266–3274
83. Fiedler WM, Ritter B, Seggewiss R, Bokemeyer C, Fettes P, Klinger M, Vieser E, Ruettinger D, Kaubitzsch S, Wolf M: **Phase I safety and pharmacology study of the EpCAM/CD3-bispecific BiTE antibody MT110 in patients with metastatic colorectal, gastric, or lung cancer.**
84. Au JL, Jang SH, Zheng J, Chen CT, Song S, Hu L, Wientjes MG: **Determinants of drug delivery and transport to solid tumors.** J Control Release 2001, **74:**31–46
85. Imrich S, Hachmeister M, Gires O: **EpCAM and its potential role in tumor-initiating cells.** Cell Adh Migr 2012, **6:**30–38
86. Bono JS de, Tolcher AW, Forero A, Vanhove GFA, Takimoto C, Bauer RJ, Hammond LA, Patnaik A, White ML, Shen S, Khazaeli MB, Rowinsky EK, LoBuglio AF: **ING-1, a monoclonal antibody targeting Ep-CAM in patients with advanced adenocarcinomas.** Clin Cancer Res 2004, **10:**7555–7565
87. Yamamoto A, Kormann M, Rosenecker J, Rudolph C: **Current prospects for mRNA gene delivery.** European Journal of Pharmaceutics and Biopharmaceutics 2009, **71:**484–489
88. Danko I, Wolff JA: **Direct gene transfer into muscle.** Vaccine 1994, **12:**1499–1502
89. van Tendeloo VF, Ponsaerts P, Lardon F, Nijs G, Lenjou M, van Broeckhoven C, van Bockstaele DR, Berneman ZN: **Highly efficient gene delivery by mRNA electroporation in human hematopoietic cells: superiority to lipofection and passive pulsing of mRNA and to electroporation of plasmid cDNA for tumor antigen loading of dendritic cells.** BLOOD 2001, **98:**49–56
90. Pascolo S: **Messenger RNA-based vaccines.** Expert Opin. Biol. Ther. 2004, **4:**1285–1294
91. Diken M, Kreiter S, Selmi A, Britten CM, Huber C, Türeci Ö, Sahin U: **Selective uptake of naked vaccine RNA by dendritic cells is driven by macropinocytosis and abrogated upon DC maturation.** Gene Ther 2011, **18:**702–708
92. Kuhn AN, Beiβert T, Simon P, Vallazza B, Buck J, Davies BP, Tureci O, Sahin U: **mRNA as a versatile tool for exogenous protein expression.** Curr Gene Ther 2012, **12:**347–361
93. Sohn RL, Murray MT, Schwarz K, Nyitray J, Purray P, Franko AP, Palmer KC, Diebel LN, Dulchavsky SA: **In-vivo particle mediated delivery of mRNA to mammalian tissues: ballistic and biologic effects.** Wound Repair Regen 2001, **9:**287–296
94. SHEIN HM, ENDERS JF: **Transformation induced by simian virus 40 in human renal cell cultures. I. Morphology and growth characteristics.** Proc Natl Acad Sci U S A 1962, **48:**1164–1172
95. Zur Hausen H: **Induction of specific chromosomal aberrations by adenovirus type 12 in human embryonic kidney cells.** J. Virol 1967, **1:**1174–1185
96. Akiyama S, Amo H, Watanabe T, Matsuyama M, Sakamoto J, Imaizumi M, Ichihashi H, Kondo T, Takagi H: **Characteristics of three human gastric cancer cell lines, NU-GC-2, NU-GC-3 and NU-GC-4.** The Japanese Journal of Surgery 1988, **18:**438–446
97. Sekiguchi M, Sakakibara K, Fujii G: **Establishment of cultured cell lines derived from a human gastric carcinoma.** Jpn J Exp Med 1978, **48:**61-8
98. Chu MYW, Naguib FNM, Iltzsch MH, el Kouni MH, Chu SH, Cha S, Calabresi P: **Potentiation of 5-Fluoro-2′-deoxyuridine Antineoplastic Activity by the Uridine Phosphorylase Inhibitors Benzylacyclouridine and Benzyloxybenzylacyclouridine.** Cancer Research 1984, **44:**1852–1856
99. Sambrook J: *Molecular cloning.* Cold Spring Harbor, NY: Cold Spring Harbor Laboratory Press; 2001.
100. Holtkamp S, Kreiter S, Selmi A, Simon P, Koslowski M, Huber C, Türeci Ö, Sahin U: **Modification of antigen-encoding RNA increases stability, translational efficacy, and T-cell stimulatory capacity of dendritic cells.** BLOOD 2006, **108:**4009–4017

101. Waggoner SA, Liebhaber SA: **Identification of mRNAs Associated with CP2-Containing RNP Complexes.** Molecular and Cellular Biology 2003, **23:**7055–7067
102. Jemielity J, Stepinski J, Jaremko M, Haber D, Stolarski R, Rhoads RE, Darzynkiewicz E: **Synthesis of novel mRNA 5' cap-analogues: dinucleoside P1, P3-tri-, P1, P4-tetra-, and P1, P5-pentaphosphates.** Nucleosides Nucleotides Nucleic Acids 2003, **22:**691–694
103. Pasquinelli AE, Dahlberg JE, Lund E: **Reverse 5' caps in RNAs made in vitro by phage RNA polymerases.** RNA 1995, **1:**957–967
104. Stepinski J, Waddell C, Stolarski R, Darzynkiewicz E, Rhoads RE: **Synthesis and properties of mRNAs containing the novel "anti-reverse" cap analogs 7-methyl(3'-O-methyl)GpppG and 7-methyl (3'-deoxy)GpppG.** RNA 2001, **7:**1486–1495
105. Mockey M, Gonçalves C, Dupuy FP, Lemoine FM, Pichon C, Midoux P: **mRNA transfection of dendritic cells: synergistic effect of ARCA mRNA capping with Poly(A) chains in cis and in trans for a high protein expression level.** Biochem. Biophys. Res. Commun. 2006, **340:**1062–1068
106. Dübel S, Rohrbach P, Schmiedl A: **Rekombinante Antikörper: Werkzeuge gegen Krebs, Infektionen und Autoimmunerkrankungen?** Biologie in unserer Zeit 2004, **34:**372–379
107. Hoedemaeker FJ: **A Single Chain Fv Fragment of P-glycoprotein-specific Monoclonal Antibody C219. DESIGN, EXPRESSION, AND CRYSTAL STRUCTURE AT 2.4 A RESOLUTION.** Journal of Biological Chemistry 1997, **272:**29784–29789
108. Shalaby MR, Shepard HM, Presta L, Rodrigues ML, Beverley PC, Feldmann M, Carter P: **Development of humanized bispecific antibodies reactive with cytotoxic lymphocytes and tumor cells overexpressing the HER2 protooncogene.** J. Exp. Med. 1992, **175:**217–225
109. Beverley PCL, Callard RE: **Distinctive functional characteristics of human „T" lymphocytes defined by E rosetting or a monoclonal anti-T cell antibody.** Eur. J. Immunol. 1981, **11:**329–334
110. van Lier RA, Brouwer M, Rebel VI, van Noesel CJ, Aarden LA: **Immobilized anti-CD3 monoclonal antibodies induce accessory cell-independent lymphokine production, proliferation and helper activity in human T lymphocytes.** Immunology 1989, **68:**45–50
111. Alberts B, Wilson JH: *Molecular biology of the cell.* New York [u.a.]: Garland; 2002.
112. Bonifacino JS, Dasso M, Harford JB, Lippincott-Schwartz J, Yamada KM: *Current Protocols in Cell Biology.* Hoboken, NJ, USA: John Wiley & Sons, Inc; 2001.
113. Gomi K: **Oxyluciferin, a Luminescence Product of Firefly Luciferase, Is Enzymatically Regenerated into Luciferin.** Journal of Biological Chemistry 2001, **276:**36508–36513
114. Coligan JE, Dunn BM, Speicher DW, Wingfield PT: *Current Protocols in Protein Science.* Hoboken, NJ, USA: John Wiley & Sons, Inc; 2001.
115. BISELLI R, MATRICARDI PM, AMELIO RD, FATTOROSSI A: **Multiparametric Flow Cytometric Analysis of the Kinetics of Surface Molecule Expression after Polyclonal Activation of Human Peripheral Blood T Lymphocytes.** Scand J Immunol 1992, **35:**439–447
116. Sakaguchi S, Yamaguchi T, Nomura T, Ono M: **Regulatory T Cells and Immune Tolerance.** Cell 2008, **133:**775–787
117. Sakaguchi S, Wing K, Onishi Y, Prieto-Martin P, Yamaguchi T: **Regulatory T cells: how do they suppress immune responses?** International Immunology 2009, **21:**1105–1111
118. Choi BD, Kuan C, Cai M, Archer GE, Mitchell DA, Gedeon PC, Sanchez-Perez L, Pastan I, Bigner DD, Sampson JH: **Systemic administration of a bispecific antibody targeting EGFRvIII successfully treats intracerebral glioma.** Proceedings of the National Academy of Sciences 2013, **110:**270–275
119. Feldmann A, Arndt C, Topfer K, Stamova S, Krone F, Cartellieri M, Koristka S, Michalk I, Lindemann D, Schmitz M, Temme A, Bornhauser M, Ehninger G, Bachmann M: **Novel Humanized and Highly Efficient Bispecific Antibodies Mediate Killing of Prostate Stem Cell Antigen-Expressing Tumor Cells by CD8+ and CD4+ T Cells.** The Journal of Immunology 2012, **189:**3249–3259
120. Klinger M, Brandl C, Zugmaier G, Hijazi Y, Bargou RC, Topp MS, Gokbuget N, Neumann S, Goebeler M, Viardot A, Stelljes M, Bruggemann M, Hoelzer D, Degenhard E, Nagorsen D, Bäuerle

PA, Wolf A, Kufer P: **Immunopharmacologic response of patients with B-lineage acute lymphoblastic leukemia to continuous infusion of T cell-engaging CD19/CD3-bispecific BiTE antibody blinatumomab.** BLOOD 2012, **119:**6226–6233
121. Tax WJ, Willems HW, Reekers PP, Capel PJ, Koene RA: **Polymorphism in mitogenic effect of IgG1 monoclonal antibodies against T3 antigen on human T cells.** Nature 1983, **304:**445–447
122. Tunnacliffe A, Olsson C, La Hera A de: **The majority of human CD3 epitopes are conferred by the epsilon chain.** Int Immunol 1989, **1:**546–550
123. Roosnek EE, Van Lier RA, Aarden LA, Roosnek EE, van Lier RA, Aarden LA: **Two monoclonal anti-CD3 antibodies can induce different events in human T lymphocyte activation.** EUR J IMMUNOL 1987, **17:**1507–1510
124. Lu D, Jimenez X, Witte L, Zhu Z: **The effect of variable domain orientation and arrangement on the antigen-binding activity of a recombinant human bispecific diabody.** Biochem Biophys Res Commun 2004, **318:**507–513
125. Fath S, Bauer AP, Liss M, Spriestersbach A, Maertens B, Hahn P, Ludwig C, Schäfer F, Graf M, Wagner R, Kudla G: **Multiparameter RNA and Codon Optimization: A Standardized Tool to Assess and Enhance Autologous Mammalian Gene Expression.** PLoS ONE 2011, **6:**e17596
126. Riethmüller G: **Symmetry breaking: bispecific antibodies, the beginnings, and 50 years on.** Cancer Immun. 2012, **12:**12
127. Bortoletto N, Scotet E, Myamoto Y, D'Oro U, Lanzavecchia A: **Optimizing anti-CD3 affinity for effective T cell targeting against tumor cells.** Eur. J. Immunol 2002, **32:**3102–3107
128. Jacobs N, Mazzoni A, MEZZANZANICA D, Negri DR, Valota O, Colnaghi MI, Moutschen MP, Boniver J, Canevari S, Jacobs N, Mazzoni A, Mezzanzanica D, Negri DRM, Valota O, Colnaghi MI, Moutschen MP, Boniver J, Canevari S: **Efficiency of T cell triggering by anti-CD3 monoclonal antibodies (mAb) with potential usefulness in bispecific mAb generation // Efficiency of T cell triggering by anti-CD3 monoclonal antibodies (mAb) with potential usefulness in bispecific mAb generation.** Cancer Immunol Immunother 1997, **44:**257–264
129. Dreier T, Lorenczewski G, Brandl C, Hoffmann P, Syring U, Hanakam F, Kufer P, Riethmuller G, Bargou RC, Bäuerle PA: **Extremely potent, rapid and costimulation-independent cytotoxic T-cell response against lymphoma cells catalyzed by a single-chain bispecific antibody.** Int. J. Cancer 2002, **100:**690–697
130. Bird RE, Walker BW: **Single chain antibody variable regions.** Trends in Biotechnology 1991, **9:**132–137
131. Kumagai I, Tsumoto K (Eds): *Antigen-Antibody Binding:* Nature Publishing Group; 2001.
132. Suntharalingam G, Perry MR, Ward S, Brett SJ, Castello-Cortes A, Brunner MD, Panoskaltsis N: **Cytokine Storm in a Phase 1 Trial of the Anti-CD28 Monoclonal Antibody TGN1412.** N Engl J Med 2006, **355:**1018–1028
133. Viola A, Lanzavecchia A: **T cell activation determined by T cell receptor number and tunable thresholds.** Science 1996, **273:**104–106
134. Van W, Goossens JG, Beverley PC: **Human T lymphocyte activation by monoclonal antibodies; OKT3, but not UCHT1, triggers mitogenesis via an interleukin 2-dependent mechanism.** J Immunol 1984, **133:**129–132
135. Jiang N: **Selection of Linkers for a Catalytic Single-chain Antibody Using Phage Display Technology.** Journal of Biological Chemistry 1996, **271:**15682–15686
136. Digiammarino EL, Harlan JE, Walter KA, Ladror US, Edalji RP, Hutchins CW, Lake MR, Greischar AJ, Liu J, Ghayur T, Jakob CG: **Ligand association rates to the inner-variable-domain of a dual-variable-domain immunoglobulin are significantly impacted by linker design.** mabs 2011, **3:**487–494
137. Dörken B, Riethmüller G, Kufer P, Lutterbüse R, Bargou R, Loffler A: *CD19xCD3 specific polypeptides and uses thereof* 2006.
138. Moore PA, Zhang W, Rainey GJ, Burke S, Li H, Huang L, Gorlatov S, Veri MC, Aggarwal S, Yang Y, Shah K, Jin L, Zhang S, He L, Zhang T, Ciccarone V, Koenig S, Bonvini E, Johnson S: **Application of dual affinity retargeting molecules to achieve optimal redirected T-cell killing of B-cell lymphoma.** BLOOD 2011, **117:**4542–4551

139. Kipriyanov SM, Moldenhauer G, Strauss G, Little M: **Bispecific CD3 x CD19 diabody for T cell-mediated lysis of malignant human B cells.** Int J Cancer 1998, **77:**763–772
140. Kipriyanov SM, Moldenhauer G, Schuhmacher J, Cochlovius B, Lieth CW von der, Matys ER, Little M: **Bispecific tandem diabody for tumor therapy with improved antigen binding and pharmacokinetics.** J Mol Biol 1999, **293:**41–56
141. Kufer P, Zettl F, Borschert K, Lutterbüse R, Kischel R, Riethmüller G: **Minimal costimulatory requirements for T cell priming and TH1 differentiation: activation of naive human T lymphocytes by tumor cells armed with bifunctional antibody constructs.** Cancer Immun. 2001, **1:**10
142. Loffler A, Kufer P, Lutterbuse R, Zettl F, Daniel PT, Schwenkenbecher JM, Riethmuller G, Dorken B, Bargou RC: **A recombinant bispecific single-chain antibody, CD19 x CD3, induces rapid and high lymphoma-directed cytotoxicity by unstimulated T lymphocytes.** BLOOD 2000, **95:**2098–2103
143. Brandl C, Haas C, d'Argouges S, Fisch T, Kufer P, Brischwein K, Prang N, Bargou RC, Suzich J, Bäuerle PA, Hofmeister R: **The effect of dexamethasone on polyclonal T cell activation and redirected target cell lysis as induced by a CD19/CD3-bispecific single-chain antibody construct.** Cancer Immunol. Immunother 2007, **56:**1551–1563
144. Hoffmann P, Hofmeister R, Brischwein K, Brandl C, Crommer S, Bargou RC, Itin C, Prang N, Bäuerle PA: **Serial killing of tumor cells by cytotoxic T cells redirected with a CD19-/CD3-bispecific single-chain antibody construct.** Int. J. Cancer 2005, **115:**98–104
145. Renner C, Bauer S, Sahin U, Jung W, van Lier R, Jacobs G, Held G, Pfreundschuh M: **Cure of disseminated xenografted human Hodgkin's tumors by bispecific monoclonal antibodies and human T cells: the role of human T-cell subsets in a preclinical model.** Blood 1996, **87:**2930–2937
146. Hauff C: **Aspects of the mode of action of bispecific T cell engager (BiTE) antibodies.** Universitätsbibliothek der Universität Würzburg; 2010.
147. Cochlovius B, Kipriyanov SM, Stassar MJ, Christ O, Schuhmacher J, Strauss G, Moldenhauer G, Little M: **Treatment of human B cell lymphoma xenografts with a CD3 x CD19 diabody and T cells.** J Immunol 2000, **165:**888–895
148. Franco R, Schoneveld O, Georgakilas AG, Panayiotidis MI: **Oxidative stress, DNA methylation and carcinogenesis.** Oxidative Stress and Carcinogenesis Special Issue 2008, **266:**6–11
149. Mehta AK, Majumdar SS, Alam P, Gulati N, Brahmachari V: **Epigenetic regulation of cytomegalovirus major immediate-early promoter activity in transgenic mice.** Gene 2009, **428:**20–24
150. Kong Q, Wu M, Huan Y, Zhang L, Liu H, Bou G, Luo Y, Mu Y, Liu Z: **Transgene expression is associated with copy number and cytomegalovirus promoter methylation in transgenic pigs.** PLOS ONE 2009, **4:**e6679
151. Legrand N, Weijer K, Spits H: **Experimental models to study development and function of the human immune system in vivo.** J Immunol 2006, **176:**2053–2058
152. McCune JM: **SCID mice as immune system models.** Current Opinion in Immunology 1991, **3:**224–228
153. Tary-Lehmann M, Saxon A, Lehmann PV: **The human immune system in hu-PBL-SCID mice.** Immunology Today 1995, **16:**529–533
154. Lutterbuese R, Raum T, Kischel R, Hoffmann P, Mangold S, Rattel B, Friedrich M, Thomas O, Lorenczewski G, Rau D, Schaller E, Herrmann I, Wolf A, Urbig T, Bäuerle PA, Kufer P: **T cell-engaging BiTE antibodies specific for EGFR potently eliminate KRAS- and BRAF-mutated colorectal cancer cells.** Proceedings of the National Academy of Sciences 2010, **107:**12605–12610
155. Reagan-Shaw S, Nihal M, Ahmad N: **Dose translation from animal to human studies revisited.** FASEB J 2008, **22:**659–661
156. Klamp T, Schumacher J, Huber G, Kuhne C, Meissner U, Selmi A, Hiller T, Kreiter S, Markl J, Türeci Ö, Sahin U: **Highly specific auto-antibodies against claudin-18 isoform 2 induced by a chimeric HBcAg virus-like particle vaccine kill tumor cells and inhibit the growth of lung metastases.** CANCER RES 2011, **71:**516–527

157. Huang RR, Jalil J, Economou JS, Chmielowski B, Koya RC, Mok S, Sazegar H, Seja E, Villanueva A, Gomez-Navarro J, Glaspy JA, Cochran AJ, Ribas A: **CTLA4 blockade induces frequent tumor infiltration by activated lymphocytes regardless of clinical responses in humans.** Clin. Cancer Res. 2011, **17:**4101–4109
158. **Stages of Drug Development** [http://www.pacificbiolabs.com/drug_stages.asp]
159. Lenkkeri-Schütz U, Kohleisen B, Itin C, Hofmeister R: *Multispecific deimmunized CD3-binders Multispezifische, deimmunsierte CD3-bindende Moleküle* 15-Oct-2004.
160. Sharan SK, Thomason LC, Kuznetsov SG, Court DL: **Recombineering: a homologous recombination-based method of genetic engineering.** Nat Protoc 2009, **4:**206–223
161. Carralot J, Probst J, Hoerr I, Scheel B, Teufel R, Jung G, Rammensee H, Pascolo S: **Polarization of immunity induced by direct injection of naked sequence-stabilized mRNA vaccines.** Cell. Mol. Life Sci. 2004, **61:**2418–2424
162. Castle JC, Kreiter S, Diekmann J, Löwer M, van de Roemer N, Graaf J de, Selmi A, Diken M, Boegel S, Paret C, Koslowski M, Kuhn AN, Britten CM, Huber C, Türeci O, Sahin U: **Exploiting the mutanome for tumor vaccination.** Cancer Res. 2012, **72:**1081–1091
163. Kormann MSD, Hasenpusch G, Aneja MK, Nica G, Flemmer AW, Herber-Jonat S, Huppmann M, Mays LE, Illenyi M, Schams A, Griese M, Bittmann I, Handgretinger R, Hartl D, Rosenecker J, Rudolph C: **Expression of therapeutic proteins after delivery of chemically modified mRNA in mice.** Nat Biotechnol 2011, **29:**154–157
164. Kreiter S, Selmi A, Diken M, Koslowski M, Britten CM, Huber C, Tureci O, Sahin U: **Intranodal Vaccination with Naked Antigen-Encoding RNA Elicits Potent Prophylactic and Therapeutic Antitumoral Immunity.** Cancer Research 2010, **70:**9031–9040
165. Scheel B, Braedel S, Probst J, Carralot J, Wagner H, Schild H, Jung G, Rammensee H, Pascolo S: **Immunostimulating capacities of stabilized RNA molecules.** Eur. J. Immunol. 2004, **34:**537–547
166. Kreiter S, Diken M, Selmi A, Türeci Ö, Sahin U: **Tumor vaccination using messenger RNA: prospects of a future therapy.** Curr Opin Immunol 2011, **23:**399–406
167. Diken M, Kreiter S, Selmi A, Türeci O, Sahin U: **Antitumor vaccination with synthetic mRNA: strategies for in vitro and in vivo preclinical studies:**235–246. In *Synthetic Messenger RNA and Cell Metabolism Modulation.* Edited by Rabinovich PM. Totowa, NJ: Humana Press; 2013. [Methods in Molecular Biology]
168. Kreiter S, Diken M, Selmi A, Diekmann J, Attig S, Husemann Y, Koslowski M, Huber C, Tureci O, Sahin U: **FLT3 Ligand Enhances the Cancer Therapeutic Potency of Naked RNA Vaccines.** Cancer Research 2011, **71:**6132–6142
169. Hoerr I, Probst J, Pascolo S: *RNA-CODED ANTIBODY.* CURVAC GMBH 8. Jan. 2008.
170. Rabinovich PM, Komarovskaya ME, Wrzesinski SH, Alderman JL, Budak-Alpdogan T, Karpikov A, Guo H, Flavell RA, Cheung N, Weissman SM, Bahceci E: **Chimeric Receptor mRNA Transfection as a Tool to Generate Antineoplastic Lymphocytes.** Human Gene Therapy 2009, **20:**51–61
171. Rabinovich PM, Weissman SM: **Cell Engineering with Synthetic Messenger RNA:**3–28. In *Synthetic Messenger RNA and Cell Metabolism Modulation.* Edited by Rabinovich PM. Totowa, NJ: Humana Press; 2013. [Methods in Molecular Biology]
172. Phua KK, Leong KW, Nair SK: **Transfection efficiency and transgene expression kinetics of mRNA delivered in naked and nanoparticle format.** Journal of Controlled Release 2013, **166:**227–233
173. Probst J, Weide B, Scheel B, Pichler BJ, Hoerr I, Rammensee H, Pascolo S: **Spontaneous cellular uptake of exogenous messenger RNA in vivo is nucleic acid-specific, saturable and ion dependent.** Gene Ther. 2007, **14:**1175–1180
174. Hoerr I, Obst R, Rammensee H, Jung G: **In vivo application of RNA leads to induction of specific cytotoxic T lymphocytes and antibodies.** Eur. J. Immunol. 2000, **30:**1–7
175. Tavernier G, Andries O, Demeester J, Sanders NN, Smedt SC de, Rejman J: **mRNA as gene therapeutic: how to control protein expression.** J Control Release 2011, **150:**238–247

176. Warren L, Manos PD, Ahfeldt T, Loh Y, Li H, Lau F, Ebina W, Mandal PK, Smith ZD, Meissner A, Daley GQ, Brack AS, Collins JJ, Cowan C, Schlaeger TM, Rossi DJ: **Highly Efficient Reprogramming to Pluripotency and Directed Differentiation of Human Cells with Synthetic Modified mRNA.** Cell Stem Cell 2010, **7:**618–630
177. Xu L, Anchordoquy T: **Drug delivery trends in clinical trials and translational medicine: challenges and opportunities in the delivery of nucleic acid-based therapeutics.** J Pharm Sci 2011, **100:**38–52
178. Scott McIvor R: **Therapeutic Delivery of mRNA: The Medium Is the Message.** Mol Ther 2011, **19:**822–823
179. Kuhn AN, Diken M, Kreiter S, Selmi A, Kowalska J, Jemielity J, Darzynkiewicz E, Huber C, Türeci Ö, Sahin U: **Phosphorothioate cap analogs increase stability and translational efficiency of RNA vaccines in immature dendritic cells and induce superior immune responses in vivo.** Gene Ther 2010, **17:**961–971
180. Sahin U, Poleganov M, Beissert T: *USE OF RNA FOR REPROGRAMMING SOMATIC CELLS* 16.02.2013.
181. Üzgün S, Nica G, Pfeifer C, Bosinco M, Michaelis K, Lutz J, Schneider M, Rosenecker J, Rudolph C: **PEGylation Improves Nanoparticle Formation and Transfection Efficiency of Messenger RNA.** Pharm Res 2011, **28:**2223–2232
182. Ponsaerts P, van TENDELOO VFI, Berneman ZN: **Cancer immunotherapy using RNA-loaded dendritic cells.** Clin Exp Immunol 2003, **134:**378–384
183. Thompson MR, Kaminski JJ, Kurt-Jones EA, Fitzgerald KA: **Pattern Recognition Receptors and the Innate Immune Response to Viral Infection.** Viruses 2011, **3:**920–940
184. Clemens MJ: **PKR--a protein kinase regulated by double-stranded RNA.** Int. J. Biochem. Cell Biol. 1997, **29:**945–949
185. Takeuchi O, Akira S: **Pattern Recognition Receptors and Inflammation.** Cell 2010, **140:**805–820
186. van Tendeloo VFI, Ponsaerts P, Berneman ZN: **mRNA-based gene transfer as a tool for gene and cell therapy.** Curr. Opin. Mol. Ther. 2007, **9:**423–431
187. Karikó K, Muramatsu H, Ludwig J, Weissman D: **Generating the optimal mRNA for therapy: HPLC purification eliminates immune activation and improves translation of nucleoside-modified, protein-encoding mRNA.** Nucleic acids research 2011.
188. Weissman D, Pardi N, Muramatsu H, Karikó K: **HPLC purification of in vitro transcribed long RNA.** Methods Mol. Biol. 2013, **969:**43–54
189. Geall AJ, Verma A, Otten GR, Shaw CA, Hekele A, Banerjee K, Cu Y, Beard CW, Brito LA, Krucker T, O'Hagan DT, Singh M, Mason PW, Valiante NM, Dormitzer PR, Barnett SW, Rappuoli R, Ulmer JB, Mandl CW: **Nonviral delivery of self-amplifying RNA vaccines.** Proc Natl Acad Sci U S A 2012, **109:**14604–14609

6 APPENDIX

6.1 INFORMATION ON USED BIMAB PROTEIN ELEMENTS

Table 18: Linker amino acid sequences used in BiMAB formats

NC	5'-VH-VL	5'-LL	3'-VH-VL	3'-LL	SL
1BiMAB	IMAB362	(GGGGS)3	TR66	VE(GGSGGS)2GGVD	SGGGGS
3'UCHT1-HS	IMAB362	(GGGGS)3	UCHT1-HS	(GGGGS)3	SGGGGS
3'UCHT1-MM	IMAB362	(GGGGS)3	UCHT1-MM	(GGGGS)3	SGGGGS
3'CLB-T3	IMAB362	(GGGGS)3	CLB-T3	(GGGGS)3	SGGGGS
3'TR66	IMAB362	(GGGGS)3	TR66	(GGGGS)3	SGGGGS
5'UCHT1-HS	UCHT1-HS	(GGGGS)3	IMAB362	(GGGGS)3	SGGGGS
5'UCHT1-MM	UCHT1-MM	(GGGGS)3	IMAB362	(GGGGS)3	SGGGGS
5'CLB-T3	CLB-T3	(GGGGS)3	IMAB362	(GGGGS)3	SGGGGS
5'TR66	TR66	(GGGGS)3	IMAB362	(GGGGS)3	SGGGGS
BIMAB4	HMFG2	(GGGGS)3	TR66	(GGGGS)3	SGGGGS
BiMAB2	TR66	VE(GGSGGS)2GGVD	IMAB362	(GGGGS)3	SGGGGS
5'Plac1	78H11	(GGGGS)3	TR66	(GGGGS)3	SGGGGS

Table 19: Secretion signal of BiMABs

NC	sec. signal
1BiMAB	MGWSCIILFLVATATGVHS
3'UCHT1-HS	MGWSCIILFLVATATGVHS
3'UCHT1-MM	MGWSCIILFLVATATGVHS
3'CLB-T3	MGWSCIILFLVATATGVHS
3'TR66	MGWSCIILFLVATATGVHS
5'UCHT1-HS	MGWSCIILFLVATATGVHS

NC	sec. signal
5'UCHT1-MM	MNSGLQLVFFVLTLKGIQG
5'CLB-T3	MNFGLSLIFLALILKGVQC
5'TR66	MEWSWIFLFLLSVTTGVHS
BIMAB4	MGWSCIILFLVATATGVHS
BiMAB2	MGWSCIILFLVATATGVHS
BiMAB3	MGWLWNLLFLMAAAQSAQA

6.2 INFORMATION ON BIMAB PROTEINS

Table 20: BiMAB protein size

BiMAB	AA	kDa
3'145-2C11	496	53.47
3'UCHT1-HS	499	54.00
3'UCHT1-MM	502	54.13
3'CLB-T3	500	53.70
3'TR66	496	53.54
5'145-2C11	495	53.39
5'UCHT1-HS	499	54.00
5'UCHT1-MM	502	54.13
5'CLB-T3	500	53.70
5'TR66	496	53.55
3'Plac1-3'TR66	495	53.37
1BiMAB	501	54.19

6.3 ABBREVIATIONS

Table 21: List of abbreviations

Abbreviation	
µL	micro liters
µM	micro molar
1ry	primary
1st	first
2nd	second
2ry	Secondary
6×His-Tag	hexahistidyl-tag
AA	amino acid
ADCC	antibody dependent cellular cytotoxicity
Amp.	ampicillin
APC	allophycocyanin
APS	ammoniumpersulfate
ATP	adenosine triphosphate
ATPase	adenosine 5`-triphosphatase
BD	Becton, Dickinson and Company
BiMAB	bispecific ideal monoclonal antibody
bs	bispecific
BSA	bovine serum albumin
bs-scAb	bispecific-single-chain-antibody
bs-td-sc-Fv	bispecific tandem single chain variable fragment
C terminus	Carboxy-terminus
CD	cluster of differentiation
CD3ε	CD3 epsilon chain
CD8/4/25/69/3+	CD8/4/25/69/3-positive
CD8+ & CD4+	CD8-positives and CD4-positives
CD8+/CD4+	CD8 and CD4 double-positive
CDC	complement dependent cytotoxicity
CDS	coding sequence
CFSE	carboxyfluorescein diacetate succinimidyl ester
CHO	chinese hamster ovary cell line
CLDN18.2	claudin 18.2
CLDN18.2+	claudin 18.2-positive
cm	centimeters
co	codon optimized
DC	dendritic cell
DEPC	diethylenpyrocarbonate
DMEM	dulbeccos modified eagle medium
DMSO	dimethyl sulfoxide
e.g.	in example
E:T	effector to target ratio
EDTA	ethylendiamintetraacetate
eGFP	enhanced green fluorescence protein
ELISA	enzyme linked immunosorbent assay
Ext. Coeff.	extinctions coefficient
Fc	fragment crystalline
FCS	Fetal calf serum
FDA	food and drug administration
FITC	Fluorescein isothiocyanate
Fv	variable fragment
GIST	gastro intestinal stromal tumor
h	hours
HEK293	human embryonic kidney cell line
HEK293T	human embryonic kidney cell line transfected with the large T antigen from SV40 virus
HPRT	hypoxanthine-guanine phosphoribosyltransferase
HS	Homo sapiens
-HS	humanized
HSA	human serum albumin
ICC	immuno-cyto-chemical
IL-2	Interleukin-2
IMAB	ideal monoclonal antibody
IMAC	immobilized metal affinity chromatography
ip	intraperitoneal
iv	intra venous
IVT	*in vitro* transcription
IVT-RNA	*in vitro* transcribed RNA
kDa	kilo Dalton
Km.	kanamycin
M&M	materials and methods
mAb	monoclonal antibody
MACS	magnetic cell separation
MFI	mean fluorescence intensity
MHC	major histocompatibility complex
min	min
mL	milliliter
MM	mus musculus
-MM	murine
MW	molecular weight
N terminus	Amino-terminus
NC	nomenclature
NEAA	non-essential amino acids
NEB	new england biolabs
Ni-NTA	nickel-nitrilotriacetic acid
nt	nucleotides
p.A.	pro analysis
PBS	Phosphate buffered saline
PE	phycoerythrin
PEI	polyethylenimine
PI	propidium iodide
qRT-PCR	qualitative real-time PCR
RT	room temperature
sc	subcutaneous
scFv	single chain variable fragment
SD	standard deviation
SDS-PAGE	sodium dodecyl sulfate polyacrylamide gel electrophoresis
Seq.	sequencing
SN	supernatant
TAA	tumor associated antigen
TAA+	tumor associated antigen-positive
TCR	T cell receptor
td	tandem
TRIS	trishydroxymethylaminomethan
V_H	variable heavy
V_L	variable light
w/o	without
ZA	Zoledronic acid
αHS	anti-human
αMM	anti-murine
γδ T cells	Vgamma9/Vdelta2 T cells

7 ACKNOWLEDGEMENTS

A project such as a dissertation is not completed without the support of many people especially the select few I am about to mention.

First and foremost, I would especially like to thank Prof. Dr. XXXX and PD Dr.YYYYY who gave me the opportunity to join their team, for being in charge of this remarkable and challenging subject and for their advice, as well as the persistent interest in my work.

My gratitude goes to my co-advisors Dr. XXXX and Dr. YYYY, for numerous fruitful scientific discussions to overcome occurring hurdles and I wish to thank for their steady encouragement, guidance, suggestions throughout the past years. From the start of the project up to the final proof-reading of this manuscript.

I want to thank Prof. Dr. XXXX for his kindness to render his expert opinion on my doctoral thesis.

Special thanks to Mrs. XXXX for her all-embracing assistance during my work as a doctoral candidate in the AG Sahin.

I am grateful to all of my colleagues, especially the whole BiMAB group as well as all fellow doctoral candidates in the group of Sahin for providing an inspiring atmosphere in the lab. I want to thank everybody who contributed to finish this work and for all the fun, we have had in the last five years.

I specially appreciated the "boulder-evenings" and conversations with Dr. XXXX.

Outside the lab, I would like to thank my best friend Antonia who always helped me to find further perspectives. Thank you Antonia for being persistent and encouraging, for believing in me, and for the many precious memories along the way.

I want to acknowledge my husband XXXX, for his love, support, and understanding in dealing with every challenge I have faced. XXXX has been central to my completion of this study as he has given me confidence and motivated me in so many ways. Without his help and belief in me this dissertation would not have been possible.

I would like to end with thanking my wonderful family–
–thank-you for the tremendous support you gave me. To them, I dedicate this thesis.

8 CURRICULUM VITAE JULIA HOLLAND

Julia Holland

Diplom-Biologist

Address:

Mail:

PERSONAL INFORMATION

Date of Birth:	08. November 1981
Nationality	born in Mainz, Germany

EDUCATION

PhD Thesis	November 2008— January 2014 Group of Prof. Sahin at Department of Experimental and Translational Oncology Johannes Gutenberg University -Mainz, GERMANY
Diploma graduation	December 2006 Degree "Diplom-Biologin" at the Ruhr-University Bochum; Final grade A (sehr gut, 1.3).
Diploma thesis	Jan.-Oct. 2006 "Characterization of silencing suppressor of Tombus viruses by means of molecular-biological techniques" at the Institute VII of Molecular Biotechnology at the University of Technology Aachen (RWTH Aachen).
Study of biology	Nov. 2005 at the Ruhr-University Bochum
Major subjects	Microbiology specialized in molecular genetics,
Minor subjects	Biochemistry specialized in biotechnology Medical science specialized in vegetative physiology.
Undergraduate study	October 2001-2003 at the Ruhr-University Bochum.
School graduation	June 2001 Degree "Abitur" Maria Wächtler Gymnasium, in Essen, Germany

PROFESSIONAL EXPERIENCE

Scientific employee	May 2007-October 2008 GeneArt AG in the R&D department of Dr. Matthias Arnold. Establishment of molecular biological methods to improve various processes of gene synthesis and cloning techniques.
Internship	January-April 2007 Internship at pharmaceutical company Pfizer (Karlsruhe) in the department Brand-Marketing Oncology. Tasks involved supporting the development of marketing plans, conception of documents and brochures for field services, assisting events such as congresses and symposia.
Student research and teaching assistant	February -July 2006 Institute VII of Molecular Biotechnology at the University of Technology Aachen (RWTH Aachen).

ACHIEVEMENTS

Patent protection	**PCT/EP2012/004712 (13.11.2012):** **"Agents for Treatment of Claudin Expressing Cancer diseases";** **Applicant: BioNTech AG, Ganymed Pharmaceuticals AG and** **TRON gGmbH;** **Inventor: U. Sahin, Ö. Türeci, J. Holland, C. Stadler und H. Bähr-Mahmud**
Poster presentations	**11th annual CIMT meeting 2013** **"Effective Recruitment and Activation of T cells by a Bispecific Single Chain Antibody leading to the Elimination of CLDN18.2 Positive Carcinoma Cells" - Mainz (Germany)** **Empowered antibodies June 2013 - Recombinant & Bispecific Antibodies** **"Redirection of T cell effector functions towards CLDN18.2 positive carcinoma cells by the novel bispecific single chain antibody 1BiMAB" - Barcelona (Spain)**
Short talk	**11th annual CIMT meeting 2013 Mainz (Germany) –** **"Development of highly potent bispecific antibody formats targeting the novel tumor specific tight junction antigen CLDN18.2"**

LANGUAGE SKILLS

German	**Native**
English	**Fluent**
French	**Moderate**

FURTHER EDUCATION

Laboratory animal science	**Course FELASA Category B**
Post graduate and doctoral certificate program	**Participant of the "Promotionskolleg Mainz"**